Not Simply the Induction of Alternative Oxidase: The AOD2 and AOD5 Transcription Factors Play Roles in Regulation of Metabolism and Energy Production in *Neurospora crassa*

by

Zhigang Qi

A thesis submitted in partial fulfillment of the requirements for the degree of

Doctor of Philosophy

in

Molecular Biology and Genetics

Department of Biological Sciences

University of Alberta

ABSTRACT

Mitochondria are important organelles in most eukaryotic organisms as they supply the majority of the ATP needed for cellular functions. Although mitochondria contain their own DNA, the vast majority of mitochondrial proteins are encoded in the nucleus. Thus, when mitochondria experience stress they signal the nucleus to alter gene expression and provide a response to the stress. In *Neurospora crassa*, one model for studying mitochondrial signaling is the induction of alternative oxidase (AOX). This enzyme is a mitochondrial protein encoded by the nuclear *aod-1* gene and serves as an alternative terminal oxidase in the electron transport chain. Under normal growth conditions, AOX is not expressed. However, induction of the AOX occurs when cells are grown in the presence of drugs that decrease the function of the standard electron transport chain or when they carry mutations affecting the standard electron transport chain. The induction of AOX requires the function of two Zn(II)Cys6 transcription factors named AOD2 and AOD5. In this study, I demonstrated that both AOD2 and AOD5 localize to the nucleus regardless of whether or not cells are grown under conditions that induce AOX. AOD2 and AOD5 were also shown to exist as a heterodimer *in vivo*.

The orthologues of AOD2 and AOD5 in other fungi have been shown to regulate the expression of genes required for gluconeogenesis. Here, I have shown that the growth of *N. crassa* on poor carbon sources was severely impaired in the absence of AOD2 or AOD5. Moreover, the expression of the gene encoding phosphoenolpyruvate carboxylase (PEPCK), which is required for gluconeogenesis, was greatly reduced in the absence of AOD2. However, no AOX was detected in cells grown in poor carbon sources, suggesting that the action of AOD2 and AOD5 in

regulating gluconeogenesis and AOX is complex and might occur via response to different signals.

To investigate whether AOD2 and AOD5 are involved in other cellular functions, I performed chromatin immunoprecipitations followed by next generation sequencing (ChIP-seq) to investigate the global binding of AOD2 and AOD5 in cells grown in the presence and absence of chloramphenicol, a drug that inhibits mitochondrial protein synthesis and, thus, indirectly affects the function of the standard electron transport chain. I focused on the 65 ChIP-seq peaks that exhibited more than four-fold enrichment from strains expressing tagged versions of AOD2 and AOD5 that could be immunoprecipitated with commercial antibodies as compared to a wild-type control strain with no tagged proteins. ChIP-seq was done following growth in both AOX inducing and non-inducing conditions. I found that the 5' regions of *aod-1* and PEPCK are constitutively bound by AOD2 and AOD5. Furthermore, AOD2 and AOD5 also bind to the 5' regions of many other genes. Most of the binding sites for the 65 peaks contain at least one AOX induction motif, which was previously shown to bind AOD2 and AOD5 using *in vitro* assays. Several of the genes associated with the 65 peaks were validated as requiring AOD2 and AOD5 for normal expression using RT-qPCR. This study suggests that not only do AOD2 and AOD5 regulate the AOX induction pathway and gluconeogenic pathway, but they also appear to play larger roles in energy homeostasis and reprogramming of metabolism under oxidative stress.

ACKNOWLEDGEMENTS

I feel very grateful to many people who helped me throughout the years I pursued my Ph.D. degree. The most important person I want to thank is my supervisor Dr. Frank Nargang, who is always very patient with me even though I had never received training in critical thinking skills. There were a great many frustrating times when experiments did not work out but thanks to Frank's encouragement and guidance, I got a lot of experimental data at the end. I especially want to express my gratitude to Frank for his advice on preparing for my candidacy and defense exams. He is indeed a very nice person, as I was told by the people I met during the first few days I was in the Department of Biological Sciences.

The second person I want to thank is Jeremy Wideman. He was always willing to help me. He taught me countless things, ranging from doing a Western, to English, to understanding American football games. I feel really lucky that I met such a person in the lab, although he left the lab in third year of my Ph. D. Other lab members were also important to me: Natasa Bosnjak, Sebastian Lackey, Beau Desaulniers, Michael Chae, Cornelia Rub, and Nancy Easton. I also want to thank the three technicians, Kelly Adames, Annie Wong, and Nancy Go, for their technical as well as emotional support. The lab was really a happy and warm environment for life.

Our collaborators in the Oregon State University did a great job on my ChIP-seq data and I am thankful to them: Kristina Smith, Erin Bredeweg, and Michael Freitag. All the qPCR experiments were performed in Kirst King-Jones's lab and I appreciate Kirst for allowing access to the qPCR machine and his lab members for technical support and advice.

Last but not least, my special thanks go to my parents. I was not around for so many years, and I feel so bad that I was not able accompany my dad when he got the diagnosis of his fatal disease. However, I am very grateful to my wife, Shiyin Chang, who was always with me during the hard times.

TABLE OF CONTENTS

LIST OF FIGURES

LIST OF TABLES

LIST OF ABBREVIATIONS

A	adenine
A. fumigatus	*Aspergillus fumigatus*
A. nidulans	*Aspergillus nidulans*
ABC	ATP-binding cassette
ADP	adenosine diphosphate
AOD	AOX deficient
AOX	alternative oxidase
ATP	adenosine triphosphate
BLAST	Basic Local Alignment Search Tool
C	cytosine
C. albicans	*Candida albicans*
C. elegans	*Caenorhabditis elegans*
CARE	cis-acting regulatory element
cDNA	complementary deoxyribonucleic acid
ChIP	chromatin immunoprecipitation
CIP	calf intestine phosphatase
CM	chloramphenicol
Complex I	NADH:ubiquinone oxidoreductase
Complex II	succinate:ubiquinone oxidoreductase
Complex III	ubiquinol:cytochrome *c* oxidoreductase
Complex IV	cytochrome *c* oxidase
Complex V	ATP synthase
conidia	conidiaspores
CSRE	carbon source-responsive element
Cys	cysteine
dH_2O	distilled water
DNA	deoxyribonucleic acid
dNTP	deoxynucleotide triphosphate
E. coli	*Escherichia coli*
EDTA	ethylenediaminetetraacetic acid
EMSA	electrophoretic mobility shift assay
ER	endoplasmic reticulum
ERMES	ER-mitochondrial encounter structure
FAD	flavin adenine dinucleotide
FBP	fructose 1,6-bisphosphatase
FDR	false discovery rate
Fe-S	iron-sulfur
FGSC	Fungal Genetic Stock Center
FMN	flavin mononucleotide
g	gravity force
G	guanine
gm	gram

GSH	reduced glutathione
GSSG	oxidized glutathione
GTP	guanosine triphosphate
H_2O_2	hydrogen peroxide
HA	hemagglutinin
HEPES	4-(2-hydroxyethyl)-1-piperazineethanesulfonic acid
hr	hour
IMS	mitochondrial intermembrane space
JA	jasmonic acid
kDa	kilodalton
L	liter
M	molar
Max	maximum
mg	milli gram
MIA	mitochondrial IMS import and assembly machinery
MICOS	mitochondrial contact site and cristae organizing system
MIM	mitochondrial inner membrane
min	minute
Min	minimum
mL	milli liter
mM	milli molar
MOM	mitochondrial outer membrane
MOPS	3-(N-morpholino)propanesulfonic acid
ms	milli second
mtDNA	mitochondrial DNA
N. crassa	*Neurospora crassa*
NAD	nicotinamide adenine dinucleotide
ND	NADH dehydrogenase
ng	nano gram
NO	nitric oxide
O_2^-	superoxide anion
ºC	degree celcius
OH·	hydroxyl radical
OXPHOS	oxidative phosphorylation
P. anserina	*Podospora anserina*
PAGE	polyacrylamide gel electrophoresis
PAS	Per-Arnt-Sim
PBS	phosphate buffered saline
PCR	polymerase chain reaction
PEPCK	phosphoenolpyruvate carboxykinase
PMSF	phenylmethanesulfonylfluoride
PTOX	plastid terminal oxidase
qPCR	quantitative polymerase chain reaction
RIP	repeat induced point mutation

RNA	ribonucleic acid
ROS	reactive oxygen species
rpm	revolutions per minute
rTAO	*Trypanosoma brucei* AOX
RTG	retrograde
S. cerevisiae	*Saccharomyces cerevisiae*
SA	salicylic acid
SAM	sorting and assembly machinery
SDS	sodium dodecyl sulfate
sec	second
SEMP	sucrose, EDTA, MOPS, PMSF
sETC	standard electron transport chain
SGD	*S. cerevisiae* genome database
SOD	superoxide dismutase
T	thymine
TCA	tricarboxylic acid
TIM	translocase of the inner membrane
Tm	melting temperature
TOM	translocase of the outer membrane
TOR	target of rapamycin
Tris	trisaminomethane
TSS	translation start site
UAS	upstream activation sequence
UPR	unfolded protein response
UTR	untranslated region
V	volt
VDAC	voltage-dependent anion channel
Y. lipolytica	*Yarrowia lipolytica*
µF	micro farad
µg	micro gram
µL	micro liter
µM	micro molar

1 Introduction

1.1 Mitochondrial structure

The mitochondrion is a well-known organelle that is harbored in eukaryotic cells. It is the power-house of the cell that produces adenosine triphosphate (ATP) via oxidative phosphorylation (OXPHOS). It is a double membraned structure that is composed of the mitochondrial outer membrane (MOM), the mitochondrial inner membrane (MIM), the mitochondrial intermembrane space (IMS), and the mitochondrial matrix (Fig. 1.1). The enzyme complexes involved in OXPHOS locate to the MIM. Although the MOM and MIM are distinct structures, interactions between them occur at sites of contact between these two membranes (Reichert & Neupert 2002). The MIM can be subdivided into three functionally distinct domains: the inner boundary membrane (IBM), which runs parallel to the MOM; the cristae membrane, which protrudes into the mitochondrial matrix; and a special structure that connects the latter two domains called the crista junction (Kuhlbrandt 2015; Vogel *et al.* 2006) (Fig. 1.1). Four separate studies revealed that the contact sites between the MOM and MIM are formed by a complex that is located mainly at crista junctions and is required to maintain cristae structure (Alkhaja *et al.* 2012; Harner *et al.* 2011; Hoppins *et al.* 2011; von der Malsburg *et al.* 2011). The complex contains six proteins in yeast. The complex also appears to play a role in mitochondrial protein import and lipid trafficking (van der Laan *et al.* 2012; Zerbes *et al.* 2012). Recently, the naming of this complex and its proteins was standardized to the "mitochondrial contact site and cristae organizing system" (MICOS) (Fig. 1.1) for the complex; and Mic10,

Figure 1.1. Basic structure of a mitochondrion. A mitochondrion has a double membrane-bound structure composed of the MOM and the MIM, as well as two inner compartments, the IMS and the matrix. The inward folding of the MIM forms compartments named cristae. As shown in the zoomed-in window, the MIM can be further subdivided into the IBM and the cristae membrane. The opening of crista, at the point where the IBM and the cristae membrane meet, is called the crista junction. The cristae structure is maintained by MICOS, which also has interactions with the MOM. The MOM interacts with the endoplasmic reticulum (ER) via the ER mitochondrial encounter structure (ERMES) complex.

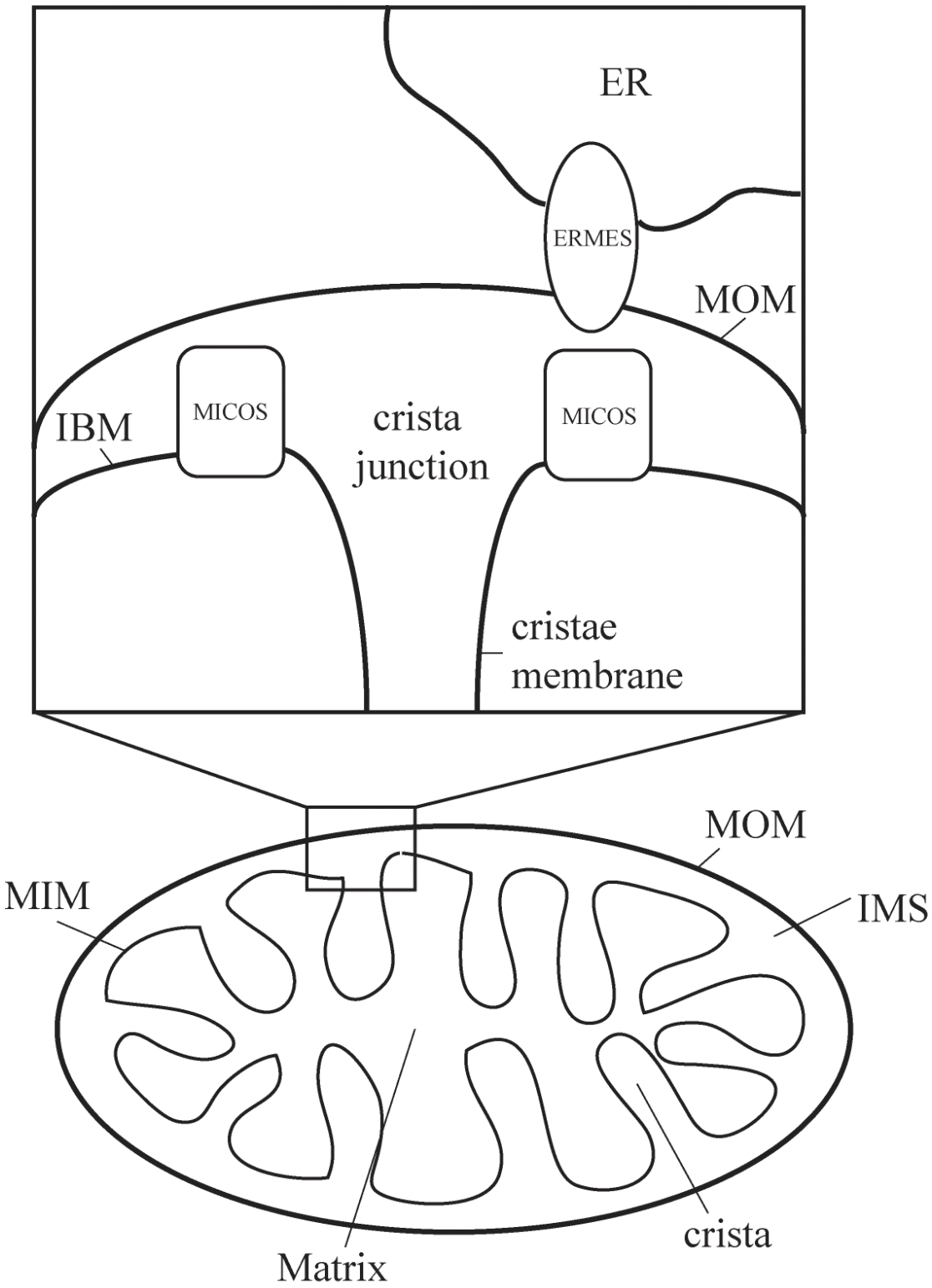
ER
ERMES
MOM
IBM
MICOS
crista
junction
MICOS
cristae
membrane
MOM
MIM
IMS
Matrix
crista

Mic12, Mic19, Mic26, Mic27, Mic60 for the proteins (Pfanner *et al.* 2014).

1.2 Mitochondrial dynamics

Mitochondria cannot be produced via *de novo* synthesis but have to emerge from an existing mitochondrion. This requires fission from an existing mitochondrion to give rise to two new mitochondria. In fact, not only do mitochondria perform fission during their biogenesis, but they are dynamic and undergo fission and fusion constantly under normal conditions. Mitochondria can maintain stable tubular structures and are often organized in a connected network in many types of cells. Environmental and metabolic conditions can influence the level of fission or fusion that occurs (Mishra & Chan 2016; Wai & Langer 2016). These behaviors are beneficial because they allow cells to remove aged and damaged mitochondria and replenish the mitochondria pool with healthy ones (Chan 2012; Labbe *et al.* 2014). These processes are mainly mediated by dynamin-related GTPases (DRPs). Mitochondrial fusion involves MFN1 (mitofusin 1) and MFN2 in mammals, or Fzo1p (fuzzy onions 1) in yeast, which are responsible for merging the MOMs of separate mitochondria. The OPA1 (optic atrophy 1) protein in mammals, or the Mgm1p (mitochondrial genome maintenance 1) protein in yeast, are required for the fusion of MIMs (Chan 2012; Labbe *et al.* 2014). On the other hand, DRP1 (dynamin-related protein 1) in mammals, Dnm1p (dynamin 1) in yeast, mediate mitochondrial fission.

Non-DRP proteins also participate in mitochondrial fusion/fission processes. In mammals, DRP1 also interacts with MFF (mitochondrial fission factor), MID49

(mitochondrial dynamics proteins of 49 kDa), and MID51 to mediate mitochondrial division (Gandre-Babbe & van der Bliek 2008; Palmer *et al.* 2011). In yeast, the non-DRP proteins Ugo1p (ugo means fusion in Japanese) (Sesaki & Jensen 2001) and Mdm30p (mitochondrial distribution and morphology 30) participate in MOM fusion (Anton *et al.* 2011; Cohen *et al.* 2011), while Fis1p (fission 1) (Mozdy *et al.* 2000) and Mdv1p (Tieu & Nunnari 2000) are components of the mitochondrial division machinery.

Interestingly, the sites where mitochondria divide in yeast were found to be wrapped by the endoplasmic reticulum (ER), before recruitment of the fission protein Dnm1p (Friedman *et al.* 2011), indicating that the ER marks mitochondrial division sites. The structure that tethers the ER and mitochondria is termed the ER-mitochondrial encounter structure (ERMES) (Kornmann *et al.* 2009) (Fig. 1.1). It consists of Mmm1p (maintenance of mitochondrial morphology 1), Mdm10p (mitochondrial distribution and morphology 10), Mdm12p, Mdm34p (Kornmann *et al.* 2009), and Gem1p (Kornmann *et al.* 2011). The ERMES has also been linked to a wide variety of mitochondrial structures and functions (Kornmann & Walter 2010; Lang *et al.* 2015; Michel & Kornmann 2012). However, ERMES is absent in animals (Wideman *et al.* 2013).

1.3 Mitochondrial DNA

Mitochondria harbor their own DNA in the matrix. In humans, the approximate 16,500 bp mitochondrial DNA (mtDNA) encodes 13 proteins, 2

ribosomal RNAs and 22 transfer RNAs (Anderson *et al.* 1981). Even though mitochondria are involved in a great many cellular functions, the 13 mtDNA-encoded proteins of humans are only found in components of the OXPHOS system including cytochrome *b* of Complex III, seven subunits of Complex I, three subunits of Complex IV, and two subunits of Complex V. The size and coding capacity of mtDNA varies considerably among different organisms (Gray 2015). The Jakobid protists such as *Reclinomonas americana* and *Andalucia godoyi* have the largest number of total genes in their mtDNA (97 and 100, respectively), and 67 and 72, respectively, are protein coding (Burger *et al.* 2013). In *Neurospora crassa*, the mitochondrial genome encodes 14 protein subunits involved in the OXPHOS system (Davis 2000). Given that there are over 1000 mitochondrial proteins in mammals (Calvo & Mootha 2010; Gregersen *et al.* 2012), it is obvious that the vast majority is encoded by the nuclear genome, translated in the cytosol, and imported into mitochondria.

1.4 Origin of the mitochondrion

The idea of endosymbiosis was first proposed in 1905 by a Russian scientist named Constantin Sergeevich Merezhkowsky who suggested that plastids arose from cyanobacteria (as reviewed in Sapp *et al.* 2002). The hypothesis was revived in 1970 by Lynn Margulis and extended to mitochondria (Margulis 1970). It is now accepted that the contemporary mitochondrion shares a common ancestor with α-proteobacteria. This point of view was first developed from phylogentic analysis of ribosomal RNA sequences (Cedergren *et al.* 1988; Gray *et al.* 1984). As genome sequences from

different prokaryotes became available, more and more phylogenetic constructions supported the α-proteobacterial ancestry of mitochondria (Esser *et al.* 2004), with the mitochondrial group placing close to the *Rickettsiales* (Brindefalk *et al.* 2011; Fitzpatrick *et al.* 2006; Georgiades *et al.* 2011; Thrash *et al.* 2011; Wang & Wu 2015; Williams *et al.* 2007).

The host that engulfed the endosymbiont ancestor of mitochondria has been long debated. Recent data appear to favor the eocyte hypothesis (Lake *et al.* 1984) which states that there are only two domains of life, Bacteria and Archaea, with eukaryotes originating within the Archaea group. It has been shown that the Archaea in the TACK superphylum (Thaumarchaeota, Aigarchaeota, Crenarchaeota, and Korarchaeota) encode various proteins related to eukaryotic signature proteins (such as those involved in the cytoskeleton system) and therefore represent the closest relatives of the original host that engulfed the mitochondrial ancestor (Archibald 2015; Williams & Embley 2015; Williams *et al.* 2013). The most promising of these is the recently discovered Lokiarcheota (Embley & Williams 2015; Koonin 2015; Spang *et al.* 2015) which harbors the most eukaryotic signature proteins that have been found thus far in an Archaea species (Koonin 2015; Saw *et al.* 2015).

1.5 Mitochondrial protein import

The mitochondrial genome only encodes a small proportion of mitochondrial proteins while the vast majority is encoded by the nuclear genome (Calvo & Mootha 2010; Schmidt *et al.* 2010). Thus, mitochondria are equipped with a protein

translocation system to import proteins that are encoded in the nucleus and produced on cytosolic ribosomes. This system consists of a series of translocases and chaperones in mitochondria that direct and escort precursor proteins (preproteins) to their target subcompartments. Many mitochondrial proteins contain an N-terminal presequence of 15 to 50 amino acids containing an alpha helix with a net positive charge on one face and hydrophobic residues on the other. These features target the protein to the mitochondrial matrix or the MIM (Schulz *et al.* 2015). The presequence normally forms an amphipathic α-helix. Once the presequence is imported to the matrix, the presequence is proteolytically removed by peptidases (Mossmann *et al.* 2012; Teixeira & Glaser 2013). Other mitochondrial proteins contain non-cleavable targeting signals that reside in internal positions of the proteins (Chacinska *et al.* 2009). These targeting signals are not removed upon import.

Most mitochondrial preproteins interact with the translocase of the outer membrane (TOM) complex where they are translocated across the MOM (Becker *et al.* 2012; Dudek *et al.* 2013; Wenz *et al.* 2015b). Tom40 is the major component of the actual import pore of the TOM complex. Tom40 has a β-barrel structure (Gessmann *et al.* 2011; Lackey *et al.* 2014; Mager *et al.* 2011; Zeth 2010). Recent data shows that Tom40 forms a trimeric complex with Tom22 (3×Tom40-3×Tom22), another component of the TOM complex, and other small Tom proteins, during preprotein translocation through the TOM complex (Shiota *et al.* 2015).

The MOM also harbors another type of protein import machinery called the SAM (sorting and assembly machinery) complex. This complex serves as an insertase

for assembling precursors of β-barrel proteins into the MOM. Once β-barrel precursors have been translocated across the MOM via the TOM complex into the IMS, they are chaperoned by the small Tim (translocase of the inner membrane) proteins (Klein *et al.* 2012; Kutik *et al.* 2008) to the SAM complex. Thus, insertion of these proteins into the MOM occurs from the IMS side. Recent findings suggest that the TOM and SAM complexes form a supercomplex via interactions between Tom22 and Sam37 (Qiu *et al.* 2013; Wenz *et al.* 2015a; Wenz *et al.* 2014), which are subunits of the TOM and SAM complexes, respectively. The supercomplex promotes the assembly of β-barrel proteins. Mic60, a component of the MICOS complex, also interacts with the TOM and SAM complexes to facilitate the import of β-barrel proteins (Horvath *et al.* 2015; Wenz *et al.* 2015b). A third complex in the MOM is the MIM complex. This complex is involved in insertion of MOM proteins with single or multiple transmembrane helices from the cytosolic side of the membrane (Becker *et al.* 2008; Becker *et al.* 2011; Papic *et al.* 2011).

Many proteins targeted to the IMS contain an internal IMS-targeting signal that features either a twin Cys-X_3-Cys or a twin Cys-X_9-Cys motif (Milenkovic *et al.* 2009; Sideris *et al.* 2009). These proteins are imported via the MIA (mitochondrial IMS import and assembly machinery) system (Chacinska *et al.* 2004). The Mia40 protein of the MIA system forms transient disulfide bonds with the reduced precursor proteins, ultimately oxidizing them to assist their folding. The sulfhydryl oxidase Erv1 then reoxidizes Mia40 to enable a new cycle of reduced precursor protein oxidation (Hell 2008; Riemer *et al.* 2011). Mic60 also plays a role in the MIA system

by mediating the interaction between Tom40 and Mia40 to promote the import of IMS precursor proteins (von der Malsburg *et al.* 2011). Not only does Mia40 support IMS protein import, but it has also been shown to promote the import of Atp23, a protease that is targeted to the MIM (Weckbecker *et al.* 2012), and Mrp10, a component of the mitochondrial ribosome that is targeted to the mitochondrial matrix (Longen *et al.* 2014), in *Saccharomyces cerevisiae*.

After translocation through the MOM via the TOM complex, precursor proteins with presequences are transported through the MIM via the TIM23 (translocase of the inner membrane 23) complex (Mokranjac & Neupert 2010; Schulz *et al.* 2015; Wenz *et al.* 2015b). The translocation requires the membrane potential across the MIM (Malhotra *et al.* 2013; Martinez-Caballero *et al.* 2007). Another driving force is provided by the PAM (presequence translocase-associated import motor) complex, which includes the ATP-dependent mitochondrial Hsp70 (heat-shock protein 70) (Wenz *et al.* 2015b). Precursor proteins that are targeted to the matrix are recognized by the MPP (mitochondrial processing peptidase), which cleaves their targeting signal presequence (Teixeira & Glaser 2013).

Some preproteins are released into the MIM laterally by the TIM23 complex and therefore are not targeted to the matrix (Botelho *et al.* 2011; Popov-Celeketic *et al.* 2011). These proteins contain a stop-transfer signal that resides C-terminal to presequences (Schulz *et al.* 2015). Release into the MIM was recently shown to be regulated by Mgr2 (mitochondria genome required 2) (Ieva *et al.* 2014), a small subunit of the TIM23 complex. Some preproteins targeted to the MIM use a different

import pathway. This involves transient translocation into the matrix by the TIM23 complex, and then insertion into the MIM from the matrix side by the OXA (oxidase assembly translocase 1) machinery (Saller *et al.* 2012). The OXA is also required for integrating some of the mtDNA-encoded proteins into the MIM (Hennon *et al.* 2015; Horvath *et al.* 2015; Neupert 2015).

Another large complex in the MIM is the TIM22 complex, which is responsible for insertion of a large class of carrier proteins into the MIM. The substrates of the TIM22 complex do not possess an N-terminal presequence but do contain several hydrophobic transmembrane domains. After translocation through the MOM via the TOM complex, the precursors of these proteins are guided by the small Tims in the IMS to the TIM22 complex where they are inserted into the MIM with the need of membrane potential (Becker *et al.* 2012; Wenz *et al.* 2015b). Interestingly, one of the subunits of the TIM22 complex, Sdh3 (Gebert *et al.* 2011), is also a subunit of Complex II, suggesting a possible connection between respiration and protein import.

1.6 Mitochondria and human diseases

Because mitochondria are involved in many important cell functions, compromised mitochondria often associate with complex human diseases. Mutations in mtDNA can directly affect subunits of the OXPHOS complexes, which lead to disease phenotypes in humans. For instance, mtDNA mutations in genes that encode subunits of Complex I can cause Leber's hereditary optic neuropathy (LHON),

mitochondrial encephalopathy with lactic acidosis and stroke-like episodes (MELAS), and Leigh syndrome (Ylikallio & Suomalainen 2012). Mutations affecting tRNA genes encoded in mtDNA have been shown to give rise to diseases such as myoclonus epilepsy and ragged red fibres (MERRF) and MELAS (Schon *et al.* 2012). A large-scale deletion in mtDNA (more than 1 kbp) can cause one of the following diseases: Pearson syndrome, Kearns-Sayre syndrome (KSS), or chronic progressive external ophthalmoplegia (CPEO) (Pinto & Moraes 2014).

Some diseases are caused by mutations in nuclear genes that are involved in mtDNA functions. Mutations affecting the nuclear encoded Pol γ (mtDNA polymerase) and TWINKLE (mtDNA helicase) significantly compromise mtDNA replication and associate with several diseases including Alpers syndrome, mitochondrial recessive ataxia syndrome (MIRAS), Parkinsonism, and progressive external ophthalmoplegia (PEO) (Copeland 2012, 2014; Sarzi *et al.* 2007; Stumpf & Copeland 2011; Stumpf *et al.* 2013; Wanrooij & Falkenberg 2010). Since most mitochondrial proteins are encoded by the nuclear genome, the integrity of the respiratory complexes requires the coordination of expression and assembly of subunits encoded by both mtDNA and nuclear DNA. Therefore, mutations in nuclear genes of the complexes can lead to similar disease phenotypes as found for mtDNA mutations. For instance, some mutations found in the nuclear gene NDUFS1, which encodes a subunit of Complex I, caused Leigh syndrome (Zhu *et al.* 2009).

Apart from OXPHOS dysfunctions, there are also connections between mitochondrial quality control and diseases. For instance, as mentioned above (section

1.2), MFN2 and OPA1 are two key proteins involved in mitochondrial fusion, and mutations affecting their functions cause Charcot Marie Tooth 2A syndrome and dominant optic atrophy (Burte *et al.* 2015; Chen *et al.* 2014a; Escobar-Henriques & Anton 2013; Zorzano & Claret 2015). In addition to mitochondrial fusion, dysfunction in PINK1 (PTEN-induced putative kinase 1)/parkin mediated mitophagy have been implicated in familial early-onset Parkinson's disease (Durcan & Fon 2015; Kazlauskaite & Muqit 2015; Pickrell & Youle 2015). In fact, mitochondrial dysfunction has been associated with the pathogenesis of many human neurodegenerative diseases including Alzheimer's disease, Huntington's disease, and amyotrophic lateral sclerosis. The connections between these diseases and mitochondria have been discussed recently (Cabezas-Opazo *et al.* 2015; Carri *et al.* 2015; Chaturvedi & Flint Beal 2013; Cozzolino *et al.* 2015).

The relationship between ageing and mitochondrial dysfunction in human cells is also intriguing. This is because aged human cells often possess characteristics such as accumulated somatic mtDNA mutations, reduced sETC (standard electron transport chain, see section 1.7) activities, and elevated oxidative stress in mitochondria (Payne & Chinnery 2015; Schon *et al.* 2012; Wang & Hekimi 2015). It is conceivable that ageing is due to the accumulation of mtDNA mutations. This hypothesis was tested in "mutator" mice, which contain homozygous nuclear mutations that affect the proofreading function of the mtDNA polymerase (Kujoth *et al.* 2005; Trifunovic *et al.* 2004). These mice accumulated more somatic mtDNA mutations and had shortened life time. However, the mice did not exhibit elevated

oxidative stress as expected for ageing phenotypes. Moreover, heterozygous mice possessing the same mutations in the mtDNA polymerase had normal lifespan, although the mutation frequency in the heterozygous mice was about 30 times higher than that in the aged wild-type mice (Vermulst *et al.* 2007). These findings suggest that accumulation of mtDNA mutations is not the only factor that accelerates ageing.

Although reduced sETC activities is one of the hallmarks of aged human cells, mutations affecting some nuclear genes which encode components of individual sETC complexes surprisingly extend *Caenorhabditis elegans* lifespan (Chang *et al.* 2015). Knocking down some nuclear genes involved in respiration by RNA interference has also been shown to extend the lifespan in *C. elegans* (Dillin *et al.* 2002; Hamilton *et al.* 2005; Lee *et al.* 2003) and *Drosophila melanogaster* (Copeland *et al.* 2009). The mechanism of how defects in components of the sETC prolong lifespan is not known. One possibility is the activation of the mitochondrial unfolded protein response (UPR^{mt}, see section 1.9.2). However, this suggestion seems unlikely since a recent study, performed in *C. elegans*, showed that activation of the UPR^{mt} did not lead to lifespan extension (Bennett *et al.* 2014).

1.7 The sETC, OXPHOS, and the tricarboxylic acid (TCA) cycle

The mitochondrial sETC, consists of four large enzyme complexes as well as ubiquinone (coenzyme Q) and cytochrome *c*. The sETC and the ATP synthase complex (Complex V) of mitochondria are important apparatuses that are involved in ATP production (Fig. 1.2). They are predominantly located in the cristae membrane

Figure 1.2. Schematic of ETC and OXPHOS. Complex I and II oxidize NADH + H^+ and $FADH_2$, respectively, and transfer electrons (direction of flow is indicated black arrows) to ubiquinone, reducing it to ubiquinol. Complex III removes electrons from ubiquinol and relays them to cytochrome *c*. Finally, Complex IV removes electrons from cytochrome *c* and combines them with protons and molecular oxygen to form water. Complexes I, III, and IV contribute to proton pumping (blue arrows) which results in the formation of a proton gradient across the MIM. The number of protons pumped by Complex I, III, and IV shown on the figure is based on transfer of pairs of electrons. Complex V harnesses the gradient (orange arrow) to produce bioenergy by converting ADP and phosphate to ATP. The F_1, F_0 domains, central and peripheral stalk of Complex V are indicated. These complexes are located in the MIM and their orientations are shown relative to the mitochondrial matrix and the IMS. In some organisms, under certain conditions, there is an alternative respiration pathway where electrons from ubiquinol are extracted by the alternative oxidase (AOX) (section 1.10). AOX also reduces oxygen to water but does not pump protons.

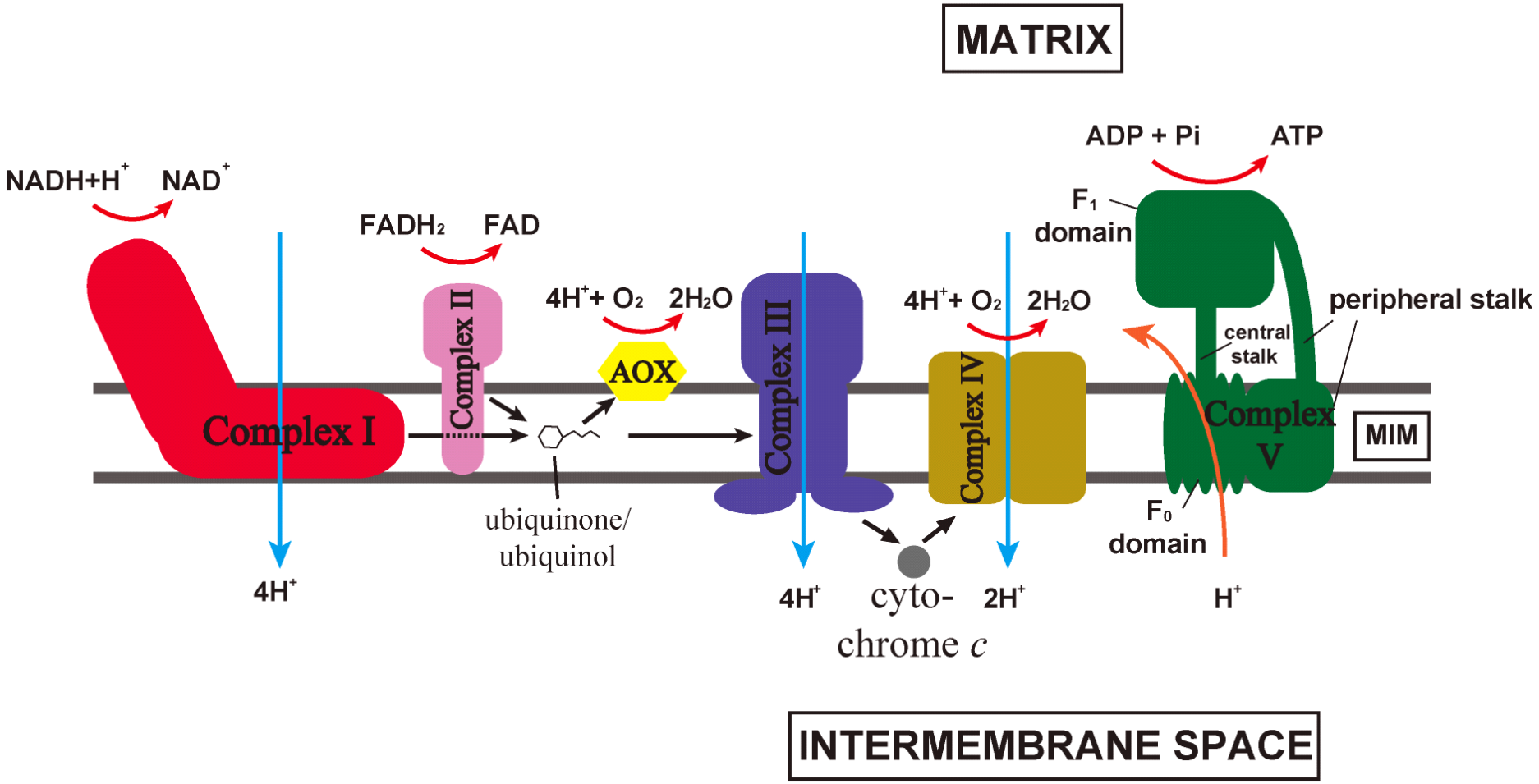
MATRIX
NADH+H+
NAD+
FADH2
FAD
ADP + Pi
ATP
F1
domain
peripheral stalk
central
stalk
4H+ + O2
2H2O
4H+ + O2
2H2O
Complex I
Complex II
AOX
Complex III
Complex IV
Complex
V
MIM
ubiquinone/
ubiquinol
F0
domain
4H+
4H+
cyto-
chrome c
2H+
H+
INTERMEMBRANE SPACE

(Vogel *et al.* 2006). Reduced nicotinamide adenine dinucleotide (NADH + H^+) is oxidized by Complex I (NADH:ubiquinone oxidoreductase) and the electrons are passed to ubiquinone. This also results in the pumping of protons from the mitochondrial matrix to the IMS. Complex II (succinate:ubiquinone oxidoreductase), which contains an FAD (flavin adenine dinucleotide) prosthetic group, also contributes to electron transport by oxidizing succinate to fumurate and reducing ubiquinone to ubiquinol. However, it does not participate in proton pumping. Ubiquinol is oxidized by Complex III (ubiquinol:cytochrome *c* oxidoreductase) and the electrons are passed to cytochrome *c*. This is coupled to proton translocation to the IMS by Complex III. Electrons are then transferred from cytochrome *c* to Complex IV (cytochrome *c* oxidase). Complex IV is the final complex in the sETC. It uses the electrons to reduce oxygen to water and also transfers protons to the IMS from the mitochondrial matrix (Sun *et al.* 2013).

1.7.1 Complexes I, II, III, IV, and V

Complex I is the first and largest enzyme in the sETC. In *Bos taurus*, Complex I from heart mitochondria is composed of 45 proteins (Carroll *et al.* 2006). Most of these are accessory subunits and only 14 are core subunits. The latter are conserved in both prokaryotes and eukaryotes and play significant roles in energy transduction. The accessory subunits are thought to be involved in assembly of the Complex and in protection from oxidative stress (Hirst 2011; Kmita & Zickermann 2013). The crystal structure of eukaryotic Complex I was recently determined from

Yarrowia lipolytica (Zickermann *et al.* 2015). It was found to be an L-shaped enzyme composed of a peripheral domain (hydrophilic) and a membrane domain (hydrophobic). The peripheral domain extends to the mitochondrial matrix and contains seven of the 14 core subunits. The peripheral domain also contains an FMN (flavin mononucleotide) and eight iron-sulfur (Fe-S) clusters. The Fe-S cluster that is closest to the MIM is named N2 and is the one that actually reduces ubiquinone (Hunte *et al.* 2010). The membrane domain contains the remaining seven core subunits. Unlike other core subunits in Complex I, these seven core subunits are encoded by the mitochondrial genome (Hirst 2013). Three of the subunits, ND2 (NADH dehydrogenase 2), ND4, and ND5, are structurally similar and belong to the multiple resistance and pH adaptation (Mrp) Na^+/H^+ antiporter family, making them strong candidates for proton translocation (Moparthi *et al.* 2014; Moparthi *et al.* 2011). Between the peripheral domain and the ND1 in the membrane domain, there is a small chamber that is thought to be an entry path to the Fe-S cluster N2 (Hirst 2013; Tocilescu *et al.* 2007). This chamber is suspected to be the binding site for the hydrophobic ubiquinone headgroup.

Not only is Complex II a component of the sETC, but it is also an enzyme involved in the TCA cycle where it catalyzes the conversion of succinate to fumarate. The crystal structure of Complex II has been determined from *Escherichia coli*, porcine heart, and chicken (Huang *et al.* 2006; Sun *et al.* 2005; Yankovskaya *et al.* 2003). In eukaryotes, Complex II is composed of two hydrophilic subunits, a flavoprotein and an iron-sulfur protein, both of which are located in the mitochondrial

matrix; and two hydrophobic subunits that are embedded in the MIM. The flavoprotein covalently binds an FAD whereas the iron-sulfur protein contains three different iron-sulfur clusters. The hydrophilic subunits are both required to convert succinate to fumarate and transfer electrons to ubiquinone, which is reduced within the hydrophobic subunits. There are two ubiquinone binding sites in the hydrophobic subunits of Complex II. One of them is close to the iron-sulfur clusters (and also close to the mitochondrial matrix) and this is thought to be the primary site of ubiquinone reduction (Sun *et al.* 2005). The second binding site is distal from the mitochondrial matrix and the ubiquinone that binds to the site probably accepts electrons from a *b*-type heme bound to the hydrophobic subunits.

Complex III transfers electrons from ubiquinol to cytochrome *c*. The crystal structure from several organisms revealed that Complex III exists as a homodimer (Berry *et al.* 2010; Esser *et al.* 2008; Gao *et al.* 2002; Huang *et al.* 2005; Hunte *et al.* 2000; Iwata *et al.* 1998; Xia *et al.* 1997; Zhang *et al.* 1998). In bovine heart, each Complex III monomer contains 11 subunits and two *b*-type hemes (b_L and b_H), one *c*-type heme (c_1), and a Rieske Fe-S protein containing one 2Fe-2S cluster. Interestingly, there are two quinone binding sites (Q_o and Q_i) in Complex III. Two electrons from a ubiquinol entering the Q_o site, which is close to the IMS, are separated. One of them proceeds to the Rieske Fe-S cluster, heme c_1, and ultimately cytochrome *c*, while the other is handed over to heme b_L and b_H and then transferred to a ubiquinone or semiubiquinone that is in the Q_i site (Sarewicz & Osyczka 2015). Meanwhile, protons are released to the IMS at the Q_o site, but ubiquinone or

semiubiquinone at the Q_i site accepts protons from the mitochondrial matrix. However, the four Q sites in the dimer are not isolated from each other. Rather, they are proposed to constitute an H-shaped electron-transfer system (Swierczek *et al.* 2010), in which an electron-transfer bridge between two heme b_Ls in a dimer is postulated to be able to transfer electrons from one monomer to the other. This was based on the study of cytochrome *b* gene in *Rhodobacter capsulatus*. Two identical cytochrome *b* genes were fused in the cells and hence mimicked a Complex III dimer. When one of the four Q sites was removed from the modified cytochrome *b* gene, the reduction rate of cytochrome *c* was only slightly reduced when compared to the duplicated cytochrome *b* without any Q sites removed (Swierczek *et al.* 2010). When one of the two Q sites in a wild-type cytochrome *b* was removed, almost no reduction of cytochrome *c* was detected (Swierczek *et al.* 2010).

Crystal structures of Complex IV revealed that it is comprised of Cu_A, heme *a*, and a binuclear complex which includes heme a_3 and Cu_B (Iwata *et al.* 1995; Ostermeier *et al.* 1997; Svensson-Ek *et al.* 2002; Tsukihara *et al.* 1996; Yoshikawa *et al.* 1998). The Cu_A contains two copper atoms whereas the Cu_B contains one (Nelson & Cox 2013). In bovine heart mitochondria, the crystallographic data revealed that Complex IV had a dimeric structure and each monomer contained 13 subunits (Tsukihara *et al.* 1996). Electrons from cytochrome *c* are passed to Cu_A, then to heme *a*, and ultimately end up in the binuclear complex where water is produced.

The protons pumped into the IMS by Complex I, III, and IV generate a proton electrochemical gradient across the MIM. The energy in the gradient is

harvested by Complex V, an ATP synthase. Complex V has a catalytic F_1 domain and a membrane-bound motor F_0 domain connected by a central and a peripheral stalk, as shown by crystal structures (Fig. 1.2) (Abrahams *et al.* 1994; Dickson *et al.* 2006; Gibbons *et al.* 2000; Rastogi & Girvin 1999; Stock *et al.* 1999). The function of these domains was recently reviewed by Walker (2013). The F_0 domain contains an oligomeric ring named the c-ring. The number of subunits in the c-ring varies in different species (Stock *et al.* 1999; Watt *et al.* 2010). Proton passage through the F_0 domain causes rotation of the c-ring. The F_1 domain is composed of three α-subunits and three β-subunits. The arrangement of alternate α-subunits and β-subunits forms a ring structure. These six subunits are organized around the central stalk which follows the rotation of the c-ring and changes the conformation of β-subunits. Synthesis of ATPs only occurs in β-subunits and α-subunits do not seem to be involved in the catalytic process. One ATP molecule is synthesized in every 120° step of the rotation of the central stalk following proton influx to the mitochondrial matrix (Yasuda *et al.* 2001). The possible role of the peripheral stalk, which connects on one side of the F_1 and F_0 domains, is thought to assist the F_1 domain in resisting the rotational torque of the rotor (Rees *et al.* 2009).

1.7.2 Respiratory supercomplexes

Complexes I, III, and IV of the sETC can be organized to form supercomplexes in which two or three complexes associate with each other (Cruciat *et al.* 2000; Schagger & Pfeiffer 2000). Based on the recently proposed plasticity model

(Acin-Perez & Enriquez 2014), the single respiratory complexes can either diffuse freely or assemble into supercomplexes, depending on the environment that the cell is exposed to. This model appears to be becoming well accepted (Porras & Bai 2015). Various supercomplexes have been identified with different make-up. These include one Complex I with two Complex IIIs; one Complex I with two Complex IIIs plus up to four Complex IVs; and two Complex IIIs with up to two Complex IVs (Eubel *et al.* 2003; Heinemeyer *et al.* 2007; Schagger & Pfeiffer 2000; Vartak *et al.* 2013). It has been proposed that the supercomplex I-III_2 may serve as a platform for the formation of the supercomplex I-III_2-IV_n. In addition, Complex I in the supercomplex I-III_2 is more stable than its freely diffusing form (Vartak *et al.* 2013). In rare cases, Complex II may also associate with supercomplexes. Conceivably, formation of supercomplexes facilitates the channeling of electrons between complexes and increases electron flux rate. Indeed, cryo electron microscopy experiments have shown that the distance between the quinol binding sites in Complex I and III and the cytochrome *c* binding sites of Complex III and IV are very short (13 nm and 10 nm, respectively) when the Complexes are in supercomplexes (Althoff *et al.* 2011; Dudkina *et al.* 2011). In addition, the generation of reactive oxygen species (ROS, see section 1.9.1) is also attenuated in supercomplexes (Ghelli *et al.* 2013; Maranzana *et al.* 2013). A recent study proposed that the assembly of various supercomplexes depends on two ubiquinone/ubiquinol pools, one derived from NADH, and the other from $FADH_2$ (Lapuente-Brun *et al.* 2013). This proposal was based on the observation of changes in the electron flux in response to different carbon substrates. However,

this point of view was challenged by Blaza *et al.* (Blaza *et al.* 2014).

Although Complex V is not part of the supercomplexes, many studies show that Complex V has a dimeric structure (Arnold *et al.* 1998; Brunner *et al.* 2002). The function of the dimeric Complex V is largely unknown, but because the dimerized form was found to cluster in the apex of cristae membranes (Strauss *et al.* 2008), it was suggested that the dimeric Complex V shapes the cristae membranes by inducing membrane curvature (Davies *et al.* 2012).

1.7.3 TCA cycle

In addition to producing ATP as an energy source for the cell via OXPHOS, the mitochondrion is also a metabolic hub of the cell because it harbors the TCA cycle (also known as the citric acid cycle or Krebs cycle). The role of the TCA cycle in metabolism was recently reviewed by Akram (Akram 2014). Pyruvate, the end product of glycolysis, enters the TCA cycle via conversion into acetyl-CoA, which is then condensed with oxaloacetate to form citrate. At the completion of the cycle, citrate is converted back to oxaloacetate and oxaloacetate reacts with acetyl-CoA to begin the cycle again. The consumption of each acetyl-CoA in the cycle gives rise to 3 NADH, 1 $FADH_2$, and 1 GTP. NADH and $FADH_2$ are oxidized by the sETC to generate ATP. In addition to feeding the ETC, some of the intermediates of the TCA cycle are precursors for synthesizing amino acids and nucleic acids (Akram 2014).

1.8 Retrograde regulation

The term “retrograde regulation” is used to describe the signaling events from mitochondria to the nucleus. Signals generated from poorly functioning mitochondria are conveyed to the nucleus resulting in altered expression of some nuclear-encoded genes. The term was first proposed in 1993 when Liao et al. studied the expression of two citrate synthases in ρ^0 petites (cells devoid of mtDNA) in *S. cerevisiae* (Fig. 1.3). It was found that the expression of CIT2, which encodes a peroxisomal citrate synthase, was greatly increased in ρ^0 cells (Liao & Butow 1993; Liao *et al.* 1991). A genetic screen revealed that CIT2 expression in ρ^0 cells required the function of at least three genes RTG1 (retrograde 1), RTG2, and RTG3 (Jia *et al.* 1997; Liao & Butow 1993; Rothermel *et al.* 1997). Both RTG1 and RTG3 encode basic helix-loop-helix leucine zipper transcription factors. They localize to the cytoplasm in ρ^+ wild-type cells but are translocated to the nucleus when mitochondria are dysfunctional, such as in ρ^0 cells. The translocation requires dephosphorylation of Rtg3p and was shown to be dependent on Rtg2p (Sekito *et al.* 2000).

Further work, most notably genetic screens for mutants that could activate the RTG response in the absence of Rtg2p, revealed that the system was more complicated, involving several additional proteins (Fig. 1.3). For example, in cells devoid of the Mks1p, the RTG response is constitutively on, and does not require Rtg2p. Under normal conditions, dephosphorylation of Rtg3p is inhibited by Mks1p, itself a phosphoprotein. When the RTG pathway is off, Mks1p is hyperphosphorylated by unknown kinases and binds to the 14-3-3 proteins Bmh1p and Bmh2p. This complex prevents dephosphorylation of Rtg3p by an unknown mechanism, and

Figure 1.3. Schematic of the RTG pathway. The RTG pathway shown in the figure applies to yeast cells grown using glucose as the carbon source. Left: In ρ^+ cells, where mtDNA (indicated by red circles) is present in the mitochondrion (top left), Mks1p is hyperphosphorylated (indicated by three yellow ovals) and is bound by the 14-3-3 proteins Bmh1p and Bmh2p. In this form Mks1p inhibits the dephosphorylation of Rtg3p and prevents its translocation to the nucleus with Rtg1p. Lst8p, which is a component of the TORC complex, promotes the hyperphosphorylation of Mks1p. Right: In ρ^0 cells where mtDNA is absent, the defective mitochondrion (top right) sends signals to activate Rtg2p. Mks1p is hypophosphorylated (indicated by a single yellow oval) by unknown mechanisms and binds to Rtg2p. The formation of the Rtg2-Mks1p complex promotes the partial dephosphorylation of Rtg3p and the translocation of both Rtg1p and Rtg3p to the nucleus. The Rtg1p/Rtg3p complex binds to the promoter of the CIT2 gene and activates its transcription. Since Mks1p is hypophosphorylated, Bmh1p and Bmh2p no longer bind to Mks1p. Some excess Mks1p which binds to neither Bmh1p-Bmh2p nor Rtg2p is recognized by Grr1p, a subunit of the E3 ubiquitin ligase complex, and processed for degradation (striped green rectangle).

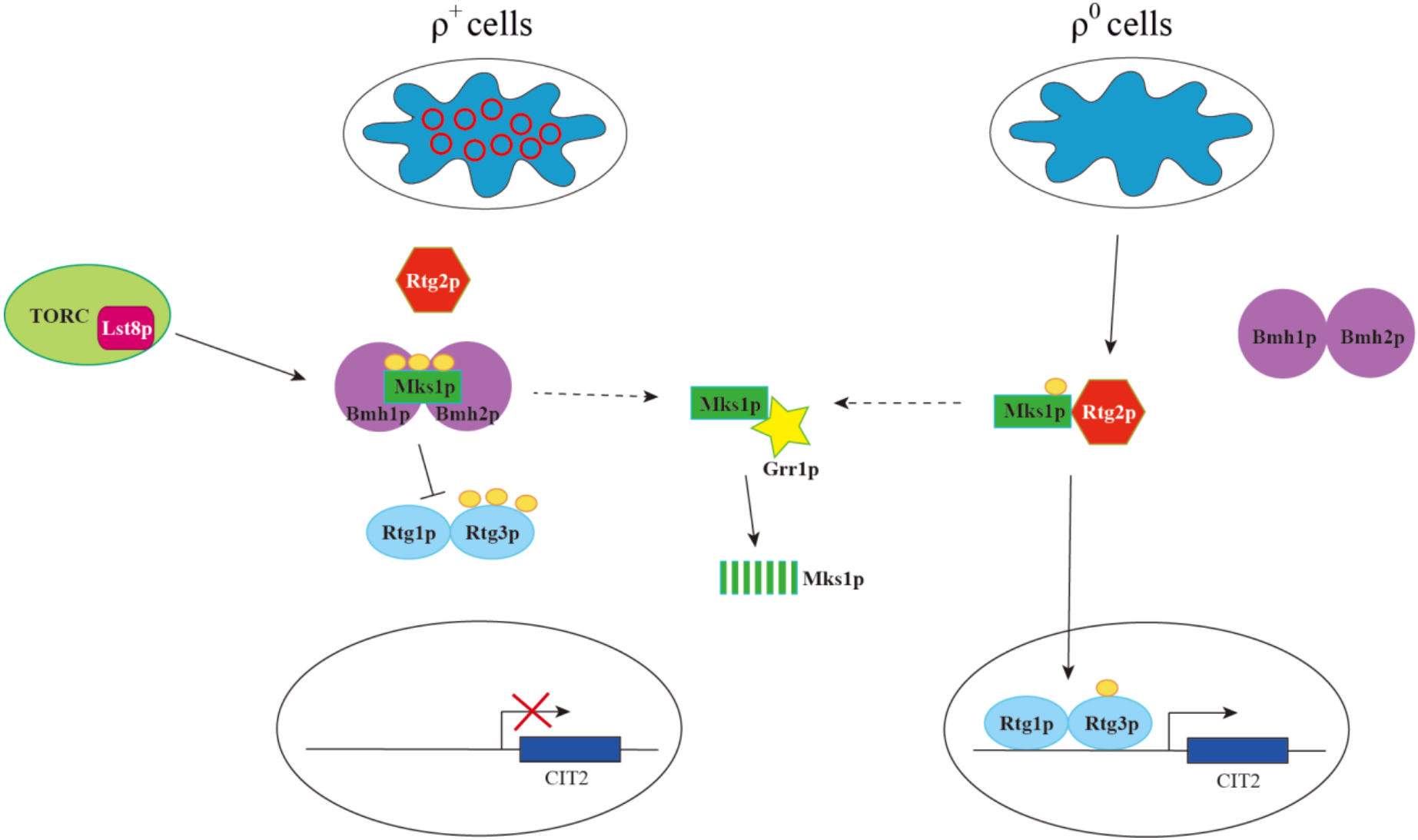
ρ+ cells
ρ0 cells
TORC
Lst8p
Rtg2p
Mks1p
Bmh1p
Bmh2p
Rtg1p
Rtg3p
Grr1p
Mks1p
CIT2
Mks1p
Rtg2p
Bmh1p
Bmh2p
Rtg1p
Rtg3p
CIT2

therefore inhibits Rtg3p nuclear translocation (Liu *et al.* 2003; Liu *et al.* 2005). When the RTG pathway is active, Mks1p is hypophosphorylated and dissociates from the Bmh1p-Bmh2p complex. Instead, it forms a complex with Rtg2p, which inhibits Mks1p and promotes the dephosphorylation of Rtg3p (Sekito *et al.* 2002). Furthermore, the stability of Mks1p is modulated by Grr1p, which is a subunit of the SCF^{Grr1} (Skp1-Cdc53/Cullin-F box protein) E3 ubiquitin ligase complex (Liu *et al.* 2005). It has been shown that the expression of CIT2, the usual indicator of a functional RTG pathway, was increased in dominant GRR1 mutants (Grr1p is hyperactive), which had a Δrtg2 and ρ^+ genetic background, as compared to wild-type cells (Liu *et al.* 2005). The effect is mediated by Mks1p degradation by hyperactive Grr1p. Mks1p was also degraded in Δrtg2 cells expressing loss-of-function *bmh1* and wild-type GRR1 (Liu *et al.* 2005). Therefore, Grr1p facilitates the removal of Mks1p that is not bound to a partner protein (either Rtg2p or the Bmh1p-Bmh2p complex).

Lst8p, a seven WD40-repeat protein, negatively regulates the RTG pathway, as *lst8* mutants restored CIT2 expression when RTG2 was deleted (Liu *et al.* 2001). It was also shown to be a component of TORC1 (target of rapamycin complex 1). Thus, Lst8p links TOR pathways to the regulation of the RTG pathway (Giannattasio *et al.* 2005) (Fig. 1.3). The TOR pathway was found in yeast mutants that showed resistance to rapamycin, an antifungal drug (Conrad *et al.* 2014; Loewith & Hall 2011). TOR regulates cell growth in response to alteration of nutrients. Mks1p has been shown to be one of the downstream targets of TOR (Dilova *et al.* 2004; Dilova *et al.* 2002), as inhibition of TOR by rapamycin caused dephosphorylation of Mks1p. Thus, TOR

indirectly affects the translocation of Rtg1/3p (Dilova *et al.* 2004; Komeili *et al.* 2000). In addition to the TOR pathway, RAS2 (resistance to audiogenic seizures 2, the yeast homologue of the RAS proto-oncogene) also regulates the RTG pathway since in *ras2* mitochondrial petite cells the expression of CIT2 is dramatically reduced (Kirchman *et al.* 1999).

Initial genetic screening showed that *rtg1*, *rtg2* and *rtg3* deletion mutants were also glutamate auxotrophs in ρ^+ cells grown on glucose medium. Growth of yeast cells on glucose does not require respiration and leads to glucose repression of several genes encoding mitochondrial proteins (Jia *et al.* 1997; Liao & Butow 1993), However, *rtg* deletion mutants were no longer glutamate auxotrophs in ρ^+ cells grown on medium that required respiration (Liu & Butow 1999). This is because under conditions of respiratory chain activation Hap2-5p, a heteromeric transcriptional complex that is involved in respiratory metabolism, takes control of the expression of genes involved in the TCA cycle. However, in cells with very low respiratory activity, these genes are controlled by the RTG system. Specifically, RTG genes are required for the normal expression of CIT1, ACO1 (aconitase 1), IDH1 (isocitrate dehydrogenase 1), and IDH2 (Epstein *et al.* 2001; Liu & Butow 1999). These TCA cycle genes encode enzymes that lead to the production of α-ketoglutarate, which can be converted to glutamate by glutamate synthase. Thus, RTG genes are required for the expression of the above TCA cycle genes in ρ^0 cells (unable to respire) regardless of the medium, and in ρ^+ cells on medium that does not require respiration and results in glucose repression.

The RTG pathway has also been shown to be involved in yeast chronological lifespan (CLS, the length of time that yeast cells stay alive without cell divisions, measured in the postdiauxic state of a yeast culture, see Longo *et al.* (2012) for detailed definition) extension, as deletion of RTG genes reduced the CLS of yeast cells (Barros *et al.* 2004; Hashim *et al.* 2014). Rtg1p and Rtg3p have also been shown to be required for cell survival in response to osmostress (Ruiz-Roig *et al.* 2012). In this circumstance, the transcriptional activity and nuclear translocation of the Rtg1/3 complex is regulated by Hog1p (high osmolarity glycerol 1).

1.9 Mitochondrial signaling

1.9.1 ROS-dependent signal transduction

ROS include the superoxide anion (O_2^-), hydrogen peroxide (H_2O_2), and the hydroxyl radical ($OH\cdot$). The mitochondrion is considered to be the main ROS generation site in the cell since, as pairs of electrons flow down the respiratory chain, there is a chance for one-electron reduction taking place. Instead of reducing oxygen to water, the reaction produces superoxide anion radicals (Quinlan *et al.* 2012). Under normal conditions, superoxide is predominantly generated from Complex I. When OXPHOS is inhibited, both Complexes I and III become the contributors to O_2^- production (Quinlan *et al.* 2012). Apart from the respiratory chain, superoxide can also be produced at some other sites within mitochondria such as glycerol 3-phosphate dehydrogenase and 2-oxoglutarate dehydrogenase (see review Brand (2010)). However, these sites are considered as generating less significant amount of

O_2^- than that from Complexes I and III (Holmstrom & Finkel 2014).

Frequently, the O_2^- generated from the ETC is converted to H_2O_2 by superoxide dismutases (SODs). SOD2 (MnSOD) is responsible for the dismutation of O_2^- in the mitochondrial matrix (O_2^- + Mn(III)SOD → Mn(II)SOD + O_2, Mn(II)SOD + O_2^- + $2H^+$ → Mn(III)SOD + H_2O_2), whereas SOD1 (Cu/ZnSOD) eliminates O_2^- in the cytoplasm or mitochondrial IMS (O_2^- + Cu(II)ZnSOD → Cu(I)ZnSOD + O_2, Cu(I)ZnSOD + O_2^- + $2H^+$ → Cu(II)ZnSOD + H_2O_2) (Fukai & Ushio-Fukai 2011). A few ROS scavengers are able to reduce H_2O_2 to water. They include glutathione peroxidases (GPXs), peroxiredoxins (PRXs), and catalase (Reczek & Chandel 2015; Sena & Chandel 2012; Shadel & Horvath 2015). H_2O_2 can further react with iron or copper to produce OH· via the Fenton reaction (Winterbourn 2013).

Although ROS have generally been considered to be harmful products of energy metabolism, much evidence has now implicated ROS in important cell signaling roles (Finkel 2012; Sena & Chandel 2012). Among ROS, H_2O_2 is the primary candidate for being a signaling molecule because it is relatively stable and able to diffuse through biological membranes (Cadenas & Davies 2000). In contrast, O_2^- and OH· have limited diffusion due to their high reactivity, short half-life, and charged nature (Cadenas 2004), though it should be noted that diffusion through the MOM is possible via the voltage-dependent anion channel (VDAC) (Han *et al.* 2003). The main physiological role of H_2O_2 is to oxidize cysteine residues and to convert the thiolate anion (S^-) to the sulfenic form (SO^-) (Cys-SH + H_2O_2 → Cys-SOH + H_2O). In some cases, oxidation by H_2O_2 occurs at the catalytic site of a protein, such as the

cysteine in tyrosine phosphatase (Boivin *et al.* 2010; Karisch *et al.* 2011), and thus can directly affect the function of the protein. Protein modifications by H_2O_2 can often be reversed. This requires the action of glutaredoxins (GRXs) and thioredoxins (TRXs), which reduce the oxidized protein to its functional form (Schieber & Chandel 2014).

One well-studied example where H_2O_2 directly affects transcriptional regulation is the KEAP1 (Kelch-like ECH-associated protein 1) -NRF2 (nuclear factor erythroid 2-related factor 2) pathway. Under normal conditions, mammalian transcription factor NRF2 is constantly targeted for proteasomal degradation due to association with the KEAP1 and CUL3 (E3 ubiquitin ligase cullin 3) proteins (Furukawa & Xiong 2005). Upon exposure to stressed environments such as the presence of H_2O_2, reactive cysteines in KEAP1 are oxidized, leading to the disruption of the KEAP1-CUL3 complex. NRF2 is released from the complex and translocates to the nucleus, resulting in transcription of antioxidant genes such as TRX1, PRX1, and glutathione S-transferase (GST) (D'Autreaux & Toledano 2007; Holmstrom & Finkel 2014; Richardson *et al.* 2015).

1.9.2 Unfolded protein response (UPR)

Mitochondria possess protein quality control systems to maintain protein homeostasis. Molecular chaperones are capable of assisting the folding of polypeptides that have translocated through the protein import machinery (Tatsuta 2009). Misfolded or unfolded proteins in the mitochondrial matrix are recognized by

the ATP-dependent proteases ClpXP and Lon resulting in their degradation (Tatsuta 2009). These processes are part of the mitochondrial quality control (mQC) system. However, when unfolded proteins accumulate in mitochondria due to stresses such as mutations affecting sETC genes that lead to imbalance of protein homeostasis and exceed the capacity of mQC systems, mitochondria will activate the mitochondrial UPR (UPR^{mt}) signaling pathways to alter the expression of various nuclear genes (Jovaisaite *et al.* 2014).

In *C. elegans*, UPR^{mt} is initiated by CLPP-1 which is a protease located in the mitochondrial matrix and cleaves unfolded proteins in stressed mitochondria (Haynes *et al.* 2007) (Fig 1.4A). Inhibitors affecting the activity of CLPP-1 abolish the UPR^{mt}. The cleaved peptides of unfolded proteins are exported to the mitochondrial IMS via an ABC (ATP-binding cassette) transporter named HAF-1 (Haynes *et al.* 2010). How the peptides are exported to the cytosol is not known, but may simply proceed by passive diffusion via VDAC in the MOM. These peptides may be a signal for initiation of the UPR^{mt}. The efflux of peptides is thought to result in the nuclear localization of ZC376.7 (Haynes *et al.* 2010). This protein was later shown to be a leucine zipper transcription factor named ATFS-1 (activating transcription factor associated with stress–1) (Nargund *et al.* 2012). ATFS-1 contains both an N-terminal MTS and a NLS (nuclear localization sequence). Normally, ATFS-1 is preferentially imported into mitochondria (probably because the protein is translated in the vicinity of mitochondria) and degraded by the mitochondrial protease Lon. However, upon UPR^{mt} activation, import into mitochondria is partially impaired, possibly due to the

Figure 1.4. UPR^{mt} in *C. elegans* and mammalian cells. A. The ATFS-1 transcription factor plays a central role in the UPR^{mt} in *C. elegans*. Unfolded peptides (red twisted threads) are fragmented by the CLPP-1 protease. The fragments (short red bars) are exported to the IMS by HAF-1. The release of peptides into the cytoplasm, presumably by passive diffusion via VDAC in the MOM, prevents ATFS-1 from being imported into the mitochondria where ATFS-1 is degraded by the Lon mitochondrial protease. Instead, ATFS-1 is translocated from the cytoplasm to the nucleus. UBL-5 and DVE-1 are also imported to the nucleus under conditions of mitochondrial stress. These three proteins coordinate to drive the expression of mitochondrial chaperones. B. One possible pathway of the UPR^{mt} in mammalian cells is via the JNK signaling pathway. C-Jun is activated by JNK2 and binds to the AP1 element of both the CHOP and C/EBPβ promoters. These two proteins subsequently bind to the CHOP site in the promoter region of the Cpn60, Cpn10, ClpP, and mtDnaJ genes and induce their expression. This figure was adapted from Jovaisaite *et al.* (2014).

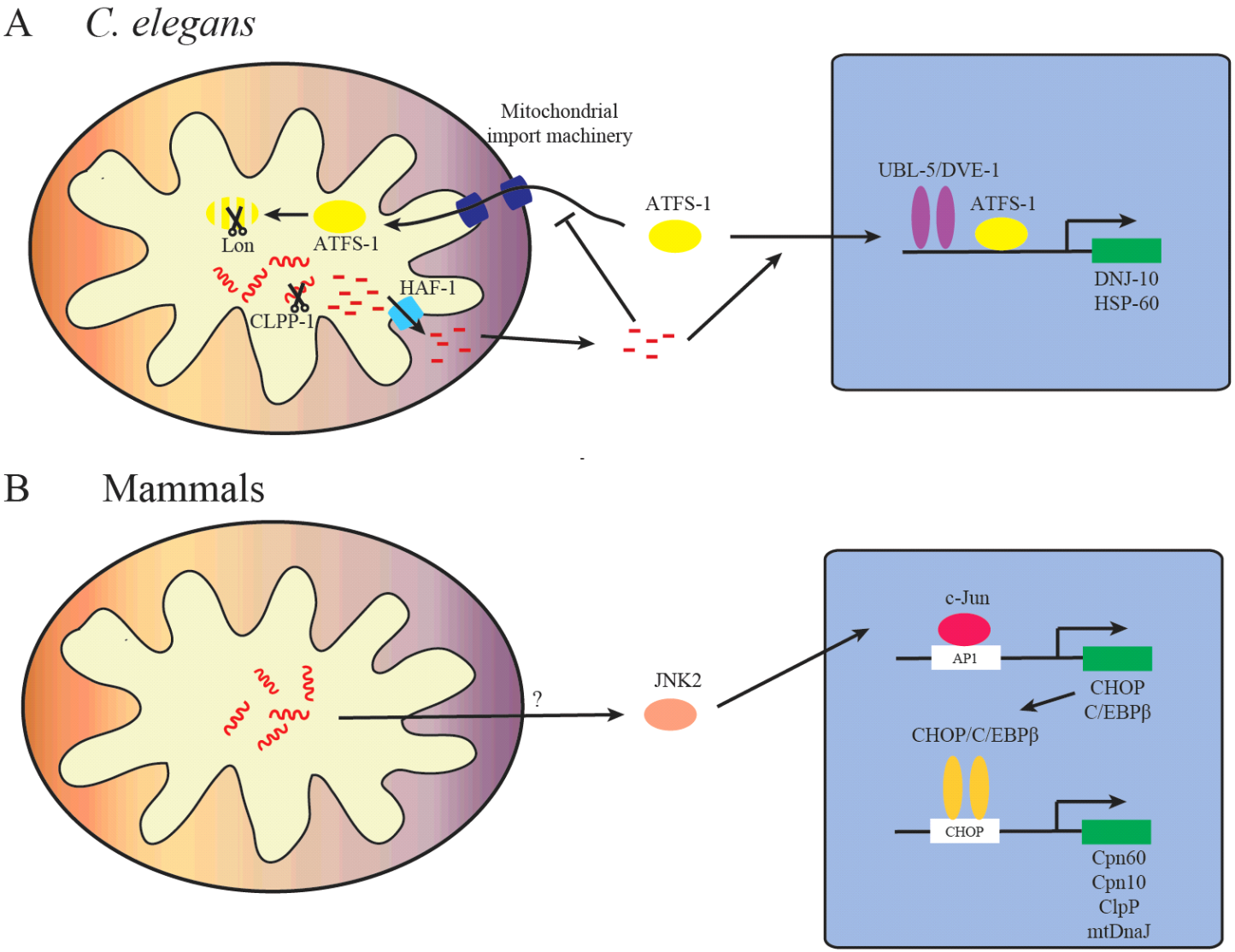
A C. elegans
Mitochondrial
import machinery
Lon
ATFS-1
HAF-1
CLPP-1
ATFS-1
UBL-5/DVE-1
ATFS-1
DNJ-10
HSP-60
B Mammals
?
JNK2
c-Jun
AP1
CHOP
C/EBPβ
CHOP/C/EBPβ
CHOP
Cpn60
Cpn10
ClpP
mtDnaJ

efflux of cleaved peptides. ATFS-1 then translocates into the nucleus where it induces the transcription of genes encoding mitochondrial chaperones such as DNJ-10 and HSP-60 (Nargund *et al.* 2012).

Two additional proteins, UBL-5 (ubiquitin-like protein 5) (Benedetti *et al.* 2006) and a homeodomain-containing transcription factor named DVE-1 (Haynes *et al.* 2007), are also involved in UPR^{mt} in *C. elegans*. They both localize to the nucleus in response to mitochondrial stress and form a complex to regulate HSP-60 transcription (Benedetti *et al.* 2006; Haynes *et al.* 2007). It is not well understood how the UBL-5/DVE-1 complex coordinates with ATFS-1, but because the mammalian homologues of DVE-1 (SATB1 and SATB2) are involved in chromatin remodeling (Cai *et al.* 2003; Dobreva *et al.* 2003), it is conceivable that the binding of ATFS-1 to DNA is facilitated by the UBL-5/DVE-1 complex (Jovaisaite *et al.* 2014) (Fig. 1.4A).

In mammalian cells, expression of a truncated version of the mitochondrial matrix protein OTC (ornithine transcarbamylase) that lacks the carbamyl phosphate-binding domain, resulted in transcription of genes encoding molecular chaperones Cpn60 and Cpn10 (homologues of HSP60 and HSP10), ClpP, and mtDnaJ, due to activation of the UPR^{mt} (Zhao *et al.* 2002) (Fig 1.4B). An element in the upstream region of these genes that is recognized by the leucine zipper transcription factor CHOP (C/EBP (CCAAT/enhancer-binding protein)-homologous protein), as well as its binding partner C/EBPβ, has been identified (Zhao *et al.* 2002). Moreover, the CHOP element is also found in the promoters of mitochondrial proteases YME1L1 and MPPβ, the mitochondrial import component Tim17A, a subunit of

Complex I NDUFB2, endonuclease G, and TRX2 (Aldridge *et al.* 2007). These genes were also shown to be upregulated in cells expressing truncated OTC (Aldridge *et al.* 2007). Two additional conserved elements, named mitochondrial unfolded protein response element 1 (MURE1) and MURE2, are also found on both sides of CHOP element in those promoters (Fig. 1.4B) and they have also been shown to be required for activation of the UPR^{mt} (Aldridge *et al.* 2007). Examination of both the CHOP and C/EBPβ promoters revealed a regulatory element called the AP-1 (activator protein-1) binding site (Horibe & Hoogenraad 2007). This binding site is essential for the CHOP-mediated UPR^{mt} in cells expressing truncated OTC. The AP-1 site is occupied by the phosphorylated transcription factor c-Jun and hence transcription is activated (Weiss *et al.* 2003). Because c-Jun is activated by JNK (c-Jun N-terminal kinase) via phosphorylation (Sabapathy 2012), it is conceivable that the UPR^{mt} is mediated by the JNK signaling pathway. In fact, it has been shown that inhibition of the phosphorylation of JNK2, which activates the JNK signaling pathway, abolished the activation of UPR^{mt} induced by the truncated OTC (Horibe & Hoogenraad 2007). The mechanism of how truncated OTC leads to the phosphorylation of JNK2 is yet to be elucidated.

A complementary pathway to the ATFS-1 pathway was discovered recently in *C. elegans*. When mitochondrial dysfunction occurs, the GCN-2 (general control nonderepressible-2) protein inhibits protein translation by altering the phosphorylation of eIF2α (eukaryotic initiation factor 2α) (Baker *et al.* 2012). A similar finding was observed in mammalian systems where truncated OTC induced UPR^{mt} in mouse

intestinal epithelial cells is associated with phosphorylation of eIF2α by PKR (double stranded-RNA-activated protein kinase) (Rath *et al.* 2012). The reason for this may be to limit protein production to alleviate protein folding stress in mitochondria that overwhelms mitochondrial chaperones. In addition to truncated OTC, Papa and Germain (2011) found another UPR^{mt} in breast adenocarcinoma MCF-7 cells which was caused by overexpressing an endonuclease G mutant that lead to aggregates of the protein in the IMS. This stress in the IMS induced phosphorylation of ERα (estrogen receptor α) and hence activated it. Activation of ERα further induced expression of NRF1 and subsequently increased the activity of the proteasome, which alleviated the IMS stress (Papa & Germain 2011).

A general scheme outlining the process of mitochondrial signaling is shown in Fig. 1.5.

1.10 AOX

AOX is a quinol terminal oxidase. It acts in an alternative, cyanide-resistant, respiration pathway. AOX accepts electrons from the ubiquinol pool and converts molecular oxygen to water via a four-electron reduction reaction. Thus, the reaction bypasses the energy coupling sites of Complexes III and IV in the sETC (Vanlerberghe & McIntosh 1997) (Fig 1.1). AOX does not contribute to proton pumping and the lost energy is dissipated as heat. AOX is sensitive to salicylhydroxamic acid and n-propyl gallate (Schonbaum *et al.* 1971; Siedow & Bickett 1981).

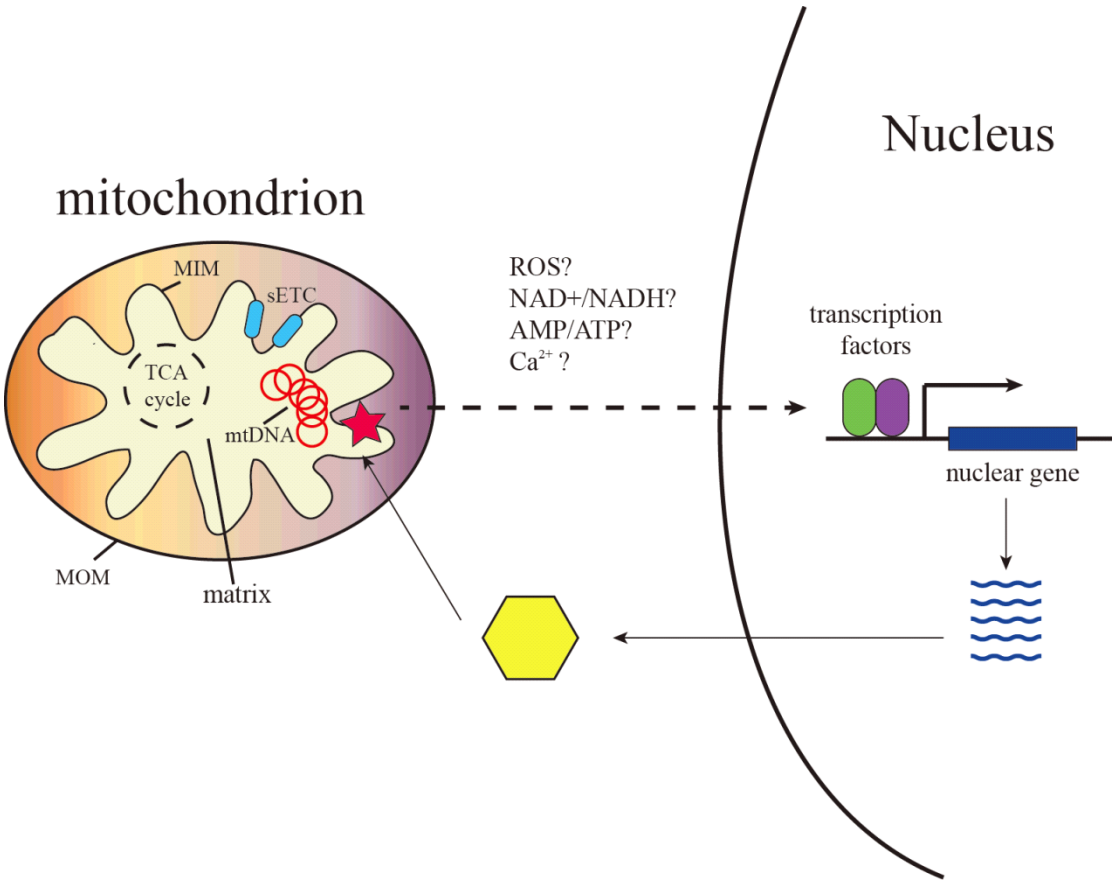

Figure 1.5. Schematic of mitochondrial signaling. Mitochondria house the TCA cycle (dashed circle) and the sETC (blue small rods) in most eukaryotic cells. They contain their own DNA (mtDNA, red circles). When mitochondria are under stress (represented by a red star), such as in the presence of inhibitors of the sETC, mitochondria may produce signals that affect the expression of nuclear genes. This may result in the production of proteins (yellow hexagon) that help alleviate the stress. The signals may include, but are not restricted to: ROS, reduced NAD^+/NADH ratio, increased AMP/ATP ratio, or calcium ions. The signals are thought be directly or indirectly transduced to the nucleus where they alter the expression of certain nuclear genes, possibly via activation of transcription factors (green and purple rods).

1.10.1 Taxonomic distribution of AOX

AOX is widely distributed in the Kingdom Plantae. It also occurs in many fungi, some protists that lack plastids, and several primitive animals which are represented in nine separate phyla (McDonald & Vanlerberghe 2004; McDonald & Vanlerberghe 2006; McDonald *et al.* 2009; Neimanis *et al.* 2013). Examples of animals possessing AOX include *Meloidogyne hapla* (root-knot nematode) and *Ciona intestinalis* (sea squirt) (McDonald *et al.* 2009). However, no vertebrate has been found to contain the enzyme, suggesting it was lost in that lineage.

AOX has also been identified in prokaryotes such as the soil bacterium *Novosphingobium aromaticivorans* (Stenmark & Nordlund 2003). However, AOX is restricted to α-proteobacteria and no other bacterial groups or Archaea have yet been found to encode the protein (McDonald *et al.* 2003; McDonald & Vanlerberghe 2005, 2006). This suggests that the ancient α-proteobacterium that was the ancestor of modern mitochondria probably contained AOX-encoding gene(s) that were subsequently lost in many eukaryotic species (Atteia *et al.* 2004; Finnegan *et al.* 2003).

Interestingly, a separate protein with high sequence similarity to AOX was identified in *Arabidopsis thaliana*. This protein localizes to the thylakoid membrane of plastids and is called plastid terminal oxidase (PTOX) (Carol *et al.* 1999; Wu *et al.* 1999). It branches from the normal electron transport pathway in plastids and reduces O_2 using electrons from plastoquinol. The protein is essential for chloroplast biogenesis and carotenoid biogenesis (McDonald *et al.* 2011). Given that PTOX is

also found in cyanobacteria, and the similarity between PTOX and AOX (McDonald *et al.* 2003), it is conceivable that PTOX and AOX evolved from a common AOX ancestor protein. The genes found in modern eukaryotic genomes probably arose via endosymbiosis of cyanobacteria and α-proteobacteria, respectively (McDonald & Vanlerberghe 2006).

1.10.2 AOX gene families

In eukaryotes, AOX is encoded by a nuclear gene and localizes to the matrix side of the MIM. The first cloning of an AOX gene was in 1991 by Rhoads and McIntosh when screening a cDNA library of *Sauromatum guttatum* (voodoo lily) (Rhoads & McIntosh 1991). Subsequently, AOX has been cloned from many plants and other organisms.

Based on genomic sequences and expressed sequence tag data of AOX genes, it has been shown that there are two AOX subfamilies (AOX1 and AOX2) in angiosperms (Considine *et al.* 2002). The AOX1 subfamiliy is widely found in both monocots and eudicots whereas the AOX2 subfamily is limited to eudicots (Considine *et al.* 2002). It was originally proposed that each subfamily had specific functions since AOX1 was thought to be responsive to oxidative stress while AOX2 was thought to be tissue specific and not stress responsive (Considine *et al.* 2002). However, more recent findings suggest that there are some exceptions to this rule, since the AOX2 in some plants is also induced by stress (Cavalcanti *et al.* 2013; Costa *et al.* 2010). Analysis of genomic sequence from *A. thaliana* revealed a third AOX

subfamily (AOX3) which might be involved in response to chilling stress (Borecky *et al.* 2006). A recent study reclassified the AOX1 and AOX2 subfamilies into four phylogenetic clades (AOX1a, b, c/1e, AOX1d, AOX2a, b, c, and AOX2d) in angiosperms (Costa *et al.* 2014). The AOX2d group includes the aforementioned AOX3 group. They also found that some eudicots have only one of the two subfamilies. The AOX1 and AOX2 subfamilies are also present in some gymnosperms such as Coniferophyta (Frederico *et al.* 2009; Neimanis *et al.* 2013).

Of the fungal species described in the literature, most contain only a single AOX gene (Albury *et al.* 2009; Rogov *et al.* 2014). Exceptions include *Candida albicans* (Huh & Kang 1999, 2001), and *N. crassa* (Tanton *et al.* 2003), which were found to have two AOX gene copies. However, a BLAST search of fungi in recent fungal genomic databases reveals that many species have two or more genes (F. Nargang, unpublished).

1.10.3 Structure of AOX

AOX belongs to the R2-type diiron carboxylate protein family, which includes methanemonooxygenase, ribonucleotide reductase subunit R2, and the stearoyl-ACP Δ^9-desaturase (Berthold *et al.* 2000). To reduce oxygen to water, the diiron center in the AOX protein is required, and ferrous iron is essential for the formation of active AOX (Minagawa *et al.* 1990). Based on the result of modeling, alignments, and mutagenesis studies, a model was proposed for AOX as an interfacial membrane protein with four glutamate and two histidine residues binding the two iron

atoms of the diiron center within a bundle of four α-helices (Andersson & Nordlund 1999; Berthold *et al.* 2000).

Recently, many aspects of the model were confirmed by examination of the crystal structure of a recombinant *Trypanosoma brucei* AOX (rTAO) expressed in *E. coli* (Shiba *et al.* 2013) (Fig. 1.6). The result showed that the rTAO forms a homodimer. In each monomer, there are six long α helices (α1–α6) and four short helices. The four-helical bundle proposed in the above model (Berthold *et al.* 2000) was found to coordinate the diiron center of rTAO and involves helices α2, α3, α5, and α6. Although the two histidine residues predicted to be involved in coordinating the iron atoms do help form the active site, they do not appear to directly bind the iron atoms because they are too distant from the diiron center. The N-terminus is thought to be responsible for dimer formation, since it protrudes from one monomer into the other. The crystallographic data, however, is contradictory to the previous findings that suggested the *T. brucei* AOX exists as a monomer (Chaudhuri *et al.* 2005). In addition, it has been long thought that fungal AOX is monomeric since it has been reported that *Pichia stipites* and *N. crassa* lack AOX dimers (Umbach & Siedow 2000). However, the crystallographic data also show that six amino acids located at the interface between rTAO monomers are highly conserved, suggesting a universal dimeric AOX structure (Moore *et al.* 2013; Shiba *et al.* 2013) .

The crystal structure of rTAO shows a hydrophobic surface containing α1, α4 and part of α2 and α5 (Shiba *et al.* 2013). These regions are thought to interact with one leaflet of the MIM with α1 and α4 being buried in the leaflet. Besides the iron

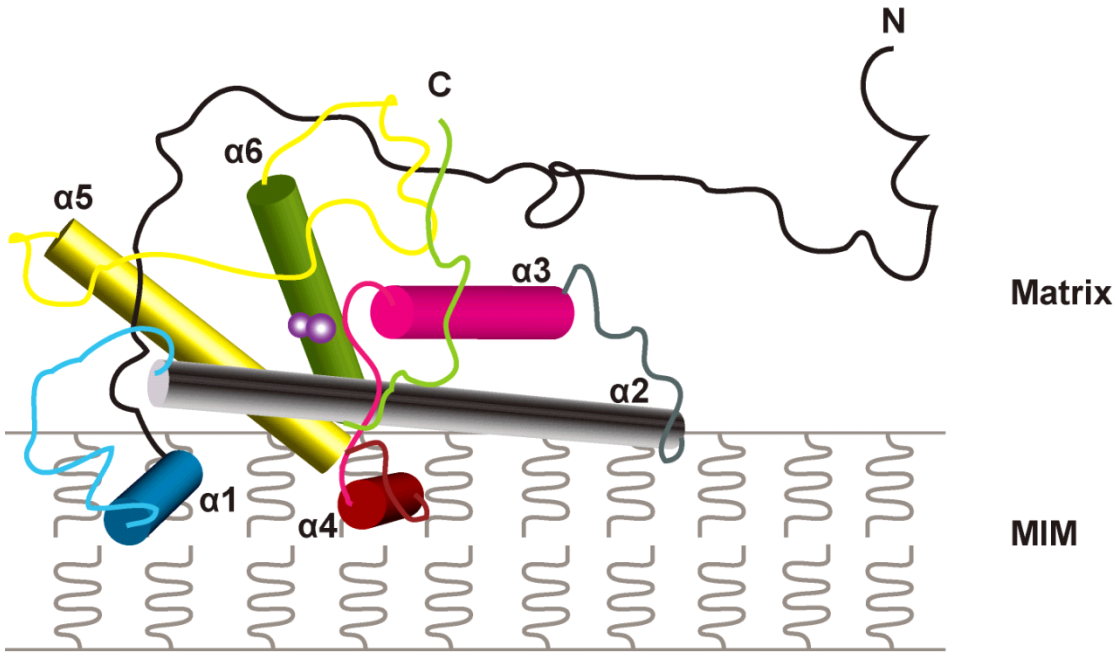

Figure 1.6. Structure of *T. brucei* AOX (rTAO). The rTAO contains six long α-helices and four short helices but only the six long α-helices are shown here. The C-terminal loop following a helix is colored the same as the helix. The N-terminal region of the protein, preceding the α1 helix, is in black. The N- and C- terminus of the rTAO are indicated. Note that the rTAO is dimeric but only one monomer is shown. The N-terminal part extends to the other monomer which is not shown here. The α2, α3, α5, and α6 helices are associated with the diiron (purple circles). The AOX is thought to attach to one leaflet of the MIM by the α1 and α4 helices, which are buried in the MIM. The horizontal lines and squiggles represent the lipid bilayer of the MIM. The figure was adapted from the crystal structure published in Shiba *et al.* (2013).

binding motif, the structure also suggests that tyrosine-122, which is the closest tyrosine to the diiron center, is critical for the catalytic activity (reduction of oxygen to water) of AOX, consistent with previous mutational studies (Albury *et al.* 2002; Nakamura *et al.* 2005). Using protein tunnel visualization software called CAVER (Chovancova *et al.* 2012), three channels that lead to the diiron center were predicted. Two of them were thought to be possible ubiquinol-binding sites based on their size, and the third one was thought to facilitate the transport of oxygen and water (Moore *et al.* 2013).

1.10.4 Functions of AOX

Early studies linked cyanide-insensitive respiration with heat generation in thermogenic plants such as *Arum italicum* and *Sauromatum guttatum* (Meeuse 1975), even though AOX was not characterized at that time. In fact, thermogenesis is critical in some plants that maintain a relatively high temperature in comparison to their surroundings to facilitate volatilization of odors in flowers to attract pollinators (Zhu *et al.* 2011). For example, in floral tissues of the sacred lotus (*Nelumbo nucifera*), the temperature is 16 to 20 ºC higher than the ambient environment during flowering. This floral thermogenesis occurs via increased alternative respiratory activity (Watling *et al.* 2006) and was shown to associate with elevated AOX protein (Grant *et al.* 2008).

However, there are many plants that are not thermogenic. Perhaps the most important function of AOX in these species is to prevent the sETC from

over-reduction and to reduce ROS production by the sETC (Feng *et al.* 2013; Rogov *et al.* 2014; Vanlerberghe 2013). Over-reduction of all or part of the sETC can be caused by inhibition of electron flow from the ubiquinol pool, excess input of reducing equivalents such as NADH, and a high ATP/ADP ratio. For instance, it has been observed that mitochondrial superoxide and nitric oxide (NO) levels were increased in tobacco leaves when AOX was knocked down with RNA interference (Cvetkovska *et al.* 2014; Cvetkovska & Vanlerberghe 2012). The generation of NO by the sETC is likely due to reduction of nitrate by electron leaks from Complexes III and IV (Gupta *et al.* 2011; Igamberdiev *et al.* 2014). The increase in levels of superoxide and NO was also observed in wild-type tobacco cells treated with antimycin A, but was greatly reduced in a transgenic line that overexpressed AOX (Cvetkovska & Vanlerberghe 2013). Therefore, AOX functions to ensure the continuation of electron flow and respiration. In addition, since respiration consumes NADH mostly generated by the TCA cycle, AOX may help allow continuation of the TCA cycle and carbon metabolism for growth and development by increasing oxidation of NADH and replenishing NAD^+ as a substrate for the TCA cycle (Millenaar 2003).

Rapid accumulation of ROS by inhibition of the respiratory chain can lead to programmed cell death (PCD) in plants. Many studies have suggested an important role of AOX in suppression of PCD, since cells lacking AOX become more sensitive to PCD upon treatment with antimycin A, salicylic acid (SA), aluminum, and azide than wild-type cells (Amirsadeghi *et al.* 2006; Li & Xing 2011; Robson &

Vanlerberghe 2002; Vanlerberghe *et al.* 2002). In AOX mutant plant cells that do not express functional AOX, signaling networks that induce antioxidant defense systems such as MnSOD, GPXs, and catalase, are activated under stresses such as low temperature, light, drought (Giraud *et al.* 2008; Watanabe *et al.* 2008), and under normal conditions (Amirsadeghi *et al.* 2006). On the other hand, overexpressing AOX in transgenic tobacco lines did not induce genes encoding antioxidant defense systems in response to ozone exposure, whereas these genes were induced in wild-type cells (Pasqualini *et al.* 2007), suggesting that AOX limits ROS production and thus antioxidant defense systems are not activated. AOX also plays an indispensable role in plants under biotic stress. For instance, it has been shown that transgenic tobacco plants in which AOX is silenced exhibit higher H_2O_2 levels and faster cell death in leaves than wild-type plants when infected by a bacterial pathogen (Zhang *et al.* 2012).

Interestingly, AOX can also be important to certain pathogens. In some fungal pathogens such as *Cryptococcus neoformans* and *Aspergillus fumigatus*, decrease in fungal AOX expression or inhibition of AOX activity by SHAM, greatly reduces the viability of these pathogens in the host (Akhter *et al.* 2003; Magnani *et al.* 2008; Ruiz *et al.* 2011; Thomazella *et al.* 2012). The protective role of AOX in pathogens is likely due to the ability of AOX to allow bypass of the inhibition of their cytochrome respiratory pathway which occurs due to NO generated by the host defense system (Hanqing *et al.* 2010). In African trypanosomes, which cause sleeping sickness, AOX is used as the terminal oxidase (instead of Complex IV) to support

respiration when the pathogen is in its bloodstream form (Chaudhuri *et al.* 2006). Because AOX is not found in the mammalian hosts of trypanosomes, it provides a potential target for therapy of the disease. Consequently, some inhibitors targeting trypanosome AOX have been developed to effectively limit the growth of *T. brucei* in bloodstream cells (Saimoto *et al.* 2013).

1.10.5 Studies of AOX in animal models

Although most species in the animal kingdom have lost AOX during evolution, the potential therapeutic benefit of introducing AOX to compensate for mitochondrial dysfunction is being explored. In 2006, Hakkaart et al. successfully expressed AOX from the ascidian *Ciona intestinalis* (sea squirt) in human embryonic kidney HEK cells (Hakkaart *et al.* 2006). AOX localized to mitochondria and cells expressing the enzyme displayed respiration that was resistant to cyanide. Since then, AOX has been expressed in different types of COX-deficient human cells and was found to restore their growth defects (Dassa *et al.* 2009a; Dassa *et al.* 2009b). However, a recent study showed that the AOX-driven respiration did not function in human cells grown in the presence of high glucose when the cells were treated with antimycin A (Cannino *et al.* 2012). It was suggested that this might have been due to activation of fermentation at high glucose when respiration was inhibited.

Drosophila has also been used as a model to study the role of AOX in OXPHOS deficient cells. Expression of *C. intestinalis* AOX rescued the detrimental phenotypes caused by addition of antimycin A to fly food or by knockdown of various

subunits of Complex IV (Fernandez-Ayala *et al.* 2009; Kemppainen *et al.* 2014b). The fly model was also used to study human diseases that are caused by mitochondrial dysfunction (Chen *et al.* 2014b; Humphrey *et al.* 2012; Kemppainen *et al.* 2014a; Vartiainen *et al.* 2014). For instance, downregulation of the catalytic subunit of mtDNA polymerase in flies results in premature aging and progressive neurodegeneration, but expressing *C. intestinalis* AOX in flies is able to reverse these phenotypes (Humphrey *et al.* 2012). *C. intestinalis* AOX has also been expressed in mice and found to confer cyanide-resistant respiration and limit ROS production (El-Khoury *et al.* 2013). It is of note that the above studies emphasized that the expression of AOX in flies, mice, and human cells appeared not to have deleterious effects on the sETC and OXPHOS functions.

1.10.6 Transcriptional control of AOX genes in plants

AOX is a good model to study mitochondrial retrograde regulation (MRR) since it is encoded in the nuclear genome but localizes to the MIM. Also, in many cases, it is produced in response to mitochondrial dysfunction (Rhoads & Subbaiah 2007), implying that a signal is generated that induces its expression. For instance, it has been shown that inhibition of Complex III by antimycin A in the electron transport chain leads to the increased expression of AOX genes in tobacco, soybean, and *A. thaliana* (Djajanegara *et al.* 2002; Saisho *et al.* 1997; Vanlerberghe & McIntosh 1994, 1996). In maize, there are three AOX paralogues and treatment with antimycin A induces all three AOX genes. However, rotenone induces only the AOX2 gene and

cyanide induces only the AOX3 gene (Karpova *et al.* 2002). Inhibition of ATP synthesis with oligomycin also leads to AOX induction in *A. thaliana* (Saisho *et al.* 2001). In addition to OXPHOS malfunctions, increased levels of citrate (either by supplementation of citrate to the medium or by inhibiting aconitase, the enzyme that converts citrate to isocitrate in the TCA cycle) also induce AOX genes in tobacco (Vanlerberghe & McIntosh 1996) and *Poa annua* (Millenaar *et al.* 2002). Interestingly, since treatment with antimycin A does not cause citrate accumulation (Vanlerberghe & McIntosh 1996), it seems likely that signaling via citrate or antimycin A occur by separate pathways.

Exogenous H_2O_2 treatment has been shown to induce AOX genes in *A. thaliana* (Clifton *et al.* 2005; Ho *et al.* 2008; Vanlerberghe & McIntosh 1996), maize (Polidoros *et al.* 2005), and rice (Feng *et al.* 2010). ROS may serve as signaling molecules in inducing AOX genes since addition of intracellular ROS scavengers weakened the induction by ROS (Feng *et al.* 2010; Maxwell *et al.* 2002). Other molecules found to induce AOX genes in plants include NO, SA, jasmonic acid (JA), and ethylene (Djajanegara *et al.* 2002; Ederli *et al.* 2006; Huang *et al.* 2002; Rhoads & McIntosh 1993). SA, JA, and ethylene are key hormones involved in plant development that are capable of inducing ROS production in plants. The relationship between these plant hormones and ROS production was recently reviewed by Xia *et al.* (2015). NO has a detrimental impact on Complex IV (Hill *et al.* 2010) and thus has the potential to generate ROS. Whether these signaling molecules induce AOX genes by ROS production or by activating other signaling pathways remains to be

elucidated.

It has been shown that AOX transcripts are greatly increased in plants under abiotic stresses such as chilling, drought, high salt, light, and limited nutrients (Feng *et al.* 2013; Vanlerberghe 2013). Some of these stresses induce AOX via a hormone signaling pathway. For instance, it has been shown that inhibition of the production of ethylene abolishes the induction of *AOX1a* under salt stress in *A. thaliana* (Wang *et al.* 2010). However, the exact physiological role that AOX plays under these different abiotic stresses is not well elucidated.

Analysis of the upstream region of AOX genes in soybean identified regions that either positively or negatively regulate AOX gene expression (Thirkettle-Watts *et al.* 2003). In *A. thaliana*, there are five AOX genes (*AtAOX1a-d* and *AtAOX2*) but only *AtAOX1a* is highly expressed in all tissue tested under normal conditions (Thirkettle-Watts *et al.* 2003). Investigation of the promoter of *AtAOX1c*, which is an oxidative stress non-responsive gene, revealed seven sequence elements that were similar to the elements found in soybean (Ho *et al.* 2007). On the other hand, *AtAOX1a* has 10 CAREs (cis-acting regulatory elements) that are responsible for response to oxidative stress within its promoter (Ho *et al.* 2008). One of the CAREs, which is a strong repressor element of the *AtAOX1a*, contains the binding site of the transcription factor ABI4 (abscisic acid insensitive 4) (Koussevitzky *et al.* 2007). Indeed, ABI4 was shown to bind to the CARE by an electrophoretic mobility shift assay (EMSA) and the expression of *AtAOX1a* was significantly increased in an abscisic acid signaling mutant that contains a mutation in the ABI4 gene (Giraud *et al.*

2009). Since ABI4 also has important functions in the plastid retrograde response, it is a critical factor in both mitochondrial and plastid retrograde signaling pathways in plants (Leon *et al.* 2012).

Recently, the role of Trp-Arg-Lys-Thr (WRKY) proteins in the plant MRR has been investigated. WRKY proteins are transcription factors that contain a WRKY amino acid sequence near the N-terminus and a zinc finger motif near the C-terminus (Rushton *et al.* 2010). They are involved in many processes including abscisic acid signaling (Rushton *et al.* 2012). They target a binding motif named the W box (TTGACC/T) (Rushton *et al.* 2010). Three W boxes were found in the promoter of *AtAOX1a* (Dojcinovic *et al.* 2005). One study revealed that the overexpression of AtWRKY15, a ROS-induced transcription factor, repressed the salt-induced expression of *AtAOX1a* (Vanderauwera *et al.* 2012). However, there was no direct evidence that AtWRKY15 was actually bound to the promoter of *AtAOX1a*. A separate study using a yeast one-hybrid system to screen 72 AtWRKY proteins revealed that 12 AtWRKY proteins were able to bind two W boxes of the *AtAOX1a* promoter, although the binding intensity varied (Van Aken *et al.* 2013). An EMSA further confirmed that individual AtWRKY57, AtWRKY63, and AtWRKY75 were able to bind one of the two W boxes tested above (Van Aken *et al.* 2013). Furthermore, among the 12 AtWRKY proteins, it was shown that AtWRKY40 negatively regulated the expression of *AtAOX1a* when cells were treated with antimycin A, or were under high light stress. AtWRKY63 positively regulated the expression of *AtAOX1a* under high light stress (Van Aken *et al.* 2013).

The NAC (no apical meristem/*Arabidopsis* transcription activation factor/ cup-shaped cotyledon) transcription factors (Olsen *et al.* 2005) have been the focus of a recent study of plant MRR. Through a yeast one-hybrid assay, *Arabidopsis* NAC domain-containing protein 13 (ANAC013), ANAC016, ANAC017, ANAC053, and ANAC078 were shown to bind the so-called "mitochondrial dysfunction motif" in the promoter of *AtAOX1a* (De Clercq *et al.* 2013). Only ANAC013 and ANAC017 have been characterized so far (De Clercq *et al.* 2013; Ng *et al.* 2013b). Both proteins localize to both the nucleus and the ER and positively regulate the expression of *AtAOX1a*. The mechanism by which regulation is achieved is not yet well understood.

Apart from transcription factors, a recent genetic screen using a cell line, which harbored an *AtAOX1a* promoter fused to a luciferase reporter gene, to look for regulators of alternative oxidase (*rao* mutants), identified the CDKE1 (cyclin dependent kinase E1) (*rao1*) which positively regulated the expression of *AtAOX1a* when cells were treated with antimycin A (Ng *et al.* 2013a). However, the mechanism of the CDKE1 regulation is unknown. In addition, mutations in four *rao* genes (*rao*3, 4, 5, and 6), which are deficient for auxin transport, resulted in significantly greater induction of *AtAOX1a* in cells treated with antimycin A as compared to wild-type cells (Ivanova *et al.* 2014). Addition of auxin analogues inhibited the induction of *AtAOX1a* caused by antimycin A treatment in the wild-type strain, indicating crosstalk between the auxin signaling pathway and the induction of *AtAOX1a* (Ivanova *et al.* 2014).

1.10.7 Induction of AOX in fungi

Similar to some plants, AOX in three yeast species *C. parapsilosis*, *C. albicans*, and *Debaryomyces occidentalis* is constantly found throughout various growth stages (Veiga *et al.* 2003). As mentioned in section 1.10.2, *C. albicans* possesses two AOX-encoding genes. One of them has been shown to be constitutively expressed, whereas the expression of the other gene is induced when cells are in the early stationary phase of growth. Even greater induction occurs by treatment with drugs such as cyanide and paraquat (Huh & Kang 2001). In *Pichia pastoris*, maximum AOX expression was observed upon glucose depletion when cells enter the stationary phase (Kern *et al.* 2007). Similarly, it has also been shown that AOX is produced upon glucose depletion in stationary phase in *Y. lipolytica* (Medentsev & Akimenko 1999). In addition to growth in stationary phase on glucose, growth utilizing non-fermentable carbon sources such as glycerol and ethanol induces the expression of AOX in *C. albicans* (Huh & Kang 2001).

Since AOX is known to lower the levels of ROS, the induction of AOX under oxidative stress has been widely studied. Addition of H_2O_2 to the medium or treatment with ETC inhibitors such as cyanide or antimycin A has been shown to induce AOX in *C. albicans* (Huh & Kang 2001), *A. fumigatus* (Magnani *et al.* 2007), *A. niger* (Honda *et al.* 2012), *Magnaporthe grisea* (Yukioka *et al.* 1998), *Paracoccidioides brasiliensis* (Martins *et al.* 2011), and *P. anomala* (Minagawa *et al.* 1992). However, induction of AOX by ROS does not seem to occur in all fungal species. For example, addition of H_2O_2 or paraquat to the medium reduces the

transcript levels of AOX in *Podospora anserina* (Borghouts *et al.* 2001). In *A. nidulans*, long-term exposure to menadione, a reagent that decreases the reduced glutathione pool and causes oxidative stress (Ross *et al.* 1985), does not induce the expression of AOX (Pusztahelyi *et al.* 2011). In line with the latter observation, a recent study showed that sensitivity of *A. nidulans* to H_2O_2 or menadione was not altered in a strain that lacked AOX (Suzuki *et al.* 2012).

1.10.8 Post-translational regulation of AOX

As described in section 1.10.3, the crystallographic data showed that rTAO exists as a dimer and indicated that the dimeric structure could be universal to AOX in other species. In plants, an early study showed that AOX existed as a mixture of covalent and non-covalent dimers in soybean (Umbach & Siedow 1993). Two conserved cysteine residues were found at the N-terminus of plant AOX (Vanlerberghe & McIntosh 1997) and they were named CysI and CysII (Berthold *et al.* 2000) (CysI is closer to the N-terminus of the protein). These cysteine residues are conserved in the vast majority of plant AOXs, but rare exceptions are known (see below). Using site-directed mutagenesis to convert the two cysteine residues to alanine in *A. thaliana* AOX (Rhoads *et al.* 1998) and tobacco AOX (Vanlerberghe *et al.* 1998), it was revealed that only CysI is responsible for the formation of a disulfide bond between two monomers. Thus, the covalently joined plant dimer results from a disulfide bond between the CysI residues in two monomers.

The reduced form of plant AOX, which exists as a non-covalently joined

dimer, exhibits higher activity than the oxidized form (Umbach & Siedow 1993). The activity of the reduced form of most plant AOXs increases even further in the presence of α-keto acids such as pyruvate (Millar *et al.* 1993; Vanlerberghe *et al.* 1995). The activation by α-keto acids is dependent on the presence of CysI but CysII also appears to play a minor role. The mechanism of activation is yet to be elucidated. Some plants possess AOXs in which the CysI is substituted by a serine residue but CysII is unchanged (Grant *et al.* 2009; Holtzapffel *et al.* 2003). These AOX isoforms have been shown to be activated by succinate instead of pyruvate. CysII was suggested to be involved in the activation of AOX by glyoxylate when *AtAOX1a* was expressed in *Escherichia coli* (Umbach *et al.* 2002). In contrast, CysI and CysII are absent in fungi, protists, and animals (Moore *et al.* 2013). In fungi such as *N. crassa* and *Y. lipolytica*, it has been shown that AOX is activated by the presence of purine nucleoside 5'-monophosphates (see review McDonald (2008)).

1.10.9 AOX in *N. crassa* and other filamentous fungi

In *N. crassa*, AOX is encoded by the nuclear *aod-1* (alternative oxidase deficient) gene (Li *et al.* 1996). Under normal conditions, the AOX protein is undetectable in cells. However, conditions that reduce the function of the sETC lead to induction of the enzyme (Bertrand *et al.* 1983). For example, growth in the presence of inhibitors of OXPHOS complexes such as antimycin A and cyanide, will induce *aod-1*, as will mutations in mitochondrial or nuclear genes involved in the function or assembly of the sETC (Bertrand *et al.* 1983; Tanton *et al.* 2003). Growth

in the presence of chloramphenicol (CM) which specifically affects mitochondrial translation, and thus the function of OXPHOS complexes containing mtDNA encoded subunits of Complexes I, III, IV, and V, is also an effective inducer of AOX expression (Li *et al.* 1996).

Several years ago, another nuclear gene, *aod-2*, was found to be essential for the induction of AOX (Bertrand *et al.* 1983) and more recently the Nargang lab identified four additional mutants that showed defects in AOX induction. The latter were named *aod-4*, *aod-5*, *aod-6,* and *aod-7* (Descheneau *et al.* 2005). Both *aod-2* and *aod-5* have been shown to encode proteins that belong to the Zn(II) Cys6 binuclear cluster family of fungal transcription factors (Chae *et al.* 2007b). Analysis of their protein sequence predicted that each contained a nuclear localization signal and a possible PAS (Per-Arnt-Sim) domain. Analysis of the promoter of the *aod-1* gene identified an AOX induction motif (AIM) at positions -172 to -184 bp upstream of the translation start site. This sequence was shown to be required for the expression of the enzyme under inducing conditions (Chae *et al.* 2007a). The AIM contains two CGG repeats separated by 7 bp. Tandem CGGs are common binding sites for members of the Zn(II) Cys6 binuclear cluster family of transcription factors (MacPherson *et al.* 2006; Schjerling & Holmberg 1996). EMSA analysis showed that the DNA-binding domains of AOD2 and AOD5 synergistically bound the AIM in a sequence-specific manner (Chae *et al.* 2007b), which suggested that AOD2 and AOD5 may form a heterodimer to activate expression of the *aod-1* gene. Using tagged proteins that contained the DNA binding domains of AOD2 and AOD5, *in vitro* experiments

verified the physical interaction between these two proteins (Chae & Nargang 2009). Quantitative PCR revealed that transcripts of *aod-2* and *aod-5* were not increased when AOX was induced (Chae *et al.* 2007b), indicating that AOD2 and AOD5 are likely to be activated post-translationally.

In addition to induction of AOX, it has been discovered that the homologues of AOD2 and AOD5 in other fungi are involved in the regulation of gluconeogenesis. Rds2p, which is the *S. cerevisiae* homologue of AOD2, binds to the promoter of a number of genes when cells are shifted from medium containing glucose to ethanol (Soontorngun *et al.* 2007). These genes included PEPCK (phosphoenolpyruvate carboxykinase) and FBP (fructose-1,6-bisphosphatase), which catalyze two key steps in gluconeogenesis. Moreover, Rds2p was shown to be phosphorylated by Snf1p, an AMPK (AMP activated protein kinase). Interestingly, Snf1p was also found in a screen of an *N. crassa* knock-out library for strains that were unable to grow in the presence of antimycin A (Nargang *et al.* 2012). This suggests that Snf1p may play a role in the induction of AOX in *N. crassa*. The binding of Rds2p to the yeast genome when cells were shifted from medium containing glucose to glycerol was also investigated (Soontorngun *et al.* 2012). The result showed that Rds2p bound to the promoter of about 150 genes. These genes included PEPCK, FBP, two transcription factors SIP4 and ADR1, as well as HAP4, a subunit of the Hap2/3/4/5 complex involved in regulation of respiration. RDS2 has also been shown to play a critical role in oxidative stress survival in a clinical isolate of *S. cerevisiae* (Diezmann & Dietrich 2011). The *aod-5* homologue in *S. cerevisiae*, ERT1, has also been characterized

using ChIP-chip analysis (Gasmi *et al.* 2014). Similar to Rds2p, Ert1p was detected in the promoter of PEPCK and FBP in cells grown in the presence of ethanol. In addition, Ert1p also binds to the PDC1 (pyruvate decarboxylase 1) promoter and negatively regulates its expression. Because PDC1 is an important enzyme for fermentation, it is conceivable that Ert1p represses the expression of PDC1 when ethanol is used as a sole carbon source.

In *A. nidulans*, two genes AcuM and AcuK, identified in a genetic screen for acetate utilization mutants, are the homologues of *aod-2* and *aod-5*, respectively. They were found to be essential for growth in poor carbon sources because PEPCK and FBP were severely deficient in both mutants (Hynes *et al.* 2007). They have also been shown to bind an AIM sequence upstream of the PEPCK gene (Suzuki *et al.* 2012). In a search for metabolites that induced the PEPCK gene when cells were grown in poor carbon sources, Suzuki *et al.* (2012) found that cells with a deletion of the cytosolic malate dehydrogenase gene showed greater induction the PEPCK gene when grown in the presence of acetate or proline when compared to wild-type cells. However, this induction was abolished when AcuM or AcuK were absent. Because it was conceivable that malate accumulated when the cytosolic malate dehydrogenase was absent in cells grown in acetate or proline, it was suggested that malate might be the metabolite responsible for the induction of the PEPCK gene and the activation of AcuM and/or AcuK in *A. nidulans*. Suzuki *et al.* (2012) also showed that the transcript levels of AOX were increased when cells were grown in the presence of acetate and proline when compared to glucose, and they hypothesized that malate also

induced AOX via activation of AcuM and/or AcuK.

In *A. fumigatus*, in addition to regulating gluconeogenesis, AcuM is also required for iron uptake and high levels of virulence (Liu *et al.* 2010). However, deletion of AcuM in *A. nidulans* does not affect iron acquisition. A recent transcriptome study in *A. fumigatus* revealed that a Δ*acu*K mutant had defects similar to the Δ*acu*M mutant, and both mutants exhibited similar transcriptional profiles during growth outside the host (Pongpom *et al.* 2015). Nevertheless, the study also showed that the deletion mutants had different transcriptional profiles during murine pulmonary infection, indicating that the two proteins may act independently in certain cases.

P. anserina is an unusual fungus in that it has a finite lifespan and cannot be cultured indefinitely. In this organism, increased lifespan is often associated with a deficient sETC. Mutants with an extended lifespan phenotype caused by deficiencies in Complex III or IV, were screened for spontaneous revertants of the extended lifespan. Mutations were found to affect several genes including *rse2* and *rse3* (Sellem *et al.* 2009). These mutants exhibited much higher expression levels of AOX, PEPCK, and FBP than the wild type strain even under normal conditions. The RSE2 and RSE3 proteins were found to be homologues of AOD2 and AOD5, respectively, and the study revealed that the mutants expressed constitutively active RSE2 and RSE3 (Sellem *et al.* 2009). A microarray analysis with these mutants identified several genes that show altered expression in the mutants including PEPCK and FBP (Bovier *et al.* 2014). Metabolome profiling of an *rse2* mutant showed that it was

similar to wild type cells that had been treated with antimycin A.

1.11 Objectives of this study

In *N. crassa*, previous work on AOD2 and AOD5 has focused on *in vitro* biochemical analysis such as EMSA. However, little is known about how they act to induce AOX *in vivo*. Obviously, questions regarding their functions include: What is the subcellular localization of AOD2 and AOD5 under normal conditions? Does the localization change in response to mitochondrial dysfunction? Do they have posttranslational modifications that are associated with the induction of AOX? Therefore, the first goal of this investigation was to investigate the behavior of AOD2 and AOD5 in response to mitochondrial dysfunction *in vivo*. My hypothesis was that, as in the RTG system of yeast (section 1.8), the subcellular localization of the proteins would change in response to a signal(s) from dysfunctional mitochondria. My investigation included determination of the subcellular localization of AOD2 and AOD5 under normal and AOX-inducing conditions. This would allow me to differentiate between two major hypotheses (Chae & Nargang 2009). The first would be that AOD2 and AOD5 are sequestered in the cytosol under normal conditions, and translocate to the nucleus when an inducing signal(s) is released from dysfunctional mitochondria. Relocalization from cytosol to nucleus is a strategy used by some other Zn(II) Cys6 transcription factors (MacPherson *et al.* 2006). For instance, the Zn(II) Cys6 transcription factor Sef1p in *C. albicans* is sequestered in the cytoplasm by Sfu1 under iron-replete conditions, but is phosphorylated and localizes to the nucleus under iron-depleted conditions (Chen & Noble 2012). As described in section 1.8, the classic RTG system of yeast also depends on localization of transcription factors from cytosol to nucleus in response to mitochondrial dysfunction, although they are not

Zn(II)Cys6 cluster transcription factors. Another possibility would be that AOD2 and AOD5 are located in the nucleus at all times and become activated under inducing conditions. Thus, I began by performing cell fractionation experiments to determine the location of AOD2 and AOD5 so that I could distinguish between these two possibilities. As shown in subsequent chapters, my initial hypothesis was rejected since no evidence for re-location of the proteins under inducing conditions could be found.

As mentioned in section 1.10.9, the orthologues of AOD2 and AOD5 in other fungal species have been shown to play a role in gluconeogenesis. Therefore, it is very likely that AOD2 and AOD5 in *N. crassa* are also involved in gluconeogenesis, and my hypothesis was that the proteins are required for transcription of PEPCK and FBP. I began to investigate this second goal by determining whether or not lack of AOD2 or AOD5 affects the growth of *N. crassa* cells in poor carbon sources. This was coupled to a transcriptional analysis of the PEPCK and FBP genes under various conditions. In this case, evidence was obtained for a role of AOD2 and AOD5 in the expression of PEPCK, but not for FBP.

A third goal towards understanding the functions of AOD2 and AOD5 was to obtain genome-wide binding data of AOD2 and AOD5. This was because AOD2 and AOD5 were already shown to be involved in the regulation of gluconeogenesis and the induction of AOX in various organisms, and it was possible that they also regulate other genes under certain conditions. My hypothesis was that AOD2 and AOD5 would be implicated in the regulation of several genes. This hypothesis was explored by a ChIP-seq analysis using strains expressing tagged version of AOD2 and AOD5. Cells grown under both AOX inducing and non-inducing conditions were analyzed.

This analysis showed several genes were regulated by AOD2 and AOD5.

2 Materials and methods

2.1 Growth of *N. crassa* and strains used

Unless otherwise stated, *N. crassa* was grown on Vogel's medium as described (Davis & De Serres 1970; Nargang & Rapaport 2007). Solid medium (containing 1.25% agar) was used for production of conidiaspores (conidia). To produce small amounts of conidia for freezer stocks and transformation screening, strains were inoculated on slants containing 2 to 5 mL agar solidified medium. To produce large amounts of conidia, strains were inoculated into 250 mL flasks containing 50 mL of solid medium. Cultures were grown in the dark at 30ºC for 1 to 2 days, until hyphae covered the surface of the agar and began to grow up the sides of the slant or flask. Cultures were then exposed to the light for 2 to 5 days at room temperature to allow formation of conidia. Conidia were used for inoculation of liquid medium within three weeks of conidia formation. Between 10^6 and 2.5×10^6 conidia were used per ml of liquid medium for inoculation. Inhibitors used in this study were CM (Fisher Scientific, Pittsburgh, USA, catalogue number: BP904-100) at a final concentration of 2 gm/L of medium, antimycin A at 500 µg/L medium, and hygromycin (Calbiochem, USA) at 500 mg/L medium.

N. crassa strains used in this study are described in Table 2.1.

2.2 Crossing

The procedure for crossing two *N. crassa* strains was as described in (Davis & De Serres 1970) with modifications. Briefly, conidia from the parent chosen to act as the female were spotted at the center of a piece of filter paper which was laid on Westergaard medium in a petri dish. The plates were incubated at room temperature for one week until protoperithecia formed. To fertilize the protoperithecia, conidia

Table 2.1. *N. crassa* strains used in this study.

Strain	Origin[1]	Genotype
NCN251	FGSC # 987 (74-OR23-1A)	*A*
CNA33	Chae *et al.* (2007)	*aod-2*, *pan-2*, *a*
PL23-40	Descheneau *et al.* (2005)	*aod-5*, *pan-2*, *A*
AOD2-N-HA-3	This study. Transformation of CNA33 with p*aod-2*hyg N-HA	*aod-2*, *pan-2*, *a* Contains an ectopic copy of genomic *aod-2* with N-terminal 3× HA tag Hygromycin resistant.
AOD2-N-HA-10	This study. Transformation of CNA33 with p*aod-2*hyg N-HA	*aod-2*, *pan-2*, *a* Contains an ectopic copy of genomic *aod-2* with N-terminal 3× HA tag Hygromycin resistant.
AOD2-C-HA-8	This study. Transformation of CNA33 with p*aod-2*hyg C-HA	*aod-2*, *pan-2*, *a* Contains an ectopic copy of genomic *aod-2* with C-terminal 3× HA tag Hygromycin resistant.
AOD2-C-Myc-4	This study. Transformation of CNA33 with p*aod-2*hyg C-Myc	*aod-2*, *pan-2*, *a* Contains an ectopic copy of genomic *aod-2* with C-terminal 3× Myc tag Hygromycin resistant.
AOD5-N-HA-1	This study. Transformation of PL23-40 with p*aod-5*hyg N-HA	*aod-5*, *pan-2*, *A* Contains an ectopic copy of genomic *aod-5* with N-terminal 3× HA tag Hygromycin resistant.
AOD5-C-HA-22	This study. Transformation of PL23-40 with p*aod-5*hyg C-HA	*aod-5*, *pan-2*, *A* Contains an ectopic copy of genomic *aod-5* with C-terminal 3× HA tag Hygromycin resistant.

AOD5-C-Myc-4	This study. Transformation of PL23-40 with p*aod-5*hyg C-Myc	*aod-5*, *pan-2*, *A* Contains an ectopic copy of genomic *aod-5* with C-terminal 3× Myc tag Hygromycin resistant.
DX13	CNA33 × PL23-40 (Cheryl Nargang and Nancy Easton)	*aod-2*, *aod-5*, *pan-2*
AOD2-C-Myc AOD5-N-HA A1	This study. Transformation of DX13 with p*aod-2*hyg C-Myc and p*aod-5*hyg N-HA	*aod-2, aod-5, pan-2* Contains an ectopic copy of genomic *aod-5* with N-terminal 3× HA tag and of genomic *aod-2* with C-terminal 3× Myc tag
96H9	FGSC # 18947	Δ*aod-1*::hygR *A*
44H6	FGSC # 16838	Δ*aod-3*::hygR *a*
97B1	FGSC # 19465	Δ*aod-2*::hygR *a*
1C3	FGSC # 11227	Δ*aod-5*::hygR
44H6-3	This study. 44H6 × 96H9 (44H6 was the female parent)	Δ*aod-1*::hygR, Δ*aod-3*::hygR

[1] See Appendix Table 1 for a description of the plasmids used in transformations to generate many of these strains.

from the male parent were spread on the filter paper with an inoculation loop. The petri dish was incubated in the dark at room temperature for two weeks and then removed to a lab bench in the light.

Upon exposure to light, fertilized perithecia shoot ascospores onto the lid of the petri dish. To collect the ascospores, 1 mL of sterile dH_2O was added to the lid and swirled to suspend the ascospores. The water containing the ascospores was then transferred to a 1.5 mL Eppendorf tube and incubated at room temperature overnight to hydrate the spores. The spores were then heat shocked at 60ºC for 45 min in a water bath. The ascospores were spread onto a plate containing Vogel's sorbose medium. The plate was incubated at 30ºC overnight. Germinated ascospores were identified using a dissecting microscope on the next day. A sterile Pasteur pipette was used to pick single germinated ascospores onto a slant containing Vogel's medium with the appropriate supplements and/or antibiotics.

2.3 Construction of plasmids containing tagged version of *aod-2* or *aod-5*

The genomic versions of the *aod-2* and *aod-5* genes, including upstream and downstream regions (1509 bp upstream from *aod-2* coding region and 783 bp downstream, 609 bp upstream from *aod-5* coding region and 470 bp downstream) were previously cloned from the *N. crassa* pMOcosX cosmid library into pBSKII by Michael Chae in the Nargang lab. Briefly, a *Hind*III/*Xba*I fragment (from the cosmid on plate X14, position D3 of the library) containing the *aod-2* gene was cloned into plasmid pBSKII at the *Hind*III and *Xba*I sites to give plasmid p*aod-2*-9. The *aod-5* gene was contained on an *Nru*I/*Pvu*II fragment (from the cosmid on plate X15, position B9 of the library). This fragment was inserted into the *EcoR*V site of pBSKII to give p*aod-5*-6. A hygromycin resistance cassette from pCSN44 (Staben *et al.* 1989)

contained on an *Apa*I/*Hind*III fragment was cloned into p*aod-2*-9 to yield p*aod-2*hyg-3. An *Xho*I fragment from pCSN44 was cloned into the *Sal*I site of p*aod-5*-6 to give p*aod-5*hyg-69.

Both the p*aod-2*hyg-3 and p*aod-5*hyg-69 plasmids contained a *Not*I site in the pBSKII plasmid backbone. Because our protein tags were designed to be cloned into *Not*I sites, I removed the plasmid *Not*I sites before I introduced *Not*I sites into the *aod-2* and *aod-5* coding sequence where the tags were desired. To remove the *Not*I sites, the p*aod-2*hyg-3 and p*aod-5*hyg-69 plasmids were digested with *Not*I and the 5' sticky-end overhang were filled in using Klenow DNA polymerase and dNTPs. The plasmids were then religated and transformed into *E. coli*. Plasmids were isolated from selected transformants and tested for loss of the *Not*I sites. Plasmid p*aod-2*hyg-3 Δ*Not*I and p*aod-5*hyg-69 Δ*Not*I were selected for further work. I then performed polymerase chain reaction (PCR) mutagenesis to introduce *Not*I restriction sites into both the p*aod-2*hyg-3 Δ*Not*I and p*aod-5*hyg-69 Δ*Not*I plasmids. For each plasmid, *Not*I sites were introduced individually at two locations. In one case the site was inserted right after the start codon. In a separate mutagenesis, a *Not*I site was inserted right before the stop codon. This resulted in plasmids p*aod-2*hyg N *Not*I, p*aod-2*hyg C *Not*I, p*aod-5*hyg N *Not*I, and p*aod-5*hyg C *Not*I. These *Not*I sites were then used to clone 3× HA or 3× Myc tags into the plasmids (Fig. 2.1). The tags were derived from plasmids pFN-*Not*I-HA3 and pFN-*Not*I-Myc3, respectively, that had been constructed according to our specifications by Integrated DNA Technologies (IDT, Coralville, USA). The resulting plasmids were named p*aod-2*hyg N-HA, p*aod-2*hyg C-HA, p*aod-2*hyg N-Myc, p*aod-2*hyg C-Myc, p*aod-5*hyg N-HA, p*aod-5*hyg C-HA, p*aod-5*hyg N-myc, p*aod-5*hyg C-myc (see Appendix Table 1 for details). The triple

Figure 2.1. Construction of plasmids containing HA or Myc tags. *aod-2* and *aod-5* (blue arrows), as well as a hygromycin resistant cassette (hygromycin B, red arrows), were cloned into plasmid pBSKII by Michael Chae (resulting in p*aod-2*hyg-3 and p*aod-5*hyg-69, respectively). The *Not*I site on the pBSKII backbone was then removed by *Not*I digestion, end-filling, and religation to give the plasmids shown in the figure. *Not*I sites were then separately introduced at the N- and C-terminus of the coding region of the *aod-2* and *aod-5* genes. 3× HA and 3× Myc tags were cloned separately into these *Not*I sites as indicated in the boxes. The start codon (ATG) and stop codon of *aod-2* and *aod-5* are shown in red. Amp, ampicillin resistant cassette. Plasmids were drawn using online software named PlasMapper (http://wishart.biology.ualberta.ca/PlasMapper/). Restriction sites indicated on the plasmid map were used for construction of the p*aod-2*hyg-3 Δ*Not*I and p*aod-5*hyg-69 Δ*Not*I plasmids. It is of note that the restriction sites used for cloning in p*aod-5*hyg-69 are no longer available due to mixed blunt-end ligations and non-identical sticky-end ligations.

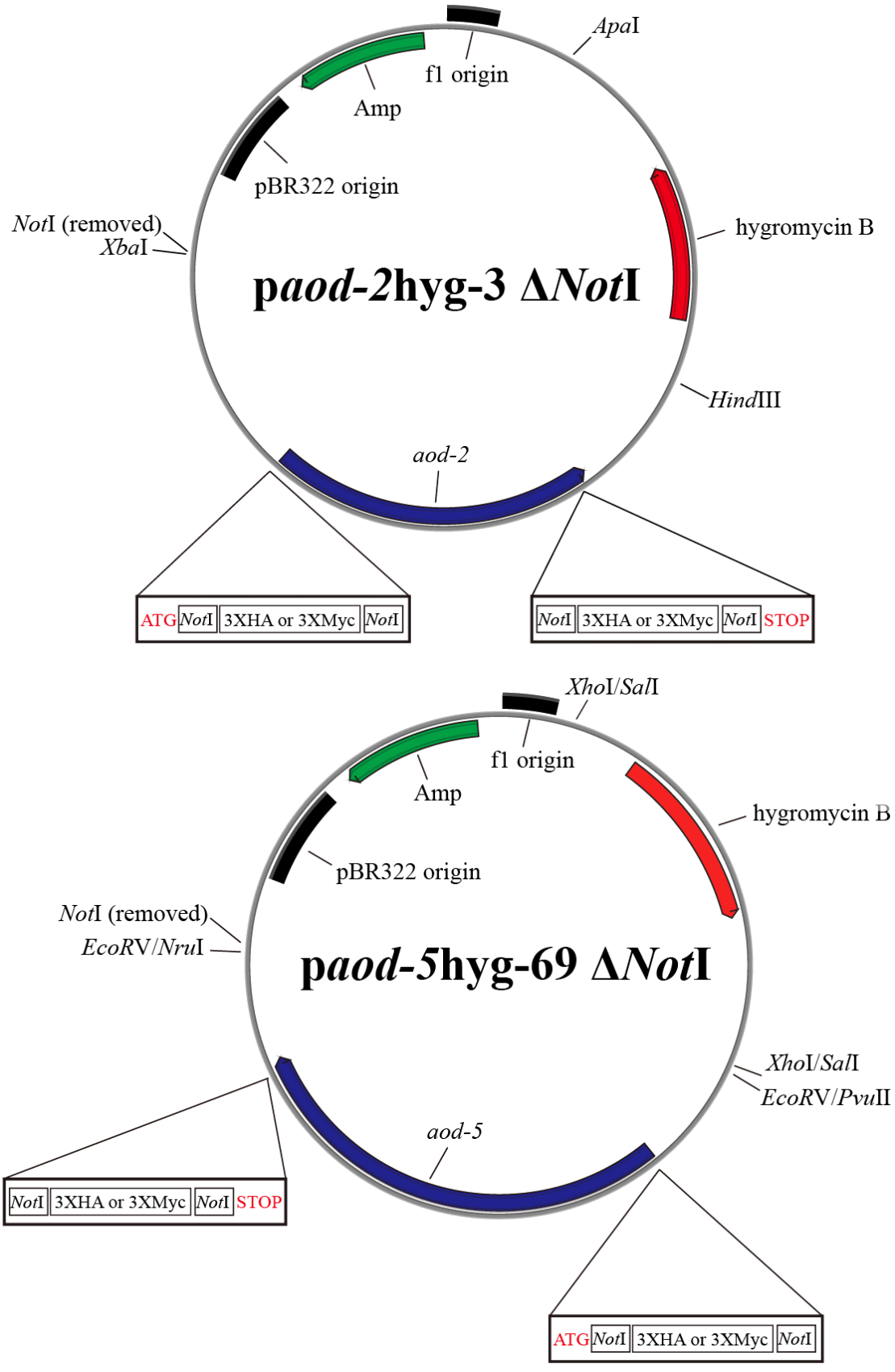
ApaI
f1 origin
Amp
pBR322 origin
NotI (removed)
XbaI
hygromycin B
paod-2hyg-3 ΔNotI
HindIII
aod-2
ATG NotI 3XHA or 3XMyc NotI
NotI 3XHA or 3XMyc NotI STOP
XhoI/SalI
f1 origin
Amp
hygromycin B
pBR322 origin
NotI (removed)
EcoRV/NruI
paod-5hyg-69 ΔNotI
XhoI/SalI
EcoRV/PvuII
aod-5
NotI 3XHA or 3XMyc NotI STOP
ATG NotI 3XHA or 3XMyc NotI

nature and orientation of all tags in the correct reading frames was verified by Sanger sequencing using appropriate primers (see Appendix Table 2 for details).

2.4 *N. crassa* strains expressing tagged AOD2 and/or AOD5

HA or myc tagged *aod-2* and *aod-5* constructs were transformed into either the *aod-2* mutant strain CNA33 or the *aod-5* mutant strain PL23-40, respectively (see Table 2.1 for genotypes) by electroporation. Transformed conidia were plated on medium containing hygromycin. For each transformation 20 to 30 colonies, with a diameter of more than 8 millimeters after 3 to 4 days at 30ºC, were transferred to slants containing hygromycin for conidiation. Conidia were then streaked on hygromycin-containing plates to obtain single colony isolates. A single colony from each transformant was selected as a stock strain for further examination. These strains were tested for their ability to grow on plates containing antimycin A. Ability to grow on antimycin A should indicate that a functional *aod-2* or *aod-5* gene was present in a transformant. Among those strains that grew in the presence of antimycin A, about 10 strains from each tagged category were chosen for genomic DNA isolation and PCR of the introduced gene to verify the presence of a tagged *aod-2* or *aod-5* gene in the selected transformants. Mitochondria were then isolated from the verified transformants following growth in medium containing CM. Levels of AOX in the mitochondria were compared by Western blot analysis with mitochondria isolated from wild type strain NCN251, grown in the same medium. Transformants able to induce AOX to the level in the wild type control were chosen for subsequent experiments. Isolates AOD2-N-HA-10, AOD2-C-HA-8, AOD2-C-Myc-4, AOD5-N-HA-1, AOD5-C-HA-22, and AOD5-C-Myc-4 were chosen for further analysis.

I also wished to express both AOD2-Myc and AOD5-HA tagged proteins in an *aod-2 aod-5* double mutant strain DX13 (Table 2.1). Verification of the double *aod-2 aod-5* mutant genotype in DX13 was done by Nancy Easton in the Nargang lab. p*aod-2*hyg C-myc and p*aod-5*hyg N-HA were cotransformed into DX13. Transformants were sequentially selected for hygromycin and antimycin A resistance as described above. Levels of AOX in CM induced cells were examined in mitochondria by Western blot and compared to wild type. One transformant, AOD2-C-Myc AOD5-N-HA A1, that expressed AOX at wild type levels was chosen for further work.

2.5 Transformation of *N. crassa* conidia by electroporation

The electroporation procedure was as described previously (Tanton *et al.* 2003) with some modifications. Briefly, 50 mL sterile water was used to harvest conidia from a 250 mL flask containing 50 mL solid Vogel's medium (section 2.1). Conidia were suspended in the sterile water, and transferred to a sterile 50 mL tube. The conidia were then pelleted in a clinical centrifuge. The supernatant was discarded and the conidia were washed once with fresh 50 mL sterile water and three times with 50 mL of 1 M sorbitol (Sigma-Aldrich, St. Louis, USA). The final concentration of conidia was adjusted to 2 to 2.5 × 10^9 conidia per mL of 1 M sorbitol. 40 µL aliquots of conidia were made for each electroporation and mixed with 1 to 5 µg DNA that was dissolved in 5 µL dH_2O. The conidia and DNA were transferred to an electroporation cuvette (Fisher Scientific, Pittsburgh, USA) that had been chilled on ice for at least 5 min before electroporation. As a negative control, 5 µL dH_2O without DNA was used for electroporation.

To electroporate conidia, a BTX model ECM 630 machine (Harvard Apparatus, Holliston, USA) was employed. Settings were 2.1 kV, 475 Ohms, and 25 μF. For successful electroporations, the pulse was between 10 ms and 13 ms. Immediately after the electroporation, 1 mL 1M sorbitol was added to the cuvette and the mixture was transferred to a 1.5 mL tube using the sterile pipette provided with the cuvette. The conidia were then incubated at 30ºC for at least 1 hr to allow recovery from electroshock. Before plating, the conidia were added to 10 mL of warm top agar (40 to 42ºC, Vogel's sorbose medium with 1 M sorbitol, 1.25% agar, and inhibitors as required in specific transformations (hygromycin or antimycin A)) for each plate. The conidia-containing top agar was evenly poured over plates (Vogel's sorbose medium with 1.25% agar, plus appropriate inhibitor) to cover the surface. After the top agar had solidified, the plate was incubated at 30ºC for 2 to 4 days until robust colonies formed.

2.6 Isolation of crude nuclei from *N. crassa*

250 mL of Vogel's liquid medium in a 1 L baffled flask was inoculated with 10^6 conidia per mL and shaken at 200 rpm at 30ºC for 18 hr (in the absence of CM), or 20 hr (in the presence of CM) at 30ºC. Normally 5 to 10 gm of mycelium was obtained and ground in liquid nitrogen. The mycelium powder was suspended in 2 mL of SEMP buffer (0.25 M sucrose, 10 mM MOPS (Sigma-Aldrich, St. Louis, USA) [pH 7.2], 1 mM EDTA, 1 mM PMSF) per 1 gm of mycelium. After thawing on ice, the suspension was filtered twice through Miracloth (Calbiochem, USA) and then centrifuged at 5,000 rpm (3,600 × g) for 5 min at 4ºC in an SA-600 rotor (Sorvall, Mandel Scientific, Guelph, ON) using a Sorvall model RC5C plus centrifuge (Mandel Scientific, Guelph, ON). The pellet was resuspended in 100 μL SEMP buffer (0.25 M

sucrose, 10 mM MOPS [pH 7.2], 1 mM EDTA, 1 mM PMSF) per 5 gm of the starting mycelium.

2.7 Isolation of purified nuclei

The protocol for purified nuclei isolation was a modified version of the method described by Talbot and Russell (1982). 1.5 L of Vogel's liquid medium in a 2 L flask was inoculated with 10^6 conidia per mL and bubbled with filter sterilized air for 18 hr (in the absence of CM), or 20 hr (in the presence of CM) in a 30ºC water bath. Mycelium was harvested by vacuum filtration and ground in liquid nitrogen. The resulting powder was suspended in 2 mL of ice-cold Buffer A (1 M sorbitol, 5% [v/v] Ficoll 400, 20% [v/v] glycerol, 5 mM $MgCl_2$, 10 mM $CaCl_2$, 1% [v/v] Triton X-100, 50 mM Tris-HCl [pH 7.5], 1 mM PMSF, protease inhibitors (final concentrations of 2 μg/mL aprotinin, 1 μg/mL leupeptin, and 1 μg/mL pepstatin A)) per 1 gm mycelium. The homogenate was filtered twice through Miracloth (Calbiochem, USA) and then centrifuged at 2,400 × g for 10 min at 4ºC in an SA-600 rotor using a Sorvall model RC5C plus centrifuge to remove cellular debris. The supernatant was centrifuged at 9,000 × g for 50 min at 4ºC in an SA-600 rotor to yield a partially purified nuclear pellet.

To further purify nuclei, the partially purified nuclear pellet was resuspended in ice-cold Buffer B (1 M sucrose, 50 mM Tris-HCl [pH7.5], 5 mM $MgCl_2$, 10 mM $CaCl_2$, 1% Triton X-100, 1 mM PMSF, protease inhibitors (final concentrations of 2 μg/mL aprotinin, 1 μg/mL leupeptin, and 1 μg/mL pepstatin A)) using 1 mL per 3 to 5 gm of the original weight of mycelium. This nuclei-containing suspension was added to two volumes of Percoll-sucrose stock solution, which was made by adding nine volumes of Percoll (GE Healthcare, UK) to one volume of 2.5 M sucrose. The total

suspension was mixed by gentle pipetting. 3 mL aliquots of the mixture were transferred to 3.2 mL polycarbonate centrifuge tubes (Beckman, Brea, USA). These were centrifuged at 58,000 × g in a TLA-110 rotor (Beckman, Brea, USA) using a Beckman Optima™ MAX table top ultracentrifuge (Brea, USA) for 45 min at 4ºC. Following centrifugation, purified nuclei were layered between the middle position of the tube and the bottom where a yellow thick Percoll pellet was covered by a layer of white material which consisted of clumps of nuclei (Figure 2.2). The band of nuclei was collected with a pipette and transferred to a fresh 3.2 mL polycarbonate centrifuge tube without addition of any buffers. To remove Percoll particles from the collected nuclear band, the fraction was centrifuged at 100,000 × g in a TLA-110 rotor for 2 hr at 4ºC. The nuclei (white) appeared as a pellet above the Percoll pellet (yellow). Using a 1000 µL pipettor, the nuclei were mixed with the supernatant without disturbing the Percoll pellet and the mixture was transferred to fresh 2 mL Eppendorf centrifuge tubes. After centrifugation at 13,000 rpm (16,000 × g) for 30 min at 4ºC in a Sorvall Biofuge® fresco table top centrifuge (Sorvall, Mandel Scientific, Guelph, ON), the supernatant was discarded and the nuclei were suspended in 100 µL suspension buffer (25 mM sucrose, 50 mM Tris-HCl [pH7.5], 5 mM $MgCl_2$, 10 mM $CaCl_2$).

2.8 Isolation of crude mitochondria from *N. crassa*

Crude mitochondria were isolated as previously described (Nargang & Rapaport 2007) with minor modifications. Cultures were grown for 18 hr (in the absence of CM), or 20 hr (in the presence of CM) at 30ºC. Mycelium was harvested by vacuum filtration, and rinsed with dH_2O. The wet weight of the pad was measured. It was then ground using a mortar and pestle, with the same weight of sand plus 1 mL

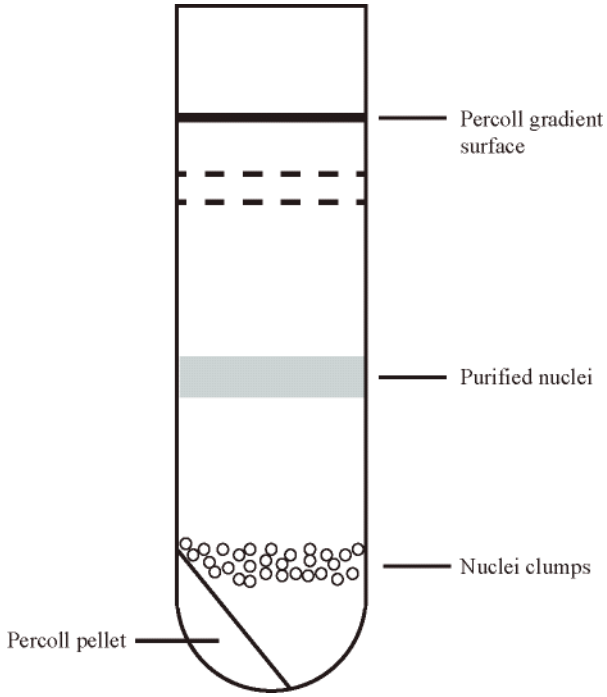

Figure 2.2. Schematic of nuclei banded in a Percoll gradient. A Percoll gradient was formed by ultracentrifugation as described in the text (section 2.7). Following centrifugation, a band of nuclei was present in the middle of the gradient as indicated by the grey band in the diagram, though the actual color of the band was white. Some Percoll particles precipitated at the bottom of the tube and appeared as a yellow pellet. A layer containing many white small clumps were visible above the Percoll pellet and they also contained nuclei as assessed by Western analysis for histone H3. Sometimes thin white bands (dashed lines) appeared beneath the gradient surface but they were found not to contain any nuclei.

SEMP buffer (0.25 M sucrose, 10 mM MOPS [pH 7.2], 1 mM EDTA, 1 mM PMSF) per 1 gm of mycelium. The ground slurry was centrifuged at 5,000 rpm (3,600 × g) for 5 min in an SA-600 rotor. The supernatant was further centrifuged at 12,000 rpm (20,800 × g) for 20 min in an SA-600 rotor to pellet mitochondria. When required, the supernatant was saved for isolation of cytosol and microsomes (section 2.10). The pellet containing mitochondria was washed twice in SEMP buffer, suspended in 50 to 500 µL SEMP buffer (depending on starting quantity of mycelium), and stored at -80ºC if not immediately used.

2.9 Isolation of purified mitochondria from *N. crassa*

When highly purified mitochondria were required, they were subjected to flotation gradient purification (Lambowitz 1979). The final pellet of crudely purified mitochondria (section 2.8) was suspended in 1 mL 60% sucrose buffer (60% [w/v] sucrose, 10 mM MOPS [pH 7.2], 1 mM EDTA) by stirring and gentle pipetting. It was then transferred to a 3.2 mL polycarbonate centrifuge tube and the volume was brought up to 1.5 mL with 60% sucrose buffer to form a uniform 60% sucrose layer. This layer was slowly overlaid with 1.5 mL of 55% sucrose buffer (55% [w/v] sucrose, 10 mM MOPS [pH 7.2], 1 mM EDTA), followed by 750 µL of 44% sucrose buffer (44% [w/v] sucrose, 10 mM MOPS [pH 7.2], 1 mM EDTA). The gradients were then centrifuged at 35,000 rpm (25,400 × g) for 2 hr at 4ºC in a TLA-110 rotor. A band with continuous clumps appeared between the 44% and 55% sucrose layers. This band was retrieved with a 1000 µL pipettor and transferred to a fresh 1.5 mL tube. The purified mitochondria were mixed with 1 mL SEMP buffer and the mitochondria were pelleted by centrifugation at 13,000 rpm (16,000 × g) for 20 min at 4ºC in a

Sorvall Biofuge® fresco centrifuge. The pellet was washed with 1 mL SEMP buffer. The final pellet was suspended in 100 µL SEMP buffer.

2.10 Purified cytosol and microsome isolation

To isolate cytosol and microsomes, 1 mL of the supernatant described in the crude mitochondria isolation procedure (section 2.8) was centrifuged at 48,000 rpm (27,900 × g) in a Beckman TLA-55 rotor for 1.5 hr at 4ºC. The pellet was suspended in 150 µL SEMP buffer as the microsomal fraction whereas the supernatant was saved as the cytosolic fraction. Both fractions were kept at -80ºC if not immediately used.

2.11 Salt extraction of proteins from nuclei

Nuclei containing 100 µg protein were brought up to 60 µL volume using the suspension buffer described at the end of the isolation of purified nuclei procedure (section 2.7). The nuclei were mixed with 60 µL of 0.4 M KCl prepared by dissolving the appropriate amount of KCl in nuclear suspension buffer (25 mM sucrose, 50 mM Tris-HCl [pH7.5], 5 mM $MgCl_2$, 10 mM $CaCl_2$) containing 1 mM PMSF and protease inhibitors (final concentrations of 2 µg/mL aprotinin, 1 µg/mL leupeptin, and 1 µg/mL pepstatin A). The suspension was gently rocked for 1.5 to 2 hr at 4ºC using an Orbitron Rotator I (Boekel Scientific, Feasterville, USA). Insoluble material was removed by centrifugation at 13,000 rpm (16,000 × g) for 30 min at 4ºC in a Sorvall Biofuge® fresco centrifuge. Meanwhile, a Zeba™ Spin Desalting column (Thermo Scientific, Rockford, USA) was activated following the manufacturer's instructions. The supernatant containing salt extracted proteins was slowly loaded onto the center of the resin bed of an activated desalting column which was placed into a fresh 1.5 mL Eppendorf tube. The desalting column was centrifuged at 1,500 × g (4,000 rpm)

for 2 min at 4ºC in a Sorvall Biofuge® fresco centrifuge with the top of the resin bed facing outward. The flow-through was immediately used for co-immunoprecipitation experiments.

2.12 Sodium dodecyl sulphate polyacrylamide gel electrophoresis (SDS-PAGE)

SDS-PAGE gels were prepared as described (Laemmli 1970). Based on the size of protein of interest, the percentage of acrylamide in the resolving gel was adjusted (from 10% to 12.5%) while keeping the stacking gel unchanged. 10 to 100 µg protein was mixed with cracking buffer (2% SDS, 10% glycerol, 5% β-mercaptoethanol, 0.005% bromphenol blue, 62.5 mM Tris-HCl [pH 6.8]) to a final volume of 30 to 50 µL. Samples were mixed for 10 min, incubated at 95ºC for 5 min, and then centrifuged at 13,000 rpm (16,000 × g) for 5 min in a Sorvall Biofuge® pico centrifuge. The supernatant of the samples, as well as 15 µL of a prestained protein marker (New England Biolabs, Ipswich, USA), were loaded into separate wells formed in the stacking gel. Electrophoresis was performed with constant current at 220 V for about 3 hr.

2.13 Western blot

Western blotting was performed as described (Towbin *et al.* 1979) with modifications. Briefly, after SDS-PAGE, proteins on acrylamide gels were transferred to a nitrocellulose membrane using a Bio-Rad (Berkeley, USA) Trans-Blot® Cell apparatus. Blots were transferred at 67 V for 1.5 to 2 hr. The membrane was then incubated in 5% skim milk buffer (milk powder dissolved in TBST: 25 mM Tris-HCl [pH7.5], 150 mM NaCl, 0.05% Tween-20) for 1 hr, followed by incubation in primary antibody for 1 to 2 hr. Primary antibodies were diluted 1:500 to 1:50,000

in 5% skim milk buffer. The degree of dilution was specific for each antibody. The membrane was then washed three times in TBST for 5 min, and incubated in secondary antibody (Bio-Rad goat anti-rabbit or anti-mouse antibody conjugated to horseradish peroxidase, diluted 1:3,000 in skim milk buffer) for 1 hr. The membrane was then washed three times in TBST for 10 min and once in TBS (25 mM Tris-HCl [pH 7.5], 150 mM NaCl) for 10 min. Illuminating reagent LumiGLO® Chemiluminescent Substrate (KPL, Maryland, USA) was evenly spread on the membrane which was then exposed to X-ray film (Eastman Kodak, New York, USA) for various time periods in a dark room. Films were developed and scanned.

2.14 Phos-tag SDS-PAGE

Phos-tag SDS-PAGE was performed as described (Kinoshita *et al.* 2009) with modifications. To prepare a Phos-tag™ solution, 10 mg Phos-tag™ AAL-107 (Wako Pure Chemical Industries, Ltd., Japan) was dissolved in 100 µL methanol and the volume was brought up to 3.2 mL with distilled water. When making a 7 mL resolving gel as described in section 2.12, 140 µL Phos-tag™ AAL solution and 140 µL 10 mM manganese chloride (Sigma-Aldrich, St. Louis, USA) were added to the gel solution. The stacking gel solution remained unchanged.

When doing a Western blot after phos-tag SDS-PAGE, additional steps were required to achieve good transfer. The phos-tag gel was soaked in transfer buffer containing 1 mM EDTA for 10 min, and then in transfer buffer without EDTA for 10 min to minimize the effect of manganese ions that inhibit transfer of phosphorylated proteins to the membrane. The gel was then ready for transfer as described in section 2.13.

2.15 Isolation of genomic DNA

The method described in Nargang and Rapaport (2007) was used to isolate genomic DNA from *N. crassa* with modifications. For each sample, 50 mL Vogel's liquid minimal medium in a 250 mL flask was used to grow cultures. To begin, approximately 4 mL from this 50 mL Vogel's liquid medium in the flask was poured into a slant containing a conidiated culture to harvest the conidia. After vigorous mixing, the conidia and medium were poured back into the flask and the culture was grown at 30ºC for at least 16 hr with constant shaking. Mycelium was harvested by vacuum filtration and ground with 1.5 gm of sand (Sigma-Aldrich, St. Louis, USA) and 5 mL Genomic DNA Isolation Buffer (100 mM Tris-HCl [pH8.0], 10 mM EDTA, 1% SDS) for each gm of mycelium. After grinding with a mortar and pestle, another 5 mL of Genomic DNA Isolation Buffer was added to make a slurry. The slurry was transferred to an SA-600 Sorvall centrifuge tube and incubated at 70ºC in a water bath for 1 hr followed by chilling on ice for at least 10 min. 640 µL 8 M potassium acetate (pH4.3) was then added and the slurry was stirred with a 5-mL pipette to achieve mixing. The tube was incubated on ice for an additional 1 hr. The slurry was centrifuged at 14,000 rpm (28,400 × g) for 15 min at 4ºC in an SA-600 rotor using a Sorvall model RC5C plus centrifuge. The supernatant was transferred to a fresh SA-600 tube. 10 mL of isopropanol was added to the supernatant and mixed to precipitate the DNA. The tube was then centrifuged at 10,000 rpm (14,500 × g) for 5 min at 4ºC in an SA-600 rotor and Sorvall centrifuge. The supernatant was discarded and the pellet was dried at room temperature for 10 min. The pellet was then dissolved in 400 µL 1 mM EDTA (pH8.0) and transferred to a 1.5 mL Eppendorf tube. To remove RNA from the genomic DNA, 200 µL Hi Salt Buffer (2.5 mM Tris-HCl [pH7.4], 0.25 mM EDTA, 1 M NaCl) and 15 µL boiled RNase A (10

mg/mL) were added, followed by incubation at 37ºC for 30 min. After digestion of the RNA, the DNA was extracted with 600 µL phenol-chloroform (1:1 [v/v]) (both from Fisher Scientific, Pittsburgh, USA) to remove proteins. This step was done twice and 400 µL of the aqueous layer was transferred to a fresh tube. To precipitate genomic DNA, 40 µL 3M sodium acetate (pH5.2) and 1 mL 95% ethanol were added and mixed. The solution was centrifuged at 13,000 rpm (16,000 × g) for 10 min at 4ºC in a Sorvall Biofuge® fresco centrifuge. The pellet was washed with 70% ethanol once and air dried for 15 min. 10 to 50 µL Milli Q water was added to dissolve the pellet and the genomic DNA was stored in a -20ºC freezer.

2.16 Co-immunoprecipitation

The Pierce® ProFound™ HA or c-Myc Tag IP/Co-IP kit (Thermo Scientific, Rockford, USA) was used for co-immunoprecipitation experiments following the manufacturer's instructions with minor modifications. A small plug provided in the kit was inserted into the bottom of an IP spin column before use. Approximately 120 µL of desalted nuclear proteins (section 2.11) were then loaded onto the column. The same volume of 2 × IP buffer (100 mM HEPES-KOH [pH7.4], 300 mM NaCl, 0.2% Triton X-100 (Sigma-Aldrich, St. Louis, USA)) containing 1 mM PMSF and protease inhibitors (final concentrations of 2 µg/mL aprotinin, 1 µg/mL leupeptin, and 1 µg/mL pepstatin A) was then added to the column, followed by addition of 20 µL anti-HA or 10 µL anti-Myc coated agarose beads (depending on which tag the IP was targeting). A lid was screwed tightly onto the IP spin column and the column was gently rocked overnight at 4ºC to allow binding of the antigen to the beads. Following the binding period, the small plug was removed from the column, the column was placed in a collection tube, and the lid was loosened. The IP spin column in the collection tube

was pulse centrifuged for 10 sec at 4ºC in a Sorvall Biofuge® fresco centrifuge. The flow-through was either saved for further analysis or discarded. The agarose beads were washed three times with 500 µL ice-cold BupH™ Tris Buffered Saline by pulse centrifugation for 10 sec at 4ºC in a Sorvall Biofuge® fresco centrifuge for each washes. The antibody-bound proteins were eluted by adding 50 µL Lane Marker Non-Reducing Sample Buffer (provided in the kit) that contained a final concentration of 12.5% β-mercaptoethanol (freshly added) and heating the column at 95ºC for 10 min in a heat block. The proteins were removed from the column by centrifugation at 13,000 rpm (16,000 × g) for 10 min in a Sorvall Biofuge® pico centrifuge at room temperature and then loaded onto an SDS-PAGE gel.

2.17 Total RNA isolation

RNA isolation was performed using the QIAGEN (Hilden, Germany) RNeasy Plant Mini Kit and followed the manufacturer's instructions. All pestles, mortars, and forceps were baked in a 240ºC oven overnight to deactivate RNase. A final concentration of 10^6 conidia/mL for normal gene expression testing was inoculated into a 1 L baffled flask containing 100 mL Vogel's liquid medium. Cultures were grown at 30ºC with constant shaking for 12 hr (in the absence of CM) or 14 hr (in the presence of CM). Approximately 100 mg mycelium was used for RNA isolation. Immediately after weighing, the mycelium was frozen in liquid nitrogen and ground to a powder. The powder was transferred to a 2 mL RNase-free tube and suspended in 450 µL RC buffer (supplied with the kit, with 10 µL β-mercaptoethanol (Sigma-Aldrich, St. Louis, USA) added per 1 mL RC buffer before use). The tube was vortexed for 1 min. The mixture was then loaded onto a QIAGEN shredder column and centrifuged at 13,000 rpm (16,000 × g) for 2 min in a Sorvall Biofuge® pico centrifuge.

The flow-through (cell lysate) was transferred to a fresh 2 mL tube, snap-frozen in liquid nitrogen, and stored at -80ºC. To isolate total RNA, frozen cell lysate was thawed in a 37ºC water bath for 15 min. The RNA isolation followed the QIAGEN kit's instructions. Briefly, the cell lysate was loaded onto an RNeasy Mini Spin column. The column was centrifuged at 13,000 rpm (16,000 × g) for 15 sec at room temperature in a Sorvall Biofuge® pico bench top centrifuge. The flow-through was discarded and the column was washed once with 700 µL RW1 buffer and twice with 500 µL RPE buffer (buffers were supplied with the kit). For each wash, the column was centrifuged at 13,000 rpm (16,000 × g) for 15 sec at room temperature. After washes, the column was centrifuged at 13,000 rpm (16,000 × g) for 1 min at room temperature to remove residual ethanol. The RNA was eluted from the column twice with 50 µL RNase-free water (supplied with the kit). The RNA was immediately examined for concentration and RNA integrity.

2.18 Measurement of RNA concentration

The concentration of total RNA was measured using a Nanodrop ND 1000 spectrophotometer (Thermo Scientific, Rockford, USA). Each RNA sample was diluted ten-fold using RNase-free water provided in the RNA isolation kit. Each sample was measured three times and the average was taken as the concentration.

2.19 Measurement of RNA integrity

RNA integrity was measured using an Agilent 2100 Bioanalyzer system and the Agilent RNA 6000 Nano kit (Agilent Technologies, USA). Each RNA sample was diluted to 250 ng/µL in RNase-free water prior to use. RNA ladder, gel-dye mix (provided in the Agilent RNA 6000 Nano kit), and samples were loaded onto an

Agilent RNA 6000 Nano chip according to the manufacturer's instructions. The loaded chip was placed in an Agilent 2100 Bioanalyzer and analyzed using Agilent 2100 Expert software for Plant Nano Assay. Only those samples that had an RNA integrity number (RIN, calculated by the software) value of greater than 9 (the maximum value is 10) were used for cDNA synthesis.

2.20 First-strand cDNA synthesis from total RNA

First-strand cDNA was synthesized using SuperScript™ III Reverse Transcriptase (Invitrogen, Carlsbad, USA) following the manufacturer's instructions. Other Invitrogen products included Oligo(dT)$_{12-18}$ Primer, RNaseOUT™ Recombinant Ribonuclease Inhibitor, and dNTPs. For each reaction, 1 μg total RNA was used. cDNA was stored at -80ºC before use.

2.21 Principals of quantitative PCR (qPCR) primer design

Either Roche probefinder (http://qpcr.probefinder.com/organism.jsp) or IDT PrimerQuest (http://www.idtdna.com/primerquest/Home/Index) was used for qPCR primer design. Roche probefinder was primarily used. "Other Organism" was selected in the dropdown menu on the website and the target sequence with exons only was pasted into the sequence box. The intron assay was opted out. When the "design" button was clicked, the system processed the target sequence and the best pair of primers was shown. To view additional primers, "More Assay" was chosen. Only those pairs of primers that either flanked an intron, or that had one of the primers spanning the splicing site of an intron, were considered. For non-intron containing genes, the pair of primers with the highest ranking was selected.

IDT PrimerQuest provided more flexible options. The target sequence with exons only was pasted into the sequence box. “Show Custom Design Parameters” was selected, and parameters were adjusted as follows:

Results to Return: 50

Primer Tm (ºC): Min 59, Opt 60, Max 63

Primer GC (%): Min 40, Opt 50, Max 60

Primer Size (nt): Min 19, Opt 20, Max 24

Amplicon Size (bp): Min 60, Opt 70, Max 100

When all parameters were entered, primers were designed accordingly by clicking the “Get Assays” button. Primer sets that flanked an intron, or where one primer of a set spanned an intron were preferred. For non-intron containing genes, the pair of primers with the highest ranking was selected.

2.22 Validation of qPCR primers

Primers for qPCR must be validated to ensure that the amplification efficiency of the gene is similar to an endogenous control and that only one product is amplified. To begin the validation, both 100 µM forward and 100 µM reverse primers were mixed and diluted to 4.8 µM per primer using DNase-free water (IDT, Coralville, USA). To obtain a standard curve, cDNA from a first-strand cDNA synthesis reaction (cDNA was synthesized from total RNA isolated from a wild-type culture grown in the presence of CM as described in section 2.20) was diluted four-fold, 16-fold, 64-fold, 256-fold, and 1024-fold. 2.5 µL diluted cDNA, 2.5 µL diluted primers, and 5 µL 2 × KAPA SYBR® Fast qPCR master mix (KAPA Biosystems, Wilmington, USA) were added to each well of a 96-well plate (BIOplastics, Landgraaf, Netherlands). For each dilution and each pair of primers,

three technical replicates were used. Loaded plates were sealed using the EU Opti-Seal (BIOplastics, Landgraaf, Netherlands) system and subjected to qPCR on a StepOnePlus qPCR machine (Applied Biosystems, Foster City, USA). StepOne software (Applied Biosystems, Foster City, USA) was used to run the qPCR programs and to generate amplification curves for each pair of primers. The amplification efficiencies were compared to the endogenous control beta-tubulin (for example, the slope of the amplification curve and R^2 value (coefficient of determination of the curve) to determine whether the primers were able to amplify the target genes as efficiently as the endogenous control. In addition, melt curves were obtained following amplification using the same qPCR machine. The melt curve gives the temperature at which the DNA double strand formed during the amplification will dissociate during increased heating. This was measured to determine whether or not the amplification generated non-specific PCR products. The goal is to identify a pair of primers where the melt curve shows only one peak, which suggests that only one PCR product was amplified from the target gene.

2.23 qPCR

Forward and reverse primers that had been validated (section 2.22) were mixed and diluted to 4.8 μM using DNase-free water (IDT, Coralville, USA). cDNA was diluted 20-fold from each first-strand cDNA synthesis reaction using the same DNase-free water. For each qPCR reaction, 2.5 μL 20-fold diluted cDNA, 2.5 μL diluted primers, and 5 μL 2 × KAPA SYBR® Fast qPCR master mix (KAPA Biosystems, USA) were added to each well of a 96-well plate (BIOplastics, Netherlands). For each condition, samples from four independent biological samples were analyzed using three technical replicates. Loaded plates were processed as

described in section 2.22. StepOne software (Applied Biosystems, Foster City, CA) was employed to run qPCR programs and to obtain Ct values.

2.24 Chromatin immunoprecipitation (ChIP)

The protocol for ChIP was as described by Guo *et al.* (2010) and Kuras and Struhl (1999) with modifications. *N. crassa* cultures were started with 2.5×10^8 conidia in 100 mL Vogel's medium and were grown for 12 hr at 30ºC in the absence of CM, or 14 hr in the presence of CM. To cross-link proteins to DNA, formaldehyde (catalogue number: F79-500, Fisher Scentific, Pittsburgh, USA) was added to each culture to a final concentration of 1% followed by constant shaking for 15 min at room temperature. Following the reaction, 20 mL of 1.25 M glycine was added to each culture and shaking was continued for 5 min to quench the cross-linking reaction. Mycelium was then harvested by vacuum filtration and washed twice with ice-cold TBS (25 mM Tris-HCl [pH7.2], 150 mM NaCl) and once with FA lysis buffer (50 mM HEPES-KOH [pH7.5], 150 mM NaCl, 1 mM EDTA, 0.1% Na deoxycholate (Thermo Scientific, Rockford, USA), 1% Triton X-100, 0.1% SDS). The washed mycelium was ground in liquid nitrogen and the resulting powder was suspended in FA lysis buffer (1 mL per 2 gm of mycelium powder) containing 1 mM PMSF and protease inhibitors (final concentrations of 2 μg/mL aprotinin, 1 μg/mL leupeptin, and 1 μg/mL pepstatin A). Once the powder had thawed in FA lysis buffer, the mixture was divided into aliquots of 2 mL and each was sonicated 30 times, each time with a 30 sec sonication pulse (Sonic Diesmembrator Model 300, Fisher Scientific, Pittsburgh, USA, 30% power with a micro-tip) followed by a 2 min cooldown on ice. This produced DNA fragments of approximately 200 to 400 bp in size. To remove cellular debris, the sonicated lysate was centrifuged at 10,000 × g at 4ºC for 15 min in an SA-600 rotor.

The supernatant was transferred to a fresh 2 mL LoBind tube (Eppendorf, Germany) and snap-frozen in liquid nitrogen. We refer to this supernatant as ChIP lysate. The ChIP lysate could be stored at -80ºC for several months. The concentration of ChIP lysates was adjusted to 2 mg protein per 750 µL before subsequent operations.

Before immunoprecipitation from the ChIP lysate, the protein A agarose beads (Invitrogen, Carlsbad, USA) used for antibody binding were blocked. 480 µL beads were washed twice in 500 µL Phosphate Buffered Saline (PBS, 137 mM NaCl, 2.7 mM KCl, 10 mM Na_2HPO_4, 2 mM KH_2PO_4 [pH7.4]), and then incubated in 1 mL FA lysis buffer containing 100 µg/mL bovine serum albumin (BSA, Sigma-Aldrich, St. Louis, USA) (dissolved in FA lysis buffer) and 100 µg/mL boiled sonicated salmon sperm DNA. The mixture was rocked at 4ºC overnight. Beads were pelleted at 4,000 × g (6,300 rpm in Sorvall Biofuge® fresco centrifuge) for 2 min at 4°C and 520 µL of the supernatant was removed to bring the volume back to 480 µL.

To prepare a pre-cleared ChIP lysate, 60 µL of blocked beads (in BSA and salmon DNA) were first incubated with 750 µL ChIP lysate at 4ºC for 5 to 7 hr by constant rocking. The beads were then removed from the lysate by centrifugation at 4,000 × g (6,300 rpm in Sorvall Biofuge® fresco centrifuge) for 2 min at 4°C. The beads were discarded and the pre-cleared lysate was transferred to a fresh 1.5 mL LoBind tube (Eppendorf, Germany) and either 24 µL anti-HA or 6 µL anti-Myc antibody (catalogue number of HA antibody: H98-63R-100; catalogue number of anti-Myc antibody: M86-61M-100, SignalChem, Canada) was added. Binding of antigen to the added antibodies was achieved by overnight incubation at 4ºC with gentle rocking. The next day, 60 µL of the blocked protein A agarose beads were added and the mixture was continuously rocked for 6 to 7 hr longer to allow the antibody to bind to the beads. The beads were then pelleted at 4,000 × g (6,300 rpm in

Sorvall Biofuge® fresco centrifuge) for 2 min at 4°C and the supernatant was removed. The beads were then consecutively washed one time in 1 mL low salt washing buffer (0.1% [w/v] SDS, 1% [v/v] Triton X-100, 2 mM EDTA, 150 mM NaCl, 20 mM Tris-HCl [pH8.0]), one time in 1 mL high salt washing buffer (0.1% [w/v] SDS, 1% [w/v] Triton X-100), 20 mM Tris-HCl [pH8.0], 500 mM NaCl), one time in 1 mL LNDET (0.25 M LiCl, 1% [w/v] NP40 (Sigma-Aldrich, St. Louis, USA), 1 mM EDTA, 10 mM Tris-HCl [pH8.0]), and two times in 1 mL TE buffer (1 mM EDTA, 10 mM Tris-HCl [pH8.0]). For each wash, beads were rocked for 5 min at 4°C after addition of buffer. After the washes, proteins and genomic DNA that was bound to the beads were eluted by adding 400 µL elution buffer (25 mM Tris-HCl [pH7.5], 10 mM EDTA, 0.5% [w/v] SDS) and incubating the tube in a 65ºC water bath for 30 min. The tube was inverted several times every 10 min to mix the buffer and the beads. The beads were then pelleted by centrifugation 4,000 × g (6,300 rpm in Sorvall Biofuge® pico centrifuge) at room temperature and the supernatant was transferred to a 1.5 mL LoBind tube. To reverse cross-linking between tagged proteins and the bound genomic DNA, 16 µL of 5 M NaCl was added to the supernatant followed by overnight incubation in a 65ºC water bath.

After reversal of cross-linking, the tagged protein-DNA mixture was treated with 2 µL of 10 mg/mL protease K (Roche, Basel, Switzerland) in a 45ºC water bath for 2 hr to degrade proteins. The sample was then extracted with 400 µL phenol-chloroform (1:1 [v/v]) (both from Fisher Scientific, Pittsburgh, USA) by vortexing for 10 sec. After centrifugation at 13,000 rpm (16,000 × g) for 1 min in a Sorvall Biofuge® pico centrifuge the top (aqueous) layer was transferred to a 1.5 mL LoBind tube and 40 µL (1/10 volume) of 3 M sodium acetate (pH5.2), 1 µL glycogen (Roche, Basel, Switzerland), and 1 mL 95% ethanol were added. The tube was inverted

several times and kept at -80ºC for 1 hr. The frozen tube was centrifuged at 13,000 rpm (16,000 × g) for 30 min at 4ºC in Sorvall Biofuge® fresco centrifuge to precipitate the ChIP DNA. The DNA pellet was washed once with 70% ethanol. The pellet was dried at room temperature for 5 to 10 min. The DNA was dissolved in 10 µL sterile MilliQ water or DNase-free water (IDT, Coralville, USA) and stored at -80ºC. The concentration of DNA was measured using a Qubit® Fluorometer (Invitrogen, Carlsbad, USA) following the manufacturer's instructions. Usually the yield of the ChIP DNA was approximately 10 ng.

To obtain DNA fragments with an average size of 200 bp, the ChIP DNA was sent to Delta Genomics for further sonication using the Covaris S2 system. The operation conditions and settings in the Application Software were as follows:

Intensity: 5

Duty cycle: 10%

Cycle per Burst: 200

Treatment Time: 3 cycles and 60 sec per cycle

Temperature: 7ºC

Power Mode: frequency sweeping

AFA Intensifier: yes

Before Covaris sonication, the volume of the DNA solution was brought up to 120 µL using TE buffer (1 mM EDTA, 10 mM Tris-HCl [pH8.0]). After sonication, the volume of the DNA solution was reduced to approximately 60 µL via evaporation in a clean fumehood for 8 to 10 hr. The concentration of DNA was then measured using a Qubit® Fluorometer. The final concentration of ChIP DNA was adjusted to 5 to 10 ng per 50 µL and samples were sent to Delta Genomics (Edmonton, Alberta, Canada). Delta Genomics used the Illumina® TruSeq® ChIP

Sample Preparation Kit (Illumina, San Diego, USA) for library preparation. They then used the Illumina sequence platform to sequence the ChIP DNA library. The sequence data for determination of binding sites of AOD2 following growth in the presence of CM were obtained using an Illumina HiScan SQ with read lengths of 51 nucleotides. All other data was obtained using an Illumina HiSeq2000 with read lengths of 101 nucleotides.

ChIP-seq was performed on eight separate samples. Four of these were from strains AOD2-C-HA-8 and AOD5-C-Myc-4 each grown in both the presence and absence of CM, and four were from a wild-type control (NCN251) which contains no tagged proteins grown under the same conditions. This resulted in four data sets when controls were subtracted from experimental results.

2.25 Analysis of ChIP-seq data

Raw sequence data from Delta Genomics was sent to our collaborators (Kristina Smith, Erin Bredeweg, Michael Freitag) at Oregon State University. Each set of experimental versus control data was analyzed using MACS2 (Zhang *et al.* 2008). The false discovery rate (FDR, q-value) cut-off was set to 0.05. The definition of FDR and it calculation was as decribed in Zhang *et al.* 2008, Johnson *et al.* 2006, and Song *et al.* 2007. Data was aligned with the *N. crassa* genome sequence in GBrowse (Stein *et al.* 2002).

2.26 Peaks count relative to translation start sites (TSS)

The distance of each ChIP-seq peak relative to the TSS was withdrawn from the ChIP-seq data files (generated by MACS2 by Kristina Smith, Erin Bredeweg, Michael Freitag). The distances were sorted from -10,000 bp to 10,000 bp in order

using Microsoft Excel. The numbers of peaks in 100-bp windows were counted using the FREQUENCY function in Microsoft Excel. The number of peaks in each window was then plotted on a graph. Peaks that are more than 10,000 bp away (either upstream or downstream) from a gene were excluded from the plots.

2.27 Standard techniques

Standard protocols were used for determination of protein concentration using the Bio-Rad protein assay reagent (Hercules, USA), agarose gel electrophoresis (Sambrook & Russell 2001), *E. coli* chemical transformation (Sambrook & Russell 2001), Sanger sequencing (performed by the Molecular Biology Service Unit), PCR reaction using *Pfu* DNA polymerase (Thermo Scientific, Rockford, USA), and nucleic acids concentration measurement using a Nanodrop ND 1000 spectrophotometer (Thermo Scientific, Rockford, USA). Plasmid DNA was extracted from *E. coli* cells using GeneJET miniprep kits according to the supplier's instructions (Thermo Scientific, Rockford, USA).

3 Results

3.1 Characterization of AOD2 and AOD5

3.1.1 Cellular localization of AOD2 and AOD5 under AOX inducing and non-inducing conditions

A major goal of this work was to gain insight into how AOD2 and AOD5 activate transcription of *aod-1*. As a first step towards this goal I wished to determine the cellular location of these transcription factors under conditions that both do, and do not, induce expression of *aod-1*.

It should be noted that the possibility of the *aod-2* and *aod-5* genes themselves being transcriptionally regulated in response to a signal from dysfunctional mitochondria seemed unlikely, since it had been previously shown that the levels of their mRNAs did not change dramatically between inducing and non-inducing conditions (Chae *et al.* 2007b). It was also conceivable that the AOD2 and/or AOD5 proteins would not be synthesized under non-inducing conditions due to a translational control mechanism. Although the possibility was not directly addressed, evidence from the experiments described below strongly suggests that this is not the case.

3.1.1.1 Tagging AOD2 and AOD5 with HA and Myc epitopes

Antibodies against AOD2 and AOD5 are not available. Therefore, to track the location of the proteins, I developed constructs of the *aod-2* and *aod-5* genes encoding three repeated 3× hemagglutinin (HA) epitopes or 3× c-Myc (Myc) epitopes at either the 5’ or 3’ end of their coding sequences. These constructs also contained more than 500 bp of the endogenous gene sequence both upstream and downstream of the coding sequence. To allow selection in *N. crassa* the constructs were cloned into a

plasmid that contained a hygromycin resistance cassette (Staben *et al.* 1989) (see section 2.3 for details). The resulting plasmids were transformed into the corresponding *aod-2* or *aod-5* mutant strains (CNA33 and PL23-40) respectively. Groups of transformants were named after the protein, with a one letter symbol for the tagged terminus, and the type of tag. Thus, there were eight different groups AOD2-N-HA, AOD2-C-HA, AOD2-N-Myc, AOD2-C-Myc, AOD5-N-HA, AOD5-C-HA, AOD5-N-Myc, and AOD5-C-Myc. Individual transformants were distinguished by isolation numbers following the group transformation name. At least 25 individual colonies that were able to grow on medium containing hygromycin were selected from each of the eight transformations and inoculated into hygromycin-containing slants. Only those that showed normal conidiation on these slants were chosen for further work. These transformants were then purified by single colony isolation as described in section 2.4. The single colonies in each transformation group were analyzed further.

The first step in the analysis of transformants was to determine if the *aod-2* or *aod-5* defects had been rescued. This was done by checking for the ability of the transformants to produce wild-type levels of AOX under inducing conditions. The first transformants analyzed were from the AOD2-N-HA group. Seven transformants were grown in the presence of CM. Mitochondria were isolated and analyzed on Western blots to determine if AOX could be induced. All seven transformants were found to contain AOX at or near wild-type levels (Fig. 3.1A). Crude nuclei were then prepared to determine if HA-tagged AOD2 could be detected. The predicted size of AOD2 with the 3× HA tag was 60.6 kDa. A band was seen at approximately this molecular weight, but this band was also present in a non-HA-tagged control (Fig. 3.1B). However, a strong band that was not present in the control was observed in all

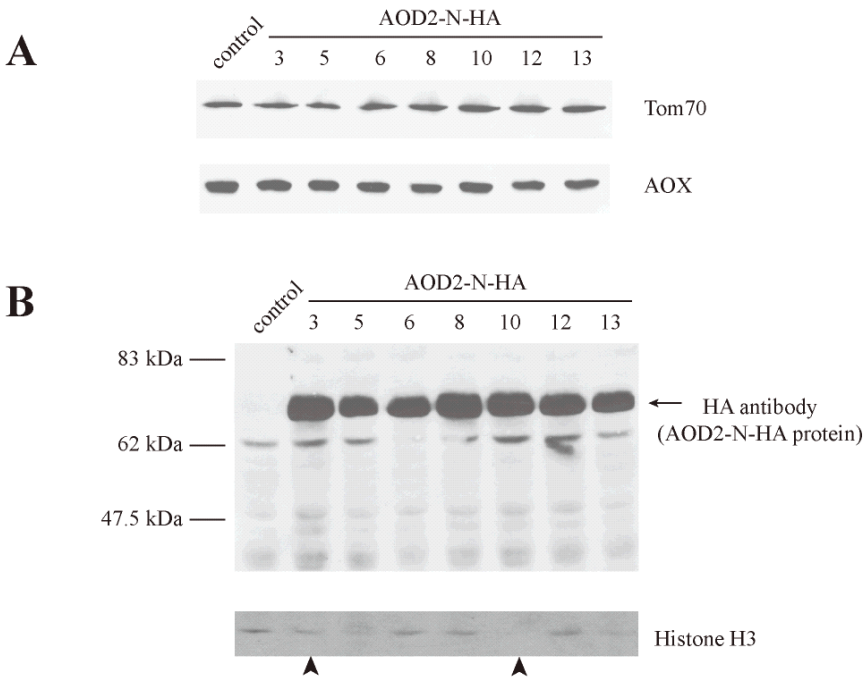

Figure 3.1. Initial examination of AOD2-N-HA transformants. A. A plasmid construct containing N-terminal 3× HA tagged *aod-2* was transformed into an *aod-2* mutant strain (CNA33) and seven transformants that exhibited good conidiation were examined for their ability to express AOX. Strains were grown in the presence of CM and mitochondria were isolated. Mitochondrial proteins were subjected to SDS-PAGE, blotted to nitrocellulose and analyzed by Western blot. The MOM protein Tom70 was used as a loading control. The control strain was the wild-type strain NCN251. B. AOD2-N-HA transformants were examined for the presence of 3× HA tagged AOD2. Crude nuclei were isolated from cells grown in the absence of CM. Nuclear proteins were extracted, subjected to SDS-PAGE, blotted to nitrocellulose, and examined by Western blot. Histone H3 was used as a loading control. Antibodies used are indicated on the right. The control strain was as for panel A. Arrowheads point to the transformants that were selected for further work. The arrow on the right indicates the position of AOD2-N-HA protein. Molecular weight markers for the HA blot are indicated on the left.

the transformants between the 62 and 83 kDa markers. Thus, it seems likely that this band represents HA-tagged AOD2. The size of the band was calculated to be about 70 kDa. Strains AOD2-N-HA-3 and AOD2-N-HA-10 were chosen for further work. A similar analysis was done for the AOD2-C-HA set of transformants (Supplementary Fig. 3.1). Again, the 70 kDa band was observed in all transformants. Strain AOD2-C-HA-8 was chosen for further analysis.

Analysis of the AOD2-N-Myc transformants showed that none of the nine transformants analyzed were capable of inducing AOX to wild-type levels following growth in CM (Supplementary Fig. 3.2). Transformants from this group were not pursued further. Analysis of more transformants may have yielded a usable strain, but given the relatively high success rate in the other groups, this seemed unlikely. It is not known why this group failed to produce rescued strains but it is conceivable that the 3× Myc tag at the N-terminus of AOD2 interferes with the function, stability, or targeting of the protein. The AOD2-C-Myc transformants were capable of expressing AOX at wild-type levels (Supplementary Fig. 3.3). The Myc Western blots sometimes showed non-specific bands at both 63 kDa and 82 kDa. However, a band of 70 kDa, similar to the size seen for HA-tagged AOD2 transformants, was also observed. Strain AOD2-C-Myc-4 was chosen for further work.

Several transformants of the AOD5-C-HA group were able to induce AOX to wild-type or near wild-type levels (Fig. 3.2A). Crude nuclear preparations of AOD5-C-HA transformants showed no band near the predicted molecular weight of the tagged AOD5 protein (83.3 kDa). However, a band specific to two transformants, and not present in the HA untagged control, was visible above the 83 kDa marker (Fig. 3.2B left panel). The size of this band was calculated to be about 100 kDa. A similar sized band was observed in other transformants (Fig. 3.2B right panel). Strain

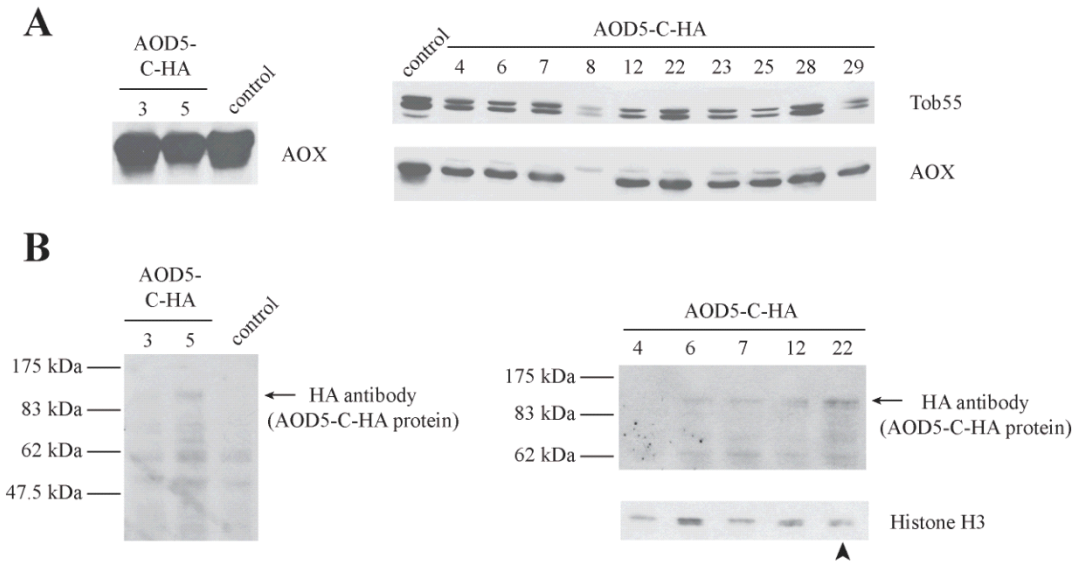

Figure 3.2. Initial examination of AOD5-C-HA transformants. A. A plasmid construct containing a C-terminal 3× HA tagged *aod-5* was transformed into an *aod-5* mutant strain (PL23-40) and 12 transformants that exhibited good conidiation were examined for their ability to express AOX. Strains were grown in the presence of CM and mitochondria were isolated. Mitochondrial proteins were subjected to SDS-PAGE, blotted to nitrocellulose and analyzed by Western blot. The MOM protein Tob55 was used as a loading control. (Tob55 appears as a doublet because alternative splicing of its transcript gives rise to different versions of the protein (Hoppins *et al.* 2007)). The control was the wild-type strain NCN251. B. Several AOD5-C-HA transformants were examined for the presence of 3× HA tagged AOD5. Crude nuclei were isolated from cells grown in the absence of CM. Nuclear proteins were extracted, subjected to SDS-PAGE, blotted to nitrocellulose, and examined by Western blot. Histone H3 was used as a loading control. Antibodies used are indicated on the right. The control was as for panel A. Arrowhead points to the transformant that was selected for further work. The arrow indicates the position of AOD5-C-HA protein. Molecular weight markers for the HA blots are indicated on the left.

AOD5-C-HA-22 was chosen for further work. Similar analysis on AOD5-N-HA transformants also detected a band of 100 kDa (Supplementary Fig. 3.4). Strain AOD5-N-HA-1 was chosen for further work.

Several AOD5-C-Myc transformants were capable of producing wild-type levels of AOX (Supplementary Fig. 3.5A). Initial attempts to detect tagged AOD5 in the AOD5-C-Myc group, showed that a band of approximately 85 kDa, close to the predicted size of the protein, was present. However, this band was also present in the Myc untagged control lane (Supplementary Fig. 3.5B). Subsequent analysis showed a band at 100 kDa that was not present in the control non Myc tagged strain (Supplementary Fig. 3.5B). The band is similar in size to that detected in the AOD5 HA tagged transformants (Fig. 3.2B). AOD5-C-Myc-4 was chosen for further work. Transformants in the AOD5-N-Myc group were able to produce varying levels of AOX (Supplementary Fig. 3.6A). Strains AOD5-N-Myc-10 and -12 were judged to produce AOX at or near wild-type levels. However, no unique Myc tagged protein was observed in crude nuclei of these strains (Supplementary Fig. 3.6B) and no further work was done with these strains.

3.1.1.2 Cell fractionation to localize AOD2 and AOD5

The AOD2-N-HA-10 strain was selected for cell fractionation experiments. Cells were grown in both the presence and absence of CM. Cultures were harvested and gradient purified nuclei and mitochondria were isolated (described in section 2.6 - 2.9). In addition, cytosolic and microsomal fractions were isolated (described in section 2.10). The fractions were subjected to SDS-PAGE and analyzed on Western blots. Histone H3, Arginase, Tom70, and Kar2 were used as markers for the nuclear, cytosolic, mitochondrial, and microsomal fractions, respectively. Fractions were also

analyzed for the presence of AOX to further demonstrate inducibility of AOX in the tagged constructs. The results (Fig. 3.3A) showed that each fraction was almost free from contamination by the other fractions, although the microsomal protein Kar2 was also found in the nuclear fraction. This is likely a reflection of the contiguous relationship of the ER and nuclear membranes. AOD2 was only detected in the nuclear fraction. It was found in nuclei isolated from cells grown under both inducing (+CM) and non-inducing (-CM) conditions (Fig 3.3A). The levels of AOD2 were similar in both conditions. AOX was present in mitochondria isolated from both the control strain and the AOD2-tagged strain only when cultures were grown under inducing conditions (+CM). Similar results were obtained from AOD5-N-HA-1 cell fractions. AOD5 was also shown to occur only in the nucleus (Fig 3.3B).

Although the above results showed nuclear localization of AOD2 and AOD5, it was possible that the N-terminal HA epitope tags interfered with the native localization of the proteins. In an attempt to rule out this possibility, I used the AOD2-C-HA-8 and AOD5-C-Myc-4 strains to repeat the cell fractionation experiments. As seen with the N-terminal tagged proteins, both of the C-terminal tagged AOD2 and AOD5 proteins were detected exclusively in the nuclear fraction. Nuclear localization was again seen to be independent of the presence or absence of CM in the growth medium (Fig. 3.3C, D). Similar amounts of both proteins were present in both +CM and –CM conditions. Taken together, the results show that AOD2 and AOD5 localize to the nucleus under both AOX inducing and non-inducing growth conditions. The amount of each protein is similar in both growth conditions. An unknown protein band seen in the cytosolic fraction of the anti-AOX blot was observed (arrows on cytosolic lanes of Fig. 3.3 A, B, C, D examined by the AOX antibody). Given its slightly larger molecular weight compared to the mature AOX

Figure 3.3. Localization of AOD2 and AOD5. A. AOD2-N-HA-10 was grown in both the presence or absence of CM. Gradient purified nuclei and mitochondria were isolated, as well as cytosolic and microsomal fractions. The wild-type strain, NCN251, served as a non-tagged control. Fractions were subjected to SDS-PAGE and proteins were transferred to nitrocellulose membrane for Western blot analysis. AOD2 was detected using antibodies against the HA tag. Other antibodies served to detect markers for the different cellular fractions as indicated on the right of the panel. Molecular weight markers for one of the HA blots are indicated on the left. B. As described for panel A using fractions isolated from strain AOD5-N-HA-1. Molecular weight markers are indicated on the left of the HA blot. C. As described for panel A using fractions isolated from strain AOD2-C-HA-8. Molecular weight markers are indicated on the left of the HA blot. D. As described for panel A using fractions isolated from strain AOD5-C-Myc-4. Detection of the tagged AOD5 protein was achieved with an antibody directed against the Myc tag. In all four panels, arrows indicate unexpected bands in the cytosolic fractions that were detected by the AOX antibody. The bands have a slightly higher molecular weight than mature processed AOX (section 3.1.1.2 and Appendix III).

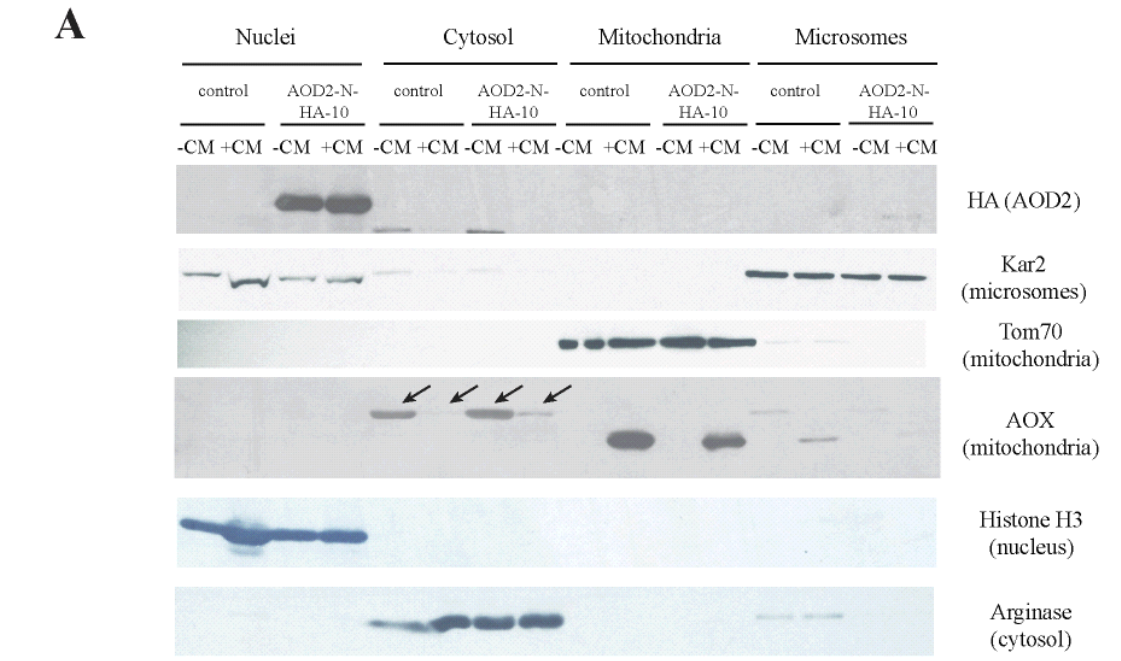
A
Nuclei
Cytosol
Mitochondria
Microsomes
control
AOD2-N-HA-10
-CM +CM
HA (AOD2)
Kar2 (microsomes)
Tom70 (mitochondria)
AOX (mitochondria)
Histone H3 (nucleus)
Arginase (cytosol)

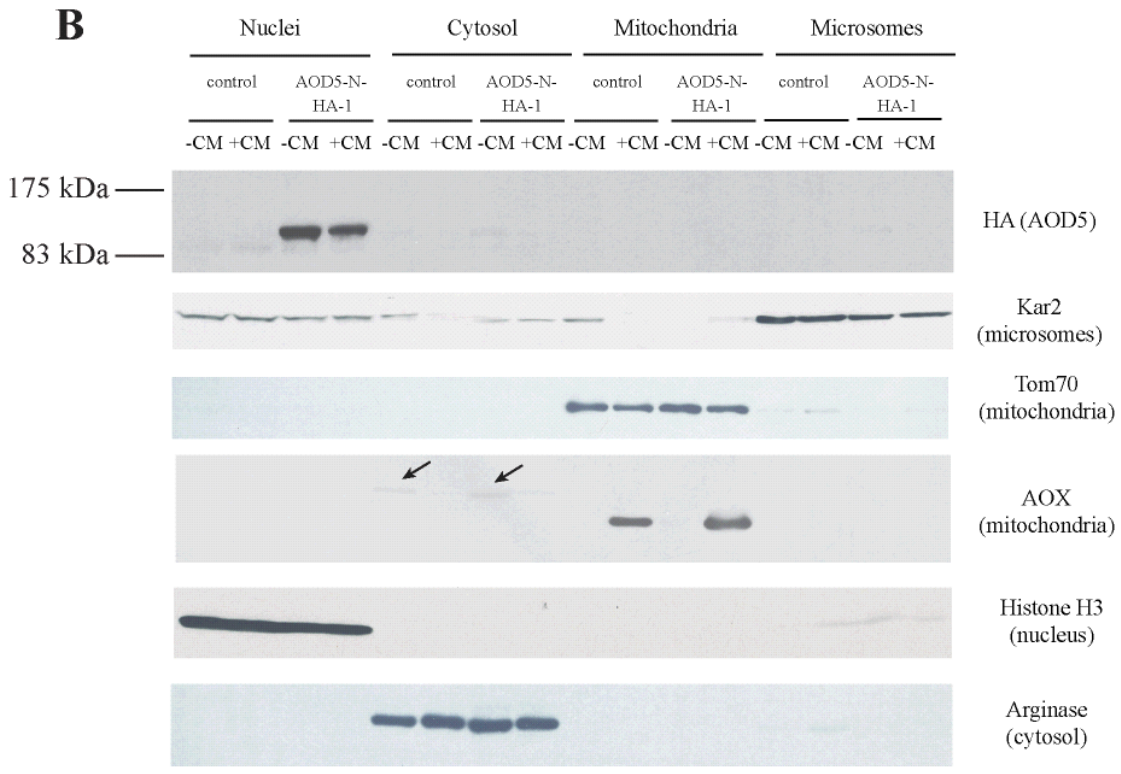
B
Nuclei
Cytosol
Mitochondria
Microsomes
control
AOD5-N-HA-1
-CM +CM
175 kDa
83 kDa
HA (AOD5)
Kar2 (microsomes)
Tom70 (mitochondria)
AOX (mitochondria)
Histone H3 (nucleus)
Arginase (cytosol)

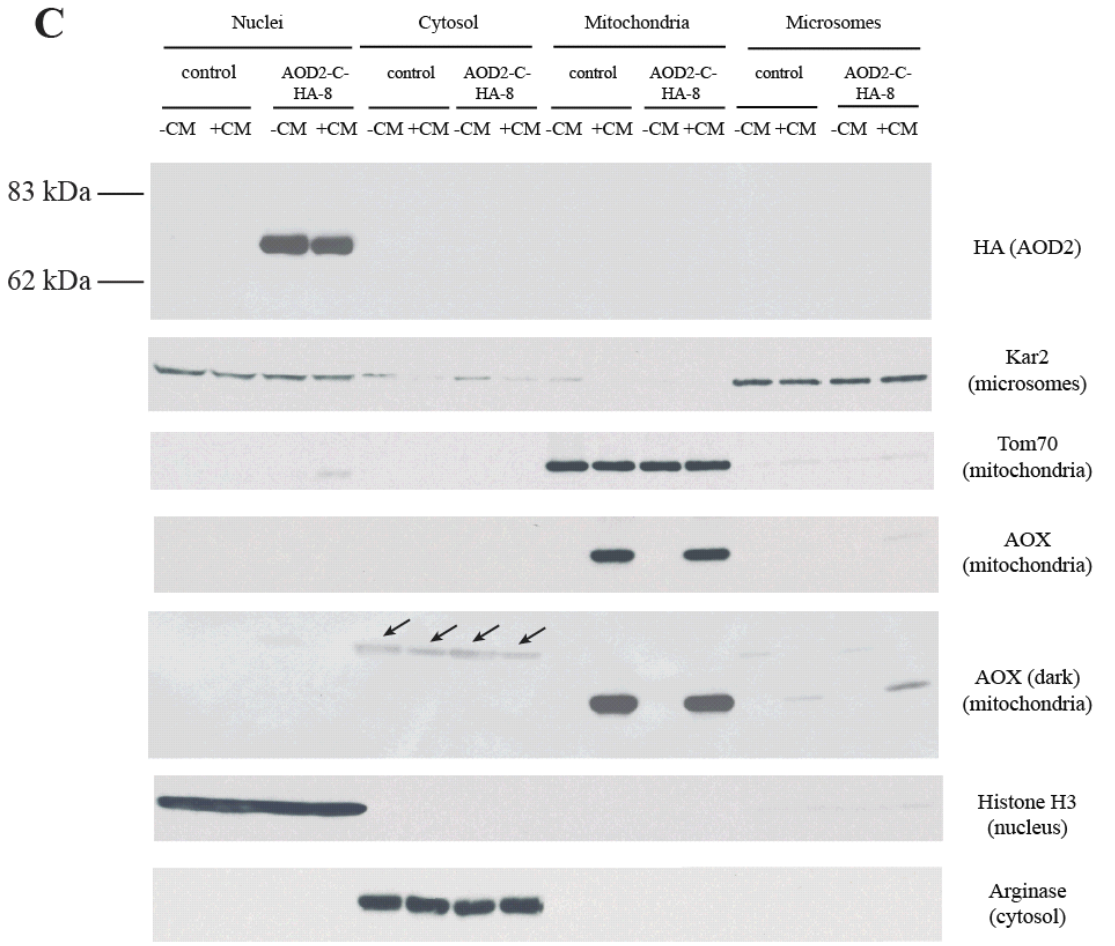
C
Nuclei
Cytosol
Mitochondria
Microsomes
control
AOD2-C-HA-8
-CM +CM
83 kDa
62 kDa
HA (AOD2)
Kar2 (microsomes)
Tom70 (mitochondria)
AOX (mitochondria)
AOX (dark) (mitochondria)
Histone H3 (nucleus)
Arginase (cytosol)

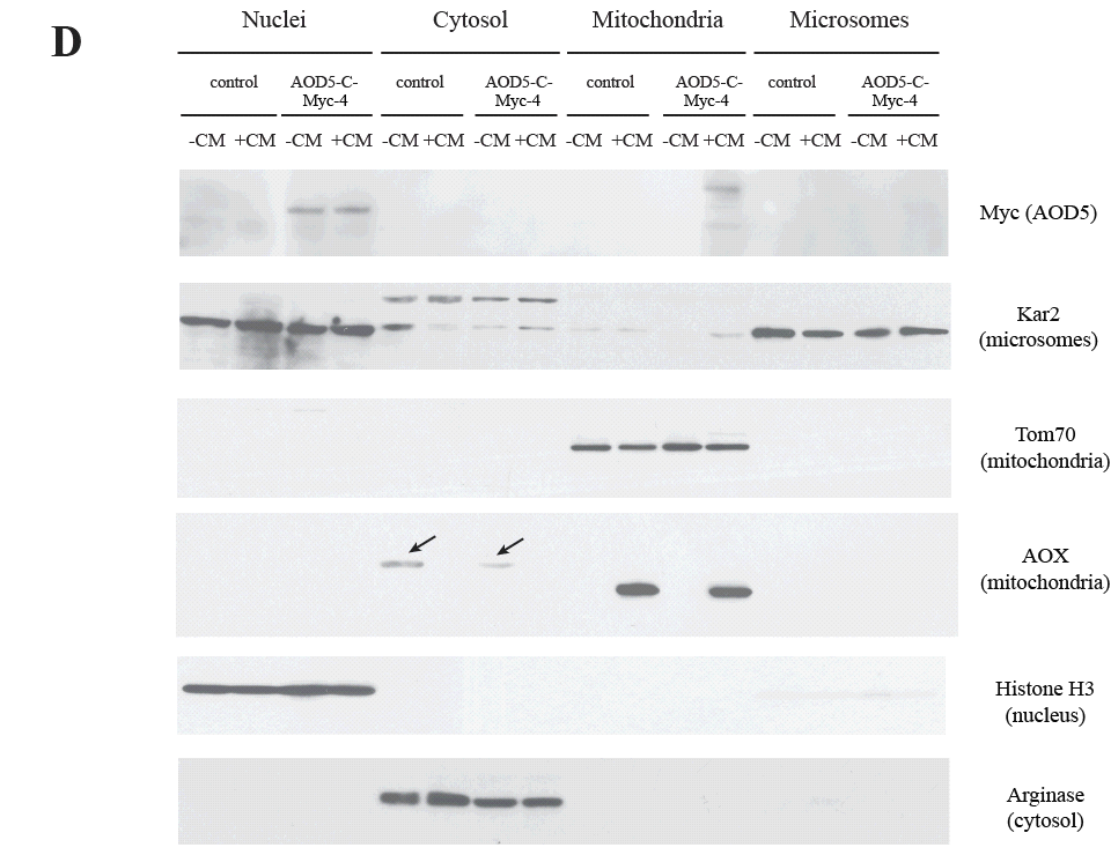
D
Nuclei
Cytosol
Mitochondria
Microsomes
control
AOD5-C-Myc-4
-CM +CM
Myc (AOD5)
Kar2 (microsomes)
Tom70 (mitochondria)
AOX (mitochondria)
Histone H3 (nucleus)
Arginase (cytosol)

seen in the mitochondria, I hypothesized that it might represent unprocessed AOX still containing its mitochondrial targeting signal (predicted molecular weight of AOX processed = 34.7 kDa, unprocessed = 41.3 kDa (Li *et al.* 1996)). This was of particular interest since the band usually seemed more prevalent in the cultures grown in non-inducing conditions. Thus, it was possible that AOX was synthesized but prevented, by some mechanism, from entering mitochondria. Another possibility was that it represented the AOD3 protein (Tanton *et al.* 2003) (predicted molecular weight of AOD3 processed = 37 kDa, unprocessed = 42.3 kDa). These possibilities were investigated by examining cytosolic fractions from double Δ*aod-1* Δ*aod-3* mutants. No evidence for either of these possibilities was found to be true since the bands were still present in the cytosolic fractions of the double mutant (Appendix III).

3.1.2 *In vivo* interaction between AOD2 and AOD5

Previous *in vitro* electrophoretic mobility shift assay (EMSA) experiments by Michael Chae in the Nargang lab showed that the DNA binding domains of both AOD2 and AOD5 must be present for binding to the AIM sequence in the *aod-1* promoter region (Chae *et al.* 2007b). A physical interaction between the proteins *in vitro* was also shown (Chae & Nargang 2009). To confirm that this interaction also occurs *in vivo*, I performed a co-immunoprecipitation (co-IP) experiment. Plasmids, which contained the *aod-2* gene with the 3× Myc tag just before the stop codon and the *aod-5* gene with the 3× HA tag just after the start codon (as described in section 2.4) were co-transformed into an *aod-2 aod-5* double mutant (DX13). Both plasmids also contained a hygromycin resistant gene. Transformants were selected either on medium containing antimycin A or hygromycin. Transformants AOD2-C-Myc AOD5-N-HA numbers A1, A2, A3, A5, and A6 were selected from antimycin

A-containing medium, whereas transformants AOD2-C-Myc AOD5-N-HA numbers 3, 5, 14, 18, and 19 were chosen from hygromycin-containing medium. All these strains were examined for AOX content following growth in the presence of CM. Surprisingly, strains A2 and A6, which were resistant to antimycin A, exhibited no AOX proteins in +CM mitochondria (Fig. 3.4A). The reason is unknown. Strains 3, 5, and 14 examined from the hygromycin resistant transformants also showed no AOX following growth in CM (Fig. 3.4A). However, strains A1, A3, 18, 19 appeared to express normal AOX levels (Fig. 3.4A). Moreover, the AOD5-N-HA and AOD2-C-Myc tagged proteins were detected in crude nuclei from all four strains (Fig. 3.4B). I selected strain AOD2-C-Myc AOD5-N-HA A1 for co-IP experiments.

The A1 strain was then grown in the presence and absence of CM, and nuclear proteins were extracted from crude nuclei (section 2.6). Immunoprecipitation was performed for AOD2-C-Myc with Myc antibody. The Western blot showed that the proteins eluted from the co-IP contained AOD2-C-Myc and AOD5-N-HA regardless of whether cells were grown under inducing or non-inducing conditions (Fig. 3.5A). In the reciprocal experiment, where AOD5-N-HA was immunoprecipitated from extracted nuclear proteins with HA antibody, AOD2-C-Myc was also eluted (Fig. 3.5B). These data strongly suggest that AOD2 and AOD5 do interact with each other *in vivo*.

3.1.3 Search for post-translational modifications of AOD2 and AOD5 in response to AOX inducing conditions

One hypothesis to explain the change in activity of AOD2 and/or AOD5 that occurs under inducing conditions is that they are post-translationally modified. One possible modification is phosphorylation. In *S. cerevisiae*, the homologue of AOD2

Figure 3.4. Examination of AOD2-C-Myc AOD5-N-HA transformants. Linearized plasmid constructs p*aod-2*hyg C-Myc and p*aod-5*hyg N-HA were cotransformed into the *aod-2 aod-5* double mutant DX13 strain and transformants were selected on medium containing either antimycin A (those designated with an "A" followed by a number) or hygromycin (those with a number only). A. Mitochondria were isolated from the indicated strains following growth in the presence of CM. The control is the wild-type strain NCN251. Proteins were subjected to SDS-PAGE and AOX levels were examined by Western blot with Tom70 serving as a loading control. B. Four transformants were tested for the presence of HA and Myc tagged proteins. Cultures were grown in the presence of CM and crude nuclei were isolated. Extracted nuclear proteins were subjected to SDS-PAGE and Western blot analysis using antibodies to the HA or Myc tag as appropriate. The control strain is the untransformed *aod-2 aod-5* double mutant strain DX13. Each lane contains the extract from crude nuclei containing 30 μg of nuclear protein. Arrows indicate the tagged AOD2 or AOD5 protein. Arrowheads point to the transformant that was selected as a representative AOD2-Myc AOD5-HA double tagged strain. Molecular weight markers for the HA and Myc blot are indicated on the left.

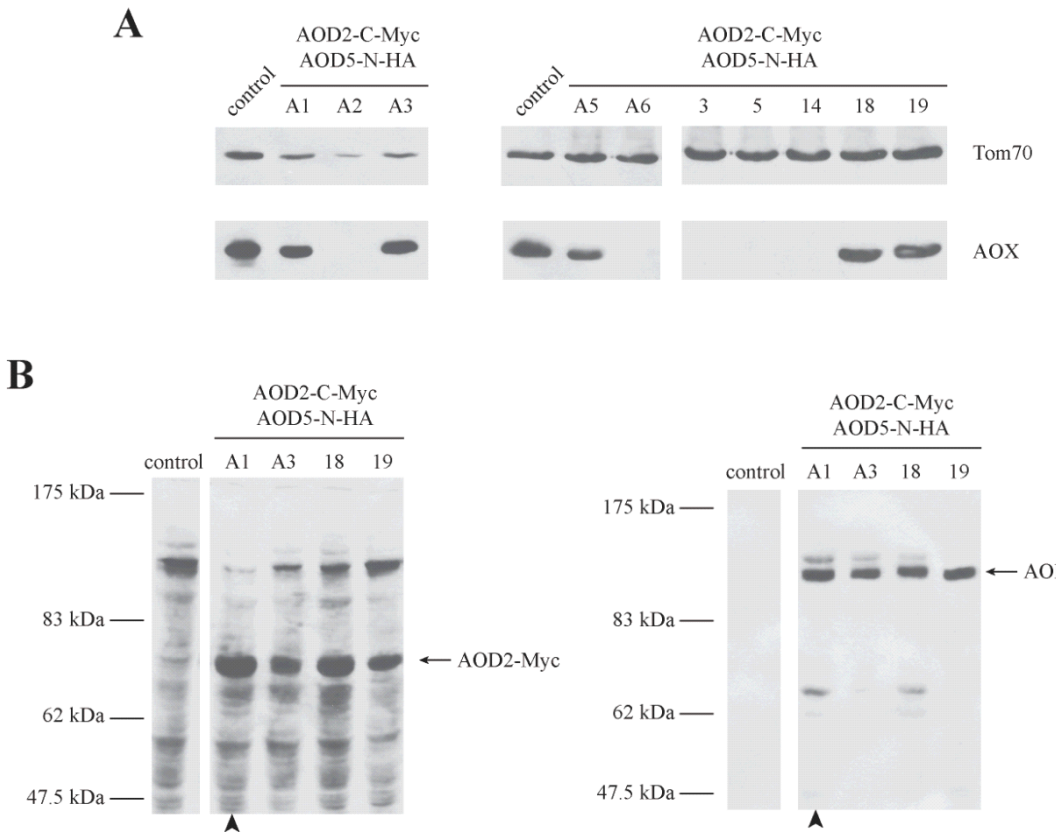
A
AOD2-C-Myc
AOD5-N-HA
control
A1
A2
A3
AOD2-C-Myc
AOD5-N-HA
control
A5
A6
3
5
14
18
19
Tom70
AOX
B
AOD2-C-Myc
AOD5-N-HA
control
A1
A3
18
19
175 kDa
83 kDa
62 kDa
47.5 kDa
AOD2-Myc
AOD2-C-Myc
AOD5-N-HA
control
A1
A3
18
19
175 kDa
83 kDa
62 kDa
47.5 kDa
AOD5-HA

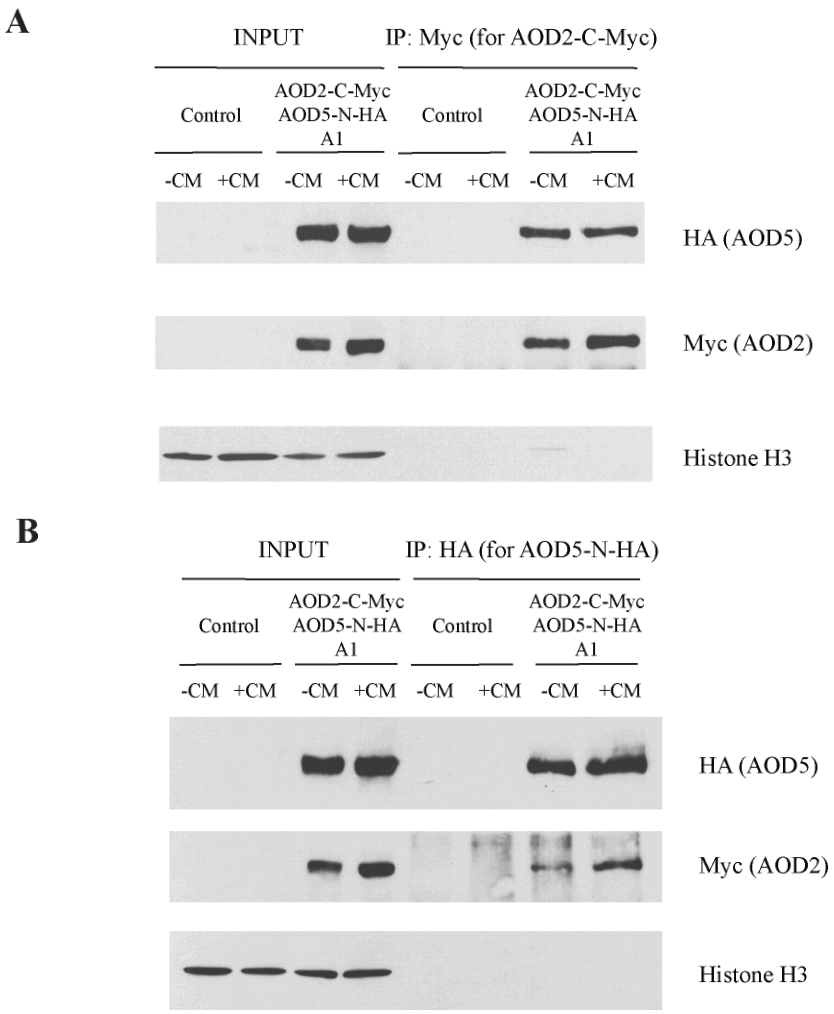

Figure 3.5. *In vivo* interaction between AOD2 and AOD5. Mycelium was harvested and gradient purified nuclei were isolated from the AOD2-C-Myc AOD5-N-HA A1 transformant, and a wild-type control (NCN251), following growth in both the presence and absence of CM. The A1 strain expresses both the AOD2-C-Myc and AOD5-N-HA tagged proteins. Immunoprecipitation (IP) was performed to pull down AOD2-C-Myc (panel A) or AOD5-N-HA (panel B) with anti-Myc and anti-HA antibodies, respectively. Elution fractions from the IPs were subjected to SDS-PAGE and the separated proteins were blotted to nitrocellulose membrane. The membranes were probed with the antibodies shown to the right of the panels. Histone H3 was used as a loading control.

(Rds2) is phosphorylated when cells use ethanol as the sole carbon source as compared to cells grown in glucose (Soontorngun *et al.* 2007). Depending on the number of phosphates added, a change in the phosphorylation status of a protein can sometimes be observed as a shift in molecular weight by traditional SDS-PAGE. However, I did not observe any mobility difference in the AOD2 or AOD5 proteins from cells grown in either inducing or non-inducing conditions in the cell fractionation experiments (Fig. 3.3). This suggests that no major change in the molecular weight of the AOD2 or AOD5 occurred upon AOX induction by growth in the presence of CM. To further investigate the phosphorylation status of AOD2 and AOD5, I used Phos-tag SDS-PAGE (Kinoshita *et al.* 2009). However, no consistent differences were observed (Appendix IV.1).

Since there are five cysteine residues C-terminal to the DNA binding domain of both AOD2 and AOD5, and because it is conceivable that growth in CM or other AOX inducers might lead to changes in the redox status of the cell, I also examined the proteins for changes in cysteine residue redox status following growth in either AOX inducing or non-inducing conditions. However, no differences were detected (Appendix IV.2).

3.2 The role of AOD2 and AOD5 in gluconeogenesis

3.2.1 Confirmation of the involvement of AOD2 and AOD5 in gluconeogenesis

As described in the introduction (section 1.10.9), studies in different fungi have identified a role for the orthologues of AOD2 and AOD5 in gluconeogenesis (Gasmi *et al.* 2014; Hynes *et al.* 2007; Liu *et al.* 2010; Sellem *et al.* 2009; Soontorngun *et al.* 2007). To determine if the proteins play a similar role in *N. crassa*, I investigated the growth rates of *aod-2* and *aod-5* mutant strains on various carbon sources. Δ*aod-2*

(97B1) and Δ*aod-5* (1C3) mutants from the *N. crassa* knock-out library were tested for growth in liquid medium containing 1.5% sucrose, 2% glycerol, 150 mM acetate, or 1% ethanol as the sole carbon source. Both mutants exhibited an approximate 40% reduction in the mass of mycelium produced following 24-hour growth in the presence of sucrose, suggesting at least some role(s) for AOD2 and AOD5 in growth in sucrose-containing medium. However, the growth relative to wild type was reduced to a much greater extent in glycerol (85%), acetate (92%), and in ethanol (99%) (Fig. 3.6A). These data indicated that AOD2 and AOD5 are both required for efficient use of these poor carbon sources.

Since it is known that AOD2 and AOD5 are transcriptional regulators for the synthesis of AOX in *N. crassa*, one possible explanation of the above data would be that AOX is required for efficient growth in poor carbon sources. Therefore, I also grew the Δ*aod-1* mutant (96H9) in media containing the same carbon sources. The *aod-1* mutant grew at near the rate of the wild-type strain in all conditions (Fig. 3.6A), thus eliminating the possibility that AOX itself plays a part in gluconeogenesis or growth on poor carbon sources.

3.2.2 Investigation of how AOD2 and AOD5 coordinate AOX induction and gluconeogenesis

The apparent involvement of *aod-2* and *aod-5* in gluconeogenesis lead me to ask if transcription of the genes encoding PEPCK and FBP are controlled by AOD2 and AOD5 as their orthologues do in *S. cerevisiae* (Gasmi *et al.* 2014; Soontorngun *et al.* 2007), *A. nidulans* (Hynes *et al.* 2007), and *P. anserina* (Bovier *et al.* 2014). These enzymes perform crucial steps in the gluconeogenic pathway that are not simply reversal of steps in glycolysis using the glycolytic enzymes (described in section 4.3).

Figure 3.6. Participation of AOD2 and AOD5 in the regulation of gluconeogenesis. A. The wild-type control strain (NCN251), and the Δ*aod-1* (96H9), Δ*aod-2* (97B1), and Δ*aod-5* (1C3) knockout strains were grown in medium containing 1.5% sucrose, 2% glycerol, 150 mM sodium acetate, or 1% ethanol. Mycelium was harvested from these cultures at 20 hr, 72 hr, 72 hr, and 96 hr, respectively, and weighed. The experiment was done in triplicate. Error bar, ±SEM. B-D. RT-qPCR was performed for the *aod-1* (panel B), PEPCK (panel C), and FBP (panel D) genes using total RNA isolated from the wild-type control strain (NCN251) and Δ*aod-2* grown in medium containing a variety of carbon sources, with or without CM, as indicated on the panels. Each experiment used four biological replicates and three technical replicates. The Student's t test was used to compare data between two different conditions. Error bar, ±SEM. n.s., not significant (p value $\geq$ 0.05). E. Mitochondria were isolated from the wild-type control strain (NCN251) and the knockout strains Δ*aod-1* and Δ*aod-2* grown in the presence or absence of CM, and in different carbon sources as indicated at the top of the panel. Mitochondrial proteins were subjected to SDS-PAGE and the proteins were transferred to nitrocellulose membranes. The blots were probed with the antibodies indicated on the right. A light and dark exposure are shown for AOX.

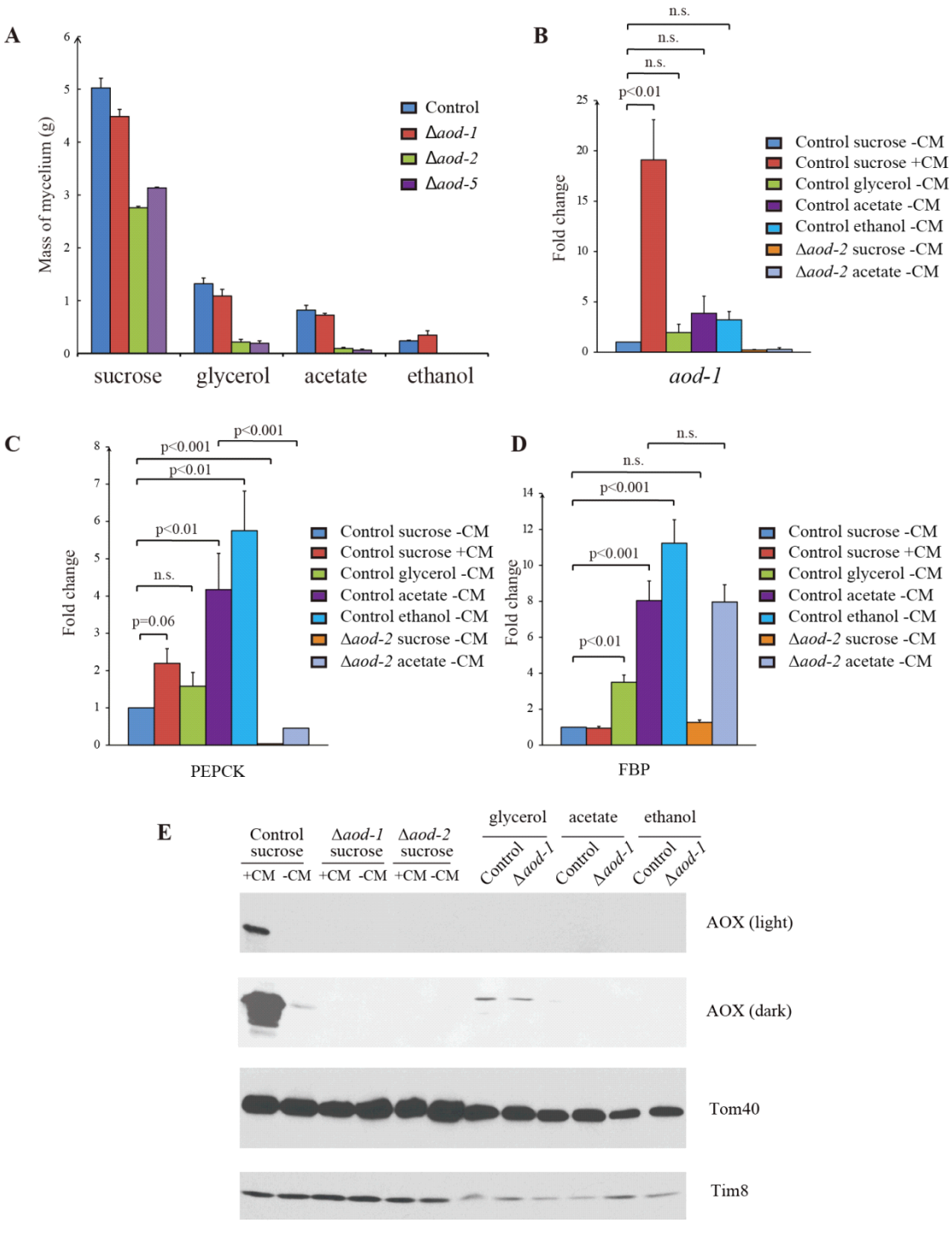
A
Mass of mycelium (g)
Control
Δaod-1
Δaod-2
Δaod-5
sucrose
glycerol
acetate
ethanol
B
n.s.
n.s.
n.s.
p<0.01
Fold change
Control sucrose -CM
Control sucrose +CM
Control glycerol -CM
Control acetate -CM
Control ethanol -CM
Δaod-2 sucrose -CM
Δaod-2 acetate -CM
aod-1
C
p<0.001
p<0.001
p<0.01
p<0.01
n.s.
p=0.06
Fold change
Control sucrose -CM
Control sucrose +CM
Control glycerol -CM
Control acetate -CM
Control ethanol -CM
Δaod-2 sucrose -CM
Δaod-2 acetate -CM
PEPCK
D
n.s.
n.s.
p<0.001
p<0.001
p<0.01
Fold change
Control sucrose -CM
Control sucrose +CM
Control glycerol -CM
Control acetate -CM
Control ethanol -CM
Δaod-2 sucrose -CM
Δaod-2 acetate -CM
FBP
E
Control sucrose
Δaod-1 sucrose
Δaod-2 sucrose
+CM -CM +CM -CM +CM -CM
glycerol
acetate
ethanol
Control
Δaod-1
Control
Δaod-1
Control
Δaod-1
AOX (light)
AOX (dark)
Tom40
Tim8

To address this question I grew wild-type strain NCN251 under various conditions (sucrose with or without CM, glycerol without CM, acetate without CM, and ethanol without CM) and measured the transcript levels for PEPCK, FBP, and *aod-1* using RT-qPCR. The results showed that the levels of *aod-1* transcript appeared to be slightly increased in all poor carbon sources (two to four fold) when compared to sucrose –CM, but the increases were not found to be statistically significant (Fig. 3.6B). About 19 fold increases in *aod-1* were observed following growth in sucrose +CM (Fig. 3.6B). On the other hand, the transcripts of PEPCK were slightly increased in sucrose +CM (two fold, just above the cutoff for statistical significance), and moderately increased in acetate –CM (four-fold) and ethanol –CM (five-fold) (Fig. 3.6C). There is apparently little induction of PEPCK in glycerol –CM. The rationale might be that the metabolism of glycerol does not require the function of PEPCK (see Fig. 4.1 in the discussion).

There was also no difference in expression for FBP following growth in sucrose with or without CM (Fig. 3.6D). Growth in poor carbon sources, in contrast, significantly induces the expression of the FBP transcript (Fig. 3.6D), which is consistent with the role that FBP plays in gluconeogenesis. Transcript levels were also measured following growth of the Δ*aod-2* strain in sucrose and acetate. A surprising observation was that while the induction of the *aod-1* and PEPCK transcripts were dependent on AOD2 (Fig. 3.6B and C), there appeared to be no effect on FBP transcript levels in the Δ*aod-2* strain (Fig. 3.6D). This demonstrates that AOD2 is not required for the induction of FBP in *N. crassa*. Since *aod-1* and PEPCK are induced to different extents in CM and poor carbon sources, these data also suggest that AOD2, and by extension its binding partner AOD5, are activated by different signals that result from growth in CM versus poor carbon sources.

It was of interest to know if the AOD1 protein was produced when cells are grown on poor carbon sources even though the transcript levels of *aod-1* are not altered significantly comparing to cells grown on sucrose. I isolated mitochondria from wild type and mutant strains and performed Western blot analysis for the presence of AOD1. As shown previously, AOD1 was readily detectable in mitochondria from strains grown in sucrose +CM (Fig. 3.6E). A small amount of AOX was also observed in sucrose –CM mitochondria after long exposure (Fig. 3.6E). On the other hand, AOD1 appeared to be absent in cultures grown in poor carbon sources (Fig. 3.6E).

3.3 Investigation of genome-wide binding of AOD2 and AOD5 by ChIP-seq

3.3.1 Summary of the ChIP-seq data by MACS2

Although I found that AOD2 and AOD5 localized to the nucleus under both –CM and +CM conditions, I was interested in knowing whether or not they are constitutively bound to the *aod-1* promoter. In addition, since they also appear to regulate the gluconeogenic gene PEPCK, it was of interest to investigate if they were bound to this promoter in cells grown in both the presence and absence of CM. Furthermore, the reduction in growth rate of the Δ*aod-2* and Δ*aod-5* mutants that was observed when sucrose was the carbon source, suggested that the proteins may have a wider role in gene expression. Thus, to obtain a fuller understanding of the function of AOD2 and AOD5, I performed chromatin immunoprecipitation assays in combination with next generation sequencing (ChIP-seq) using four sets of samples as shown in Table 3.1. Since no antibodies were available to AOD2 or AOD5, I utilized two of the strains described in the localization experiments (section 3.1.1.1). The strains chosen were AOD2-C-HA-8 and AOD5-C-Myc-4, which express a C-terminal HA

Table 3.1 Four experimental data sets of ChIP-seq.

Experiment	Strain	Protein-tag	Antibody used	CM	Mapped Reads (millions)	Peaks (>4 fold enrichment vs control)
	AOD2-C-HA-8	HA	HA	+	9.9	
1	wild-type (strain NCN251)	none	HA	+	6.9	217
	AOD2-C-HA-8	HA	HA	-	0.9	
2	wild-type (strain NCN251)	none	HA	-	1.4	303
	AOD5-C-Myc-4	Myc	Myc	+	3.3	
3	wild-type (strain NCN251)	none	Myc	+	2.5	754
	AOD5-C-Myc-4	Myc	Myc	-	2.0	
4	wild-type (strain NCN251)	none	Myc	-	1.3	243

tagged AOD2 and a C-terminal Myc tagged AOD5, respectively.

The tagged strains were grown in both the presence and absence of CM and processed as described in the Materials and Methods (section 2.24) using commercial antibodies to HA and Myc. The isolated DNA was used to develop libraries for next generation sequencing. As controls for non-specific binding of the antibodies, the same experiments were performed using the same antibodies with an untagged wild-type strain (NCN251). In each data set, the number of sequence reads that were mapped to the *N. crassa* genome is also shown in Table 3.1. Sequences were analyzed by our collaborators at Oregon State University (Kristina Smith, Erin Bredeweg, and Michael Freitag) using MACS2 software (Zhang *et al.* 2008) to call peaks and calculate p-values and false discovery rates (FDR, q-value) for the peaks. Peaks in controls were subtracted from the corresponding region of the experimental data sets for MAC2 analysis. Only those peaks with both p-value and q-value smaller than 0.05 were considered further. The data were placed in the context of the *N. crassa* genome sequence using GBrowse (Stein *et al.* 2002).

To determine whether the peaks called by MACS2 were found randomly throughout the genome or clustered in the 5' region upstream of coding sequences, I plotted the number of peaks against the distance of the peaks to their closest genes on both sides of the peaks using Microsoft Excel (see section 2.26 for details). I found that the peaks were mainly clustered at positions less than 1000 bp 5' upstream relative to the translation start site (TSS) of genes across the four experimental data sets (Fig. 3.7). This indicates that AOD2 and AOD5 were predominantly bound close to genes in the 5' upstream region of these genes. The number of peaks dramatically dropped at the vicinity of the TSSs (Fig. 3.7), though there seemed to be a smaller secondary peak around 1000 bp downstream of the TSS (Fig. 3.7). The reasons for

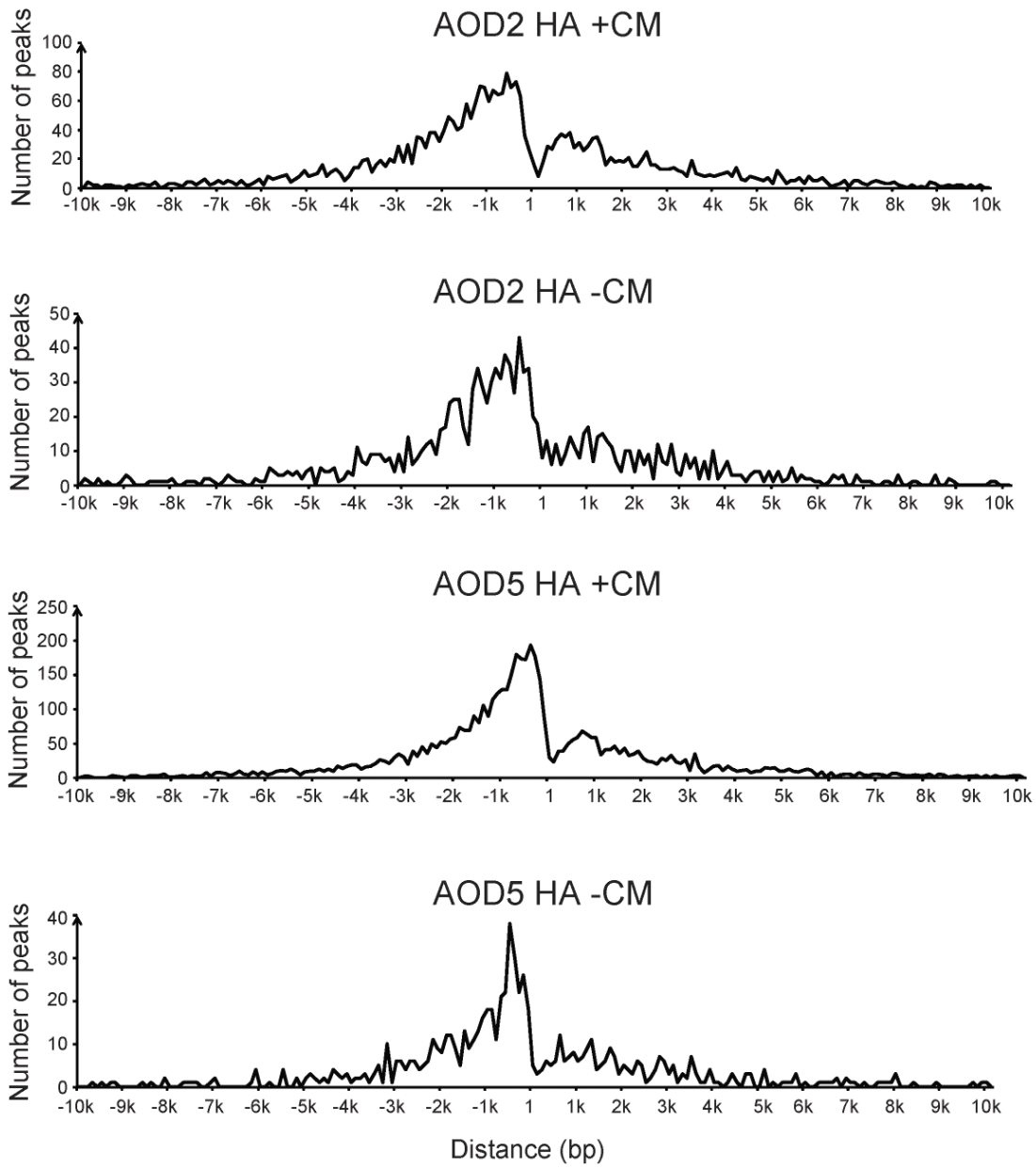

Figure 3.7. The distance between peaks called by MACS2 and the TSSs. The occurrence of ChIP-seq peaks relative to coding sequences was plotted using the Microsoft Excel. On the x-axis, the value 1 represents the position of the TSS. Negative values indicate the upstream distance from the TSS whereas positive values represent the downstream distance. The number of peaks was counted in a 100-bp window.

this are not clear. Overall, these data suggest that AOD2 and AOD5 bound predominantly in the promoter region of genes.

We arbitrarily chose to focus on peaks that had more than four-fold enrichment in a tagged strain compared to the wild-type control for the same growth condition and antibody. Given that AOD2 and AOD5 are thought to act as a heterodimer, and because both proteins were found to localize constitutively to the nucleus, we further refined the data set to those peaks in common to all four experimental conditions as determined by a Venn diagram program called VENNY (http://bioinformatics.psb.ugent.be/webtools/Venn/). Seventy peaks in common to all four categories were found (Fig. 3.8). In cases where the peak was between two genes at their 3' ends, these genes were not considered further. This left a set of 65 peaks for further analysis. The genes that are found in the vicinity of the 65 peaks are summarized in Table 3.2. When examining peaks in GBrowse, the y-axis of mapped reads for the different experiments was set based on the ratio of total mapped reads for the different experiments. However, only the experiments involving one of the antibodies, either the HA IP or the Myc IP, were compared directly. The maximum of the y-axes were then set to best reveal the peaks in the set of 65. Upon visual inspection, many of the peaks appear to have a bimodal, trimodal, or multimodal shape. These shapes were often different for the four experimental results of a single gene. This suggests that multiple binding sites may be present in a given promoter. It is also possible that other factors may influence binding.

As expected, one of the peaks within the set of 65 was found in the *aod-1* promoter region. This peak has a varying enrichment over the untagged control ranging from 6.7 to 22.7 in the four experiments (Fig. 3.9A). The data in section 3.2.2 showed that PEPCK was also regulated by AOD2, and by implication, AOD5. Thus,

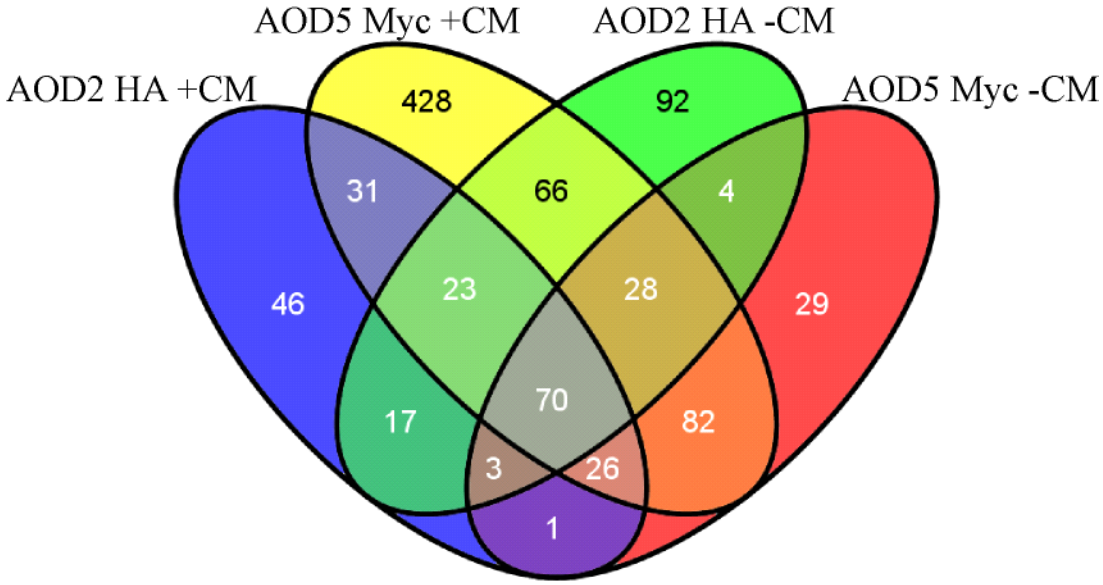

Figure 3.8. Venn diagram of the number of peaks that overlap within the four experimental data sets. Peaks with more than four-fold enrichment were analyzed by the VENNY program (http://bioinformatics.psb.ugent.be/webtools/Venn/) which searches for elements that are either unique or common within the data sets. In this study, I focused on the 70 peaks (represented in grey, at the center) that were common to all four data sets. However, some peaks that were unique to AOD2 (both –CM and +CM) or to AOD5 (both –CM and +CM) were also analyzed (section 3.3.3). From left to right: AOD2 HA +CM (purple); AOD5 Myc +CM (yellow); AOD2 HA –CM (green); AOD5 HA –CM (red).

Table 3.2 Peaks in common to all four ChIP-seq experiments with over four-fold enrichment relative to the controls. Horizontal lines separate single genes or pairs of genes that occur in the correct orientation relative to each set of peaks.

NCU number[1]	Gene name	Found in *P. anserina* microarray	Presence of AIM	Regulation by AOD2 and/or AOD5[2]
NCU00577	hypothetical protein		AIM	nd[3]
NCU00576	hypothetical protein			nd
NCU00682	serine/threonine-protein kinase PRKX		AIM	nd
NCU00866	DUF1275 domain-containing protein		AIM	nd
NCU00865	oxalate decarboxylase			nd
NCU01195	amination-deficient	Yes	AIM	no effect observed
NCU01224	26S protease regulatory subunit 4		no AIM	no effect observed
NCU01225	ubiquitin conjugating enzyme			no effect observed
NCU01744	glutamate synthase	Yes	AIM	nd
NCU01742	hypothetical protein			nd
NCU01808	cytochrome *c*		AIM	AOD2 AOD5 positive
NCU01807	hypothetical protein			nd
NCU01834	hypothetical protein		AIM	nd
NCU01944	hypothetical protein		no AIM	nd
NCU02092	hypothetical protein		AIM	nd
NCU02474	Tom5		AIM	no effect observed
NCU02475	glycine dehydrogenase			AOD2 AOD5 positive
NCU02496	M-phase inducer phosphatase 3		AIM	nd
NCU02497	hypothetical protein			nd
NCU02514	ATPase-1		AIM[4]	no effect observed
NCU02549	processing enhancing protein		AIM	nd
NCU02550	α-galactosidase			nd

NCU02720	hypothetical protein		AIM	nd
NCU02732	hypothetical protein		no AIM	no effect observed
NCU03118	hypothetical protein		AIM	nd
NCU03120	hypothetical protein			nd
NCU03257	ammonium transpoter MEP1		AIM	nd
NCU03364	DENN domain-containing protein		AIM	nd
NCU03365	hypothetical protein			nd
NCU03408	hypothetical protein	Yes	AIM[5]	AOD2 AOD5 positive
NCU03409	RNA lariat debranching enzyme			no effect observed
NCU03466	hypothetical protein		AIM	nd
NCU03548	hypothetical protein		AIM	nd
NCU03549	hypothetical protein			nd
NCU03593	kaleidoscope-1		AIM	nd
NCU03651	NADP-dependent malic enzyme		AIM	AOD2 AOD5 positive
NCU03749	hydroxyacylglutathione hydrolase		no AIM	AOD2 AOD5 negative (+CM)[6]
NCU04307	MSF1		AIM	no effect observed
NCU04569	5-oxoprolinase		AIM	AOD2 AOD5 positive
NCU04730	post-transcriptional silencing protein QDE-2		AIM[5]	no effect observed
NCU04801	hypothetical protein		AIM	nd
NCU04874	*aod-3*		AIM	AOD5 negative (-CM)
NCU04953	penicillopepsin		AIM[5]	nd
NCU04954	hypothetical protein			nd
NCU04986	hypothetical protein		no AIM	nd
NCU11067	hypothetical protein			nd

NCU05202	hypothetical protein		AIM[5]	no effect observed
NCU05203	hypothetical protein			no effect observed
NCU05299	NADH:ubiquinone oxidoreductase 29.9		no AIM	no effect observed
NCU05390	mitochondrial phosphate carrier protein		AIM	nd
NCU05391	hypothetical protein			nd
NCU05477	hypothetical protein		AIM	nd
NCU11913	hypothetical protein			nd
NCU05616	arsenite S-adenosylmethyltransferase		AIM[7]	nd
NCU05989	hypothetical protein		AIM	nd
NCU06083	hypothetical protein		AIM[5]	nd
NCU06230	serine/threonine protein kinase		AIM	AOD2 AOD5 negative
NCU06381	GPI-anchored cell wall beta-1; 3-endoglucanase EglC		AIM	nd
NCU06382	ABC transporter			AOD2 AOD5 positive
NCU06387	hypothetical protein		AIM	nd
NCU06389	DUF625 domain-containing protein			nd
NCU06424	aminomethyl transferase		AIM	nd
NCU06425	hypothetical protein		AIM	nd
NCU06426	hypothetical protein			nd
NCU06724	glutamine synthase		AIM	nd
NCU06939	endosome-associated ubiquitin isopeptidase		AIM	nd
NCU06940	hypothetical protein	Yes		AOD2 AOD5 positive[8]
NCU07098	hypothetical protein		AIM[5]	nd
NCU07099	hypothetical protein			nd
NCU07166	hypothetical protein		AIM	nd
NCU07167	isoflavone reductase			nd
NCU07327	hypothetical protein		AIM	nd

NCU07530	transporter Smf2		AIM[5]	nd
NCU07531	copper-transporting ATPase			nd
NCU07668	MFS multidrug transporter		AIM[9]	nd
NCU11717	hypothetical protein			nd
NCU07676	hypothetical protein		no AIM	nd
NCU07678	hypothetical protein			no effect observed
NCU07807	fructose bisphophatase aldolase		AIM	no effect observed
NCU07941	aspartate aminotransferase		AIM	nd
NCU07942	hypothetical protein			nd
NCU07953	*aod-1*	Yes	AIM	AOD2 AOD5 positive
NCU07954	hypothetical protein			nd
NCU08674	pentatricopeptide repeat protein		AIM[10]	AOD2 AOD5 positive
NCU08877	glycine cleavage system H protein		AIM	no effect observed
NCU08878	TEM1			no effect observed
NCU08940	ubiquinol-cytochrome *c* reductase complex protein		AIM	nd
NCU08941	calcium-binding mitochondrial carrier protein Aralar2			nd
NCU08946	hypothetical protein		no AIM[11]	no effect observed
NCU08947	ubiquinol-cytochrome *c* reductase complex protein			AOD2 AOD5 positive (+CM)
NCU08976	fatty acid elongase		AIM	nd
NCU08977	long chain fatty alcohol oxidase			nd
NCU09656	carboxymethylenebutenolidase		AIM	AOD2 positive (-CM)
NCU11414	plasma membrane zinc ion transporter	Yes		no effect observed
NCU09873	PEPCK	Yes	AIM	AOD2 AOD5 positive
NCU10007	malate synthase		AIM	AOD2 AOD5 positive
NCU10894	hypothetical protein		AIM	nd

NCU12093	N-acyl-phosphatidylethanolamine-hydrolyzing phospholipase D	no AIM	nd

[1] Genes in wrong orientation on one side or both sides of a peak were excluded from this table.

[2] As determined by RT-qPCR on cultures grown in both the presence and absence of CM. Wild-type, Δ*aod-2*, and Δ*aod-5* strains were analyzed and compared. See section 3.3.3 for details.

[3] nd, not determined.

[4] The AIM is located in the coding region of NCU11471 on the Freitag lab GBrowse version of the genome. The AIM aligns with the summit of the peak. However, NCU11471 is not found in FungiDB (Stajich *et al.* 2012) but another gene NCU16361 is present between NCU02514 and NCU02515. NCU16361 encodes a hypothetical protein of 174 amino acids distributed in four small exons. It appears that the summits of the peaks in the AOD2 –CM and +CM experiments align with one of the exons of NCU16361 whereas the ones in the AOD5 –CM and +CM experiments align with an intron of the gene.

[5] An AIM was found in the intergenic region but does not align with the summit of a peak.

[6] (-CM) or (+CM) indicates that the AOD2 and/or AOD5 positive and/or negative regulation only occurs in –CM or +CM cultures, respectively.

[7] The peak region partially overlaps with the coding region of NCU05617. There is an AIM located in the coding region of NCU05617 but it does not align with the summit of the peak.

[8] The RT-qPCR was performed by Natasa Bosnjak.

[9] Two AIMs are located in the coding region of NCU11717 on the Freitag lab GBrowse version of the genome. One of the two AIMs aligns perfectly with summit of the peak. However, NCU11717 is not found in FungiDB (Stajich *et al.* 2012) but another gene NCU16786 is present between NCU07666 and NCU07668. NCU16786 encodes a hypothetical protein of 173 amino acids distributed in five small exons. It appears that the summit of the peak in the AOD2 +CM experiment aligns with an intron of NCU16786 whereas the ones in the AOD5 –CM and +CM experiments align with an exon of the gene.

[10] Two AIMs are located in the coding region of NCU08672 and align with summit of the peak. However, NCU08672 encodes a hypothetical protein of only 107 amino acids distributed in three small exons and may not represent an actual protein coding gene.

[11] The peak region in within the coding region of NCU08947 which encodes a subunit of Complex III of the ETC.

Figure 3.9. ChIP-seq peaks in the 5' upstream region of *aod-1* and PEPCK. A. The regions of the *N. crassa* genome containing the *aod-1* and PEPCK genes with associated ChIP-seq peaks are shown. The location of the regions on the appropriate chromosomes is indicated at the top. The coding region of the genes is indicated in blue and the 5' and 3' UTRs are shown in grey. Introns are indicated by the thin folded lines and the orientation of a gene is shown by the black arrows. ChIP peaks are shown below the genes in black with the experimental data sets indicated on the left. As described in the text, the different y-axis values represent the ratio of the number of reads in the different ChIP-seq experiments (Table 3.1). The HA data sets are related to each other and the Myc data sets are related to each other, but there was no attempt to assign a ratio between the IPs involving different antibodies. The actual values of the y-axis were then chosen to best visualize peaks for all genes in the set of 65. For PEPCK, the two peak sets in the 5' upstream region are separated by approximately 27 kbp. B. The region between the PEPCK gene and its closest 5' upstream gene are shown. The PEPCK gene is highlighted in yellow and labeled. This region is neither located near the centromere (green box) of chromosome 6 (Smith *et al.* 2011), nor at one of the ends of the chromosome. The synteny of this region in *N. crassa*, *N. tetrasperma*, and *N. discreta* is shown as given at FungiDB (Stajich *et al.* 2012). Genes in the same orientation as PEPCK are shown in blue and those in opposite orientation are shown in red. Orthologues in these species are connected by two grey straight lines. The region containing the far 5' upstream ChIP-seq peak of PEPCK is indicated by a black box and an arrow in the *N. crassa* row. The numbers on the top and in the middle indicate the location on chromosome 6.

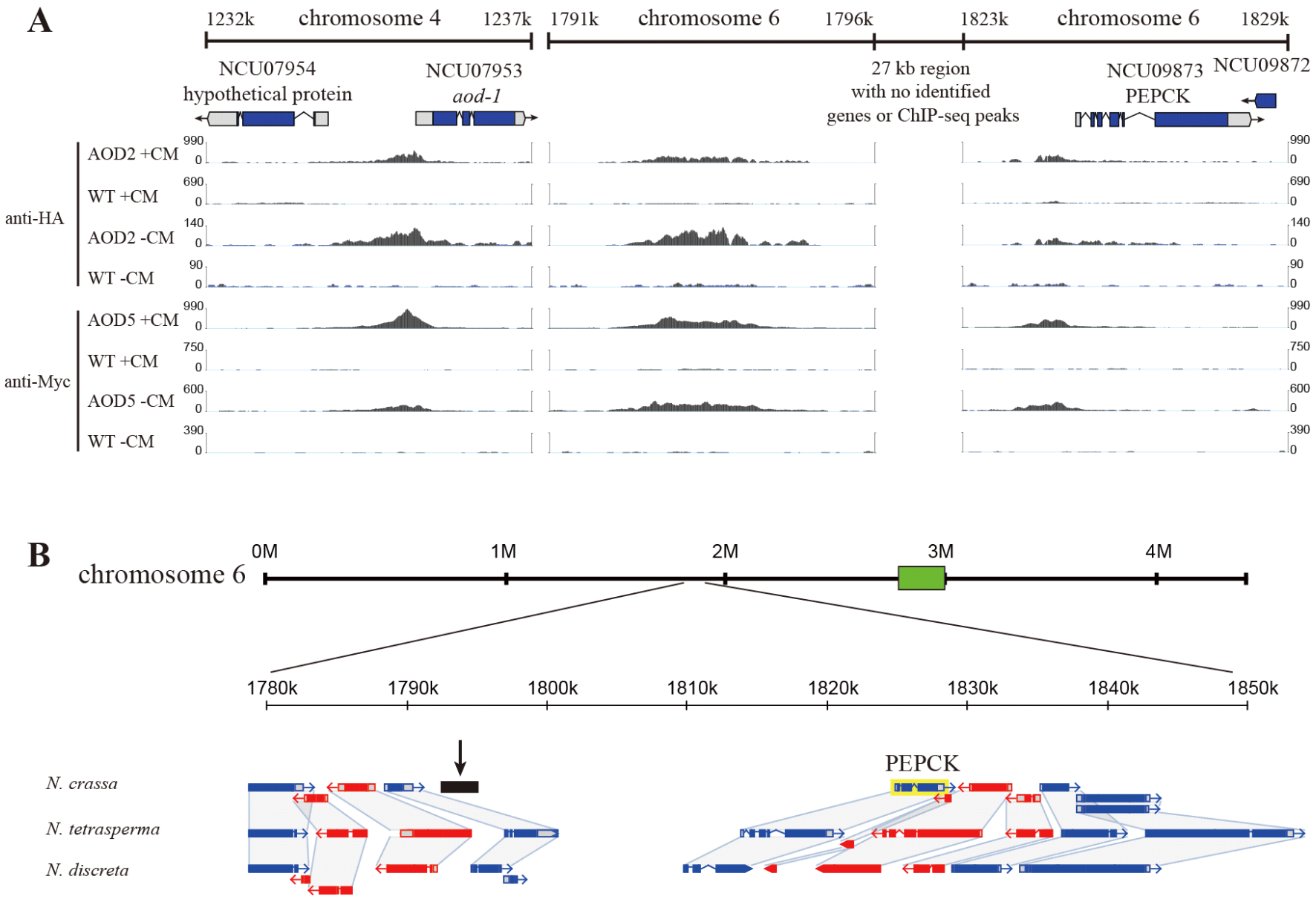
A
1232k
chromosome 4
1237k
1791k
chromosome 6
1796k
1823k
chromosome 6
1829k
NCU07954
hypothetical protein
NCU07953
aod-1
27 kb region
with no identified
genes or ChIP-seq peaks
NCU09873
PEPCK
NCU09872
anti-HA
AOD2 +CM
WT +CM
AOD2 -CM
WT -CM
anti-Myc
AOD5 +CM
WT +CM
AOD5 -CM
WT -CM
B
chromosome 6
0M
1M
2M
3M
4M
1780k
1790k
1800k
1810k
1820k
1830k
1840k
1850k
PEPCK
N. crassa
N. tetrasperma
N. discreta

as expected, PEPCK was included in the set of 65 peaks identified. By inspection, two major peaks were associated with the PEPCK gene. The first peak set was 1.3 to 1.4 kbp upstream of the coding sequence of PEPCK, the second was found 30 to 33 kbp upstream (Fig. 3.9A). Strangely, of the four experimental sets, only the "close" peak in the AOD2 –CM experiment had less than four-fold enrichment (2.1-fold). By contrast, the "far" peak set was relatively broad (Fig. 3.9A) and had more than four-fold enrichment across all four experimental sets.

Between the two major peaks that were associated with the PEPCK gene, there is an extremely long intergenic region (Fig. 3.9A). The length of this intergenic region varies among other *N. crassa* species (Fig. 3.9B). Of the species whose sequence is listed on FungiDB (Stajich *et al.* 2012), the smallest version of the region was in *N. tetrasperma* (about 13 kbp) and the largest in *N. crassa* (about 33 kbp). Moreover, this region seems not to be associated with the centromere of chromosome 6 (Fig. 3.9B) and it is unclear why such a large non-coding region exists at this position. It is not known if both regions contribute to PEPCK transcription regulation. Both regions do contain AIM sequences (see below).

3.3.2 Alignment of AIM with ChIP-seq peaks in the intergenic region

Since the AIM was shown to be bound by the AOD2/AOD5 dimer in EMSA experiments (Chae *et al.* 2007b), I next asked whether the location of the 65 peaks on the genomic DNA coincides with the position of an AIM sequence (Fig. 3.10 and Supplementary Fig. 3.7). Three AIM sequences were found at the position of the peak in the *aod-1* upstream region (Fig. 3.10A). The AIM closest to the coding sequence was the one previously characterized (Chae *et al.* 2007a). Interestingly, the peaks in the AOD2 –CM, AOD2 +CM, and AOD5 –CM experiments appear to have multiple

Figure 3.10. Position of AIM sequences in some typical peaks. Snapshots of the peak sets are taken from GBrowse for the genes indicated in panels A through G on the figure. Unlike Fig. 3.9 where the y-axis was set based on ratio of read numbers, the y-axes in this figure were set to maximize visualization of the summits and their relationship to AIM sequence positions. The control data sets are not shown. CGG(N7)CGG motifs on the + strand (DNA strand from 5' to 3' corresponds to the order from left to right on GBrowse) are indicated by black arrows whereas the palindromic counterpart CCG(N7)CCG motifs on the + strand are indicated by red arrows. In cases where CGG(N7)CGG and CCG(N7)CCG sequences are too close to each other to be resolved, green arrows are used. One green arrow signifies a mixture of a CGG(N7)CGG and a CCG(N7)CCG. Shorter green arrows with two numbers above indicate the number of CGG(N7)CGG sequences (black number) and CCG(N7)CCG sequences (red number). If there are two or more closely clustered CGG(N7)CGG repeats, the black arrows are shortened and the number on the top indicates the number of repeats. The same applies to CCG(N7)CCG repeats using shortened red arrows. The peaks are shown between two genes, with the exception of the peaks at PEPCK, which occur at two loci within a 35-kbp intergenic region. This region is divided into two separate regions (panels B and C). The orientation of the genes are indicated by the short black arrows attached to the genes. A. The peak set close to the *aod-1* gene. B and C. The "far" and "close" peak sets in the 5' upstream region of PEPCK. D. The peak set close to NCU06940. E. The peak set close to the 5-oxoprolinase gene. F. The peak set close to NCU05202. G. The peak set close to the *aod-3* gene.

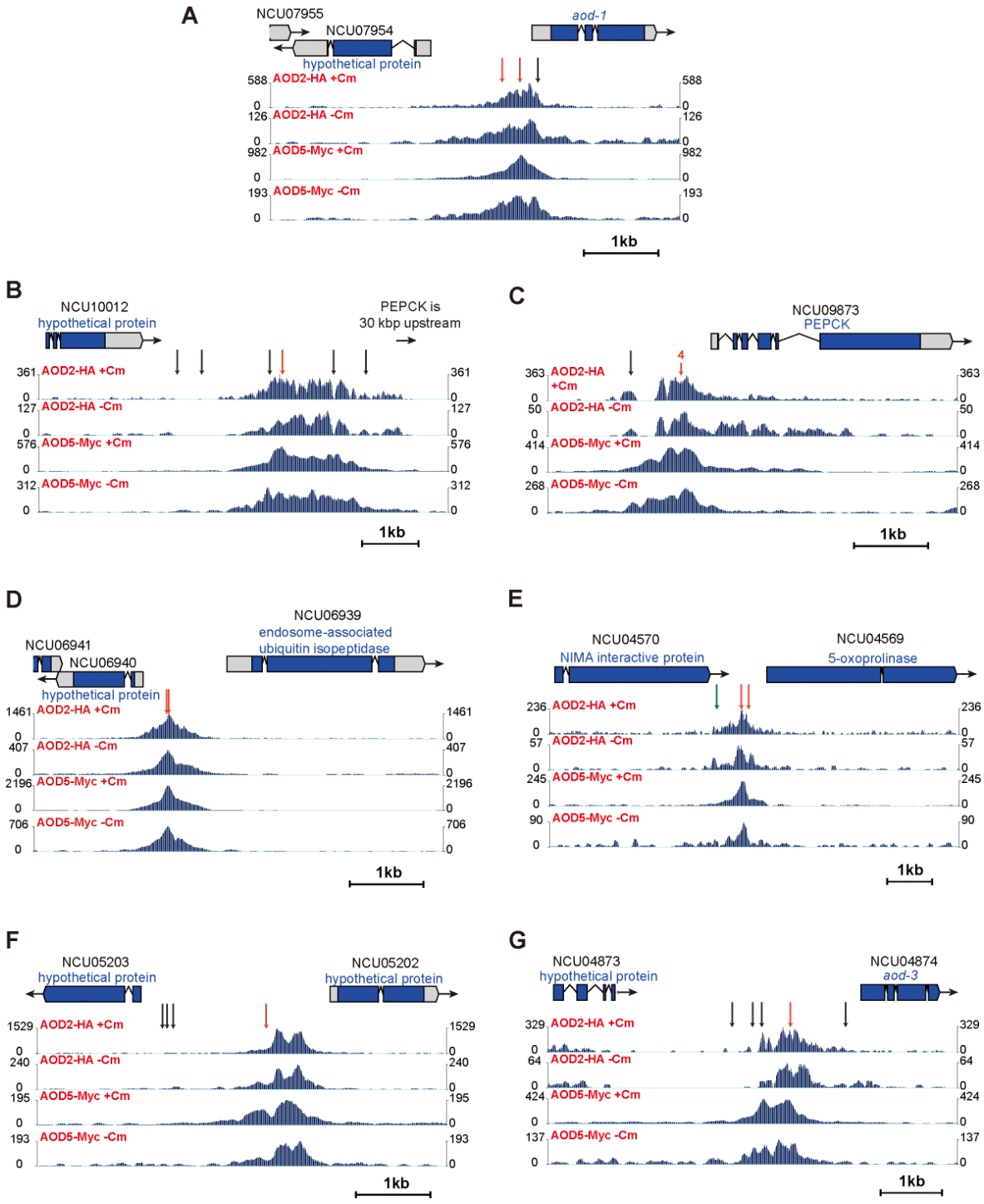
A
NCU07955
NCU07954
hypothetical protein
aod-1
588 AOD2-HA +Cm
126 AOD2-HA -Cm
982 AOD5-Myc +Cm
193 AOD5-Myc -Cm
1kb
B
NCU10012
hypothetical protein
PEPCK is
30 kbp upstream
361 AOD2-HA +Cm
127 AOD2-HA -Cm
576 AOD5-Myc +Cm
312 AOD5-Myc -Cm
1kb
C
NCU09873
PEPCK
4
363 AOD2-HA +Cm
50 AOD2-HA -Cm
414 AOD5-Myc +Cm
268 AOD5-Myc -Cm
1kb
D
NCU06941
NCU06940
hypothetical protein
NCU06939
endosome-associated
ubiquitin isopeptidase
1461 AOD2-HA +Cm
407 AOD2-HA -Cm
2196 AOD5-Myc +Cm
706 AOD5-Myc -Cm
1kb
E
NCU04570
NIMA interactive protein
NCU04569
5-oxoprolinase
236 AOD2-HA +Cm
57 AOD2-HA -Cm
245 AOD5-Myc +Cm
90 AOD5-Myc -Cm
1kb
F
NCU05203
hypothetical protein
NCU05202
hypothetical protein
1529 AOD2-HA +Cm
240 AOD2-HA -Cm
195 AOD5-Myc +Cm
193 AOD5-Myc -Cm
1kb
G
NCU04873
hypothetical protein
NCU04874
aod-3
329 AOD2-HA +Cm
64 AOD2-HA -Cm
424 AOD5-Myc +Cm
137 AOD5-Myc -Cm
1kb

summits while the AOD5 +CM has only one summit whose position coincides with the middle AIM. The AIM sequence previously investigated appears to align with a small summit in the AOD2 +CM data.

As mentioned above, there are two upstream regions of PEPCK that are enriched for peaks. I found that each region contained five AIM sequences. The region at 30 kbp upstream had multiple peaks that contained four AIMs in total. However, the peak summits did not align precisely across all four ChIP experiments (Fig. 3.10B). In contrast, among the five AIMs in the region just upstream of the PEPCK coding sequence, four of them are tandem CCG(N7)CCG repeats. There seems to be good concordance of the position of these tandem AIMs and the ChIP-seq summits (Fig. 3.10C). The fifth AIM was found in a smaller upstream summit.

Among the 65 peaks that are common to all four experimental data sets, some peaks have their summit quite precisely aligned with an AIM position, such as the peaks in the promoters of NCU06940 (hypothetical protein) (Fig. 3.10D) and NCU04569 (5-oxoprolinase) (Fig. 3.10E). Some peaks contained one or more AIMs but the summits do not match the AIMs precisely, such as the peak in the 5' region of NCU05202 (hypothetical protein) (Fig. 3.10F). Nine peak sets were not associated with any AIMs, such as the peaks in the promoter region of NCU01224 (26S protease regulatory subunit 4) and NCU03749 (hydroxyacylglutathione hydrolase) (Table 3.2 and Supplementary Fig. 3.7). Two of these nine peak sets (peaks in the 5' upstream regions of NCU07678 and NCU11067) were associated with a special binding motif for AOD2 only and are described in section 3.3.6. The peak sets associated with NCU05202 that do not align with the AIM (Fig. 3.10F) are also in this "special AOD2" group. This left seven peaks that were not associated with any AIMs or special AOD2 binding sites. When compared to the peak in the promoter region of *aod-1*, three of

the nine peak sets (peaks in the 5' upstream regions of NCU01944, NCU02732, and NCU08946) were much smaller and two of them (the peak associated with NCU01944 and NCU08946) contained multiple peak summits (Supplementary Fig. 3.7). Four additional peak sets (peaks in the 5' upstream regions of NCU01224, NCU03749, NCU05299, and NCU12093) exhibited good peak quality but were not associated with any AIMs. The reason that AOD2 and AOD5 bind to these four regions is unknown, but it may involve additional proteins or another undefined binding site. Interestingly, all four of the latter peak sets show much more efficient binding of AOD2 than AOD5 when compared to the ratios seen for *aod-1*.

I also looked for the presence of the AIM sequence in the five peak sets within the group of 70 identified by Venny (Fig. 3.8) that were found to be between the 3' downstream regions of two genes (in other words, in the wrong orientation). Four of them (peaks in the 3' downstream regions of NCU01791, NCU03614, NCU05425, and NCU06076) were associated with AIMs and one (the peak in the 3' downstream region of NCU01958) was not (Supplementary Fig. 3.7). Furthermore, the AIMs in the four 3' regions align perfectly with the summit of the peak sets (Supplementary Fig. 3.7). However, the peak sets in the 3' downstream regions of NCU01791, NCU03614, and NCU05425 were relatively small when compared to the one in the 5' upstream region of *aod-1*. It is not known if binding of AOD2 and AOD5 in these regions plays any role in regulation.

3.3.3 Validation of regulatory role of ChIP-seq peaks by RT-qPCR

To determine whether the AOD2 and AOD5 proteins actually influence the expression of genes in the set of 65, I performed RT-qPCR experiments to measure the transcript levels of 34 genes in the wild-type control strain (NCN251), as well as

Δ*aod-2* and Δ*aod-5* knockout strains, grown in the presence and absence of CM. A cutoff point of two-fold difference in expression was chosen to most likely represent actual biological significance. The selection of the 34 genes examined was influenced by a subjective judgment of peak quality and/or position of peaks in proximity to genes and/or a predicted metabolic function. I found that the expression of 11 of these 34 genes was positively regulated by AOD2 and AOD5 (Table 3.2). That is, the transcript levels were reduced by two-fold or more in the Δ*aod-2* and Δ*aod-5* knockout strains when compared to the control strain under both of the growth conditions (Fig. 3.11). As expected, *aod-1* and PEPCK were included in this group. Among these 11 genes, there appeared to be two general categories. For 8 genes there was greater than two-fold increase in the transcript levels for wild-type cells grown in the presence of CM (Fig. 3.11A). The expression of the remaining three genes was increased less than two-fold in wild-type cells grown in the presence of CM (Fig. 3.11B).

AOD2 and AOD5 were also found to negatively regulate the expression of two genes in the presence of CM, NCU03749 (hydroxyacylglutathione hydrolase) and NCU06230 (serine/threonine protein kinase), since their transcript levels were more than two-fold higher in the absence of the proteins (Fig. 3.12A). One gene NCU04874 (*aod-3*) was found with an unusual pattern of regulation. It appeared to be regulated negatively by AOD5 only in the absence of CM (Fig. 3.12B). The *aod-3* gene codes for a homologue of *aod-1*, but its transcript was found to be undetectable on Northern blots following growth with or without CM (Tanton *et al.* 2003). The *aod-3* gene was found in the 65 peaks that are common to all categories and it is unknown why loss of AOD2 had no effect on its expression. When examined for AIM sequences, the peak set in the *aod-3* upstream region covered one CCG(N7)CCG sequence, but three

Figure 3.11. Transcript levels of genes that are positively regulated by AOD2 and AOD5. RT-qPCR was performed using total RNA isolated from wild-type, Δ*aod-2* and Δ*aod-5* strains grown in both the absence and presence of CM. Primers for the indicated genes were chosen as described in section 2.21. The data was analyzed using the $\Delta\Delta C_T$ method. β-tubulin was used as an internal amplification control and data from all experimental conditions was normalized to the wild-type –CM data. Data was determined for four biological replicates, each with three technical replicates. The Student's t test was used to compare data between two different conditions. *, p value < 0.05. **, p value < 0.01. ***, p value < 0.001. Error bars, ±SEM. (The data for NCU06940 was obtained and supplied by Natasa Bosnjak.) A. Genes with increased expression in wild-type cells grown in the presence of CM compared to the absence of CM. B. Genes with expression unaffected by CM in wild-type cells.

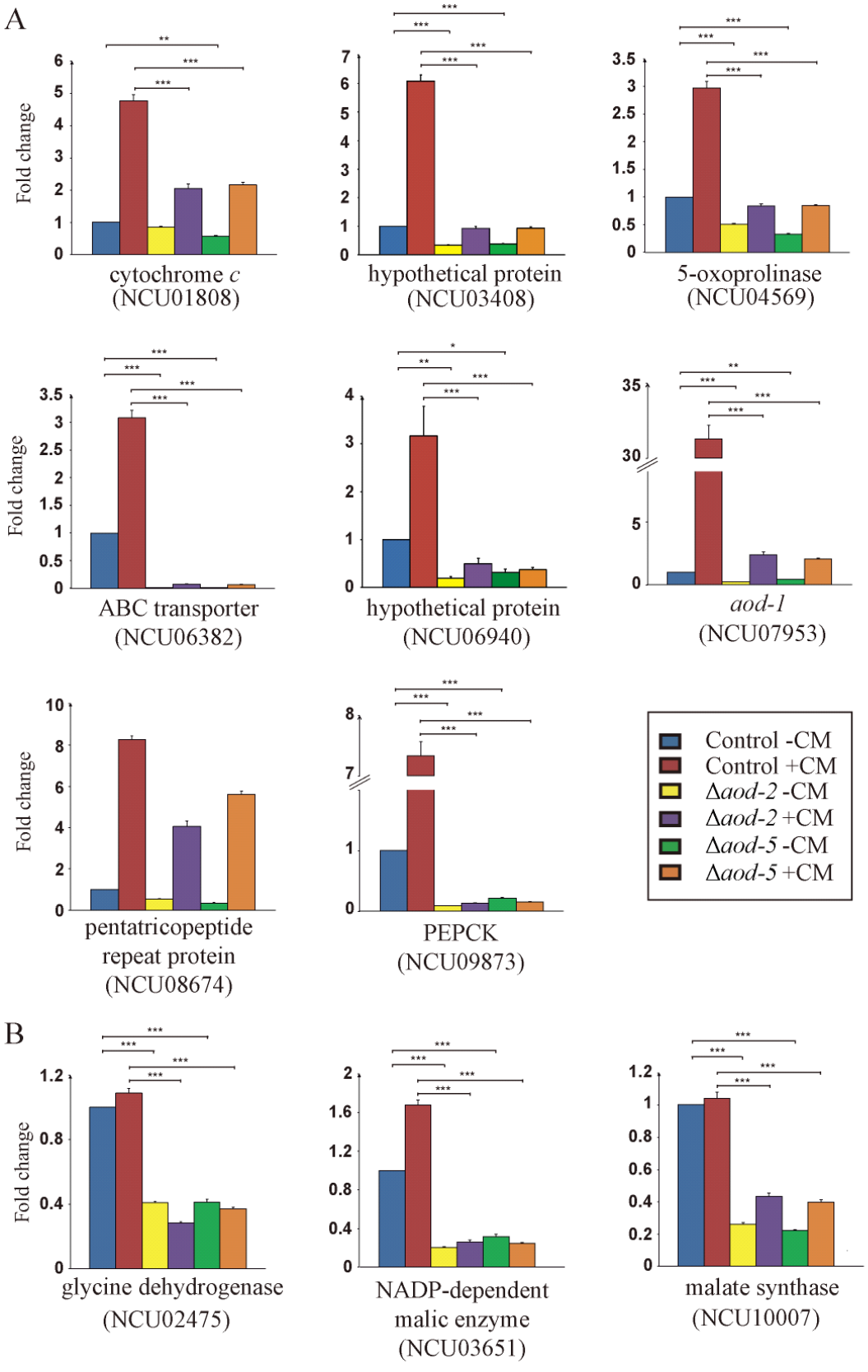
A
Fold change
cytochrome c
(NCU01808)
hypothetical protein
(NCU03408)
5-oxoprolinase
(NCU04569)
ABC transporter
(NCU06382)
hypothetical protein
(NCU06940)
aod-1
(NCU07953)
pentatricopeptide
repeat protein
(NCU08674)
PEPCK
(NCU09873)
Control -CM
Control +CM
Δaod-2 -CM
Δaod-2 +CM
Δaod-5 -CM
Δaod-5 +CM
B
glycine dehydrogenase
(NCU02475)
NADP-dependent
malic enzyme
(NCU03651)
malate synthase
(NCU10007)

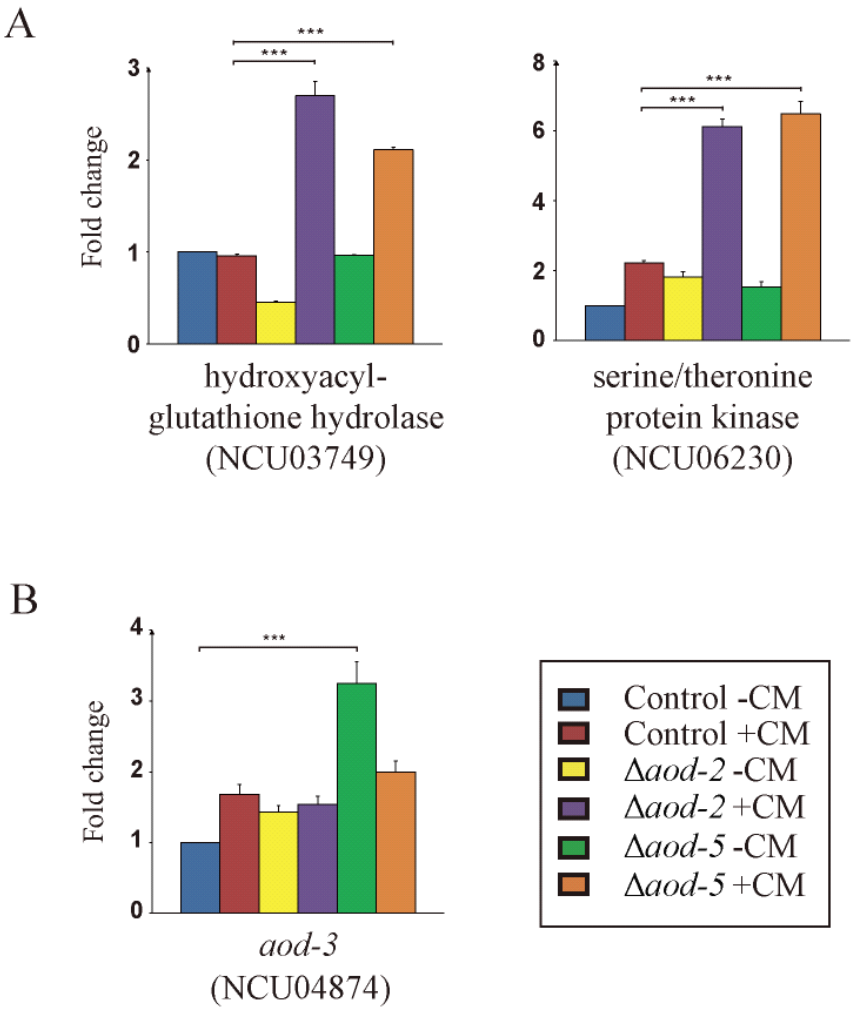

Figure 3.12. Genes that are negatively regulated by AOD2 and/or AOD5 in the presence of CM. Expression of the indicated genes was examined as described in the legend to Fig. 3.11. A. Genes that are negatively regulated by AOD2 and/or AOD5 in the presence of CM. B. The *aod-3* gene is negatively regulated by AOD5 in the absence of CM.

CGG(N7)CGG sequences were only associated with small summits (Fig. 3.10G). It is noteworthy that lack of induction of *aod-3* by growth of wild-type cells in CM shows a clear difference in regulation from *aod-1* and is in agreement with previous observations (Tanton *et al.* 2003).

The RT-qPCR data also revealed that the expression of five genes was not controlled by AOD2 and AOD5 under the -CM and +CM conditions tested (Fig. 3.13A). However, their transcript levels were moderately increased (two to four-fold) in cells grown in the presence of CM (Fig. 3.13A). Thus, other factors appear to mediate this expression. Conceivably AOD2 and AOD5 could play a role in some untested condition. It was of interest to note that the NCU02474 (Tom5) and NCU02475 (glycine dehydrogenase) genes were found on opposite sides of a single ChIP-seq peak. Strangely, Tom5 appears to respond to the presence of CM, in a manner independent of AOD2 and AOD5 (Fig. 3.13A) while expression of NCU02475 is dependent on AOD2 and AOD5 but does not respond to CM (Fig. 3.11B). The expression of NCU08947 (ubiquinol-cytochrome *c* reductase complex protein, Fig. 3.13B), which is found adjacent to NCU08946 of Fig. 3.13A was also peculiar. The gene exhibits up regulation in the presence of CM in wild-type cells. However, unlike the genes shown in Fig. 3.11A, the transcript levels of the gene were not dependent on AOD2 and AOD5 in the absence of CM. On the other hand, expression of the gene was reduced in the Δ*aod-2* and Δ*aod-5* knockout strains grown in the presence of CM (Fig. 3.13B). Unexpectedly, the ChIP-seq peak associated with NCU08946 was within the coding region of NCU08947. The peak was relatively small and not associated with any AIM sequences (Supplementary Fig. 3.7 and Table 3.2). The mechanism of how AOD2 and AOD5 regulate the expression of NCU08947 in the presence of CM remains to be elucidated.

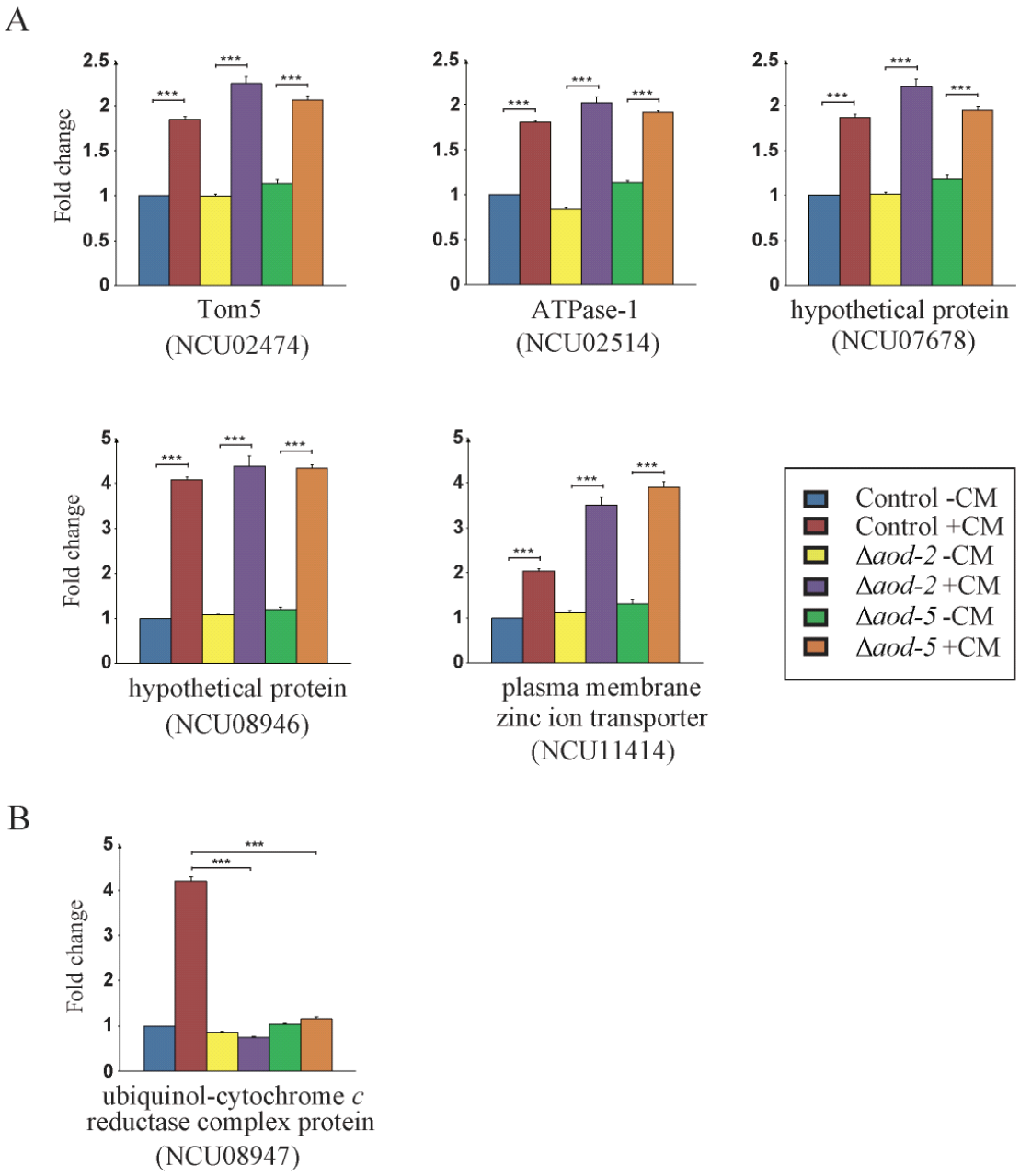

Figure 3.13. Genes showing increased expression in the presence of CM. Genes were examined by qPCR as described in the legend to Fig. 3.11. A. Genes with increased expression following growth in CM, but no dependence on AOD2 or AOD5. B. Gene with increased expression in the presence of CM. AOD2 and AOD5 are required for increased expression only in the presence of CM.

The expression of one gene NCU09656 (carboxymethylenebutenolidase) was affected by the absence of AOD2, with about three-fold reduction in the Δ*aod-2* cells grown in the absence of CM and minor reduction (about 3.3-fold) in the presence of CM when compared to the control strain (Fig. 3.14). There were 13 genes of the 34 examined that showed little or no effect on expression by AOD2 or AOD5, and no effects from growth in CM (Supplementary Fig. 3.8).

In addition to the 65 peak sets that are common to the four ChIP-seq experiments, I was interested in investigating certain peaks in other regions of the Venn diagram common to only certain experiments (Fig. 3.8). These include certain peaks that are either common to three of the four experiments, or only found in AOD2 or AOD5 experiments, or only specific to –CM or +CM experiments and that were in the correct orientation relative to the peaks. Again, the choice of genes examined was influenced by subjective consideration of peak quality and predicted gene function. As above, RT-qPCR was performed to determine whether AOD2 and/or AOD5 affected the expression of the genes. The data are summarized in Table 3.3 and Fig. 3.15.

Many of these genes showed unexpected behavior with respect to their expression. The expression of NCU00628 (hypothetical protein), though found in the 5- 5+ experimental class (see Table 3.3 for abbreviations of experimental classes), was only increased two-fold in Δ*aod-2* cells grown in the presence of CM more than two-fold and did not seem to be affected by the absence of AOD5 (Fig. 3.15A). NCU04392 (hypothetical protein), NCU04752 (hypothetical protein), and NCU09144 (hypothetical protein) showed greater than two-fold increased expression only in the Δ*aod-5* knockout cells grown in the absence of CM (Fig. 3.15B). However, of those latter three genes showing effects in the Δ*aod-5* cells, only NCU04752 was found in the 5- 5+ experimental class. NCU04392 and NCU09144 were in the 2- 2+ 5+ and 2-

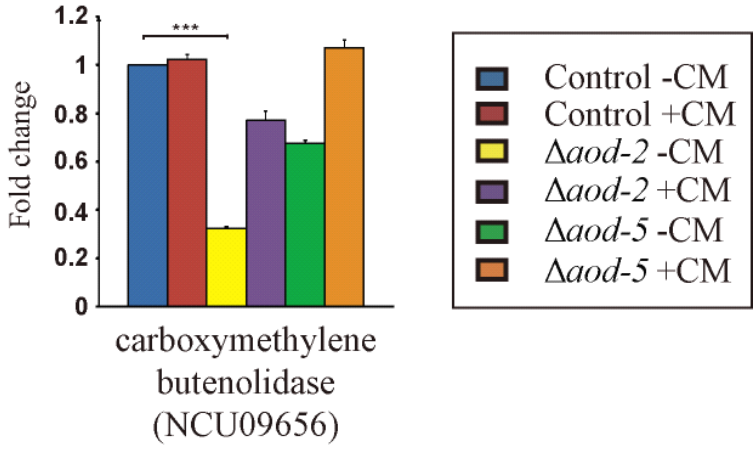

Figure 3.14. Reduced expression of NCU09656 in Δ*aod-2* cells grown in the presence of CM. The gene was examined by qPCR as described in the legend to Fig. 3.11.

Table 3.3 Summary of RT-qPCR data for genes associated with ChIP-seq peaks not included in the set of 65. The peaks are common to three of the four experiments on the Venn diagram, or are found in AOD2 or AOD5 only, or in +CM only. Horizontal lines separate single genes or pairs of genes in the correct orientation relative to each set of peaks.

Gene chosen	Experimental class	Experimental class abbreviation	Presence of AIM	Regulation by AOD2 and/or AOD5[1]
NCU00628 (hypothetical) NCU00629 (6-phosphofructokinase)	AOD5 –CM, AOD5 +CM	5- 5+	no AIM	AOD2 negative no regulation
NCU01053 (hypothetical)	AOD2 –CM, AOD2 +CM	2- 2+	no AIM	no regulation
NCU02128 (D-arabinitol dehydrogenase)	AOD2 –CM, AOD2 +CM, AOD5 +CM	2- 2+ 5+	no AIM	AOD2 positive (-CM)
NCU02623 (mitochondrial hypoxia responsive domain)	AOD5 –CM, AOD5 +CM	5-, 5+	AIM[2]	no regulation
NCU04392 (hypothetical)	AOD2 –CM, AOD2 +CM, AOD5 +CM	2- 2+ 5+	AIM[2]	AOD5 negative (-CM)
NCU04752 (hypothetical) NCU04753 (NADH:ubiquinone oxidoreductase subunit 11.6kD)	AOD5 –CM, AOD5 +CM	5- 5+	AIM	AOD5 negative (-CM) no regulation
NCU04797 (FBP)	AOD5 –CM, AOD5 +CM	5- 5+	AIM	no regulation
NCU04899 (malate dehydrogense)	AOD5 –CM, AOD5 +CM	5- 5+	no AIM	AOD2 AOD5 positive
NCU05627 (high affinity glucose transporter)	AOD2 +CM, AOD5 –CM, AOD5 +CM	2+ 5- 5+	no AIM	AOD2 AOD5 positive

NCU05995 (ubiquitin) NCU05996 (C6 finger domain-containing protein)	AOD2 –CM, AOD5 –CM, AOD5 +CM	2- 5- 5+	AIM	no regulation no regulation
NCU06211 (malate dehydrogense)	AOD2 +CM, AOD5 –CM, AOD5 +CM	2+ 5- 5+	AIM	no regulation
NCU09144 (hypothetical)	AOD2 –CM, AOD2 +CM, AOD5 -CM	2- 2+ 5-	no AIM	AOD5 negative (-CM)

[1] In some cases effects of missing AOD2 and/or AOD5 were only seen in the absence of CM (indicated as –CM) or the presence of CM (indicated as +CM). If an effect was seen in both –CM and +CM, no –CM or +CM symbol is added.

[2] An AIM is present in the region of the peak set, but does not align with the peak summit.

Figure 3.15. Expression of genes associated with ChIP-seq peaks from categories of the Venn diagram not common to all four experimental conditions. Genes were analyzed as described in the legend to Fig. 3.11. Genes were identified in either three of the four ChIP-seq experiments in the Venn diagram, or the 2- 2+, 5- 5+, 2- 5-, or 2+ 5+ experimental classes (classes defined in Table 3.3). Genes to be analyzed were chosen by inspection of peak quality and/or assigned metabolic function. A. Genes with increased transcript levels in the Δ*aod-2* cells grown in the presence of CM. B. Genes with increased transcript levels in Δ*aod-5* cells grown in the absence of CM. C. Genes with decreased transcript levels in Δ*aod-2* cells grown in the absence of CM. D. Genes with decreased transcript levels in Δ*aod-2* and Δ*aod-5* cells grown in the presence and absence of CM. E. Gene with transcript levels that were only affected by the presence of CM in all the strains tested but did not respond to presence or absence of AOD2 or AOD5.

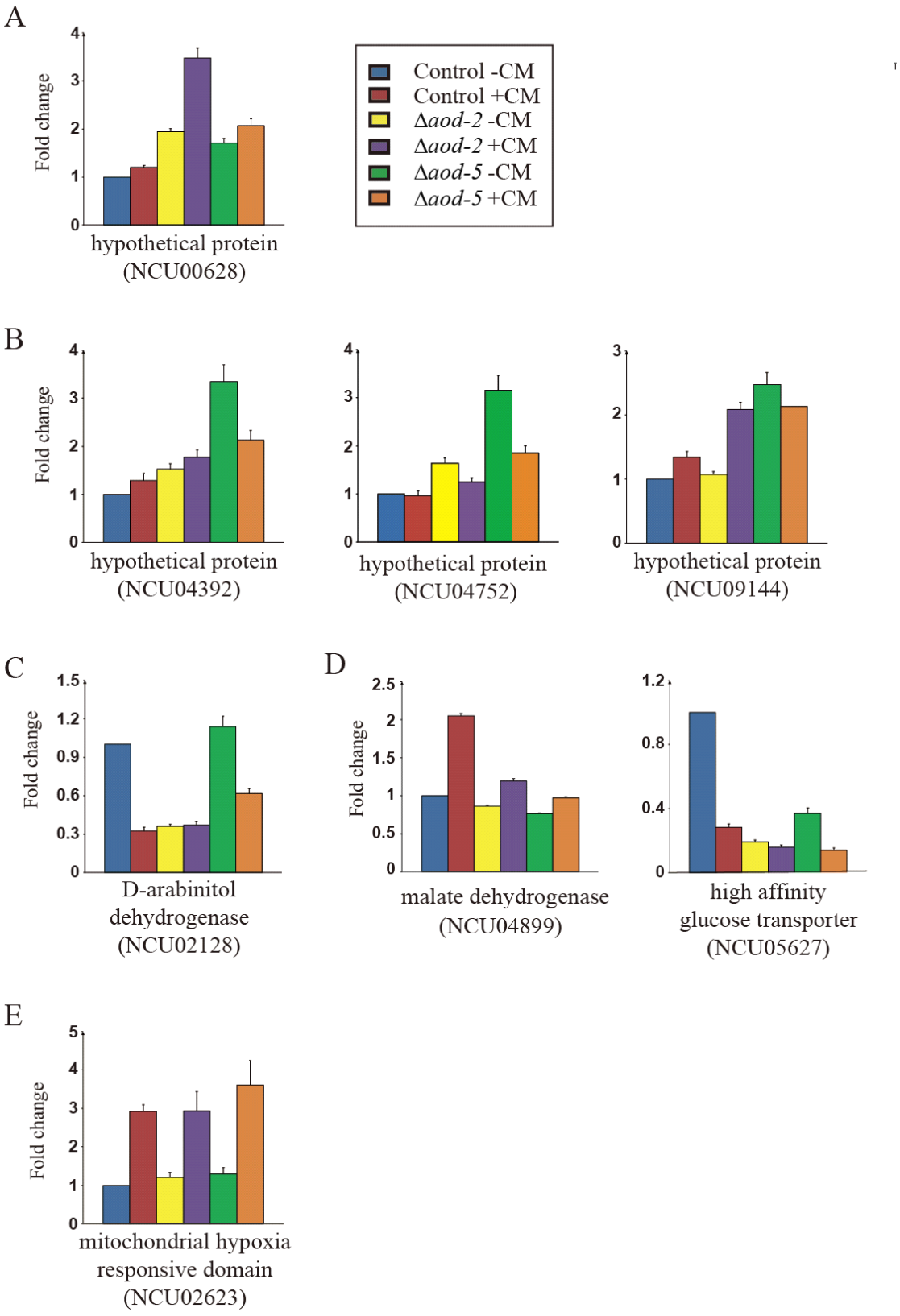
A
Fold change
hypothetical protein
(NCU00628)
Control -CM
Control +CM
Δaod-2 -CM
Δaod-2 +CM
Δaod-5 -CM
Δaod-5 +CM
B
Fold change
hypothetical protein
(NCU04392)
hypothetical protein
(NCU04752)
hypothetical protein
(NCU09144)
C
Fold change
D-arabinitol
dehydrogenase
(NCU02128)
D
Fold change
malate dehydrogenase
(NCU04899)
high affinity
glucose transporter
(NCU05627)
E
Fold change
mitochondrial hypoxia
responsive domain
(NCU02623)

2+ 5- class, respectively, but they were not seen to be controlled by AOD2 under the conditions tested.

Similar to NCU04392, NCU02128 (D-arabinitol dehydrogenase) was found in the 2- 2+ 5+ class, but was only affected by AOD2, as its expression was reduced more than two-fold in the Δ*aod-2* cells grown in the absence of CM (Fig. 3.15C). (Note that NCU02128 also belongs to a special class of genes discussed in section 3.3.6.) Two genes NCU04899 (malate dehydrogenase) and NCU05627 (high affinity glucose transporter), found in the 5- 5+ group and the 2+ 5- 5+ groups, respectively, were shown to be positively regulated by both AOD2 and AOD5. The transcript levels of NCU04899 were only slightly reduced in the Δ*aod-2* and Δ*aod-5* knockout strains grown in the absence of CM, but were reduced 1.7- and 2.1-fold in the respective cells grown in the presence of CM (Fig. 3.15D). The expression of NCU05627 was reduced more than two-fold in cells lacking AOD2 or AOD5 in –CM, but was reduced 1.8-fold and two-fold in +CM, respectively (Fig. 3.15D). These results are contradictory to the experimental class the genes are in. However, visual inspection reveals obvious peaks in the AOD2 -CM and AOD2 +CM experiments for NCU05627. For NCU04899, the ChIP-seq peaks in the 2- 2+ experiments are extremely small whereas the peaks for AOD5 experiments are obvious. This might explain why AOD2 had less impact than AOD5 on the expression of NCU04899. Given the RT-qPCR results for NCU04899, I also looked at the transcription of another malate dehydrogenase (NCU06211) but it seemed not to be dependent on AOD2 or AOD5 (Supplementary Fig. 3.9). One gene NCU02623 (mitochondrial hypoxia responsive domain) was shown to behave similar to the genes in Fig. 3.13A that showed a response to CM, but were not affected by loss of AOD2 or AOD5 (Fig. 3.15E). The gene was found in the 5- 5+ experimental class, but its expression does

not appear to be regulated by AOD5 under the conditions tested.

Seven genes were shown to have no changes greater than two-fold in their transcript levels when AOD2 or AOD5 were absent, regardless of whether the cells were grown in the presence or absence of CM (Supplementary Fig. 3.9). It is noteworthy that NCU04797 (FBP) was in this group. Found in the 5- 5+ experimental class, FBP is a gluconeogenic enzyme (discussed in section 4.3) that has been reported to be regulated by AOD2 and AOD5 orthologues in *A. nidulans*, *P. anserina*, and *S. cerevisiae* (Gasmi *et al.* 2014; Hynes *et al.* 2007; Sellem *et al.* 2009; Soontorngun *et al.* 2007). The fold-enrichments for binding the AOD2 protein in both AOD2 experiments (-CM and +CM) are more than three but less than the arbitrary four-fold cutoff in the upstream region of the FBP gene (Supplementary Fig. 3.10). In addition, inspection of the AOD2 experimental peaks shows that they are very small (Supplementary Fig. 3.10). The fold enrichments for the AOD5 +CM and AOD5 –CM experiments are 10.8 and 4.3, respectively. While it is conceivable that AOD2 and AOD5 do bind the FBP gene promoter, the RT-qPCR data for ChIP-seq peak validation (Supplementary Fig. 3.9) and for gene expression in cells grown in poor carbon sources (Fig. 3.6D) strongly suggest that AOD2 and AOD5 do not play a role in FBP induction in *N. crassa*, at least under the conditions tested. Taken together, these data show that certain genes outside the group of 65 do show dependence on AOD2 and/or AOD5 for expression. In addition, it appears that the categorization of genes by MACS2 is not always in agreement with the experimental data.

I was also interested in the expression NCU10051 (flavohemoglobin) because it was found in a microarray study of the Δ*rse2* and Δ*rse3* cells in *P. anserina* (Bovier *et al.* 2014). This gene was found in the 5+ group of the Venn diagram (Supplementary Fig. 3.11A). The expression of its orthologue was reported to be

dramatically increased when cells were grown in the presence of antimycin A in *P. anserina* (Bovier *et al.* 2014). However, induction was abolished in cells lacking the orthologues of AOD2 and AOD5 (Δ*rse2*Δ*rse3* cells). My RT-qPCR results showed that AOD2 and AOD5 do not affect expression of the gene under normal conditions, but expression was increased slightly (1.9-fold and 2.1-fold) in Δ*aod-2* and Δ*aod-5* cells, respectively, grown in the presence of CM (Supplementary Fig. 3.11B). Thus, AOD2 and AOD5 may have a slightly negative effect on flavohemoglobin expression in the presence of CM.

3.3.4 Gene expression in the Δ*aod-2* Δ*aod-5* double mutant

From Fig. 3.11, I noticed that in either Δ*aod-2* or Δ*aod-5* cells or in both mutant strains, there were slightly more transcripts of *aod-1* in +CM cells than –CM cells. A similar observation occurred for transcripts of the NCU01808 (cytochrome *c*), NCU03408 (hypothetical protein), NCU03651 (NADP-dependent malic enzyme), NCU04569 (5-oxoprolinase), NCU06382 (ABC transporter), NCU06940 (hypothetical protein), NCU08674 (pentatricopeptide repeat protein), NCU09873 (PEPCK), and NCU10007 (malate synthase) (Fig. 3.11) from the group of 65. One possible explanation for these observations is that when AOD2 is lacking, AOD5 alone is capable of facilitating a slight induction of these genes, and vice versa. Another possibility is that unknown proteins are involved in the induction. To distinguish between these possibilities, I performed RT-qPCR on an *aod-2 aod-5* double mutant (strain DX13) to test the expression of the above genes (except NCU06940). When grown in the absence or presence of CM, all genes in the double mutant background showed a pattern of transcript levels similar to the mutant strains (less than two-fold change, even though in many cases the differences are statistically

significant as judged by Student's t test), with two apparent exceptions. One exception was NCU09873 (PEPCK) (Fig. 3.16) where the transcript levels were not significantly altered in the *aod-2 aod-5* double mutant compared to Δ*aod-2* cells grown in the absence of CM. However, levels were more than three-fold reduced compared to Δ*aod-2* alone when the double mutant cells were grown in the presence of CM. In contrast, the transcript levels in the *aod-2 aod-5* double mutant was reduced (more than two-fold) when compared to the Δ*aod-5* cells following growth in both the presence or absence of CM. The other exception was NCU10007 (malate synthase) which displayed slightly decreased expression (more than two-fold) in the double mutant (Fig. 3.16). The data suggest that other factors may play a role in low level expression of these genes.

3.3.5 Functional categorization of genes found in ChIP-seq

To determine if the ChIP-seq peaks identified in this study were associated with genes of related function, I analyzed the genes identified using a web-based tool called Fungifun2 (Priebe *et al.* 2015). This tool allows gene set enrichment analyses and gene functional classification such as FunCat (Functional Catalogue) (Ruepp *et al.* 2004) analysis. It is an annotation scheme that consists of 28 main functional categories such as "metabolism" and "interaction with the cellular environment". Each category contains subcategories and different levels of categories are organized in a hierarchical structure. For the functional annotation of a certain level and a certain category of gene, a FunCat ID is assigned, which includes information about the level and category. It is noteworthy that a gene could belong to more than one category. For instance, the SNF1 gene is assigned to FunCat ID 30.01.05 (30 (main category): cellular communication/signal transduction mechanism; 30.01: cellular

Figure 3.16. Expression of genes associated with ChIP-seq peaks in a Δ*aod-2* Δ*aod-5* double mutant. The genes shown here were also shown in Fig. 3.11, but here the data from the Δ*aod-2* Δ*aod-5*double mutant strain is included. Methods of Student's t test analysis, and data collection were all as described in the legend to Fig. 3.11. Genes were selected from Fig. 3.11.

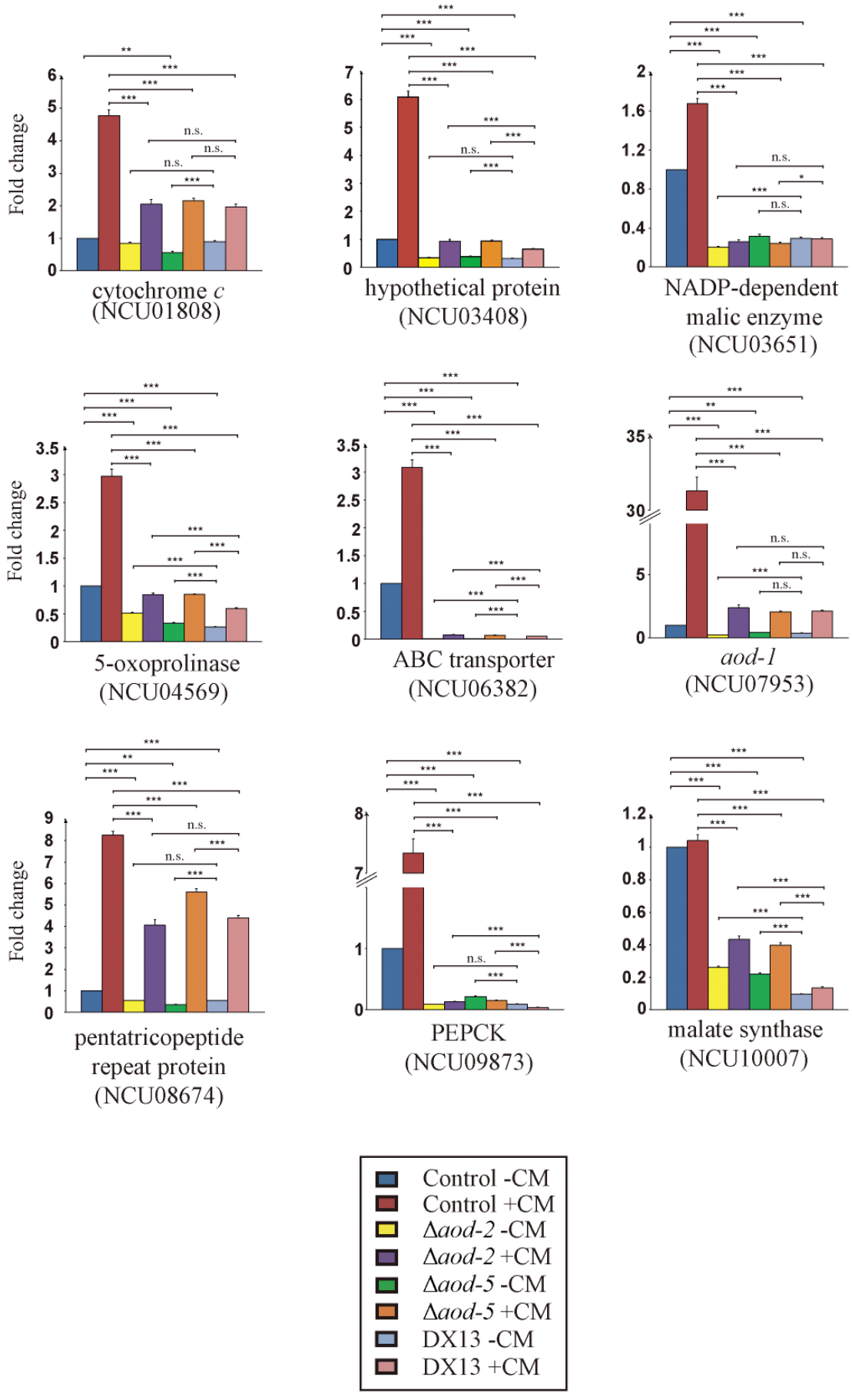
Fold change
cytochrome c
(NCU01808)
hypothetical protein
(NCU03408)
NADP-dependent
malic enzyme
(NCU03651)
5-oxoprolinase
(NCU04569)
ABC transporter
(NCU06382)
aod-1
(NCU07953)
pentatricopeptide
repeat protein
(NCU08674)
PEPCK
(NCU09873)
malate synthase
(NCU10007)
Control -CM
Control +CM
Δaod-2 -CM
Δaod-2 +CM
Δaod-5 -CM
Δaod-5 +CM
DX13 -CM
DX13 +CM

signaling; 30.01.05: enzyme mediated signaling transduction) and to FunCat ID 14.07.03 (14 (main category): protein fate; 14.07: protein modification; 14.07.03: modification by phosphorylation, dephosphorylation and autophosphorylation). Assignment to these two categories reflects: 1. Its involvement in signaling pathways and 2. The kinase activity of the protein (Ruepp *et al.* 2004).

I first used FunCat function to analyze the 98 genes that are associated with the 65 ChIP-seq peaks (Table 3.2). Note that of the 98 genes, 37 genes had no annotated functions as indicated by Fungifun2 and therefore had no FunCat IDs assigned by the system. Of the remaining 61 genes, Fungifun2 found that 43 genes were assigned to 29 FunCat IDs that were over-represented (p-value < 0.05) (Supplementary Table 3.1). These FunCat IDs were chiefly in the FunCat main categories of "metabolism" (12 IDs), "energy" (7 IDs), "cellular transport, transport facilitation and transport routes" (4 IDs), and "cellular communication/signal transduction mechanism" (3 IDs) (Fig. 3.17A and Supplementary Table 3.1). When I adjusted the p-values using the FDR correction tool available in the program, only 4 FunCat IDs were found to be over-represented. These IDs were "biosynthesis of glutamate", "degradation of glycine", "aerobic respiration", and "respiration" (Fig. 3.17B). They belonged to the "metabolism" and "energy" FunCat main categories.

I also performed FunCat analysis for those genes associated with the ChIP-seq peaks with more than four-fold enrichment in their 5' upstream region, compared to the corresponding wild-type control experiment, from the individual data sets for AOD2 +CM (280 genes), AOD2 –CM (401 genes), AOD5 +CM (1038 genes), and AOD5 –CM (325 genes) experimental data sets. Of the input genes, 115, 155, 384, and 118 genes from the AOD2 +CM, AOD2 –CM, AOD5 +CM, and AOD5 –CM experimental data sets, respectively, had no annotated functions in the database and

Figure 3.17. FunCat main categories in the 98 genes common to all four ChIP-seq experiments. The 98 genes that are associated with the 65 ChIP-seq peaks listed in Table 3.2 were entered into the Fungifun2 (https://elbe.hki-jena.de/fungifun/fungifun.php) online system. In the "Advanced Options" menu, "Hypergeometric distribution" with "over-representation (enrichment)" was chosen for p-value calculation. A. The pie chart was created based on the FunCat main categories that were over-represented and the total number of genes in 29 FunCat IDs that were calculated to be significant (p-value < 0.05, Supplementary Table 3.1). The p-values were not adjusted with the program's FDR correction. The genes in FunCat IDs that belong to the same main category were lumped together. B. As in A, but the p-values were adjusted with the FDR correction by selecting the "Benjamini-Hochberg Procedure (FDR correction)" in the "Advanced Options" menu in Fungifun2. In this case, only four FunCat IDs were found to be over-represented.

A

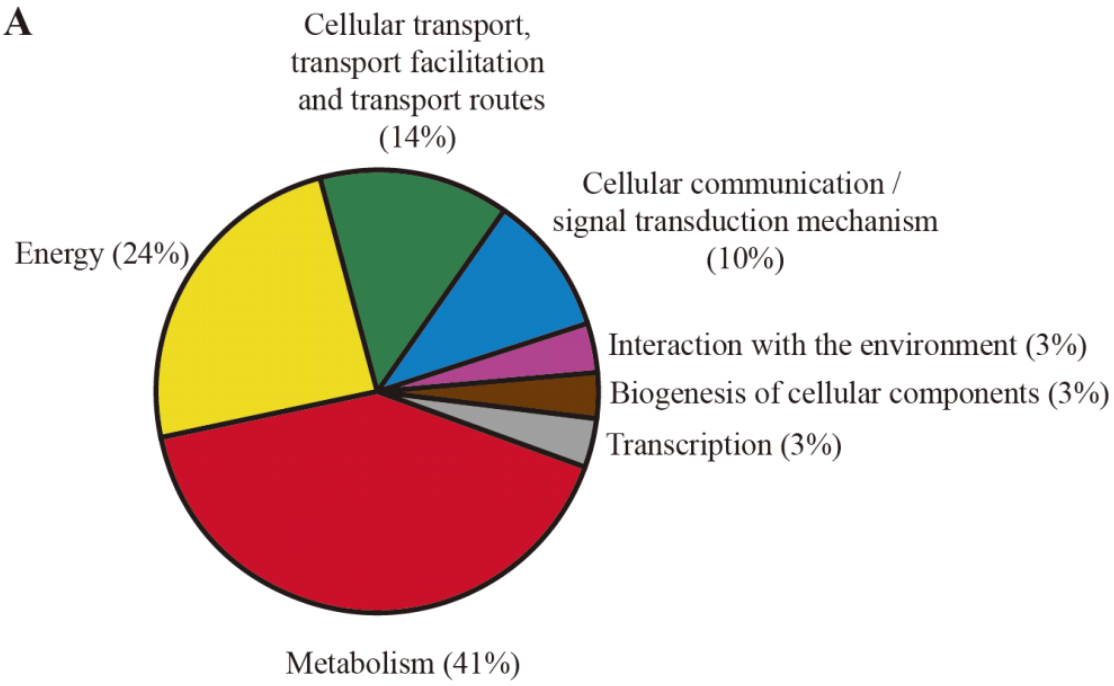
Cellular transport, transport facilitation and transport routes (14%)
Cellular communication / signal transduction mechanism (10%)
Interaction with the environment (3%)
Biogenesis of cellular components (3%)
Transcription (3%)
Metabolism (41%)
Energy (24%)

B

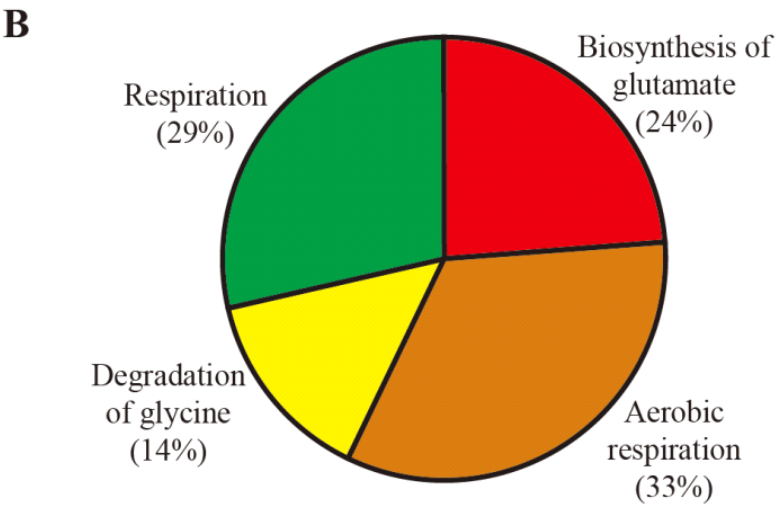
Biosynthesis of glutamate (24%)
Aerobic respiration (33%)
Degradation of glycine (14%)
Respiration (29%)

thus were not given a FunCat ID. 82, 155, 322, and 97 genes were assigned to 30, 47, 48, and 32 FunCat IDs that were overrepresented (p-value < 0.05) in the AOD2 +CM, AOD2 –CM, AOD5 +CM, and AOD5 –CM experiments, respectively (Supplementary Tables 3.2 to 3.5). Therefore, 50%, 63%, 49%, and 47% of the genes with annotated functions in the four experiments were found to be significantly enriched with respect to a related function. Among the FunCat IDs that have the 20 smallest p-values in each experiment, "biosynthesis of glutamate", "degradation of glycine", "aerobic respiration", "respiration", "mitochondrial transport", and "glycolysis and gluconeogenesis" were found in all experiments. Furthermore, three of the FunCat main categories ("metabolism", "energy", and "cellular transport, transport facilitation and transport routes") which were found within the 98 genes, as mentioned above, were also over-represented in all four experiments. These results suggest that AOD2 and AOD5 may play an import role in modulation of metabolism and energy production. Moreover, many genes not captured in our arbitrary set of genes that occurred in all four experiments may be affected by AOD2 and/or AOD5.

3.3.6 An additional binding motif for AOD2

During our general analysis of the ChIP-seq data, searches for conserved sequence motifs associated with the genes listed in Table 3.2 and 3.3 using the SCOPE motif finder (Martyanov & Gross 2011) revealed that a subset of the genes was associated with another well conserved upstream sequence that was not related to the AIM. Further investigation showed that 10 ChIP-seq peak sets were associated with a 310 bp sequence that is repeated with greater than 85% identity in 11 places throughout the *N. crassa* genome (Table 3.4). There are also smaller subsets of the

Table 3.4. A 310 bp conserved sequence associated with genes identified in the ChIP-seq analysis. The sequence upstream of NCU02128 was arbitrarily chosen as the probe to search against the *N. crassa* genome. The table includes all sites with > 85% identity over 310 base pairs.

Location	% identity to NCU02128 > 310 bp upstream region	Peak set gene(s)[1]	Gene name	Experimental class[2]
Supercontig 1 1155455-1155765	100	NCU02128	D-arabinitol dehydrogenase	2- 2+ 5+
Supercontig 1 1865502-1865814	88	NCU01957[3] NCU01958[3]	AR2 mating-type protein A-1	2- 2+ 5- 5+
Supercontig 1 5481346-5481655	87	NCU09144	hypothetical protein	2- 2+ 5-
Supercontig 2 825079-825389	100	NCU03408 NCU03409	hypothetical protein RNA lariat debranching enzyme	65
Supercontig 4 2271671-2271981	100	NCU07676 NCU07678[4]	hypothetical protein hypothetical protein	65
Supercontig 4 1096849-1097159	87	NCU04986 NCU11067	hypothetical protein hypothetical protein	65
Supercontig 4 5768811-5769121	87	NCU05202 NCU05203	hypothetical protein hypothetical protein	65
Supercontig 4 3512618-3512927	86	NCU04392	hypothetical protein	2- 2+ 5+

Supercontig 5 3654597-3654907	87	NCU01321 NCU01322	high-affinity nickel transporter transcription factor TFIIE complex alpha subunit	2+ 5- 5+
Supercontig 6 1613020-1613330	87	NCU05527	hypothetical protein	2- 2+
Supercontig 7 3974291-3974600	86	NCU09460[5] NCU09993[5]	NADH:ubiquinone oxidoreductase 20.1kD subunit helicase swr-1	N/A

[1] Gene or genes listed occurs in the 5' to 3' direction relative to the region, unless noted otherwise.

[2] Abbreviation used as described in Table 3.2. "65" indicates that the peaks are in the group of 65, whereas 2- 2+ 5- 5+ indicates that the peaks are common to all four experimental sets but the genes associated with the peaks are in the incorrect orientation relative to the peaks.

[3] Both genes are in the incorrect orientation relative to the peaks.

[4] The peak is much closer to the 5` end of this gene of the pair.

[5] These genes are at least 7 kbp distant from the repeat region and not associated with any ChIP-seq peaks.

310 bp sequence abundant in the genome. Each of the 310 bp sequences contains a set of 78 bp inverted repeats at the ends of the sequence (Fig. 3.18). The inverted repeats may have functional significance since they are more highly conserved than the region between them (Fig. 3.18A). The 310 bp repeats appear to have been subjected to the mutagenic process of repeat induced point mutation (RIP) that occurs with repeated sequences in *N. crassa* (Aramayo & Selker 2013; Gladyshev & Kleckner 2014; Selker 1990), since the majority of the changes found among the sequences are transitions, which are characteristic of RIP. Of the 80 positions containing a change in at least one of the 11 sequences, only 15 are transversions and one is in insertion of two bp. RIP was long thought to occur only with repeats greater than 400 bp (Watters *et al.* 1999) but recent data has shown that repeats as small as 155 bp may serve as substrates (Gladyshev & Kleckner 2014).

Of the 11 loci that contain the conserved sequence, five are associated with ChIP-seq peaks in the group of 65 (Table 3.4). Another five loci were found in other positions of the Venn diagram (Fig. 3.8). Only one of the repeated regions, which occurred between genes NCU09460 and NCU09993 on supercontig 7, was not found to be associated with any ChIP-seq peaks called by MACS2 (Table 3.4). A characteristic of the peak sets associated with these repeat sequences is the binding of relatively large amounts of AOD2 and smaller variable amounts of AOD5 (Fig. 3.19A) as compared to most "typical" peak sets observed in this study, such as for NCU09753 (*aod-1*) and NCU06940 (hypothetical protein) (Fig. 3.19B). One obvious exception to this rule is the repeat sequence in the region between genes NCU09460 and NCU09993 where, as mentioned above, no binding of either protein was observed. For the three repeat sequences near NCU01321, NCU03408, and NCU04986, there are higher levels of AOD5 bound than for the other repeats (Fig. 3.19A). Another

Figure 3.18. Alignment of 310 bp repeat regions. A. Schematic diagram of the repeat sequence (red) showing the inverted repeats (arrows). Two blue boxes indicate the positions of the highly conserved motif that is associated with AOD2 binding summit. The sequence of the motif is shown on the top and at the bottom of the blue boxes. The black line at the bottom of the panel defines the position of the two palindromic sequences, the sequence between them, and the percentage of overall conservation of the three regions. B. Sequences were retrieved following BLASTN of the *N. crassa* genome using the 310 bp repeat sequence upstream of NCU02128 as the probe. Clustal (Larkin *et al.* 2007) was used for the alignment. The palindromic regions are highlighted by the red lines. Asterisks indicate identical nucleotides among all sequences. Yellow shading in both panel A and panel B indicates the conserved AOD2 binding motif in each of the palindromic regions.

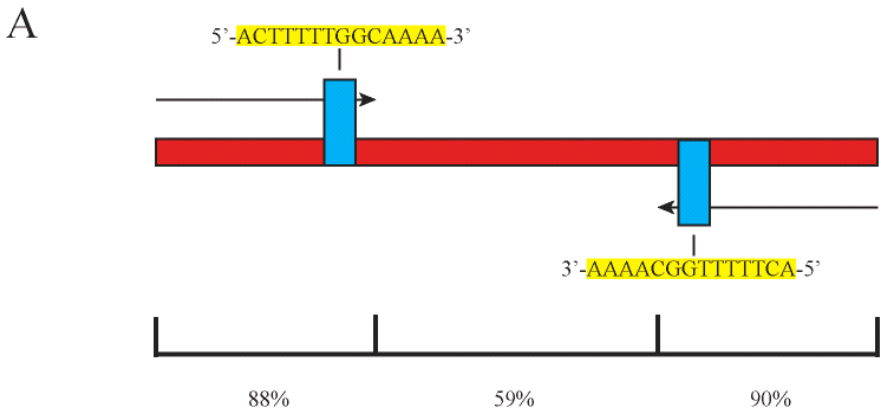

B


NCU04986 TTCCCACACTCAAACGCCTGTGCAGTCTTGGCGGACGTGTGCGTGTACACACACACACAA 60
NCU05202 TTCCCACACTCAAACGCCTGTGCAGTCTTGGCGGACGTGTGCGTGTACACACACACACAA 60
NCU09144 TTCCCACACTCAAACGCCTGTGCAGTCTTGGCGGACGTGTGCGTGTACACACACACACAA 60
NCU01957 TTCCCACACTCAAACGCCTGTGCAGTCTTGGCGGACGTGTGCGTGTACACACACACACAA 60
NCU01321 TTCCCACACTCAAACGCCTGTGCAGTCTTGGCGGACGTGTGCGTGTACACACACACACAA 60
NCU05527 TTCCCACACTCAAACGCCTGTGCAGTCTTGGCGGACGTGTGCGTGTACACACACACACAA 60
NCU04392 TTCCCACACTCAAACACCTGTGCAGTCTTGGCGGACGTGTGTGTGTACACACACACACAA 60
NCU09993 TTCCCACACTCAAACACCTGTGCAGTCTTGGCGGACGTATGTGTGTATATACACACACAA 60
NCU02128 TTCCCACACTCAATCGCCTGTGCAGTCTTGGCGGACGTGTGTGTGTACACGCACACACGA 60
NCU07676 TTCCCACACTCAATCGCCTGTGCAGTCTTGGCGGACGTGTGTGTGTACACGCACACACGA 60
NCU03409 TTCCCACACTCAATCGCCTGTGCAGTCTTGGCGGACGTGTGTGTGTACACGCACACACGA 60
NCU04986 CTTTTTGGCAAAACGGACCATCGACAAAATTTCATTTGCTTATATCTCTACCAAACGAGG 120
NCU05202 CTTTTTGGCAAAACGGACCATCGACAAAATTTCATTTGCTTATATCTCTACCAAACGAGG 120
NCU09144 CTTTTTGGCAAAACGGACCATCGACAAAATTTCATTTGCTTATATCTCTACCAAACGAGG 120
NCU01957 CTTTTTGGCAAAACGGACCATCGATGAGATTTCATTTGCTTATATCTCTACCAAACAAAG 120
NCU01321 CTTTTTGGCAAAACGGACCATCGATGAGATTTCATTTGCTTATATCTCTACTAAACAAAG 120
NCU05527 CTTTTTGGCAAAACGGACCATCGATGAGATTTCATTTGCTTATATTTCTATTAAGCGAAG 120
NCU04392 CTTTTTGGCAAAATGGACCATCGATGAGATTTCATTTGCTTATATCTCTACCAAACGGGG 120
NCU09993 CTTTTTGGCAAAATGGACTATCGATAAGATTTTATTTACTTATATCTCTACTAAACGGGG 120
NCU02128 CTTTTTGGCAAAACGGACTATCGATAAGATTTCGTTTGCTTATATCTCTACCAAACGAAG 120
NCU07676 CTTTTTGGCAAAACGGACTATCGATAAGATTTCGTTTGCTTATATCTCTACCAAACGAAG 120
NCU03409 CTTTTTGGCAAAACGGACTATCGATAAGATTTCGTTTGCTTATATCTCTACCAAACGAAG 120
NCU04986 AGATGAAAGAGAACCGACTTGAGATTTAGAATTAGAGTACTTAAAATTATCAAGAGAAAA 180
NCU05202 AGATGAAAGAGAACCGACTTGAGATTTAGAATTAGAGTACTTAAAATTATCAAGAGAAAA 180
NCU09144 AGATGAAAGAGAACCGACTTGAGATTTAGAATTAGAGTACTTAAAATTATCAAGAGAAAA 180
NCU01957 AGATAAAAGAAATCCGACTTGAGATTCAGAGTCAGCGTACTTAAGATTATTAAGAGAATA 180
NCU01321 AGATAAAAGAAATCCGACTTGAGATTCAGAATTAGCGTACTTAGGATTGTTAAGAGAGAA 180
NCU05527 AGATAAAAGAAAATTGACTTGAAATTCAAAGTTAGTGTACTTAAGATTATCAAGAGACAA 180
NCU04392 AGATAGAGGAAAACCGACTTGAGATTTAGGATCAGCGTACTTAGAACTACTAAGAAA-TA 179
NCU09993 AGATAAAGGAGAACCGACTTGAGATTTAGGATTAGCGTACTTAAAACTACTAAGAAAATA 180
NCU02128 AGATAAAAGAAAATGGACTCAAATTTTAGAATCGGCGTACCTAAGACTACTAAGACAATA 180
NCU07676 AGATAAAAGAAAATGGACTCAAATTTTAGAATCGGCGTACCTAAGACTACTAAGACAATA 180
NCU03409 AGATAAAAGAAAATGGACTCAAATTTTAGAATCGGCGTACCTGGCGGAACTAAGACAATA 180
NCU04986 GTTTTTT--CTATAGGATAATTGAATTCCTTCATCTTCGTCTTTCGTTTCAGTAGTCCAT 238
NCU05202 GTTTTTT--CTATAGGATAATTGAATTCCTTCATCTTCGTCTTTCGTTTCAGTAGTCCAT 238
NCU09144 GTTTTTT--CTATAGGATAATTGAATTCCTTCATCTTCGTCTTTCGTTTCAGTAGTCCAT 238
NCU01957 GTTTTTTTTCCATAGGATAATTGAGTTTCTTCATCTTCGTCTTTCGTTTCAATAGTCCAT 240
NCU01321 GTTTTTT--CCATAGGATAATTGAATTTATTCATCTTCGTCTTTCGTTTCAATAGTCCAT 238
NCU05527 GTTTTTT--CTATAGGATAATTGAATTTCTTCATCTTCGTCTTTCGTTTCAATAGTCCAT 238
NCU04392 GTTTTTC--CTCCAGGATAATTACATCTCGTCATCTCCATCTTTCGTTTCAATGGTCCGT 237
NCU09993 GTTTTTC--CTCTAGGATAATTGCATTTCGTCATCTCCATCTTTCGTTTCGATAGTCCGT 238
NCU02128 ATCTTTT--CTATAGTATAATTGAATTTCTTCATCTTCGTCTTTCGTTTCGATGGTCCGT 238
NCU07676 ATCTTTT--CTATAGTATAATTGAATTTCTTCATCTTCGTCTTTCGTTTCGATGGTCCGT 238
NCU03409 ATCTTTT--CTATAGTATAATTGAATTTCTTCATCTTCGTCTTTCGTTTCGATGGTCCGT 238
NCU04986 TTTGCCAAAAAGTTGTGTGTGTGTGTACACGCACACGTCCGCCAAGACTGCACAGGCGTT 298
NCU05202 TTTGCCAAAAAGTTGTGTGTGTGTGTACACGCACACGTCCGCCAAGACTGCACAGGCGTT 298
NCU09144 TTTGCCAAAAAGTTGTGTGTGTGTGTACACGCACACGTCCGCCAAGACTGCACAGGCGTT 298
NCU01957 TTTACCAAAAAGTTGTGTGTGTGTGTACACGCACACGTCCGCCAAGACTGCACAGGCGTT 300
NCU01321 TTTACCAAAAAGTTGTGTGTGTGTGTACACGCACACGTCCGCCAAGACTGCACAGGCGTT 298
NCU05527 TTTGCCAAAAAGTTGTGTGTGTGTGTACACGCACACGTCCGCCAAGACTGCACAGGCGTT 298
NCU04392 TTTGCCAAAAAGTTGTGTGTGTGTGTACACGCACACGTCCGCCAAGACTGCACAGGTGTT 297
NCU09993 TTTGCCAAAAAGTTGTGTGTGTGTGTACACGCACACGTCCGCCAAGACTGCACAGGTGTT 298
NCU02128 TTTGCCAAAAAGTCGTGTGTGCGTGTACACACACACATCCGCCAAGACTGCACAGGCGAT 298
NCU07676 TTTGCCAAAAAGTCGTGTGTGCGTGTACACACACACATCCGCCAAGACTGCACAGGCGAT 298
NCU03409 TTTGCCAAAAAGTCGTGTGTGCGTGTACACACACACATCCGCCAAGACTGCACAGGCGAT 298
NCU04986 TGAGTGTGGGAA 310
NCU05202 TGAGTGTGGGAA 310
NCU09144 TGAGTGTGGGAA 310
NCU01957 TGAGTGTGGGAA 312
NCU01321 TGAGTGTGGGAA 310
NCU05527 TGAGTGTGGGAA 310
NCU04392 TGAGTGTGGGAA 309
NCU09993 TGAGTGTGGGAA 310
NCU02128 TGAGTGTGGGAA 310
NCU07676 TGAGTGTGGGAA 310
NCU03409 TGAGTGTGGGAA 310

Figure 3.19. ChIP-seq peaks at regions containing the conserved 310 bp sequence. A. Peak sets associated with the conserved sequence are shown. The coding region of the genes is indicated by blue boxes and the 5' and 3' UTRs are indicated in grey. Introns are indicated by the thin folded lines and the orientation of a gene is indicated by a black arrow. ChIP-seq peaks are shown in blue with the y-axis representing the number of reads in the ChIP-seq. The maximum value of the y-axis in each experiment was adjusted based on the ratio of mapped reads in the anti-HA or anti-Myc data sets. The scale bar at the bottom indicates the length of 1 kbp. Note that the right side gene associated with the peak at the 5' region of NCU09144 is more than 20 kbp away from NCU09144. B. Peaks associated with NCU07953 (*aod-1*) and NCU06940 are shown for comparison. Features indicated are as in panel A.

A

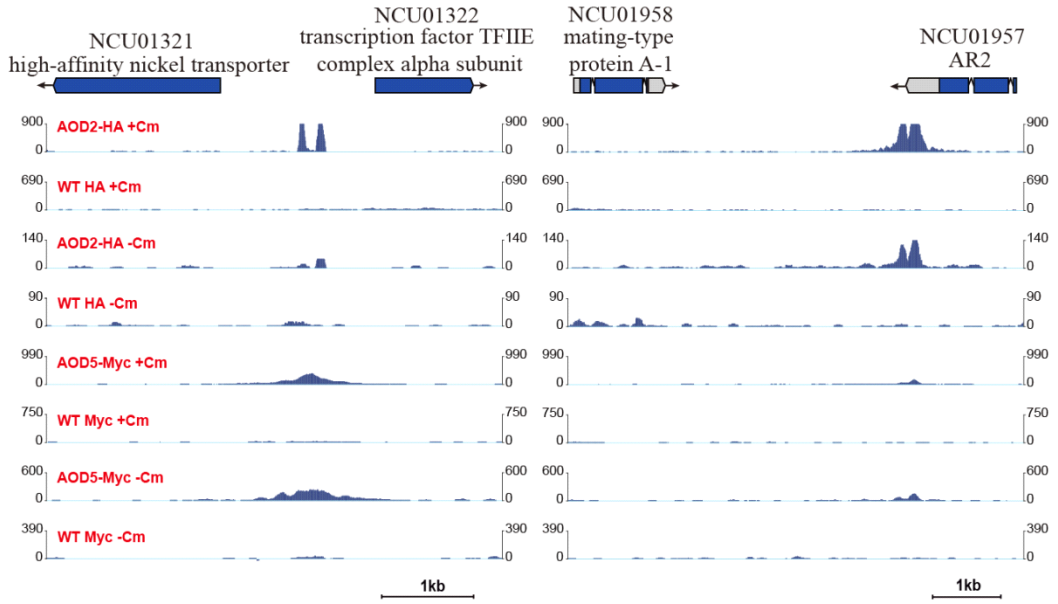
NCU01321
high-affinity nickel transporter
NCU01322
transcription factor TFIIE
complex alpha subunit
NCU01958
mating-type
protein A-1
NCU01957
AR2
AOD2-HA +Cm
WT HA +Cm
AOD2-HA -Cm
WT HA -Cm
AOD5-Myc +Cm
WT Myc +Cm
AOD5-Myc -Cm
WT Myc -Cm
1kb
1kb

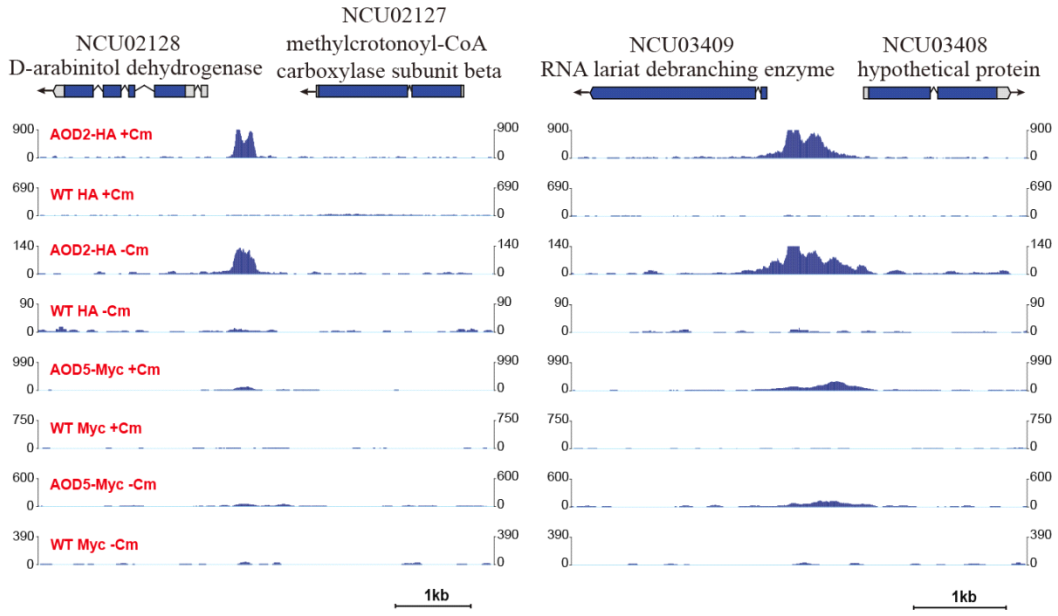
NCU02128
D-arabinitol dehydrogenase
NCU02127
methylcrotonoyl-CoA
carboxylase subunit beta
NCU03409
RNA lariat debranching enzyme
NCU03408
hypothetical protein
AOD2-HA +Cm
WT HA +Cm
AOD2-HA -Cm
WT HA -Cm
AOD5-Myc +Cm
WT Myc +Cm
AOD5-Myc -Cm
WT Myc -Cm
1kb
1kb

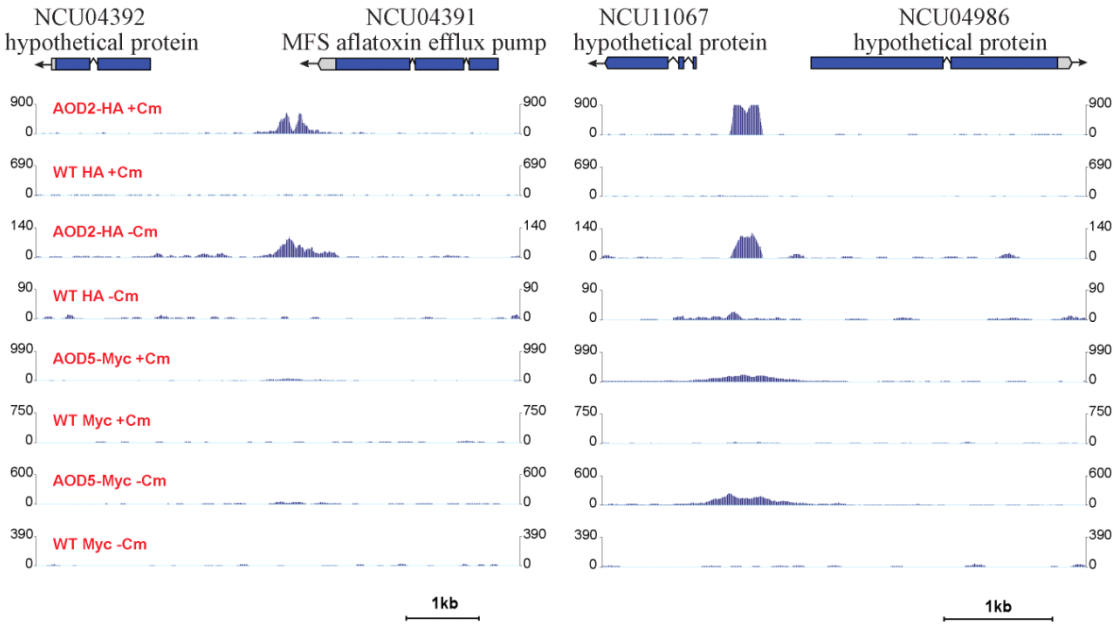
NCU04392
hypothetical protein
NCU04391
MFS aflatoxin efflux pump
NCU11067
hypothetical protein
NCU04986
hypothetical protein
AOD2-HA +Cm
WT HA +Cm
AOD2-HA -Cm
WT HA -Cm
AOD5-Myc +Cm
WT Myc +Cm
AOD5-Myc -Cm
WT Myc -Cm
1kb
1kb

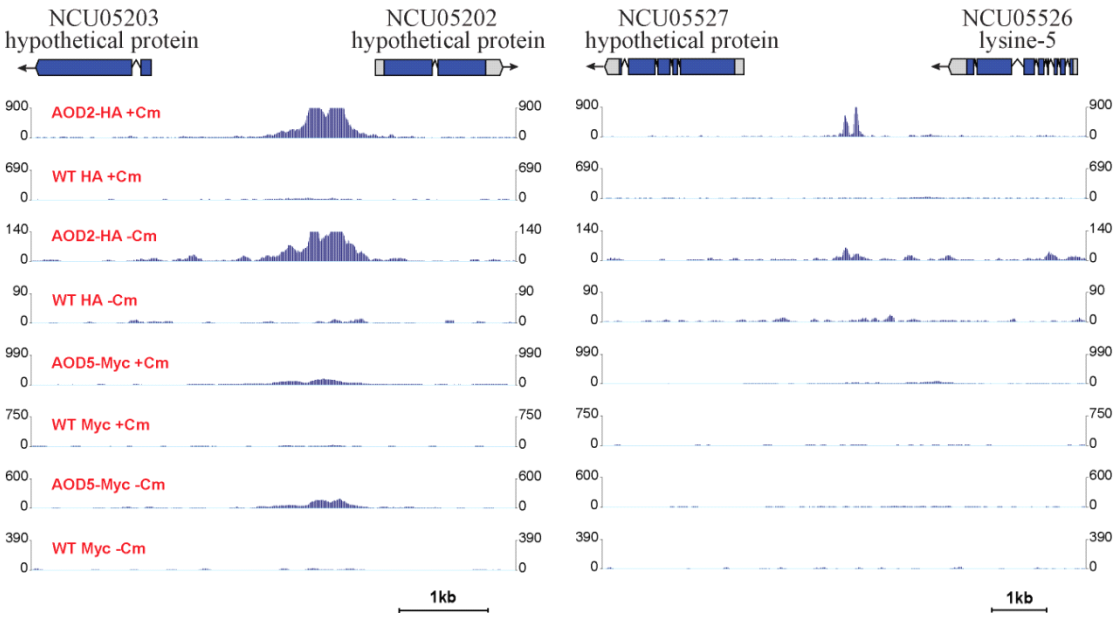
NCU05203
hypothetical protein
NCU05202
hypothetical protein
NCU05527
hypothetical protein
NCU05526
lysine-5
AOD2-HA +Cm
WT HA +Cm
AOD2-HA -Cm
WT HA -Cm
AOD5-Myc +Cm
WT Myc +Cm
AOD5-Myc -Cm
WT Myc -Cm
1kb
1kb

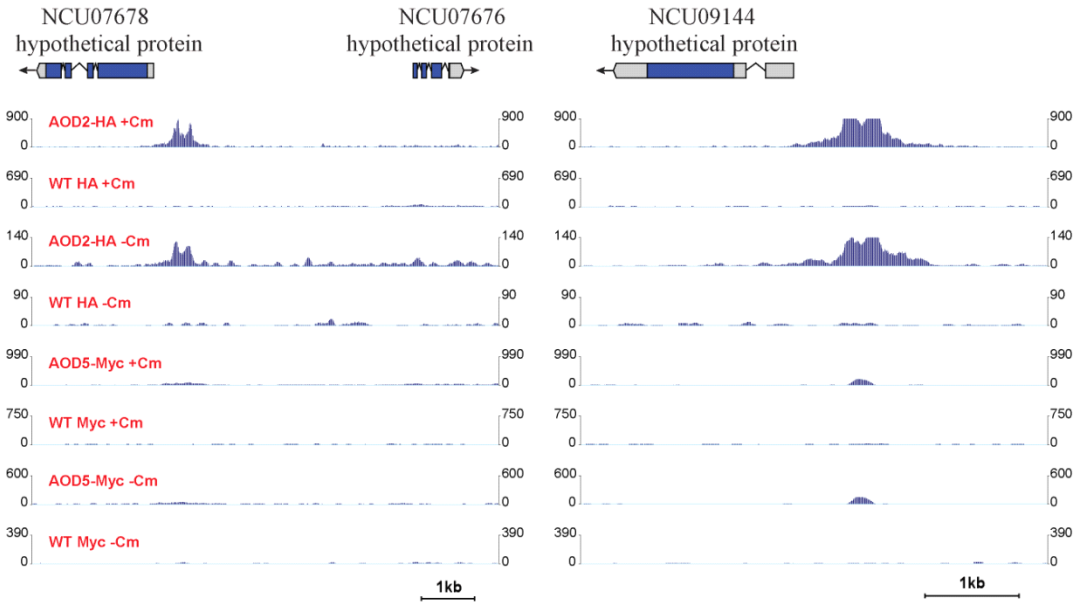
NCU07678
hypothetical protein
NCU07676
hypothetical protein
NCU09144
hypothetical protein
AOD2-HA +Cm
WT HA +Cm
AOD2-HA -Cm
WT HA -Cm
AOD5-Myc +Cm
WT Myc +Cm
AOD5-Myc -Cm
WT Myc -Cm
1kb
1kb

B

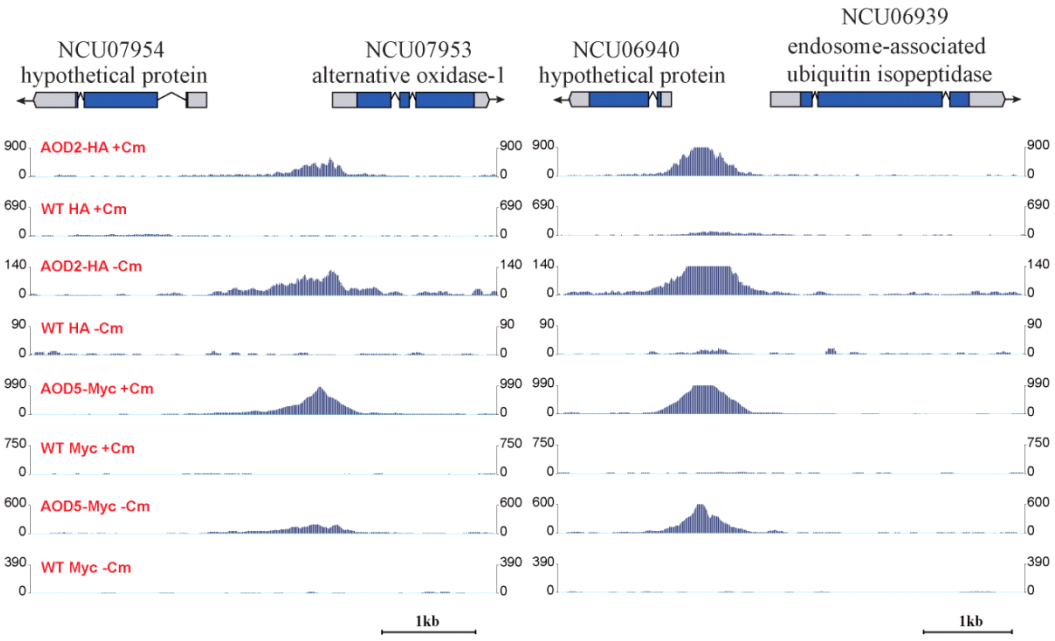
NCU07954
hypothetical protein
NCU07953
alternative oxidase-1
NCU06940
hypothetical protein
NCU06939
endosome-associated
ubiquitin isopeptidase
AOD2-HA +Cm
WT HA +Cm
AOD2-HA -Cm
WT HA -Cm
AOD5-Myc +Cm
WT Myc +Cm
AOD5-Myc -Cm
WT Myc -Cm
1kb
1kb

characteristic of these 10 binding sites is that the AOD2 peak is usually divided into two summits especially in the +CM data sets. The AOD2 peak summits at these sequences are always found associated with all or a portion of a highly conserved 14 bp sequence (Fig. 3.18), which occurs at the ends of the inverted repeats. These AOD2 peaks are located in the correct upstream position for at least one of the genes adjacent to the peaks in nine of the 10 cases (Table 3.4) and could contribute to the regulation of the genes.

Of the 18 genes listed in Table 3.4 that are associated with the 310 bp repeat, NCU01957 and NCU01958 are in the wrong orientation relative to the sequence, and NCU09460 and NCU09993 are each more than 7 kbp distant from the sequence. In the latter case, no ChIP-seq peaks present at the repeat site. RT-qPCR analysis was performed on eight of the 14 remaining genes. NCU03408 was found to be positively regulated by both AOD2 and AOD5 under the conditions tested, whereas NCU03409 was unaffected (Fig. 3.11A, Supplementary Fig. 3.8). The expression of NCU02128 (D-arabinitol dehydrogenase) was only affected by AOD2 (Fig. 3.15C), as the transcript levels were reduced more than two-fold when Δ*aod-2* cells were grown in the absence of CM. The expression of NCU07678, NCU05202, and NCU0520 was not dependent on AOD2 or AOD5 (Fig. 3.13A and Supplementary Fig. 3.8). For NCU04392 and NCU09144, an unexpected two-fold increase in their expression was observed in Δ*aod-5* cells grown in the absence of CM (Fig. 3.15B), despite the fact that little AOD5 binding is associated with these genes (Fig. 3.19A). Expression of these latter two genes was not affected by loss of AOD2 under the conditions tested (Fig. 3.15B). There is no obvious explanation for these observations. Much more work is required to gain insight into the role of this AOD2 binding motif.

With regard to preferential binding sites for AOD2, it should also be noted

that there are 17 ChIP-seq peaks in the Venn diagram that are common to only the AOD2 –CM and +CM experiments (Fig. 3.8). However, visual inspection revealed that most of the peaks are not associated with abundant AOD2 binding. Of the genes in this class, only the peak set associated with the NCU01053 gene exhibits good peak quality in the AOD2 experiments and virtually no AOD5 binding (Supplementary Fig. 3.12). Unlike the peaks listed in Table 3.4 and shown on Fig. 3.19, however, the NCU01053 peak is not bimodal in shape, nor is the 310 bp repeat sequence found at this site. RT-qPCR data showed that the expression of NCU01053 was not affected by the absence of AOD2 under the conditions tested (Supplementary Fig. 3.9).

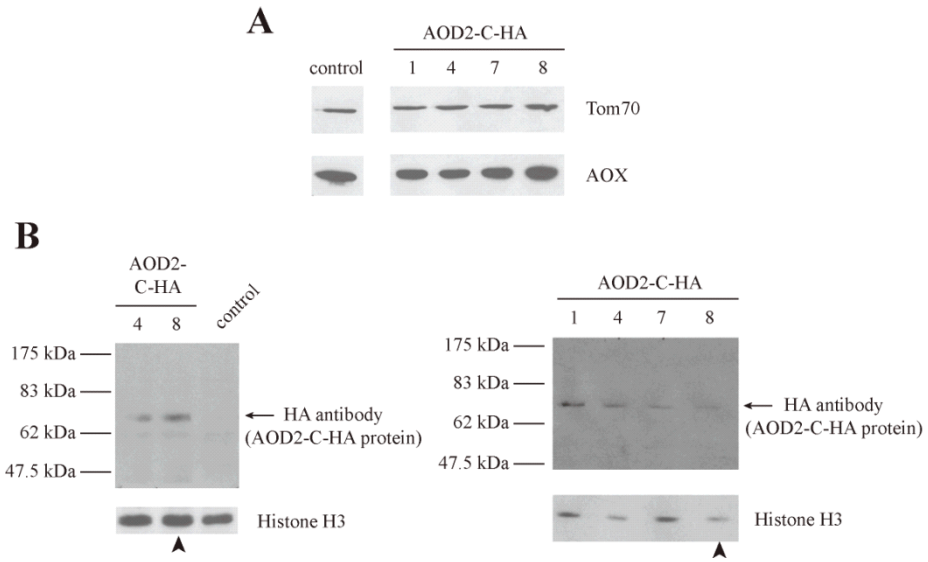

Supplementary Figure 3.1. Initial examination of AOD2-C-HA transformants. A. A plasmid construct containing C-terminal 3× HA tagged *aod-2* was transformed into an *aod-2* mutant strain (CNA33) and four transformants that exhibited good conidiation were examined for their ability to express AOX. Strains were grown in the presence of CM and mitochondria were isolated. Mitochondrial proteins were subjected to SDS-PAGE, blotted to nitrocellulose and analyzed by Western blot. The MOM protein Tom70 was used as a loading control. The control strain was the wild-type strain NCN251. B. AOD2-C-HA transformants were examined for the presence of 3× HA tagged AOD2 on two separate gels. Crude nuclei were isolated from cells grown in the absence of CM. Nuclear proteins were extracted, subjected to SDS-PAGE, blotted to nitrocellulose, and examined by Western blot. Histone H3 was used as a loading control. Antibodies used are indicated on the right. The control strain was as for panel A. Arrowheads point to the transformant that was selected for further work. The arrow on the right indicates the position of AOD2-C-HA protein. Molecular weight markers for the HA blots are indicated on the left.

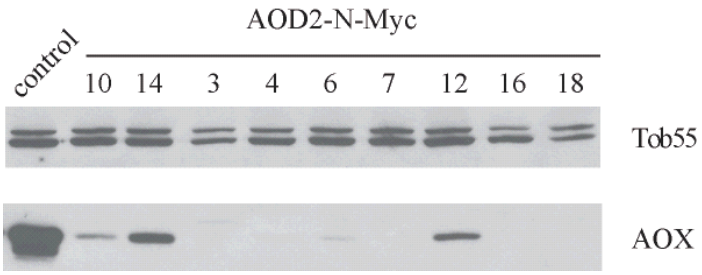

Supplementary Figure 3.2. Initial examination of AOD2-N-Myc transformants. A plasmid construct containing N-terminal 3× Myc tagged *aod-2* was transformed into an *aod-2* mutant strain (CNA33) and nine transformants that exhibited good conidiation were examined for their ability to express AOX. Strains were grown in the presence of CM and mitochondria were isolated. Mitochondrial proteins were subjected to SDS-PAGE, blotted to nitrocellulose and analyzed by Western blot. The MOM protein Tob55 was used as a loading control. (Tob55 appears as a doublet because alternative splicing of its transcript gives rise to different versions of the protein (Hoppins *et al.* 2007)). The control was the wild-type strain NCN251.

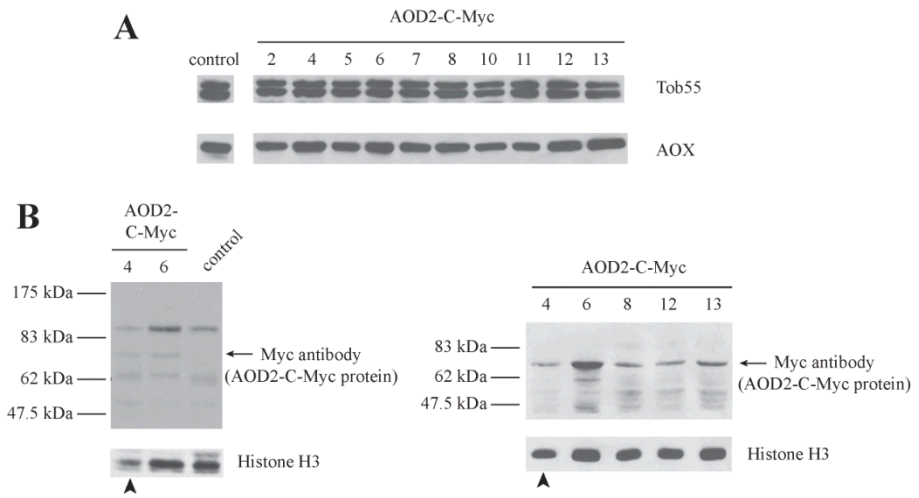

Supplementary Figure 3.3. Initial examination of AOD2-C-Myc transformants. A. A plasmid construct containing C-terminal 3× Myc tagged *aod-2* was transformed into an *aod-2* mutant strain (CNA33) and 10 transformants that exhibited good conidiation were examined for their ability to express AOX. Strains were grown in the presence of CM and mitochondria were isolated. Mitochondrial proteins were subjected to SDS-PAGE, blotted to nitrocellulose and analyzed by Western blot. The MOM protein Tob55 was used as a loading control. (Tob55 appears as a doublet because alternative splicing of its transcript gives rise to different versions of the protein (Hoppins *et al.* 2007)). The control was the wild-type strain NCN251. B). AOD2-C-Myc transformants were examined for the presence of 3× Myc tagged AOD2. Crude nuclei were isolated from cells grown in the absence of CM. Nuclear proteins were extracted, subjected to SDS-PAGE, blotted to nitrocellulose, and examined by Western blot. Histone H3 was used as a loading control. Antibodies used are indicated on the right. The control was as for panel A. Arrowheads point to the transformant that was selected for further work. Although isolate 6 expressed more of the tagged protein, it seemed likely that this was due to overexpression since all other isolates expressed a lesser, but similar, amount of the protein. The arrow on the right indicates the position of AOD2-C-Myc protein. Molecular weight markers for the Myc blots are indicated on the left.

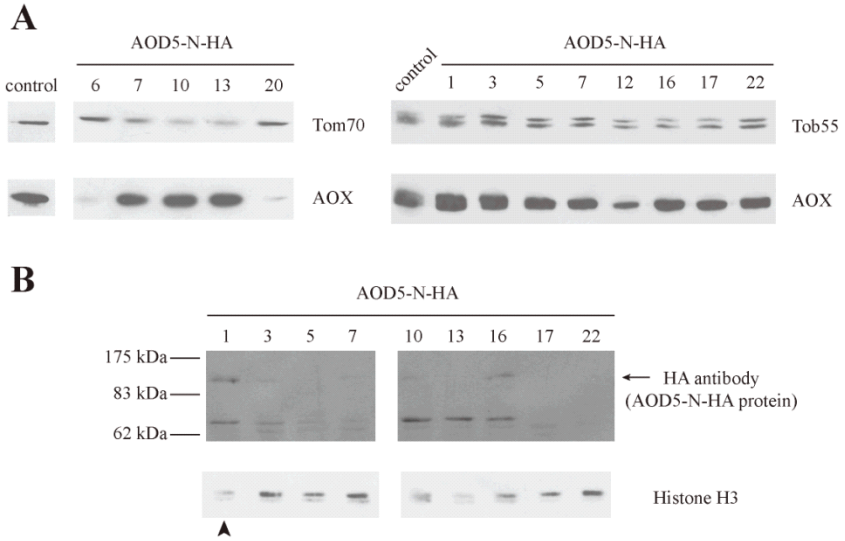

Supplementary Figure 3.4. Initial examination of AOD5-N-HA transformants. A. A plasmid construct containing N-terminal 3× HA tagged *aod-5* was transformed into an *aod-5* mutant strain (PL23-40) and 13 transformants that exhibited good conidiation were examined for their ability to express AOX. Strains were grown in the presence of CM and mitochondria were isolated. Mitochondrial proteins were subjected to SDS-PAGE, blotted to nitrocellulose and analyzed by Western blot. The MOM proteins Tom70 or Tob55 were used as loading controls. (Tob55 appears as a doublet because alternative splicing of its transcript gives rise to different versions of the protein (Hoppins *et al.* 2007)). The control was the wild-type strain NCN251. B. AOD5-N-HA transformants were examined for the presence of 3× HA tagged AOD5. Crude nuclei were isolated from cells grown in the absence of CM. Nuclear proteins were extracted, subjected to SDS-PAGE, blotted to nitrocellulose, and examined by Western blot. Histone H3 was used as a loading control. Antibodies used are indicated on the right. The control was as for panel A. Arrowheads point to the transformant that was selected for further work. The arrow on the right indicates the position of AOD5-N-HA protein. Molecular weight markers for the HA blot are indicated on the left.

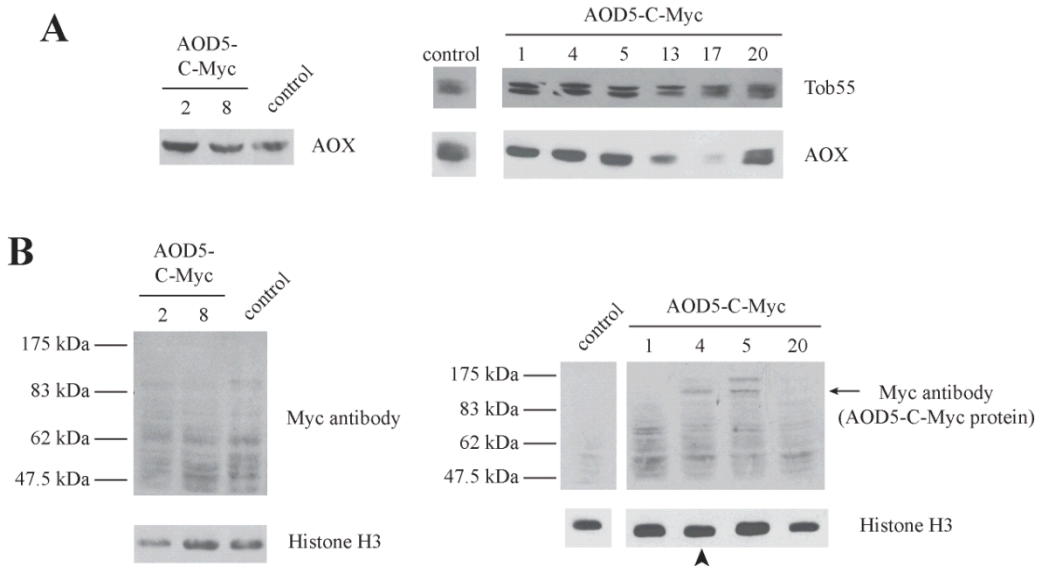

Supplementary Figure 3.5. Initial examination of AOD5-C-Myc transformants. A. A plasmid construct containing C-terminal 3× Myc tagged *aod-5* was transformed into an *aod-5* mutant strain (PL23-40) and eight transformants that exhibited good conidiation were examined for their ability to express AOX. Strains were grown in the presence of CM and mitochondria were isolated. Mitochondrial proteins were subjected to SDS-PAGE, blotted to nitrocellulose and analyzed by Western blot. The MOM protein Tob55 was used as a loading control. (Tob55 appears as a doublet because alternative splicing of its transcript gives rise to different versions of the protein (Hoppins *et al.* 2007)). The control was the wild-type strain NCN251. B. AOD5-C-Myc transformants were examined for the presence of 3× Myc tagged AOD5. Crude nuclei were isolated from cells grown in the absence of CM. Nuclear proteins were extracted, subjected to SDS-PAGE, blotted to nitrocellulose, and examined by Western blot. Histone H3 was used as a loading control. Antibodies used are indicated on the right. The control was strain AOD2-C-HA-8, which is an AOD5 untagged strain. Arrowhead points to the transformant that was selected for further work. The arrow on the right indicates the position of AOD5-C-Myc protein. Molecular weight markers for the Myc blots are indicated on the left.

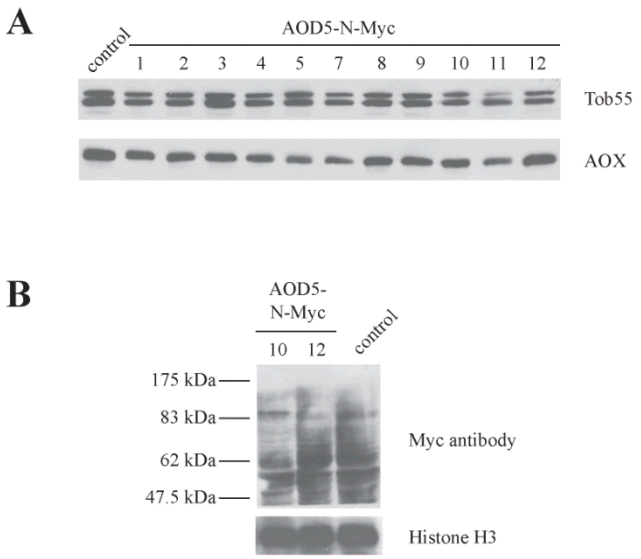

Supplementary Figure 3.6. Initial examination of AOD5-N-Myc transformants. A. A plasmid construct containing N-terminal 3× Myc tagged *aod-5* was transformed into an *aod-5* mutant strain (PL23-40) and 11 transformants that exhibited good conidiation were examined for their ability to express AOX. Strains were grown in the presence of CM and mitochondria were isolated. Mitochondrial proteins were subjected to SDS-PAGE, blotted to nitrocellulose and analyzed by Western blot. The MOM protein Tob55 was used as a loading control. (Tob55 appears as a doublet because alternative splicing of its transcript gives rise to different versions of the protein (Hoppins *et al.* 2007)). The control was the wild-type strain NCN251. B. AOD5-N-Myc transformants were examined for the presence of 3× Myc tagged AOD5. Crude nuclei were isolated from cells grown in the absence of CM. Nuclear proteins were extracted, subjected to SDS-PAGE, blotted to nitrocellulose, and examined by Western blot. Histone H3 was used as a loading control. Antibodies used are indicated on the right. The control was as for panel A. The 100 kDa protein band identified as tagged AOD5 in the previous analysis (Fig. 3.2B) was not detected in either of the transformants analyzed. Molecular weight markers for the Myc blot are indicated on the left.

Supplementary Figure 3.7. Alignment of AIM sequences with ChIP-seq peaks. The 70 peaks that are common to all four sets of experiments were examined. CGG(N7)CGG sequences on the + strand are indicated by black arrows whereas CCG(N7)CCG sequences on the + strand are indicated by red arrows. In cases where CGG(N7)CGG and CCG(N7)CCG sequences are too close to each other to be resolved, green arrows are used. One green arrow is a mixture of a CGG(N7)CGG and a CCG(N7)CCG. Shorter green arrows with two numbers above indicate the number of CGG(N7)CGG sequences (black number) and CCG(N7)CCG sequences (red number). If there are two or more closely clustered CGG(N7)CGG repeats, the black arrows are shortened and the number on the top indicates the number of repeats. The same applies to CCG(N7)CCG repeats using shortened red arrows. Note that some regions have no AIMs and thus no color arrows are shown. Peaks are shown between the two genes closest to the peak. The y-axis was adjusted for each gene set to maximize the ability to detect summits and therefore did not reflect the ratios used in other figures based on number of reads per experiment. The control experiments are not shown.

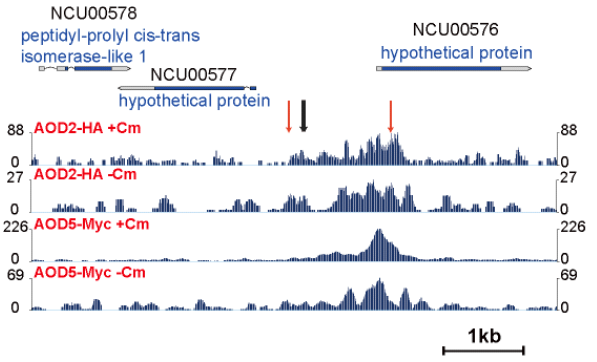
NCU00578
peptidyl-prolyl cis-trans isomerase-like 1
NCU00577
hypothetical protein
NCU00576
hypothetical protein
AOD2-HA +Cm
AOD2-HA -Cm
AOD5-Myc +Cm
AOD5-Myc -Cm
1kb

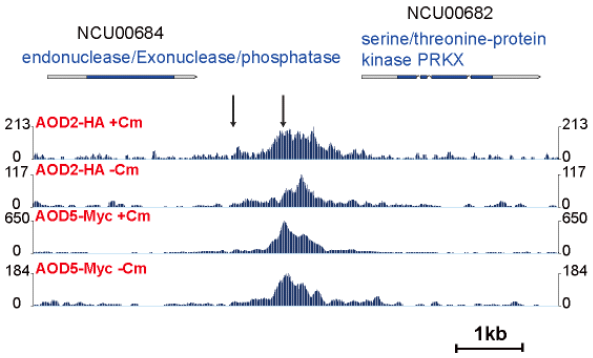
NCU00684
endonuclease/Exonuclease/phosphatase
NCU00682
serine/threonine-protein kinase PRKX
AOD2-HA +Cm
AOD2-HA -Cm
AOD5-Myc +Cm
AOD5-Myc -Cm
1kb

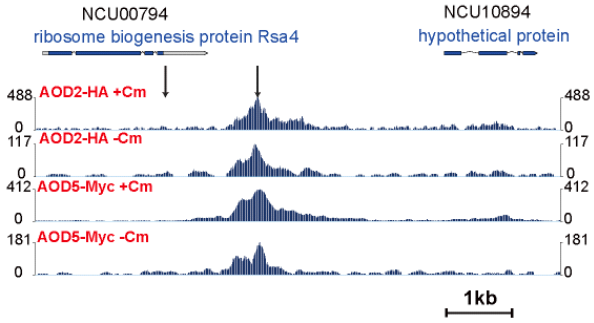
NCU00794
ribosome biogenesis protein Rsa4
NCU10894
hypothetical protein
AOD2-HA +Cm
AOD2-HA -Cm
AOD5-Myc +Cm
AOD5-Myc -Cm
1kb

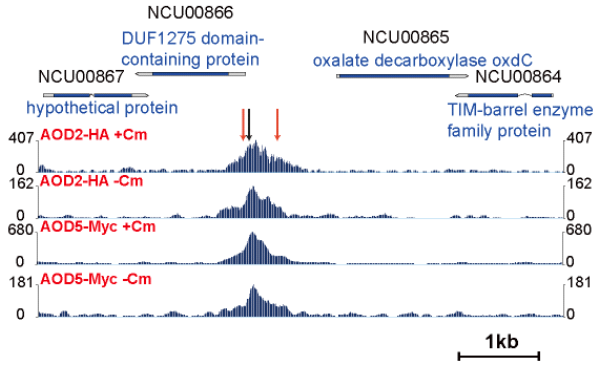
NCU00866
DUF1275 domain-containing protein
NCU00865
oxalate decarboxylase oxdC
NCU00867
hypothetical protein
NCU00864
TIM-barrel enzyme family protein
AOD2-HA +Cm
AOD2-HA -Cm
AOD5-Myc +Cm
AOD5-Myc -Cm
1kb

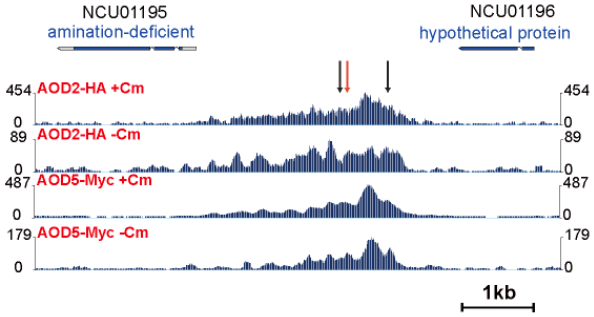
NCU01195
amination-deficient
NCU01196
hypothetical protein
AOD2-HA +Cm
AOD2-HA -Cm
AOD5-Myc +Cm
AOD5-Myc -Cm
1kb

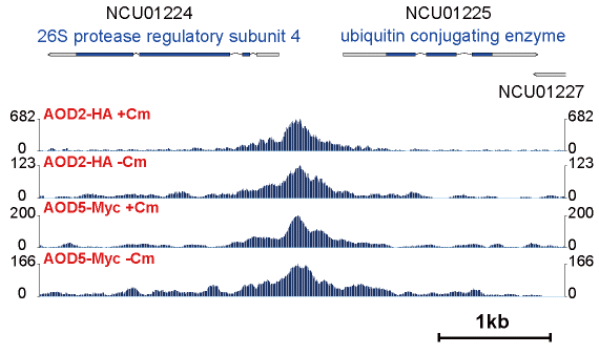
NCU01224
26S protease regulatory subunit 4
NCU01225
ubiquitin conjugating enzyme
NCU01227
AOD2-HA +Cm
AOD2-HA -Cm
AOD5-Myc +Cm
AOD5-Myc -Cm
1kb

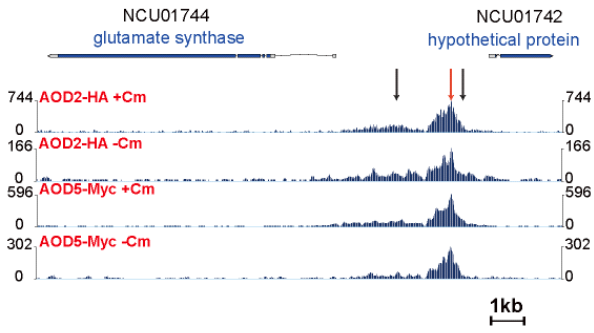
NCU01744
glutamate synthase
NCU01742
hypothetical protein
AOD2-HA +Cm
AOD2-HA -Cm
AOD5-Myc +Cm
AOD5-Myc -Cm
1kb

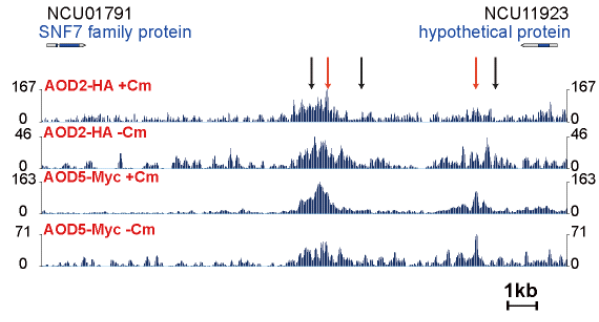
NCU01791
SNF7 family protein
NCU11923
hypothetical protein
AOD2-HA +Cm
AOD2-HA -Cm
AOD5-Myc +Cm
AOD5-Myc -Cm
1kb

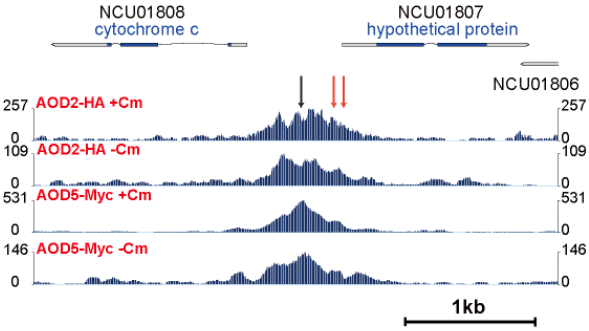
NCU01808
cytochrome c
NCU01807
hypothetical protein
NCU01806
AOD2-HA +Cm
AOD2-HA -Cm
AOD5-Myc +Cm
AOD5-Myc -Cm
1kb

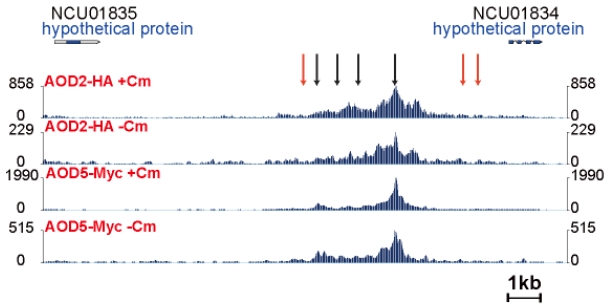
NCU01835
hypothetical protein
NCU01834
hypothetical protein
AOD2-HA +Cm
AOD2-HA -Cm
AOD5-Myc +Cm
AOD5-Myc -Cm
1kb

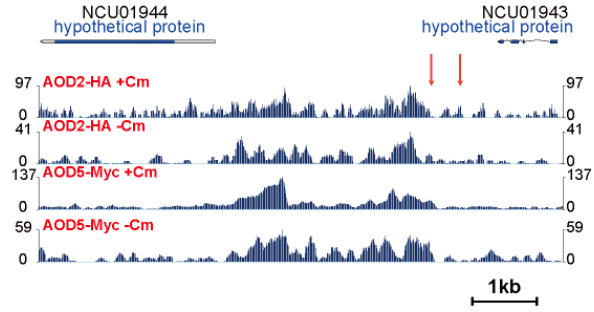
NCU01944
hypothetical protein
NCU01943
hypothetical protein
AOD2-HA +Cm
AOD2-HA -Cm
AOD5-Myc +Cm
AOD5-Myc -Cm
1kb

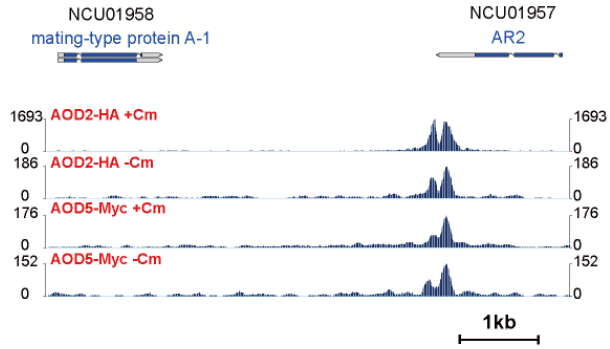
NCU01958
mating-type protein A-1
NCU01957
AR2
AOD2-HA +Cm
AOD2-HA -Cm
AOD5-Myc +Cm
AOD5-Myc -Cm
1kb

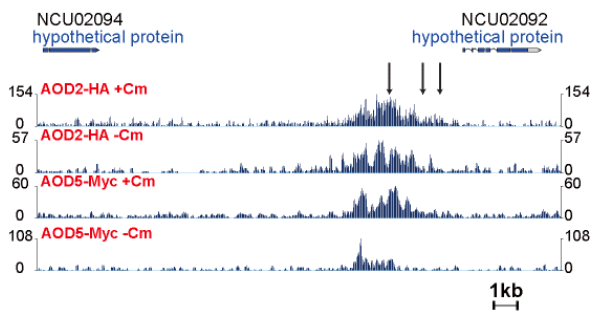
NCU02094
hypothetical protein
NCU02092
hypothetical protein
AOD2-HA +Cm
AOD2-HA -Cm
AOD5-Myc +Cm
AOD5-Myc -Cm
1kb

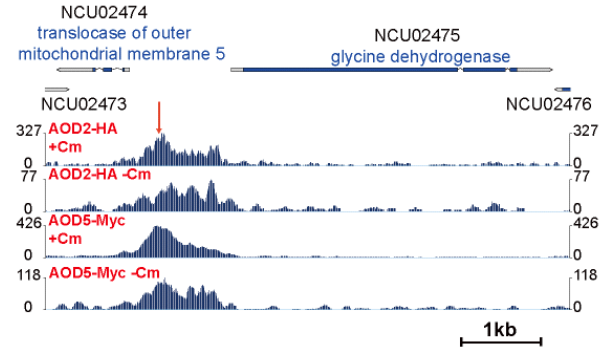
NCU02474
translocase of outer
mitochondrial membrane 5
NCU02475
glycine dehydrogenase
NCU02473
NCU02476
AOD2-HA
+Cm
AOD2-HA -Cm
AOD5-Myc
+Cm
AOD5-Myc -Cm
1kb

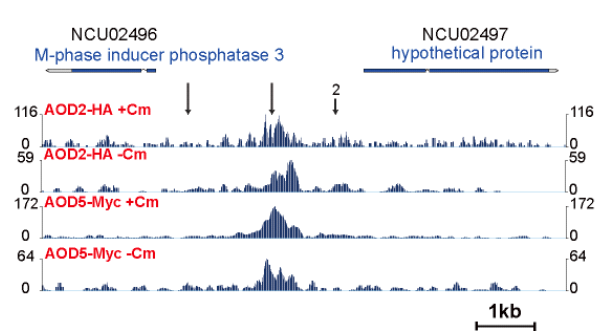
NCU02496
M-phase inducer phosphatase 3
NCU02497
hypothetical protein
2
AOD2-HA +Cm
AOD2-HA -Cm
AOD5-Myc +Cm
AOD5-Myc -Cm
1kb

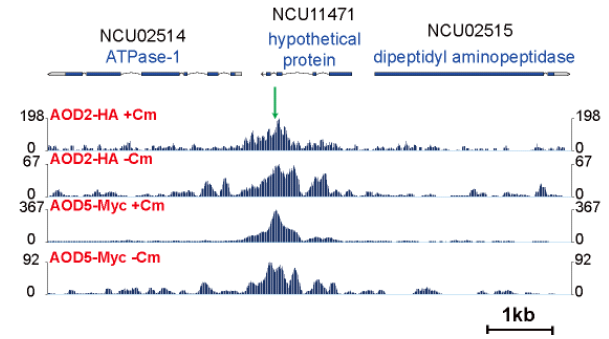
NCU02514
ATPase-1
NCU11471
hypothetical
protein
NCU02515
dipeptidyl aminopeptidase
AOD2-HA +Cm
AOD2-HA -Cm
AOD5-Myc +Cm
AOD5-Myc -Cm
1kb

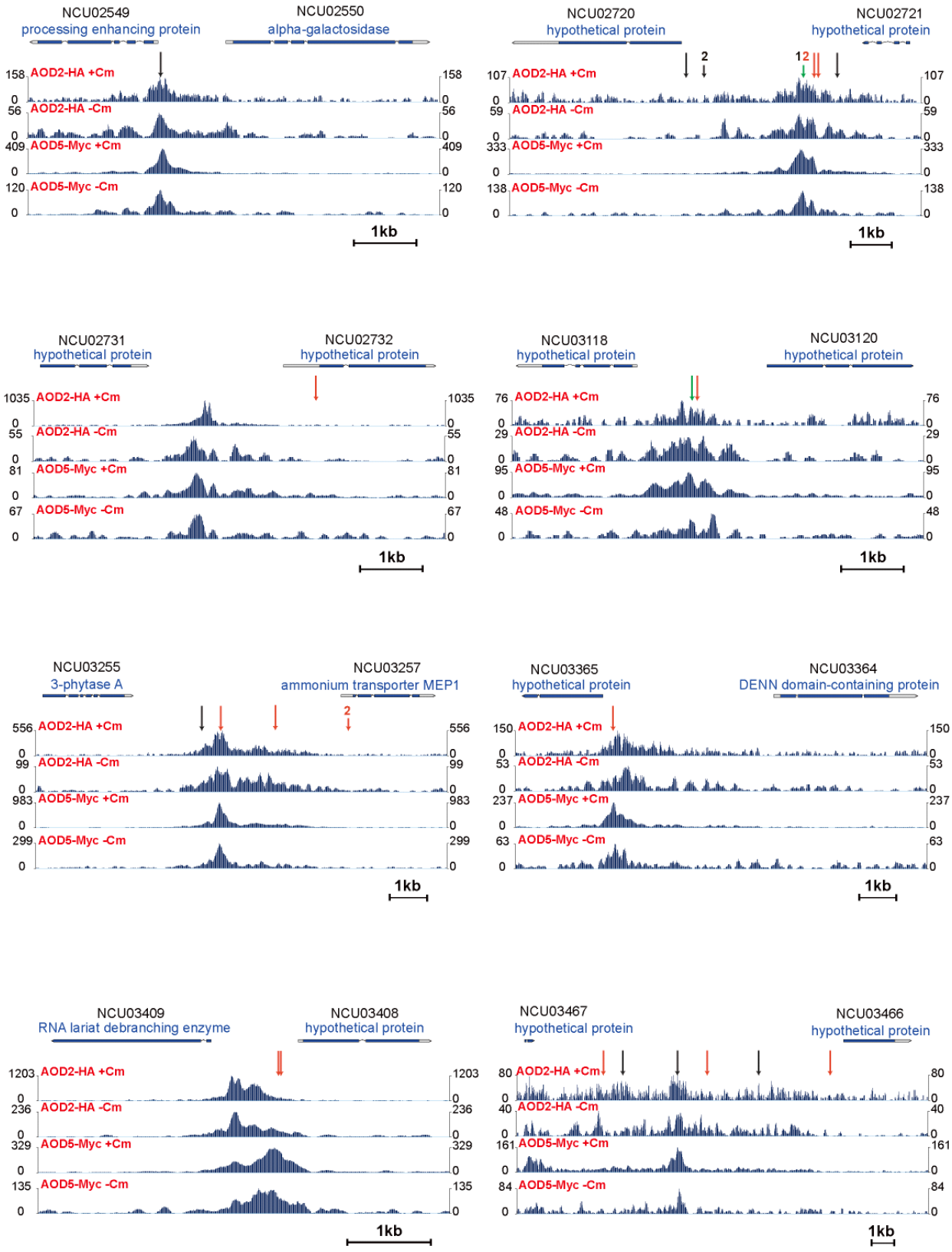
NCU02549
processing enhancing protein
NCU02550
alpha-galactosidase
AOD2-HA +Cm
AOD2-HA -Cm
AOD5-Myc +Cm
AOD5-Myc -Cm
1kb
NCU02720
hypothetical protein
NCU02721
hypothetical protein
NCU02731
hypothetical protein
NCU02732
hypothetical protein
NCU03118
hypothetical protein
NCU03120
hypothetical protein
NCU03255
3-phytase A
NCU03257
ammonium transporter MEP1
NCU03365
hypothetical protein
NCU03364
DENN domain-containing protein
NCU03409
RNA lariat debranching enzyme
NCU03408
hypothetical protein
NCU03467
hypothetical protein
NCU03466
hypothetical protein

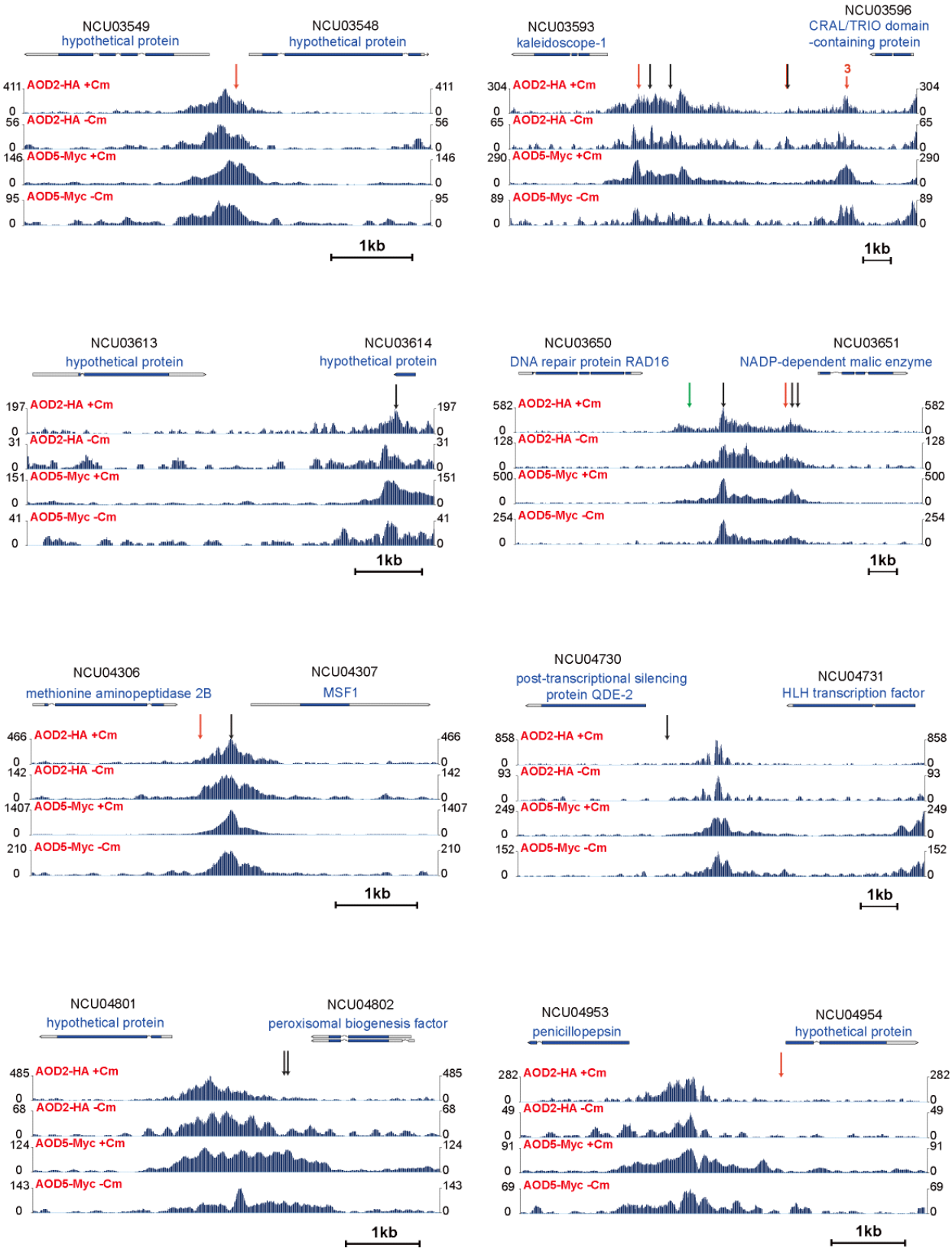
NCU03549
hypothetical protein
NCU03548
hypothetical protein
411 AOD2-HA +Cm
0
411
56 AOD2-HA -Cm
0
56
146 AOD5-Myc +Cm
0
146
95 AOD5-Myc -Cm
0
95
1kb
NCU03593
kaleidoscope-1
NCU03596
CRAL/TRIO domain
-containing protein
3
304 AOD2-HA +Cm
0
304
65 AOD2-HA -Cm
0
65
290 AOD5-Myc +Cm
0
290
89 AOD5-Myc -Cm
0
89
1kb
NCU03613
hypothetical protein
NCU03614
hypothetical protein
197 AOD2-HA +Cm
0
197
31 AOD2-HA -Cm
0
31
151 AOD5-Myc +Cm
0
151
41 AOD5-Myc -Cm
0
41
1kb
NCU03650
DNA repair protein RAD16
NCU03651
NADP-dependent malic enzyme
582 AOD2-HA +Cm
0
582
128 AOD2-HA -Cm
0
128
500 AOD5-Myc +Cm
0
500
254 AOD5-Myc -Cm
0
254
1kb
NCU04306
methionine aminopeptidase 2B
NCU04307
MSF1
466 AOD2-HA +Cm
0
466
142 AOD2-HA -Cm
0
142
1407 AOD5-Myc +Cm
0
1407
210 AOD5-Myc -Cm
0
210
1kb
NCU04730
post-transcriptional silencing
protein QDE-2
NCU04731
HLH transcription factor
858 AOD2-HA +Cm
0
858
93 AOD2-HA -Cm
0
93
249 AOD5-Myc +Cm
0
249
152 AOD5-Myc -Cm
0
152
1kb
NCU04801
hypothetical protein
NCU04802
peroxisomal biogenesis factor
485 AOD2-HA +Cm
0
485
68 AOD2-HA -Cm
0
68
124 AOD5-Myc +Cm
0
124
143 AOD5-Myc -Cm
0
143
1kb
NCU04953
penicillopepsin
NCU04954
hypothetical protein
282 AOD2-HA +Cm
0
282
49 AOD2-HA -Cm
0
49
91 AOD5-Myc +Cm
0
91
69 AOD5-Myc -Cm
0
69
1kb

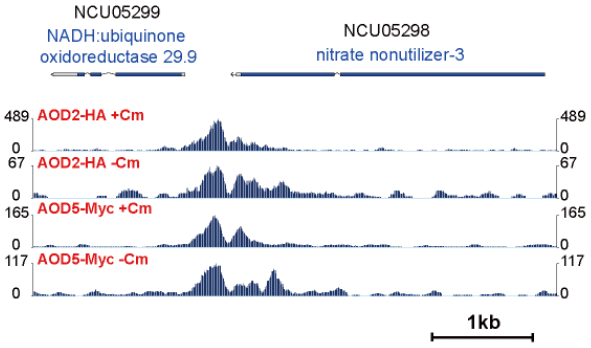
NCU05299
NADH:ubiquinone oxidoreductase 29.9
NCU05298
nitrate nonutilizer-3
AOD2-HA +Cm
AOD2-HA -Cm
AOD5-Myc +Cm
AOD5-Myc -Cm
1kb

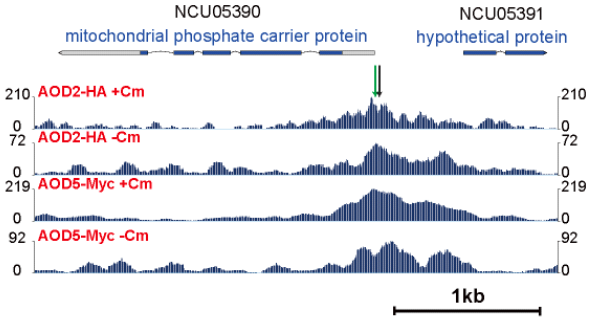
NCU05390
mitochondrial phosphate carrier protein
NCU05391
hypothetical protein
AOD2-HA +Cm
AOD2-HA -Cm
AOD5-Myc +Cm
AOD5-Myc -Cm
1kb

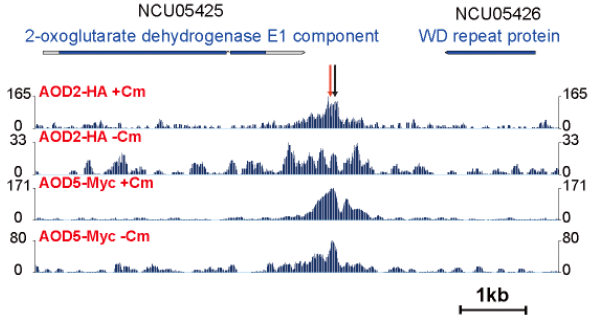
NCU05425
2-oxoglutarate dehydrogenase E1 component
NCU05426
WD repeat protein
AOD2-HA +Cm
AOD2-HA -Cm
AOD5-Myc +Cm
AOD5-Myc -Cm
1kb

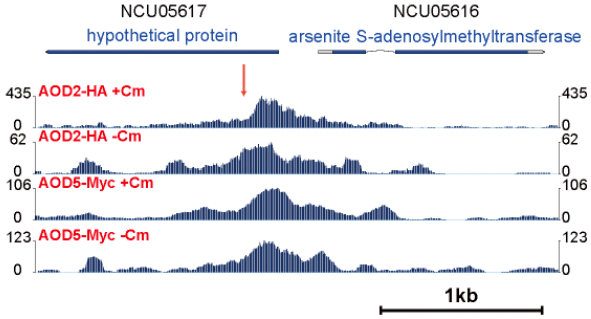
NCU05617
hypothetical protein
NCU05616
arsenite S-adenosylmethyltransferase
AOD2-HA +Cm
AOD2-HA -Cm
AOD5-Myc +Cm
AOD5-Myc -Cm
1kb

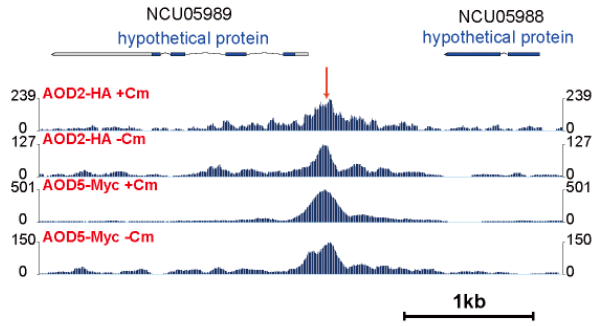
NCU05989
hypothetical protein
NCU05988
hypothetical protein
AOD2-HA +Cm
AOD2-HA -Cm
AOD5-Myc +Cm
AOD5-Myc -Cm
1kb

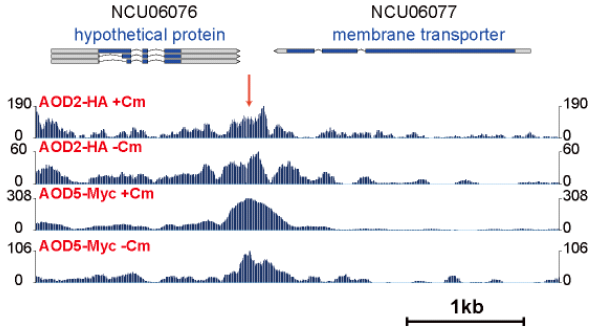
NCU06076
hypothetical protein
NCU06077
membrane transporter
AOD2-HA +Cm
AOD2-HA -Cm
AOD5-Myc +Cm
AOD5-Myc -Cm
1kb

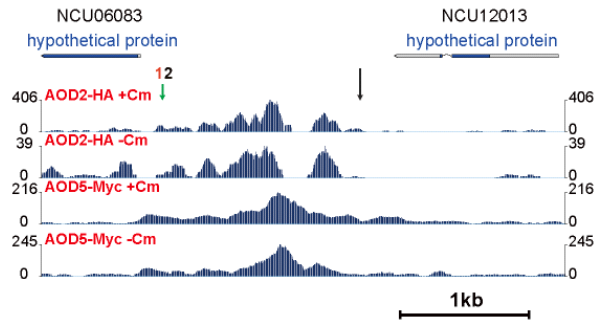
NCU06083
hypothetical protein
NCU12013
hypothetical protein
1
2
AOD2-HA +Cm
AOD2-HA -Cm
AOD5-Myc +Cm
AOD5-Myc -Cm
1kb

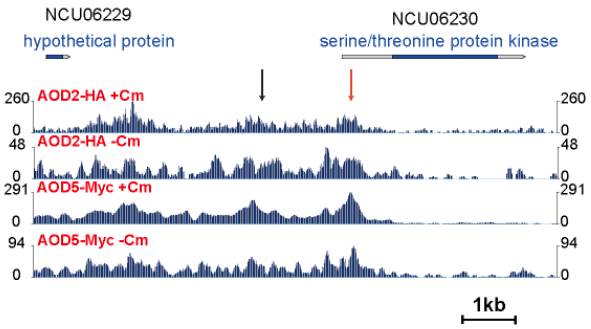
NCU06229
hypothetical protein
NCU06230
serine/threonine protein kinase
AOD2-HA +Cm
AOD2-HA -Cm
AOD5-Myc +Cm
AOD5-Myc -Cm
1kb

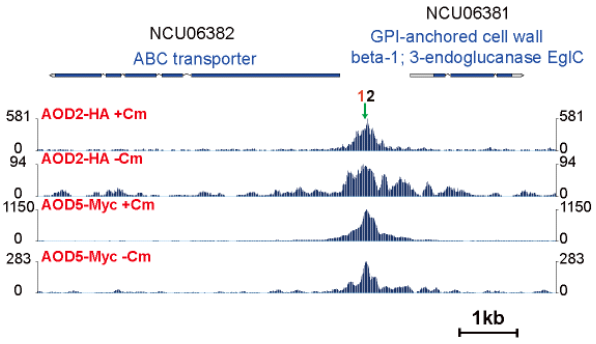
NCU06382
ABC transporter
NCU06381
GPI-anchored cell wall beta-1; 3-endoglucanase EglC
1
2
AOD2-HA +Cm
AOD2-HA -Cm
AOD5-Myc +Cm
AOD5-Myc -Cm
1kb

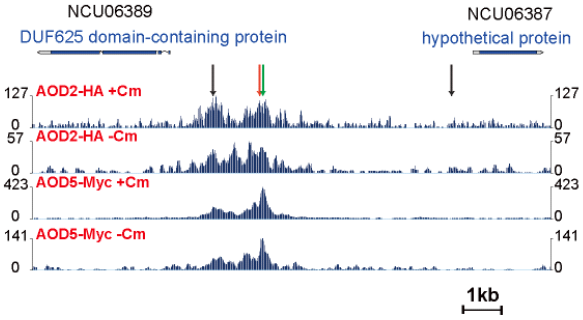
NCU06389
DUF625 domain-containing protein
NCU06387
hypothetical protein
AOD2-HA +Cm
AOD2-HA -Cm
AOD5-Myc +Cm
AOD5-Myc -Cm
1kb

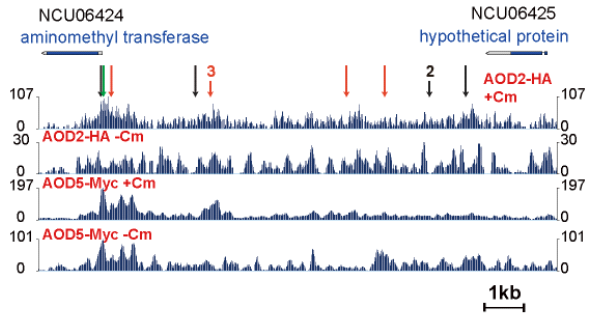
NCU06424
aminomethyl transferase
NCU06425
hypothetical protein
3
2
AOD2-HA +Cm
AOD2-HA -Cm
AOD5-Myc +Cm
AOD5-Myc -Cm
1kb

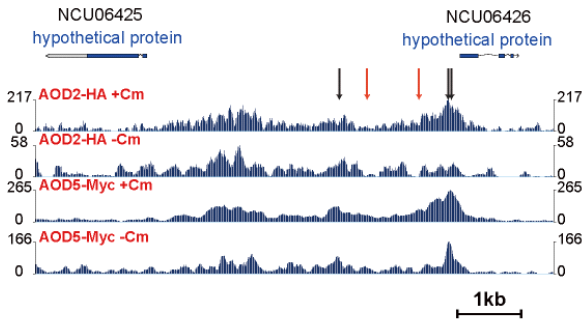
NCU06425
hypothetical protein
NCU06426
hypothetical protein
AOD2-HA +Cm
AOD2-HA -Cm
AOD5-Myc +Cm
AOD5-Myc -Cm
1kb

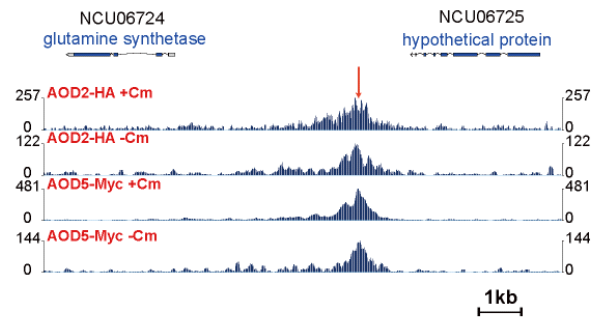
NCU06724
glutamine synthetase
NCU06725
hypothetical protein
AOD2-HA +Cm
AOD2-HA -Cm
AOD5-Myc +Cm
AOD5-Myc -Cm
1kb

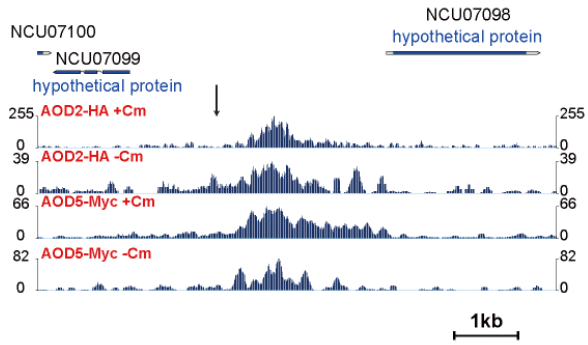
NCU07100
NCU07099
hypothetical protein
NCU07098
hypothetical protein
AOD2-HA +Cm
AOD2-HA -Cm
AOD5-Myc +Cm
AOD5-Myc -Cm
1kb

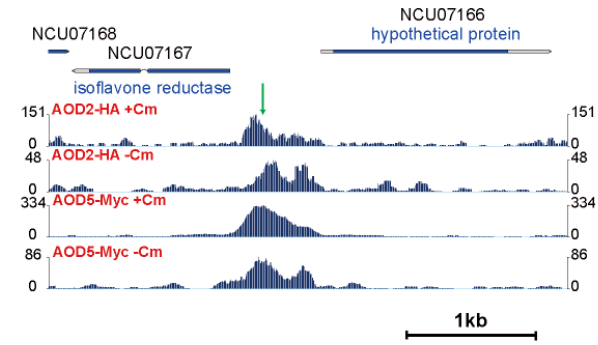
NCU07168
NCU07167
isoflavone reductase
NCU07166
hypothetical protein
AOD2-HA +Cm
AOD2-HA -Cm
AOD5-Myc +Cm
AOD5-Myc -Cm
1kb

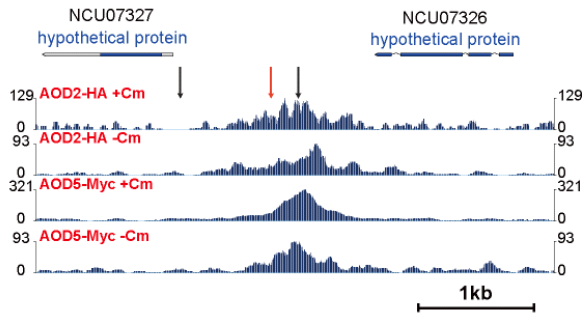
NCU07327
hypothetical protein
NCU07326
hypothetical protein
AOD2-HA +Cm
AOD2-HA -Cm
AOD5-Myc +Cm
AOD5-Myc -Cm
1kb

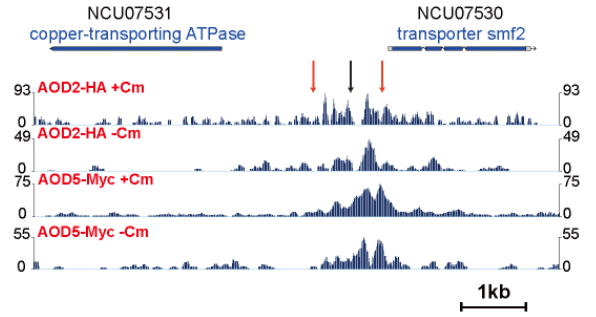
NCU07531
copper-transporting ATPase
NCU07530
transporter smf2
AOD2-HA +Cm
AOD2-HA -Cm
AOD5-Myc +Cm
AOD5-Myc -Cm
1kb

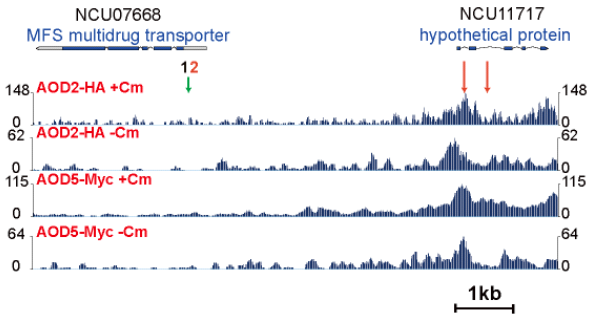
NCU07668
MFS multidrug transporter
NCU11717
hypothetical protein
AOD2-HA +Cm
AOD2-HA -Cm
AOD5-Myc +Cm
AOD5-Myc -Cm
1kb

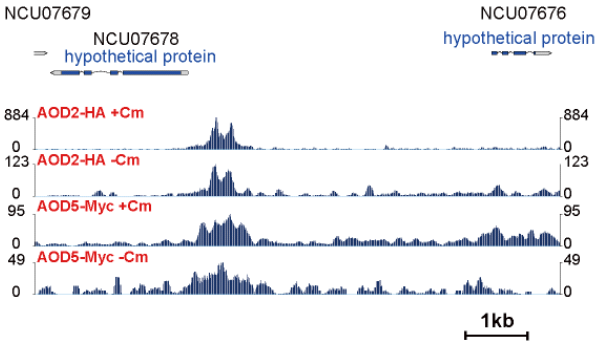
NCU07679
NCU07678
hypothetical protein
NCU07676
hypothetical protein
AOD2-HA +Cm
AOD2-HA -Cm
AOD5-Myc +Cm
AOD5-Myc -Cm
1kb

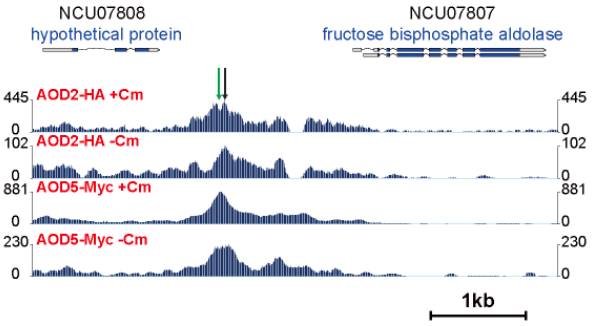
NCU07808
hypothetical protein
NCU07807
fructose bisphosphate aldolase
AOD2-HA +Cm
AOD2-HA -Cm
AOD5-Myc +Cm
AOD5-Myc -Cm
1kb

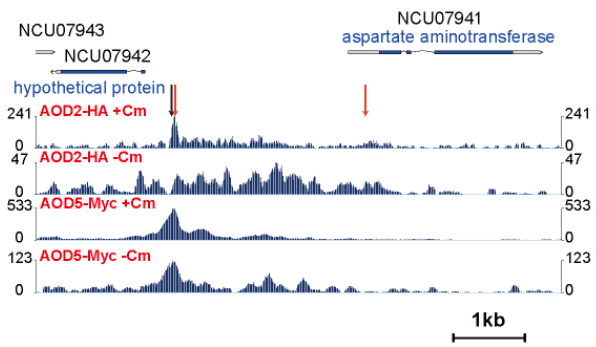
NCU07943
NCU07942
hypothetical protein
NCU07941
aspartate aminotransferase
AOD2-HA +Cm
AOD2-HA -Cm
AOD5-Myc +Cm
AOD5-Myc -Cm
1kb

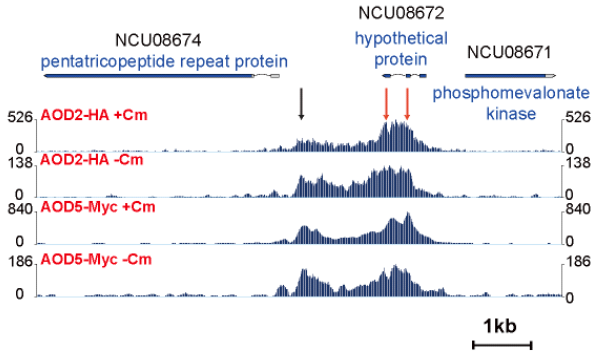
NCU08672
NCU08674
pentatricopeptide repeat protein
hypothetical protein
NCU08671
phosphomevalonate kinase
AOD2-HA +Cm
AOD2-HA -Cm
AOD5-Myc +Cm
AOD5-Myc -Cm
1kb

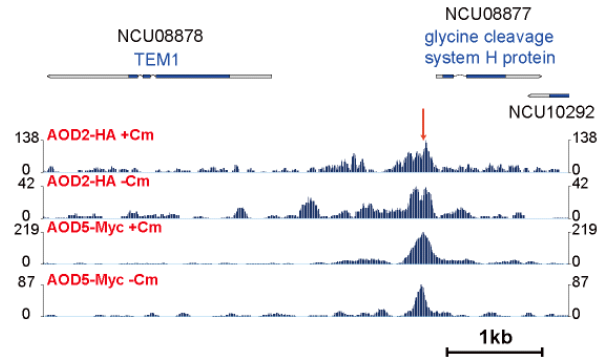
NCU08878
TEM1
NCU08877
glycine cleavage system H protein
NCU10292
AOD2-HA +Cm
AOD2-HA -Cm
AOD5-Myc +Cm
AOD5-Myc -Cm
1kb

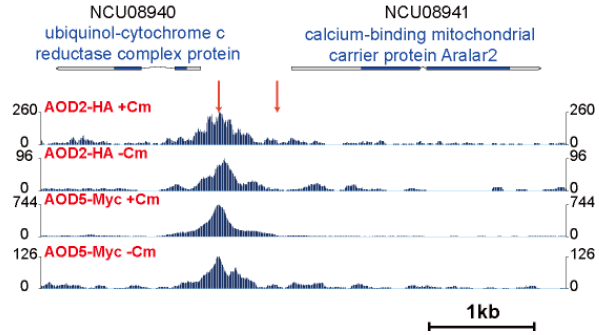
NCU08940
ubiquinol-cytochrome c reductase complex protein
NCU08941
calcium-binding mitochondrial carrier protein Aralar2
AOD2-HA +Cm
AOD2-HA -Cm
AOD5-Myc +Cm
AOD5-Myc -Cm
1kb

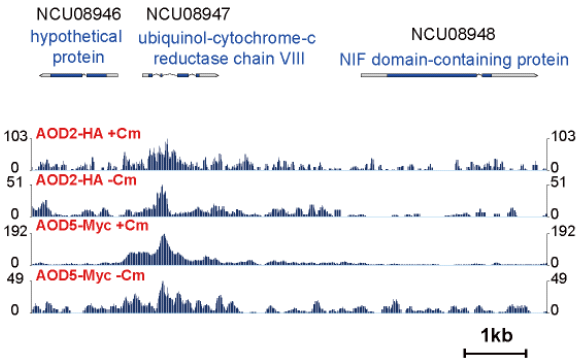
NCU08946
hypothetical protein
NCU08947
ubiquinol-cytochrome-c reductase chain VIII
NCU08948
NIF domain-containing protein
AOD2-HA +Cm
AOD2-HA -Cm
AOD5-Myc +Cm
AOD5-Myc -Cm
1kb

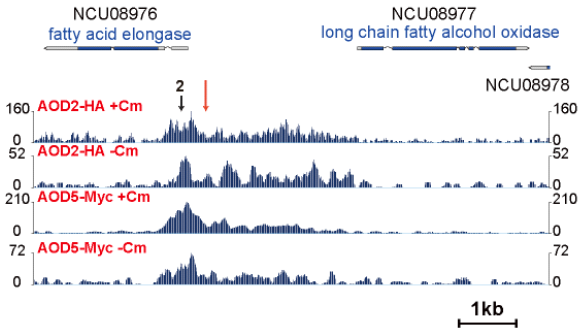
NCU08976
fatty acid elongase
NCU08977
long chain fatty alcohol oxidase
NCU08978
2
AOD2-HA +Cm
AOD2-HA -Cm
AOD5-Myc +Cm
AOD5-Myc -Cm
1kb

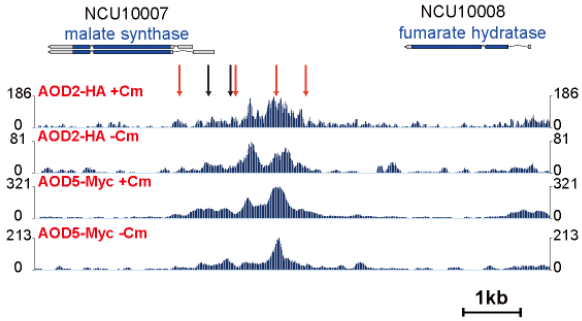
NCU10007
malate synthase
NCU10008
fumarate hydratase
AOD2-HA +Cm
AOD2-HA -Cm
AOD5-Myc +Cm
AOD5-Myc -Cm
1kb

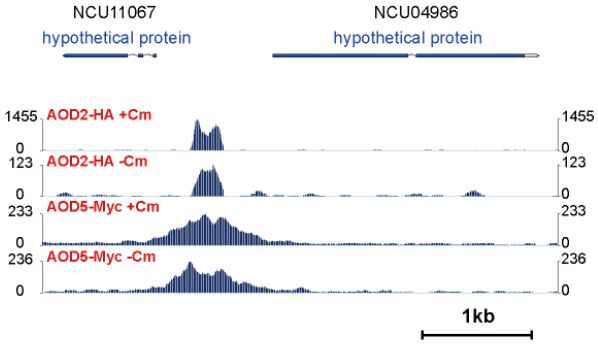
NCU11067
hypothetical protein
NCU04986
hypothetical protein
AOD2-HA +Cm
AOD2-HA -Cm
AOD5-Myc +Cm
AOD5-Myc -Cm
1kb

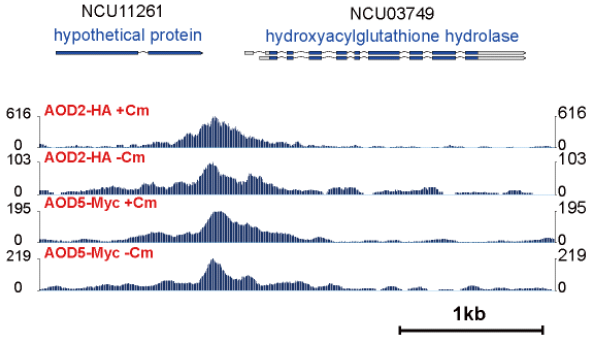
NCU11261
hypothetical protein
NCU03749
hydroxyacylglutathione hydrolase
AOD2-HA +Cm
AOD2-HA -Cm
AOD5-Myc +Cm
AOD5-Myc -Cm
1kb

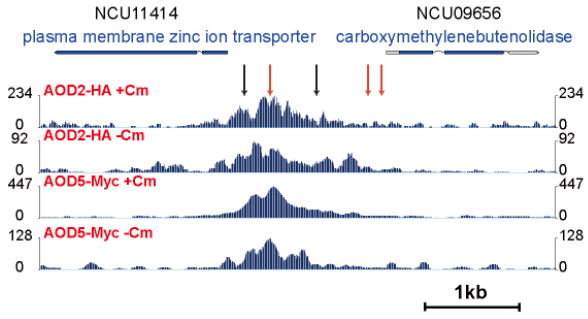
NCU11414
plasma membrane zinc ion transporter
NCU09656
carboxymethylenebutenolidase
AOD2-HA +Cm
AOD2-HA -Cm
AOD5-Myc +Cm
AOD5-Myc -Cm
1kb

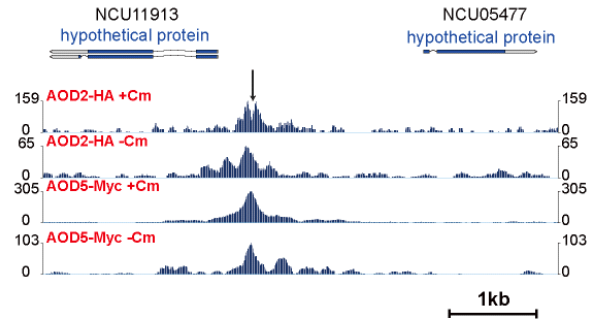
NCU11913
hypothetical protein
NCU05477
hypothetical protein
AOD2-HA +Cm
AOD2-HA -Cm
AOD5-Myc +Cm
AOD5-Myc -Cm
1kb

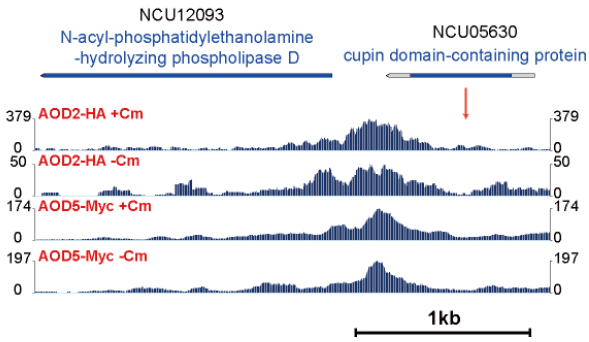
NCU12093
N-acyl-phosphatidylethanolamine -hydrolyzing phospholipase D
NCU05630
cupin domain-containing protein
AOD2-HA +Cm
AOD2-HA -Cm
AOD5-Myc +Cm
AOD5-Myc -Cm
1kb

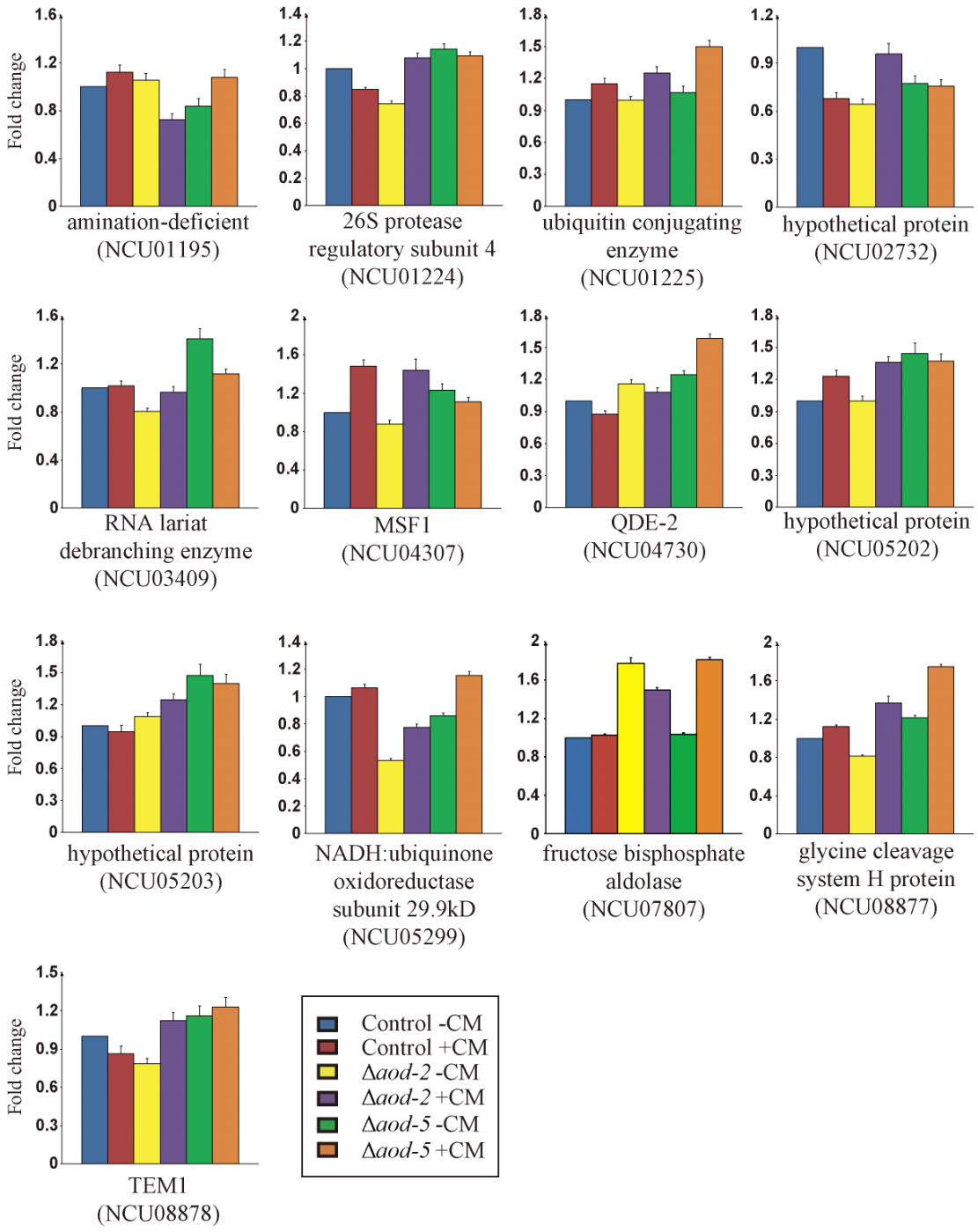

Supplementary Figure 3.8. Expression of genes associated with the group of 65 ChIP-seq peaks that show no difference greater than two-fold in mutant strains.

Analysis was performed as described in the legend to Fig. 3.11.

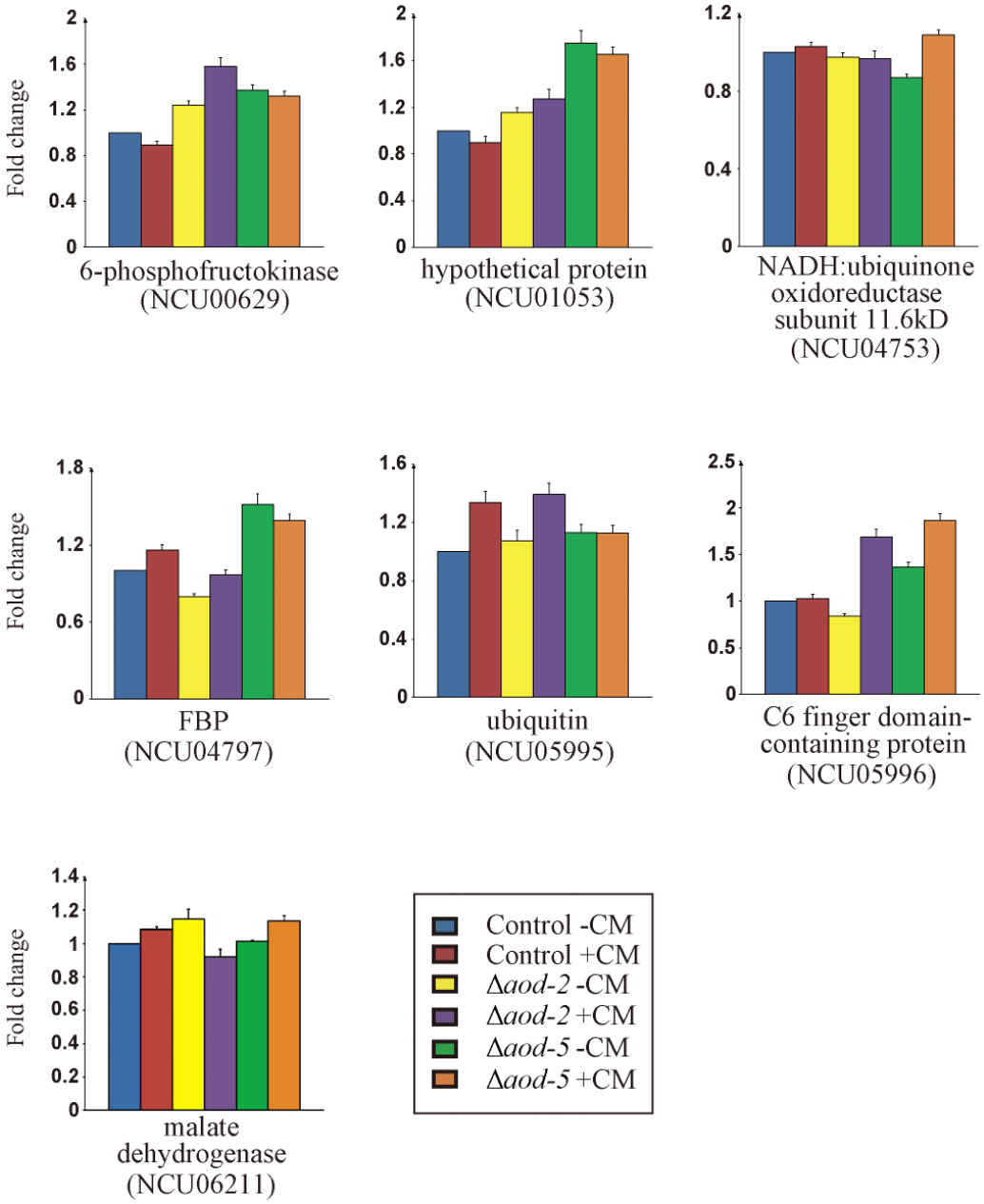

Supplementary Figure 3.9. Expression of genes associated with the ChIP-seq peaks from outside the group of 65 that show no difference greater than two-fold in mutant strains. Analysis was performed as described in the legend to Fig. 3.11.

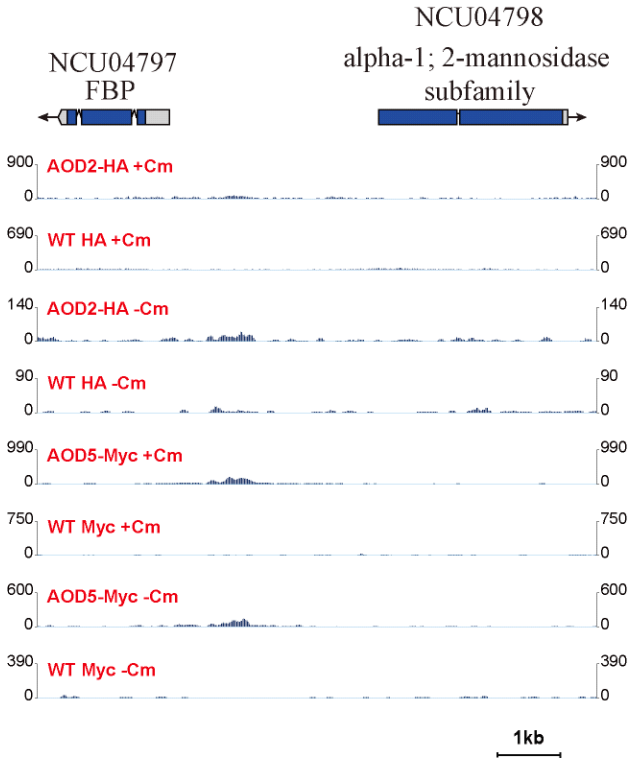

Supplementary Fig. 3.10. ChIP-seq peaks associated with FBP. Information shown is as described in the legend to Fig. 3.19. Y-axes height are shown as for other Figures (for example, Fig. 3.9, Fig. 3.19 and Supplementary Fig. 3.11 - 3.12).

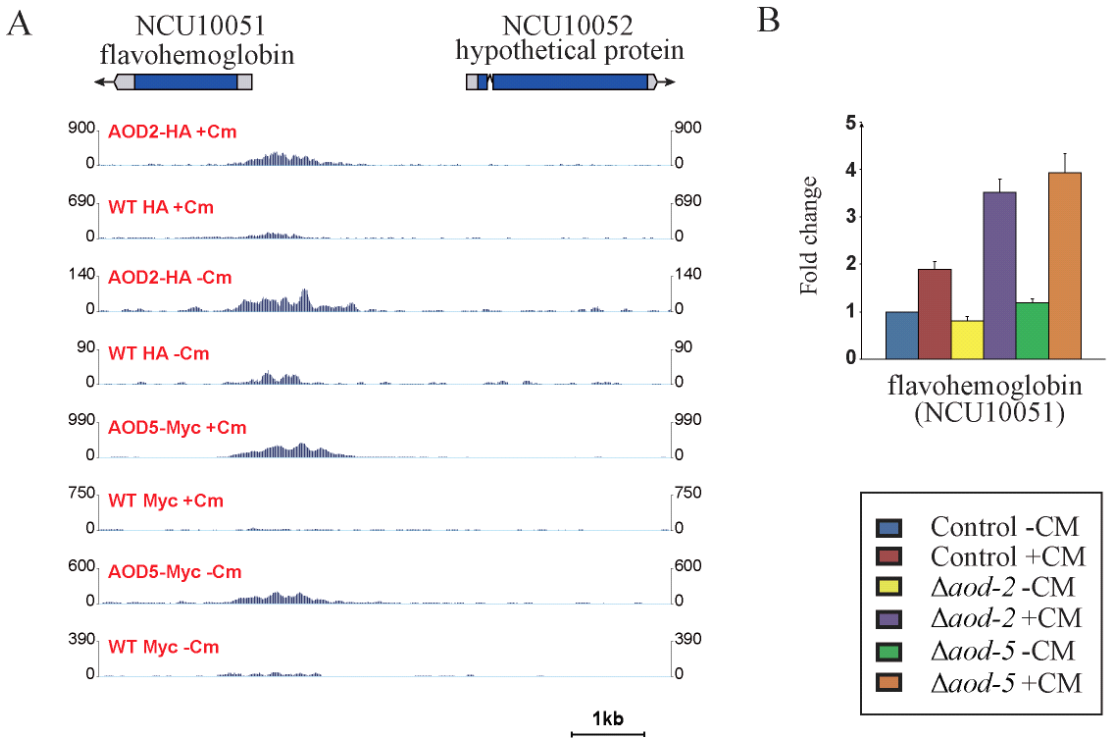

Supplementary Figure 3.11. ChIP-seq peaks associated with flavohemoglobin and expression of the gene. A. Information shown is as described in the legend to Fig. 3.19. B. The flavohemoglobin gene was analyzed as described in the legend to Fig. 3.11.

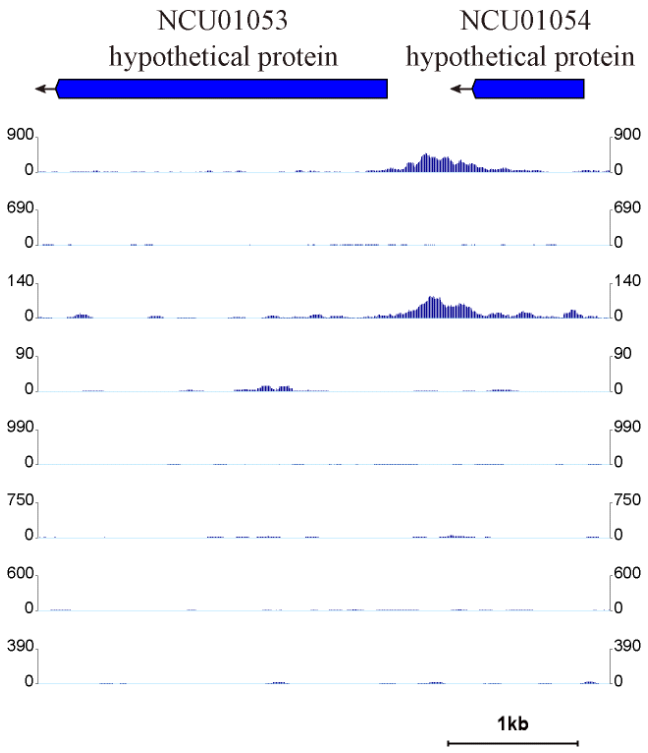

Supplementary Fig. 3.12. ChIP-seq peaks associated with NCU01053. Information shown is as described in the legend to Fig. 3.19.

Supplementary Table 3.1. FunCat analysis of the 98 genes associated with the 65 ChIP-seq peaks.

FunCat ID	FunCat description	FunCat main category	Gene ID(s)	Exact p-value	# genes found/# genes in category	# genes found/# genes input
01.01.03.02 .01	biosynthesis of glutamate	Metabolism	NCU01195, NCU01744, NCU04569, NCU06724, NCU07941	4.84E-05	5 / 39	5 / 98
02.13.03	aerobic respiration	Energy	NCU01808, NCU02514, NCU02549, NCU04874, NCU07953, NCU08940, NCU08947	0.000156	7 / 112	7 / 98
01.01.09.01 .02	degradation of glycine	Metabolism	NCU02475, NCU06424, NCU08877	0.000174	3 / 11	3 / 98
2.13	respiration	Energy	NCU00865, NCU01808, NCU02514, NCU04874, NCU05299, NCU07953	0.000769	6 / 105	6 / 98
2.11	electron transport and membrane-associated energy conservation	Energy	NCU01808, NCU02514, NCU02549, NCU05299, NCU08940, NCU08947	0.001611	6 / 121	6 / 98
20.03	transport facilities	Cellular transport, transport facilitation and transport routes	NCU01808, NCU03257, NCU05390, NCU05391, NCU06382, NCU07531, NCU07668, NCU08940, NCU08941, NCU08947	0.001816	10 / 323	10 / 98
01.01.03	assimilation of ammonia, metabolism of the glutamate group	Metabolism	NCU01744, NCU04569, NCU06724	0.00218	3 / 25	3 / 98
34.01.03.03	homeostasis of phosphate	Interaction with the environment	NCU05390, NCU05391	0.00376	2 / 9	2 / 98
20.01.01.07 .07	phosphate transport	Cellular transport, transport facilitation and transport routes	NCU05390, NCU05391	0.009186	2 / 14	2 / 98

01.20.38	metabolism of toxins/drugs	Metabolism	NCU05616	0.010552	1 / 1	1 / 98
01.05.05.07	C-1 compound catabolism	Metabolism	NCU02475, NCU08877	0.011951	2 / 16	2 / 98
01.01.03.02	metabolism of glutamate	Metabolism	NCU06724, NCU07941	0.013453	2 / 17	2 / 98
20.01.01.01 .01	heavy metal ion transport (Cu+, Fe3+, etc.)	Cellular transport, transport facilitation and transport routes	NCU07530, NCU07531, NCU11414	0.017125	3 / 52	3 / 98
01.20.37.01	metabolism of thioredoxin, glutaredoxin, glutathion	Metabolism	NCU03749, NCU04569	0.018418	2 / 20	2 / 98
1.02	nitrogen, sulfur and selenium metabolism	Metabolism	NCU01195, NCU01744, NCU02475, NCU06724, NCU07941	0.020401	5 / 150	5 / 98
30.01.05.07	two-component signal transduction system (e.g. phosphorelay)	Cellular communication / signal transduction mechanism	NCU03593	0.020994	1 / 2	1 / 98
01.01.06.02 .01	biosynthesis of asparagine	Metabolism	NCU07941	0.020994	1 / 2	1 / 98
2.45	energy conversion and regeneration	Energy	NCU00865, NCU10007	0.022093	2 / 22	2 / 98
30.01.09.07	cAMP/cGMP mediated signal transduction	Cellular communication / signal transduction mechanism	NCU00682, NCU03466	0.022093	2 / 22	2 / 98
02.11.05	accessory proteins of electron transport and membrane-associated energy conservation	Energy	NCU01808, NCU02549, NCU08940	0.022871	3 / 58	3 / 98

01.20.35.01	metabolism of phenylpropanoids	Metabolism	NCU04801, NCU07167	0.030259	2 / 26	2 / 98
2.09	anaplerotic reactions	Energy	NCU03651	0.031328	1 / 3	1 / 98
20.09.04	mitochondrial transport	Cellular transport, transport facilitation and transport routes	NCU02514, NCU05390, NCU07530, NCU08941	0.039171	4 / 122	4 / 98
42.22	endosome	Biogenesis of cellular components	NCU08878	0.041554	1 / 4	1 / 98
01.02.02.06	assimilation of ammonia	Metabolism	NCU03120	0.041554	1 / 4	1 / 98
01.01.09.01	metabolism of glycine	Metabolism	NCU08877	0.041554	1 / 4	1 / 98
30.01.05.01 .01	JAK-STAT cascade	Cellular communication / signal transduction mechanism	NCU06939	0.041554	1 / 4	1 / 98
2.01	glycolysis and gluconeogenesis	Energy	NCU07807, NCU09873, NCU10007	0.044161	3 / 75	3 / 98
11.02.01	rRNA synthesis	Transcription	NCU02497, NCU04986, NCU07166	0.04564	3 / 76	3 / 98

Supplementary Table 3.2. FunCat analysis of the genes associated with the ChIP-seq peaks that are more than four-fold enrichment in the AOD2 +CM experiment.

FunCat ID	FunCat description	FunCat main category	Gene ID(s)	Exact p-value	# genes found/# genes in category	# genes found/# genes input
16.21.15	biotin binding	Protein with binding function or cofactor requirement (structural or analytic)	NCU00050, NCU02505, NCU08535	0.000734	3 / 7	3 / 280
01.01.03.02 .01	biosynthesis of glutamate	Metabolism	NCU01195, NCU01744, NCU03500, NCU04569, NCU06724, NCU07941	0.000737	6 / 39	6 / 280
2.09	anaplerotic reactions	Energy	NCU02505, NCU03651	0.002384	2 / 3	2 / 280
2.13	respiration	Energy	NCU00385, NCU00865, NCU01808, NCU02514, NCU03031, NCU04874, NCU05299, NCU07953, NCU08093	0.002907	9 / 105	9 / 280
01.01.09.01 .02	degradation of glycine	Metabolism	NCU02475, NCU06424, NCU08877	0.003182	3 / 11	3 / 280
02.13.03	aerobic respiration	Energy	NCU00385, NCU01808, NCU02514, NCU02549, NCU03031, NCU04874, NCU07953, NCU08940, NCU09477	0.004485	9 / 112	9 / 280
01.01.03	assimilation of ammonia, metabolism of the glutamate group	Metabolism	NCU01744, NCU03500, NCU04569, NCU06724	0.005066	4 / 25	4 / 280
32.01.11	nutrient starvation response	Cell rescue, defense and virulence	NCU03118, NCU03593, NCU04637, NCU05589, NCU06182	0.007141	5 / 43	5 / 280

1.07	metabolism of vitamins, cofactors, and prosthetic groups	Metabolism	NCU00552, NCU00605, NCU02475, NCU02505, NCU04636, NCU07742, NCU08269, NCU08404, NCU08877	0.007418	9 / 121	9 / 280
20.03	transport facilities	Cellular transport, transport facilitation and transport routes	NCU01808, NCU01882, NCU03257, NCU05390, NCU05391, NCU05627, NCU06382, NCU07531, NCU07668, NCU07960, NCU08404, NCU08738, NCU08940, NCU08941, NCU09287, NCU09477, NCU09580	0.010252	17 / 323	17 / 280
20.09.16	cellular export and secretion	Cellular transport, transport facilitation and transport routes	NCU00754, NCU01674, NCU02712, NCU03300, NCU05627, NCU07531, NCU07668, NCU07960, NCU09287, NCU09580	0.012257	10 / 154	10 / 280
20.01.11	amine / polyamine transport	Cellular transport, transport facilitation and transport routes	NCU00754, NCU09580, NCU09909	0.013592	3 / 18	3 / 280
01.05.03.03 .04	chitin anabolism	Metabolism	NCU04350, NCU04352, NCU09324	0.015808	3 / 19	3 / 280
01.20.37.01	metabolism of thioredoxin, glutaredoxin, glutathion	Metabolism	NCU03749, NCU04130, NCU04569	0.018215	3 / 20	3 / 280
43.01.03.06	hyphae formation	Cell type differentiation	NCU00939, NCU03593, NCU03616	0.018215	3 / 20	3 / 280
2.01	glycolysis and gluconeogenesis	Energy	NCU00050, NCU01528, NCU02505, NCU07807, NCU09873, NCU10007	0.019617	6 / 75	6 / 280
40.2	cell aging	Cell fate	NCU01643, NCU03616, NCU04773, NCU08946	0.022206	4 / 38	4 / 280
20.09.04	mitochondrial transport	Cellular transport, transport facilitation and transport routes	NCU00385, NCU02514, NCU03031, NCU05390, NCU05593, NCU07530, NCU08941, NCU09477	0.02281	8 / 122	8 / 280

42.27	extracellular / secretion proteins	Biogenesis of cellular components	NCU04953, NCU05105, NCU07533	0.023606	3 / 22	3 / 280
30.01.09.07	cAMP/cGMP mediated signal transduction	Cellular communication / signal transduction mechanism	NCU00682, NCU03466, NCU03616	0.023606	3 / 22	3 / 280
34.01.03.03	homeostasis of phosphate	Interaction with the environment	NCU05390, NCU05391	0.02555	2 / 9	2 / 280
2.1	tricarboxylic-acid pathway (citrate cycle, Krebs cycle, TCA cycle)	Energy	NCU00050, NCU01195, NCU03031, NCU03651, NCU06211	0.025831	5 / 59	5 / 280
20.01.13	lipid/fatty acid transport	Cellular transport, transport facilitation and transport routes	NCU03596, NCU03863, NCU05591, NCU06382, NCU08404, NCU09287	0.027526	6 / 81	6 / 280
01.20.38	metabolism of toxins/drugs	Metabolism	NCU05616	0.028542	1 / 1	1 / 280
32.01.03	osmotic and salt stress response	Cell rescue, defense and virulence	NCU01940, NCU04350, NCU04352, NCU04637, NCU06182, NCU09324	0.029023	6 / 82	6 / 280
01.05.09.04	aminosaccharide anabolism	Metabolism	NCU04350, NCU04352, NCU09324	0.029768	3 / 24	3 / 280
01.25.03	extracellular protein degradation	Metabolism	NCU04953, NCU07533	0.031347	2 / 10	2 / 280
20.09.18	cellular import	Cellular transport, transport facilitation and transport routes	NCU01674, NCU01882, NCU02278, NCU03257, NCU05627, NCU07530, NCU07531, NCU08738, NCU09287	0.034955	9 / 157	9 / 280
16.21.17	pyridoxal phosphate binding	Protein with binding function or cofactor requirement (structural or analytic)	NCU02475, NCU03500, NCU04636, NCU07941	0.035833	4 / 44	4 / 280
02.45.15	energy generation (e.g. ATP synthase)	Energy	NCU00385, NCU02514, NCU08093	0.040441	3 / 27	3 / 280

Supplementary Table 3.3. FunCat analysis of the genes associated with the ChIP-seq peaks that are more than four-fold enrichment in the AOD2 -CM experiment.

FunCat ID	FunCat description	FunCat main category	Gene ID(s)	Exact p-value	# genes found/# genes in category	# genes found/# genes input
2.11	electron transport and membrane-associated energy conservation	Energy	NCU00636, NCU00644, NCU00959, NCU01606, NCU01808, NCU02514, NCU02549, NCU03031, NCU03558, NCU03559, NCU05008, NCU05225, NCU05299, NCU05430, NCU05457, NCU08940, NCU09119, NCU09816	2.81E-06	18 / 121	18 / 401
02.13.03	aerobic respiration	Energy	NCU00959, NCU01606, NCU01808, NCU02514, NCU02549, NCU03031, NCU03559, NCU04874, NCU05225, NCU05430, NCU05457, NCU07953, NCU08940, NCU09119, NCU09477, NCU09816	1.73E-05	16 / 112	16 / 401
01.01.03.02 .01	biosynthesis of glutamate	Metabolism	NCU01195, NCU01744, NCU02333, NCU03500, NCU04216, NCU04569, NCU05410, NCU06724, NCU07941	2.73E-05	9 / 39	9 / 401
2.13	respiration	Energy	NCU00636, NCU00644, NCU00865, NCU01606, NCU01808, NCU02514, NCU03031, NCU03233, NCU04874, NCU05225, NCU05299, NCU05430, NCU07953, NCU09119, NCU09816	3.18E-05	15 / 105	15 / 401
02.45.15	energy generation (e.g. ATP synthase)	Energy	NCU00636, NCU00644, NCU01606, NCU02514, NCU05430, NCU09119, NCU09816	9.91E-05	7 / 27	7 / 401

20.09.04	mitochondrial transport	Cellular transport, transport facilitation and transport routes	NCU00636, NCU01241, NCU01564, NCU01606, NCU02269, NCU02514, NCU03031, NCU05390, NCU05430, NCU07478, NCU07530, NCU08693, NCU08941, NCU09119, NCU09477	0.000184	15 / 122	15 / 401
20.03	transport facilities	Cellular transport, transport facilitation and transport routes	NCU01564, NCU01808, NCU01815, NCU01882, NCU02269, NCU02582, NCU03257, NCU03509, NCU03559, NCU05390, NCU05391, NCU05457, NCU05775, NCU05985, NCU06231, NCU06382, NCU06538, NCU07478, NCU07531, NCU07668, NCU07711, NCU08707, NCU08738, NCU08940, NCU08941, NCU09477, NCU09795, NCU09811	0.00022	28 / 323	28 / 401
01.02.07	regulation of nitrogen, sulfur and selenium metabolism	Metabolism	NCU02333, NCU03536, NCU05411, NCU05994, NCU06407, NCU07430, NCU07675	0.000671	7 / 36	7 / 401
01.01.09.01 .02	degradation of glycine	Metabolism	NCU02475, NCU05805, NCU06424, NCU08877	0.000833	4 / 11	4 / 401
01.03.13	regulation of nucleotide/nucleoside /nucleobase metabolism	Metabolism	NCU03593, NCU05994, NCU06111, NCU08651, NCU08652	0.000953	5 / 19	5 / 401
30.01.05.07	two-component signal transduction system (e.g. phosphorelay)	Cellular communication / signal transduction mechanism	NCU02413, NCU03593	0.001804	2 / 2	2 / 401
20.01.01.01 .01	heavy metal ion transport (Cu+, Fe3+, etc.)	Cellular transport, transport facilitation and transport routes	NCU02020, NCU06380, NCU07478, NCU07530, NCU07531, NCU08707, NCU11414	0.006031	7 / 52	7 / 401

20.03.22	transport ATPases	Cellular transport, transport facilitation and transport routes	NCU00636, NCU00644, NCU01606, NCU02514, NCU04218, NCU05430, NCU05591, NCU07531, NCU09119	0.006535	9 / 80	9 / 401
20.01.01.01	cation transport (H+, Na+, K+, Ca2+ , NH4+, etc.)	Cellular transport, transport facilitation and transport routes	NCU00636, NCU01564, NCU01606, NCU02514, NCU03257, NCU05430, NCU05591, NCU05775, NCU06380, NCU07711, NCU08148, NCU09119	0.00952	12 / 131	12 / 401
16.21.17	pyridoxal phosphate binding	Protein with binding function or cofactor requirement (structural or analytic)	NCU00194, NCU02475, NCU03500, NCU06112, NCU06189, NCU07941	0.010139	6 / 44	6 / 401
42.22	endosome	Biogenesis of cellular components	NCU00895, NCU08878	0.010223	2 / 4	2 / 401
02.11.05	accessory proteins of electron transport and membrane-associated energy conservation	Energy	NCU00959, NCU01808, NCU02549, NCU03031, NCU03559, NCU08940, NCU09816	0.010927	7 / 58	7 / 401
34.01.01.03	homeostasis of protons	Interaction with the environment	NCU00636, NCU00644, NCU01606, NCU02514, NCU05430, NCU07711, NCU09119	0.011962	7 / 59	7 / 401
01.01.03.05 .02	degradation of arginine	Metabolism	NCU00194, NCU01195, NCU02333	0.012587	3 / 12	3 / 401
2.01	glycolysis and gluconeogenesis	Energy	NCU00050, NCU01528, NCU04265, NCU07807, NCU09285, NCU09873, NCU10007, NCU11201	0.013772	8 / 75	8 / 401
20.03.02.02 .01	proton driven symporter	Cellular transport, transport facilitation and transport routes	NCU01241, NCU05775, NCU06231, NCU08148	0.014962	4 / 23	4 / 401

18.02.01	enzymatic activity regulation / enzyme regulator	Regulation of metabolism and protein function	NCU01224, NCU01242, NCU01498, NCU01563, NCU02114, NCU02496, NCU05973, NCU06182, NCU08693, NCU08961, NCU09085, NCU09310, NCU09377, NCU09841	0.015072	14 / 173	14 / 401
01.01.03	assimilation of ammonia, metabolism of the glutamate group	Metabolism	NCU01744, NCU03500, NCU04569, NCU06724	0.020003	4 / 25	4 / 401
20.01.13	lipid/fatty acid transport	Cellular transport, transport facilitation and transport routes	NCU02269, NCU03596, NCU04218, NCU04388, NCU05008, NCU05591, NCU06382, NCU08809	0.021137	8 / 81	8 / 401
01.03.01.03	purine nucleotide/nucleoside /nucleobase anabolism	Metabolism	NCU03117, NCU03593, NCU04202, NCU04216, NCU07015	0.021336	5 / 38	5 / 401
20.01.15	electron transport	Cellular transport, transport facilitation and transport routes	NCU00636, NCU00644, NCU00959, NCU01606, NCU01808, NCU01815, NCU02514, NCU02549, NCU02665, NCU03031, NCU03559, NCU05225, NCU05430, NCU05457, NCU05775, NCU08940, NCU09119, NCU09816	0.023174	18 / 255	18 / 401
11.02.03.04 .01	transcription activation	Transcription	NCU01722, NCU02413, NCU03033, NCU03120, NCU04050, NCU04179, NCU05308, NCU05994, NCU06407, NCU07430, NCU08651, NCU08652	0.023221	12 / 148	12 / 401
01.02.02.09	catabolism of nitrogenous compounds	Metabolism	NCU01816, NCU02333, NCU10007	0.023694	3 / 15	3 / 401

1.02	nitrogen, sulfur and selenium metabolism	Metabolism	NCU00194, NCU01195, NCU01744, NCU01779, NCU02005, NCU02475, NCU03500, NCU05410, NCU05994, NCU06724, NCU07675, NCU07941	0.025485	12 / 150	12 / 401
01.01.03.02 .02	degradation of glutamate	Metabolism	NCU01195, NCU04216, NCU06112	0.028266	3 / 16	3 / 401
01.05.05.07	C-1 compound catabolism	Metabolism	NCU02475, NCU05805, NCU08877	0.028266	3 / 16	3 / 401
16.21.15	biotin binding	Protein with binding function or cofactor requirement (structural or analytic)	NCU00050, NCU08535	0.032872	2 / 7	2 / 401
01.01.03.02	metabolism of glutamate	Metabolism	NCU06112, NCU06724, NCU07941	0.03327	3 / 17	3 / 401
32.01.11	nutrient starvation response	Cell rescue, defense and virulence	NCU03118, NCU03593, NCU04050, NCU05589, NCU06182	0.034505	5 / 43	5 / 401
16.21.08	Fe/S binding	Protein with binding function or cofactor requirement (structural or analytic)	NCU00959, NCU02549, NCU03031, NCU03559, NCU08940	0.034505	5 / 43	5 / 401
01.01.13	regulation of amino acid metabolism	Metabolism	NCU02094, NCU04050, NCU05994, NCU06407, NCU07430	0.034505	5 / 43	5 / 401
20.09.18	cellular import	Cellular transport, transport facilitation and transport routes	NCU00895, NCU01882, NCU02020, NCU02582, NCU03257, NCU03509, NCU06231, NCU07530, NCU07531, NCU08148, NCU08738, NCU09795	0.034689	12 / 157	12 / 401
01.01.09.02 .01	biosynthesis of serine	Metabolism	NCU02004, NCU02475, NCU05805	0.038702	3 / 18	3 / 401

01.02.03.03	assimilatory reduction of sulfur	Metabolism	NCU02005	0.042553	1 / 1	1 / 401
01.20.38	metabolism of toxins/drugs	Metabolism	NCU05616	0.042553	1 / 1	1 / 401
01.20.19.03	metabolism of open-chain tetrapyrrols	Metabolism	NCU06189	0.042553	1 / 1	1 / 401
43.01.03.09	development of asco- basidio- or zygospore	Cell type differentiation	NCU00007, NCU01225, NCU01498, NCU02076, NCU03596, NCU05995, NCU06111, NCU07430, NCU08423, NCU08809, NCU08948, NCU09731, NCU10046	0.044025	13 / 181	13 / 401
30.01.05.01	protein kinase	Cellular communication / signal transduction mechanism	NCU00682, NCU00914, NCU01498, NCU02496, NCU06111, NCU06182, NCU09841	0.04447	7 / 77	7 / 401
01.06.10	regulation of lipid, fatty acid and isoprenoid metabolism	Metabolism	NCU03596, NCU07430, NCU07741, NCU08535	0.04517	4 / 32	4 / 401
11.02.03.04	transcriptional control	Transcription	NCU00083, NCU00340, NCU01486, NCU01563, NCU01634, NCU01635, NCU01994, NCU02094, NCU02413, NCU02853, NCU03033, NCU03120, NCU03466, NCU03536, NCU03537, NCU03593, NCU04179, NCU04202, NCU04830, NCU05308, NCU05389, NCU05411, NCU05973, NCU05994, NCU06407, NCU06424, NCU07430, NCU07675, NCU08319, NCU08423, NCU08651, NCU08809, NCU09118, NCU09310, NCU09615, NCU09843	0.046924	36 / 640	36 / 401

34.11.12	perception of nutrients and nutritional adaptation	Interaction with the environment	NCU00340, NCU02582, NCU04005, NCU04179, NCU06111, NCU06182	0.047066	6 / 62	6 / 401

Supplementary Table 3.4. FunCat analysis of the genes associated with the ChIP-seq peaks that are more than four-fold enrichment in the AOD5 +CM experiment.

FunCat ID	FunCat description	FunCat main category	Gene ID(s)	Exact p-value	# genes found/# genes in category	# genes found/# genes input
2.13	respiration	Energy	NCU00153, NCU00385, NCU00502, NCU00636, NCU00644, NCU00865, NCU00894, NCU01479, NCU01606, NCU01808, NCU02250, NCU02274, NCU02514, NCU02807, NCU03031, NCU03112, NCU03233, NCU04874, NCU05220, NCU05225, NCU05299, NCU05430, NCU06051, NCU06606, NCU07739, NCU07953, NCU08093, NCU08272, NCU08980, NCU09119, NCU09816, NCU10051	7.2671E-08	32 / 105	32 / 1038
02.45.15	energy generation (e.g. ATP synthase)	Energy	NCU00385, NCU00502, NCU00636, NCU00644, NCU01229, NCU01606, NCU02250, NCU02514, NCU05220, NCU05430, NCU08093, NCU09119, NCU09143, NCU09816	2.4126E-07	14 / 27	14 / 1038
02.13.03	aerobic respiration	Energy	NCU00153, NCU00385, NCU00655, NCU00959, NCU01606, NCU01808, NCU02217, NCU02250, NCU02422, NCU02514, NCU02549, NCU03031, NCU03112, NCU03231, NCU03559, NCU03926, NCU04874, NCU05220, NCU05221, NCU05225, NCU05430, NCU05457, NCU06403, NCU06606, NCU07756, NCU07953, NCU08336, NCU08940, NCU08980, NCU09119, NCU09477, NCU09816	3.8094E-07	32 / 112	32 / 1038

2.11	electron transport and membrane-associated energy conservation	Energy	NCU00153, NCU00236, NCU00385, NCU00502, NCU00636, NCU00644, NCU00959, NCU01229, NCU01606, NCU01808, NCU02250, NCU02514, NCU02549, NCU03031, NCU03112, NCU03558, NCU03559, NCU04452, NCU05008, NCU05220, NCU05225, NCU05299, NCU05430, NCU05457, NCU06606, NCU07756, NCU08272, NCU08336, NCU08940, NCU08980, NCU09119, NCU09816	2.49E-06	32 / 121	32 / 1038
20.01.15	electron transport	Cellular transport, transport facilitation and transport routes	NCU00153, NCU00385, NCU00502, NCU00552, NCU00636, NCU00644, NCU00959, NCU01219, NCU01229, NCU01606, NCU01808, NCU01853, NCU02074, NCU02096, NCU02250, NCU02422, NCU02514, NCU02549, NCU02665, NCU02954, NCU03031, NCU03112, NCU03559, NCU03697, NCU04013, NCU04443, NCU04452, NCU04771, NCU04899, NCU05169, NCU05220, NCU05221, NCU05225, NCU05278, NCU05430, NCU05457, NCU05752, NCU06051, NCU06211, NCU06556, NCU06606, NCU06924, NCU07112, NCU08048, NCU08272, NCU08280, NCU08336, NCU08940, NCU08980, NCU09119, NCU09816, NCU10051	1.2E-05	52 / 255	52 / 1038
01.01.09.01.02	degradation of glycine	Metabolism	NCU02274, NCU02475, NCU02727, NCU03607, NCU05805, NCU06424, NCU08877	5.04E-05	7 / 11	7 / 1038
20.09.04	mitochondrial transport	Cellular transport, transport facilitation and transport routes	NCU00075, NCU00385, NCU00502, NCU00636, NCU01241, NCU01479, NCU01606, NCU01810, NCU02514, NCU02802, NCU03031, NCU05390, NCU05427, NCU05430, NCU05593, NCU06842, NCU07295, NCU07414, NCU07465, NCU07478, NCU07530, NCU08326, NCU08693, NCU08810, NCU08941, NCU09119, NCU09143, NCU09477, NCU10732	6.52E-05	29 / 122	29 / 1038

2.1	tricarboxylic-acid pathway (citrate cycle, Krebs cycle, TCA cycle)	Energy	NCU00050, NCU00959, NCU01195, NCU01227, NCU02366, NCU02954, NCU03031, NCU03651, NCU03857, NCU04899, NCU06211, NCU06785, NCU06836, NCU07659, NCU07756, NCU08336, NCU10008	0.000188	17 / 59	17 / 1038
01.01.03 .02.01	biosynthesis of glutamate	Metabolism	NCU01195, NCU01744, NCU02366, NCU03347, NCU03500, NCU03857, NCU04569, NCU04856, NCU05410, NCU06724, NCU07941, NCU08411	0.000863	12 / 39	12 / 1038
01.03.01	purin nucleotide/nucleoside/nucleobase metabolism	Metabolism	NCU00843, NCU00895, NCU01550, NCU01647, NCU01985, NCU02090, NCU02167, NCU02202, NCU02274, NCU02296, NCU02812, NCU02979, NCU03117, NCU03166, NCU03346, NCU04202, NCU05805, NCU07742, NCU07853, NCU07914, NCU08568, NCU08878, NCU09320, NCU09331, NCU09621, NCU10007, NCU10226	0.002057	27 / 135	27 / 1038
16.21.17	pyridoxal phosphate binding	Protein with binding function or cofactor requirement (structural or analytic)	NCU00194, NCU02475, NCU03347, NCU03500, NCU03607, NCU04292, NCU04636, NCU06112, NCU06189, NCU07941, NCU08216, NCU08411	0.002736	12 / 44	12 / 1038
02.13.01	anaerobic respiration	Energy	NCU02096, NCU05457, NCU09143, NCU09477, NCU10051	0.002826	5 / 10	5 / 1038
01.05.02 .04	sugar, glucoside, polyol and carboxylate anabolism	Metabolism	NCU00629, NCU00959, NCU02097, NCU02128, NCU02366, NCU02954, NCU03031, NCU03857, NCU04203, NCU04221, NCU04265, NCU04797, NCU04899, NCU06075, NCU06211, NCU07281, NCU07914, NCU09347, NCU10008	0.003309	19 / 87	19 / 1038

43.01.03 .09	development of asco- basidio- or zygospore	Cell type differentiation	NCU00007, NCU00269, NCU00939, NCU01225, NCU01414, NCU01498, NCU01823, NCU01833, NCU02076, NCU02273, NCU02289, NCU02295, NCU02806, NCU03171, NCU03596, NCU03771, NCU04142, NCU04350, NCU04352, NCU04376, NCU05995, NCU06111, NCU06331, NCU06821, NCU06871, NCU08423, NCU08776, NCU08936, NCU08948, NCU09205, NCU09324, NCU09731, NCU10046	0.003444	33 / 181	33 / 1038
2.01	glycolysis and gluconeogenesis	Energy	NCU00050, NCU00187, NCU00629, NCU01754, NCU02505, NCU04265, NCU04797, NCU05133, NCU06075, NCU07281, NCU07659, NCU07807, NCU07914, NCU08402, NCU09285, NCU09873, NCU10007	0.003552	17 / 75	17 / 1038
20.01.01 .01.01	heavy metal ion transport (Cu+, Fe3+, etc.)	Cellular transport, transport facilitation and transport routes	NCU02009, NCU02133, NCU03497, NCU03498, NCU05830, NCU07478, NCU07530, NCU07531, NCU08225, NCU08325, NCU08707, NCU11216, NCU11414	0.004252	13 / 52	13 / 1038
01.05.02 .07	sugar, glucoside, polyol and carboxylate catabolism	Metabolism	NCU00629, NCU00865, NCU00959, NCU01227, NCU02097, NCU02128, NCU02344, NCU02366, NCU02668, NCU02954, NCU03000, NCU03031, NCU03857, NCU04013, NCU04203, NCU04221, NCU04265, NCU04797, NCU04899, NCU05105, NCU05429, NCU05594, NCU05595, NCU06075, NCU06211, NCU07281, NCU07807, NCU07914, NCU08131, NCU08336, NCU08412, NCU09347, NCU09821, NCU10008	0.004471	34 / 191	34 / 1038
43.01.03 .06	hyphae formation	Cell type differentiation	NCU00939, NCU01823, NCU01833, NCU03593, NCU06111, NCU07296, NCU08038	0.004739	7 / 20	7 / 1038

1.02	nitrogen, sulfur and selenium metabolism	Metabolism	NCU00194, NCU00236, NCU01195, NCU01744, NCU01779, NCU01985, NCU02096, NCU02296, NCU02475, NCU03171, NCU03347, NCU03500, NCU04092, NCU04636, NCU04856, NCU05340, NCU05387, NCU05410, NCU05994, NCU06724, NCU07112, NCU07413, NCU07675, NCU07853, NCU07941, NCU08411, NCU09621, NCU10051	0.004844	28 / 150	28 / 1038
34.01.01 .03	homeostasis of protons	Interaction with the environment	NCU00385, NCU00430, NCU00502, NCU00636, NCU00644, NCU01606, NCU01735, NCU02250, NCU02514, NCU05430, NCU08325, NCU09119, NCU09143, NCU09287	0.005087	14 / 59	14 / 1038
42.22	endosome	Biogenesis of cellular components	NCU00895, NCU06183, NCU08878	0.005281	3 / 4	3 / 1038
16.21.08	Fe/S binding	Protein with binding function or cofactor requirement (structural or analytic)	NCU00959, NCU01219, NCU01229, NCU02366, NCU02549, NCU03031, NCU03559, NCU05221, NCU06606, NCU08336, NCU08940	0.006888	11 / 43	11 / 1038
01.01.09 .03.01	biosynthesis of cysteine	Metabolism	NCU00536, NCU01985, NCU04636, NCU07001, NCU08216	0.007321	5 / 12	5 / 1038

20.03	transport facilities	Cellular transport, transport facilitation and transport routes	NCU00430, NCU00821, NCU01285, NCU01411, NCU01456, NCU01763, NCU01808, NCU01810, NCU01813, NCU02422, NCU02582, NCU02802, NCU02903, NCU03112, NCU03171, NCU03257, NCU03497, NCU03498, NCU03509, NCU03559, NCU04310, NCU05180, NCU05390, NCU05391, NCU05457, NCU05546, NCU05627, NCU05830, NCU05843, NCU05985, NCU06167, NCU06231, NCU06382, NCU07295, NCU07334, NCU07465, NCU07478, NCU07531, NCU07668, NCU07960, NCU08404, NCU08707, NCU08738, NCU08895, NCU08940, NCU08941, NCU09287, NCU09477, NCU09580, NCU09874, NCU10732	0.007562	51 / 323	51 / 1038
34.01.03 .03	homeostasis of phosphate	Interaction with the environment	NCU05390, NCU05391, NCU07465, NCU08325	0.012825	4 / 9	4 / 1038
40.01.03	directional cell growth (morphogenesis)	Cell fate	NCU01797, NCU01833, NCU02216, NCU02234, NCU02558, NCU02885, NCU02984, NCU04185, NCU05314, NCU06111, NCU06182, NCU06593, NCU06815, NCU07253, NCU07378, NCU08683	0.014021	16 / 79	16 / 1038
01.01.11 .02.01	biosynthesis of isoleucine	Metabolism	NCU02954, NCU03608, NCU04292, NCU04579, NCU09331	0.015273	5 / 14	5 / 1038
01.01.06 .06.02	degradation of lysine	Metabolism	NCU00269, NCU02274, NCU03118, NCU04771, NCU05805	0.015273	5 / 14	5 / 1038
20.01.01 .07.07	phosphate transport	Cellular transport, transport facilitation and transport routes	NCU05390, NCU05391, NCU07465, NCU08325, NCU08743	0.015273	5 / 14	5 / 1038
1.07	metabolism of vitamins, cofactors, and prosthetic groups	Metabolism	NCU00552, NCU00605, NCU01157, NCU01219, NCU02274, NCU02475, NCU02505, NCU02727, NCU03857, NCU03970, NCU04013, NCU04596, NCU04636, NCU04771, NCU05278, NCU05805, NCU07112, NCU07659, NCU07742, NCU08269, NCU08404, NCU08877	0.015805	22 / 121	22 / 1038

01.20.37.01	metabolism of thioredoxin, glutaredoxin, glutathion	Metabolism	NCU01157, NCU01219, NCU03749, NCU04130, NCU04569, NCU04596	0.019752	6 / 20	6 / 1038
16.21.01	heme binding	Protein with binding function or cofactor requirement (structural or analytic)	NCU01808, NCU02624, NCU03031, NCU03492, NCU05001, NCU05169, NCU05278, NCU05752, NCU07286, NCU08138, NCU09816	0.021571	11 / 50	11 / 1038
01.01.06	metabolism of the aspartate family	Metabolism	NCU03500, NCU03607, NCU06512, NCU07941, NCU08411	0.027541	5 / 16	5 / 1038
01.05.05.07	C-1 compound catabolism	Metabolism	NCU02274, NCU02475, NCU02727, NCU05805, NCU08877	0.027541	5 / 16	5 / 1038
01.01.11.03.01	biosynthesis of valine	Metabolism	NCU02954, NCU03608, NCU04292, NCU04579	0.027941	4 / 11	4 / 1038
2.45	energy conversion and regeneration	Energy	NCU00865, NCU02979, NCU03857, NCU04452, NCU06836, NCU10007	0.03129	6 / 22	6 / 1038
34.01.01.01	homeostasis of metal ions (Na, K, Ca etc.)	Interaction with the environment	NCU00430, NCU01285, NCU01779, NCU01978, NCU02009, NCU02063, NCU02133, NCU02278, NCU03497, NCU03498, NCU03592, NCU04140, NCU04636, NCU04830, NCU05830, NCU07530, NCU07531, NCU07564, NCU07728, NCU07742, NCU08147, NCU08225, NCU08707, NCU11414	0.032211	24 / 144	24 / 1038

32.01.01	oxidative stress response	Cell rescue, defense and virulence	NCU01219, NCU02133, NCU03112, NCU03200, NCU03333, NCU03857, NCU03905, NCU04596, NCU05169, NCU05973, NCU06031, NCU06051, NCU06556, NCU07280, NCU07286, NCU07742, NCU09534	0.032935	17 / 94	17 / 1038
40.01.01	non-directional cell growth	Cell fate	NCU03117, NCU08331	0.035459	2 / 3	2 / 1038
2.09	anaplerotic reactions	Energy	NCU02505, NCU03651	0.035459	2 / 3	2 / 1038
01.01.03.02	metabolism of glutamate	Metabolism	NCU01157, NCU04856, NCU06112, NCU06724, NCU07941	0.035489	5 / 17	5 / 1038
20.01.01.01.01.01	siderophore-iron transport	Cellular transport, transport facilitation and transport routes	NCU02009, NCU03497, NCU03498, NCU07564	0.038251	4 / 12	4 / 1038
30.01.05.01.03	MAPKKK cascade	Cellular communication / signal transduction mechanism	NCU00587, NCU02133, NCU02234, NCU02885, NCU04335, NCU06182, NCU07286, NCU11215	0.044213	8 / 36	8 / 1038
01.01.09.01.01	biosynthesis of glycine	Metabolism	NCU01853, NCU02475, NCU02727, NCU03607, NCU04771	0.044712	5 / 18	5 / 1038
20.01.11	amine / polyamine transport	Cellular transport, transport facilitation and transport routes	NCU07334, NCU08148, NCU08895, NCU09580, NCU09909	0.044712	5 / 18	5 / 1038
01.20.19.01	metabolism of porphyrins	Metabolism	NCU01013, NCU01546, NCU03498, NCU06051, NCU06189, NCU08138	0.046505	6 / 24	6 / 1038
02.01.03	regulation of glycolysis and gluconeogenesis	Energy	NCU00629, NCU02401, NCU04797, NCU06075, NCU09347, NCU10046	0.046505	6 / 24	6 / 1038

20.09.18	cellular import	Cellular transport, transport facilitation and transport routes	NCU00821, NCU00895, NCU01813, NCU02009, NCU02278, NCU02582, NCU02988, NCU03257, NCU03498, NCU03509, NCU05168, NCU05627, NCU05830, NCU05843, NCU06231, NCU06821, NCU07334, NCU07530, NCU07531, NCU07564, NCU08148, NCU08225, NCU08325, NCU08738, NCU09287	0.047376	25 / 157	25 / 1038

Supplementary Table 3.5. FunCat analysis of the genes associated with the ChIP-seq peaks that are more than four-fold enrichment in the AOD5 -CM experiment.

FunCat ID	FunCat description	FunCat main category	Gene ID(s)	Exact p-value	# genes found/# genes in category	# genes found/# genes input
2.13	respiration	Energy	NCU00385, NCU00865, NCU01606, NCU01808, NCU02250, NCU02514, NCU02807, NCU03233, NCU04874, NCU05299, NCU06051, NCU06606, NCU07953, NCU08272	1.89E-05	14 / 105	14 / 325
2.11	electron transport and membrane-associated energy conservation	Energy	NCU00385, NCU00959, NCU01606, NCU01808, NCU02250, NCU02514, NCU02549, NCU03558, NCU05008, NCU05299, NCU05457, NCU06606, NCU08272, NCU08940	9.38E-05	14 / 121	14 / 325
01.01.03 .02.01	biosynthesis of glutamate	Metabolism	NCU01195, NCU01744, NCU02366, NCU04569, NCU04856, NCU06724, NCU07941	0.000395	7 / 39	7 / 325
01.01.09 .01.02	degradation of glycine	Metabolism	NCU02475, NCU05805, NCU06424, NCU08877	0.000432	4 / 11	4 / 325
02.13.03	aerobic respiration	Energy	NCU00385, NCU00959, NCU01606, NCU01808, NCU02250, NCU02514, NCU02549, NCU04874, NCU05457, NCU06606, NCU07953, NCU08940	0.000609	12 / 112	12 / 325
01.05.02 .04	sugar, glucoside, polyol and carboxylate anabolism	Metabolism	NCU00629, NCU00959, NCU01528, NCU02366, NCU04265, NCU04797, NCU04899, NCU06211, NCU09347, NCU10008	0.001003	10 / 87	10 / 325

2.1	tricarboxylic-acid pathway (citrate cycle, Krebs cycle, TCA cycle)	Energy	NCU00959, NCU01195, NCU02366, NCU03651, NCU04899, NCU06211, NCU06836, NCU10008	0.001086	8 / 59	8 / 325
20.03	transport facilities	Cellular transport, transport facilitation and transport routes	NCU00821, NCU01285, NCU01763, NCU01808, NCU01810, NCU03257, NCU03509, NCU05390, NCU05391, NCU05457, NCU05627, NCU05843, NCU05985, NCU06382, NCU07531, NCU07668, NCU08404, NCU08940, NCU08941, NCU09287, NCU09580, NCU10732	0.00254	22 / 323	22 / 325
2.09	anaplerotic reactions	Energy	NCU02505, NCU03651	0.003738	2 / 3	2 / 325
2.01	glycolysis and gluconeogenesis	Energy	NCU00629, NCU01528, NCU02505, NCU04265, NCU04797, NCU07807, NCU09873, NCU10007	0.005069	8 / 75	8 / 325
01.02.02.06	assimilation of ammonia	Metabolism	NCU03120, NCU09205	0.0073	2 / 4	2 / 325
16.13.03	fatty acid binding (e.g. acyl-carrier protein)	Protein with binding function or cofactor requirement (structural or analytic)	NCU00596, NCU05008	0.0073	2 / 4	2 / 325
01.05.02.07	sugar, glucoside, polyol and carboxylate catabolism	Metabolism	NCU00629, NCU00865, NCU00959, NCU01517, NCU01528, NCU01873, NCU02366, NCU04265, NCU04797, NCU04899, NCU06211, NCU07807, NCU09347, NCU10008	0.008235	14 / 191	14 / 325

01.01.03	assimilation of ammonia, metabolism of the glutamate group	Metabolism	NCU01744, NCU04569, NCU04856, NCU06724	0.011185	4 / 25	4 / 325
20.09.04	mitochondrial transport	Cellular transport, transport facilitation and transport routes	NCU00075, NCU00385, NCU01606, NCU01810, NCU02514, NCU05390, NCU05593, NCU07530, NCU08941, NCU10732	0.011685	10 / 122	10 / 325
01.02.07 .01	regulation of nitrogen metabolism	Metabolism	NCU03120, NCU04335, NCU09205	0.012297	3 / 14	3 / 325
02.45.15	energy generation (e.g. ATP synthase)	Energy	NCU00385, NCU01606, NCU02250, NCU02514	0.014678	4 / 27	4 / 325
16.21.08	Fe/S binding	Protein with binding function or cofactor requirement (structural or analytic)	NCU00959, NCU02366, NCU02549, NCU06606, NCU08940	0.017863	5 / 43	5 / 325
01.05.05 .07	C-1 compound catabolism	Metabolism	NCU02475, NCU05805, NCU08877	0.01795	3 / 16	3 / 325
20.01.15	electron transport	Cellular transport, transport facilitation and transport routes	NCU00385, NCU00959, NCU01606, NCU01808, NCU02250, NCU02514, NCU02549, NCU02665, NCU04899, NCU05169, NCU05457, NCU06051, NCU06211, NCU06606, NCU08272, NCU08940	0.019908	16 / 255	16 / 325
01.01.03 .02	metabolism of glutamate	Metabolism	NCU04856, NCU06724, NCU07941	0.021232	3 / 17	3 / 325

20.09.18	cellular import	Cellular transport, transport facilitation and transport routes	NCU00821, NCU02009, NCU03257, NCU03509, NCU05168, NCU05627, NCU05843, NCU07530, NCU07531, NCU07564, NCU09287	0.024661	11 / 157	11 / 325
1.07	metabolism of vitamins, cofactors, and prosthetic groups	Metabolism	NCU00596, NCU02475, NCU02505, NCU04636, NCU05805, NCU08269, NCU08404, NCU08877, NCU09770	0.02885	9 / 121	9 / 325
01.01.03 .01.01	biosynthesis of glutamine	Metabolism	NCU04856, NCU06724	0.030986	2 / 8	2 / 325
01.20.37 .01	metabolism of thioredoxin, glutaredoxin, glutathion	Metabolism	NCU03749, NCU04130, NCU04569	0.032913	3 / 20	3 / 325
20.09.18 .07	non-vesicular cellular import	Cellular transport, transport facilitation and transport routes	NCU03509, NCU05168, NCU05627, NCU05843, NCU07530, NCU07564, NCU09287, NCU11414	0.033837	8 / 105	8 / 325
01.20.38	metabolism of toxins/drugs	Metabolism	NCU05616	0.035807	1 / 1	1 / 325
01.20.19 .03	metabolism of open-chain tetrapyrrols	Metabolism	NCU06189	0.035807	1 / 1	1 / 325
34.01.03 .03	homeostasis of phosphate	Interaction with the environment	NCU05390, NCU05391	0.038913	2 / 9	2 / 325
16.17.05	sodium binding	Protein with binding function or cofactor requirement (structural or analytic)	NCU01285, NCU01321	0.038913	2 / 9	2 / 325

2.45	energy conversion and regeneration	Energy	NCU00865, NCU06836, NCU10007	0.042209	3 / 22	3 / 325
1.05	C-compound and carbohydrate metabolism	Metabolism	NCU00148, NCU00629, NCU00761, NCU00865, NCU00959, NCU01517, NCU01528, NCU02366, NCU02505, NCU02550, NCU02702, NCU03651, NCU03749, NCU04265, NCU04569, NCU04797, NCU04899, NCU05340, NCU05627, NCU05960, NCU06062, NCU06211, NCU06381, NCU06836, NCU07807, NCU08044, NCU08272, NCU08784, NCU09287, NCU09347, NCU09770, NCU09873, NCU10007, NCU10008	0.045499	34 / 711	34 / 325

4. Discussion

4.1 Protein tagging and localization

In this study, my major goal was to gain a deeper understanding of the function of AOD2 and AOD5. To address this goal, several questions needed to be addressed. What is the subcellular localization of AOD2 and AOD5 under normal conditions? Do they change localization in response to mitochondrial dysfunction? Do they form a heterodimer *in vivo*? Do they have any post-translational modifications that are associated with the induction of AOX? The first step in addressing these questions was to develop strains expressing AOD2 and AOD5 tagged with HA or Myc epitopes in the corresponding mutant strains. In addition, I also successfully expressed C-terminal Myc tagged AOD2 and N-terminal HA tagged AOD5 in DX13, an *aod-2 aod-5* double mutant.

It has occasionally been observed that the addition of HA or Myc epitopes or other protein tags can affect the activity of a tagged protein (Zhao *et al.* 2013). For instance, in *C. albicans*, a C-terminal HA-tagged Zn(II)Cys6 fungal transcription factor called MRR1 was found to be constitutively active in driving the expression of its target gene MDR1 (Schubert *et al.* 2011) whereas the wild-type MRR1 protein only induced the expression of MDR1 when cells were grown in the presence of an antifungal agent (Morschhauser *et al.* 2007). However, the tagged AOD2 and AOD5 proteins in the present study conferred neither constitutive expression of AOX in non-inducing conditions nor the abolishment of AOX expression under inducing conditions. Cell fractionation experiments showed that AOD2 and AOD5 always localize to the nucleus regardless of whether the HA or Myc epitope is at the N- or C-terminus of either protein.

The classic mitochondrial retrograde regulation RTG system of *S. cerevisiae*

functions by sequestering transcription factors Rtg1p and Rtg3p in the cytoplasm until a signal is received that results in their translocation to the nucleus (section 1.8). Although Rtg1p and Rtg3p are not Zn(II)Cys6 fungal transcription factors, this is also an example of the factors being sequestered in the cytoplasm under normal conditions, but imported into the nucleus when they are activated (MacPherson *et al.* 2006). Another example, as mentioned in section 1.11, is the *C. albicans* Zn(II)Cys6 transcription factor Sef1, which can localize to either the nucleus or the cytosol, depending on the availability of iron (Chen & Noble 2012). Under normal conditions, Sef1 is sequestered in the cytosol. Upon iron depletion, it is phosphorylated and localizes to the nucleus. Another example is Upc2p in *S. cerevisiae*. This Zn(II)Cys6 transcription factor is responsible for the expression of ergosterol biosynthesis-related genes when ergosterol is depleted (Vik & Rine 2001). Fluorescence microscopy showed that GFP (green fluorescent protein) tagged Upc2p localized to the cytoplasm when ergosterol is abundant, but is imported into the nucleus after addition of fluconazole (Yang *et al.* 2015), a drug that inhibits the conversion of lanosterol to ergosterol and hence lowers the levels of ergosterol.

Many other Zn(II)Cys6 transcription factors localize to the nucleus at all times and become activated when the proper signal is generated. Examples of such transcription factors include Leu3p in *S. cerevisiae* (Kirkpatrick & Schimmel 1995) and Trm1p in *P. pastoris* (Sahu *et al.* 2014). My results suggested that the AOD2 and AOD5 behave in a similar manner. When the cell fractionation and the ChIP-seq data are considered together, it appears that AOD2 and AOD5 constitutively reside in the nucleus and bind to the 5′ upstream region of many genes. Similarly, GFP (green fluorescent protein) tagged AcuM and AcuK, the orthologues of AOD2 and AOD5 in *A. nidulans*, respectively, were shown to localize to the nucleus when cells were

grown on media containing glucose, proline, or acetate (Suzuki *et al.* 2012). Because AOD2 and AOD5 and their target genes are not spatially isolated, it is conceivable that they are "switched on or off" *in situ*. It has been shown that the transcript levels (Chae *et al.* 2007b) and protein levels (this study) of AOD2 and AOD5 are not altered greatly between AOX inducing and non-inducing conditions. This suggests that they are regulated post-translationally. This could be achieved by covalent modification of the protein or covalent or non-covalent interactions with other proteins or unknown ligands.

4.2 Regulation of AOD2 and AOD5 activity

It has been reported in *S. cerevisiae* that the AOD2 orthologue Rds2p is phosphorylated by Snf1p when cells are grown on media shifted from glucose to ethanol. Snf1p belongs to a conserved protein kinase family and AMPK (AMP-activated protein kinase) is its mammalian orthologue. In plants, it has an orthologue named SnRK1 (SNF1-related protein kinase 1) (Crozet *et al.* 2014; Ghillebert *et al.* 2011; Polge & Thomas 2007). These kinases maintain energy homeostasis by generally switching off anabolism and activating catabolic pathways for ATP production. In yeast, SNF1 is required for cell growth when cells utilize non-fermentable carbon sources. In plants, SnRK1 is a metabolic regulator that responds to nutrient limitation and environmental stress. In mammals, AMPK senses changes in the AMP/ATP or ADP/ATP ratio (Carling & Viollet 2015; Ghillebert *et al.* 2011; Hardie 2015; Hardie *et al.* 2012).

In *S. cerevisiae*, SNF1 regulates a wide variety of genes in response to carbon source alteration. When cells are deprived of glucose, Snf1p phosphorylates the glucose repressor Mig1p which leads to the nuclear export of Mig1p and hence

derepression of glucose repressed genes (Hedbacker & Carlson 2008). SNF1 also activates the transcription of gluconeogenic genes via phosphorylation of Sip4 and Cat8 (Hedbacker & Carlson 2008; Turcotte *et al.* 2010). Cat8 has been shown to be required for Rds2 to bind to the promoters of PEPCK and FBP (Soontorngun *et al.* 2007). In *N. crassa*, deletion of SNF1 has been shown to slightly decrease AOX protein levels under AOX inducing conditions, but the mechanism by which this occurs is unknown (Nargang *et al.* 2012). It is conceivable that SNF1 plays a similar role as in *S. cerevisiae*, in which case, it would be expected that AOD2 would be differentially phosphorylated between AOX inducing and non-inducing conditions. However, using phos-tag SDS-PAGE, I was unable to show reproducible changes in phosphorylation of AOD2 or AOD5 under inducing or non-inducing conditions (Appendix IV.1). This suggests that, unlike Rds2p in yeast, AOD2 and AOD5 are not being regulated by phosphorylation, at least when comparing growth in the presence and absence of CM. So far, no phosphorylation of an AOD2 orthologue has been reported in any fungus other than *S. cerevisiae*, and no phosphorylation of an AOD5 orthologue has been reported at all.

4.3 AOD2, AOD5 and gluconeogenesis

The involvement of AOD2 and AOD5 orthologues in the regulation of genes required for gluconeogenesis in *S. cerevisiae*, *A. nidulans*, *A. fumigatus*, and *P. anserina* (Bovier *et al.* 2014; Gasmi *et al.* 2014; Hynes *et al.* 2007; Liu *et al.* 2010; Pongpom *et al.* 2015; Sellem *et al.* 2009; Soontorngun *et al.* 2012; Soontorngun *et al.* 2007; Suzuki *et al.* 2012) prompted me to ask whether or not AOD2 and AOD5 play a similar role in *N. crassa*. I first showed that AOD2 and AOD5 are required for maximal growth rate when any of sucrose, glycerol, acetate, or ethanol were supplied

as the sole carbon sources. Thus, AOD2 and AOD5 appear to have a more general role in maintaining the maximum growth rate of the organism. However, the reduction of growth of Δ*aod-2* and Δ*aod-5* strains on glycerol, acetate, and ethanol was much more pronounced than on sucrose. These findings are in agreement with the data from *A. fumigatus*, where mutants with deletion of *acuM* or *acuK* showed slightly weaker growth on standard medium with sucrose as the carbon source (Liu *et al.* 2010; Pongpom *et al.* 2015). However, the findings are slightly different from the data from *A. nidulans* (Hynes *et al.* 2007). The *acuM* and *acuK* mutant strains grew at wild-type rates on glucose and glycerol, but were not able to grow on acetate or ethanol. In *S. cerevisiae*, the data for the growth of the Δ*rds2* mutant on ethanol was contradictory in two different studies (Gasmi *et al.* 2014; Soontorngun *et al.* 2012). The Δ*rds2* strain in the FY73 background (MATα *his3*-Δ200 *ura3-52*) did not grow on media containing ethanol or acetate, weakly grew on glycerol, and grew at wild-type rates on glucose (Soontorngun *et al.* 2012). In contrast, the Δ*rds2* strain in the BY4741 background (MATa *his3*Δ1 *leu2*Δ0 *met15*Δ0 *ura3*Δ0) grew as wild-type on glucose or ethanol (Gasmi *et al.* 2014). These differences are probably due to the different genetic backgrounds of the strains used. Taken together, these studies on deletion of the AOD2 orthologue show general agreement with my study.

The general process of gluconeogenesis is shown in Fig. 4.1. In comparison to glycolysis, it converts pyruvate to glucose and, depending on the organism or tissue, can provide a source of energy and/or precursors for synthesizing important molecules such as glycoproteins and nucleotides (Nelson & Cox 2013). Many of the steps in the gluconeogenesis pathway are simply accomplished by using the glycolysis enzymes in reverse. However, glycolysis contains three irreversible steps that involve large changes in free energy. As a result, there are four enzymes that are

Figure 4.1. Glycolysis and gluconeogenesis. The black arrows from top to bottom represent the glycolysis pathway. The red arrows represent the steps of gluconeogenesis. The enzymes involved in glycolysis are shown in blue on the left of the glycolytic pathway. Most of the enzymes are shared by both glycolysis and gluconeogenesis. Four enzymes that are critical and unique for gluconeogenesis are shown in green and are highlighted by boxes on the right of the gluconeogenic pathway. The metabolic pathway from glycerol to dihydroxyacetone phosphate is indicated by green arrows and the enzymes that are involved in this pathway are indicated in pink. This figure is adapted from (Nelson & Cox 2013).

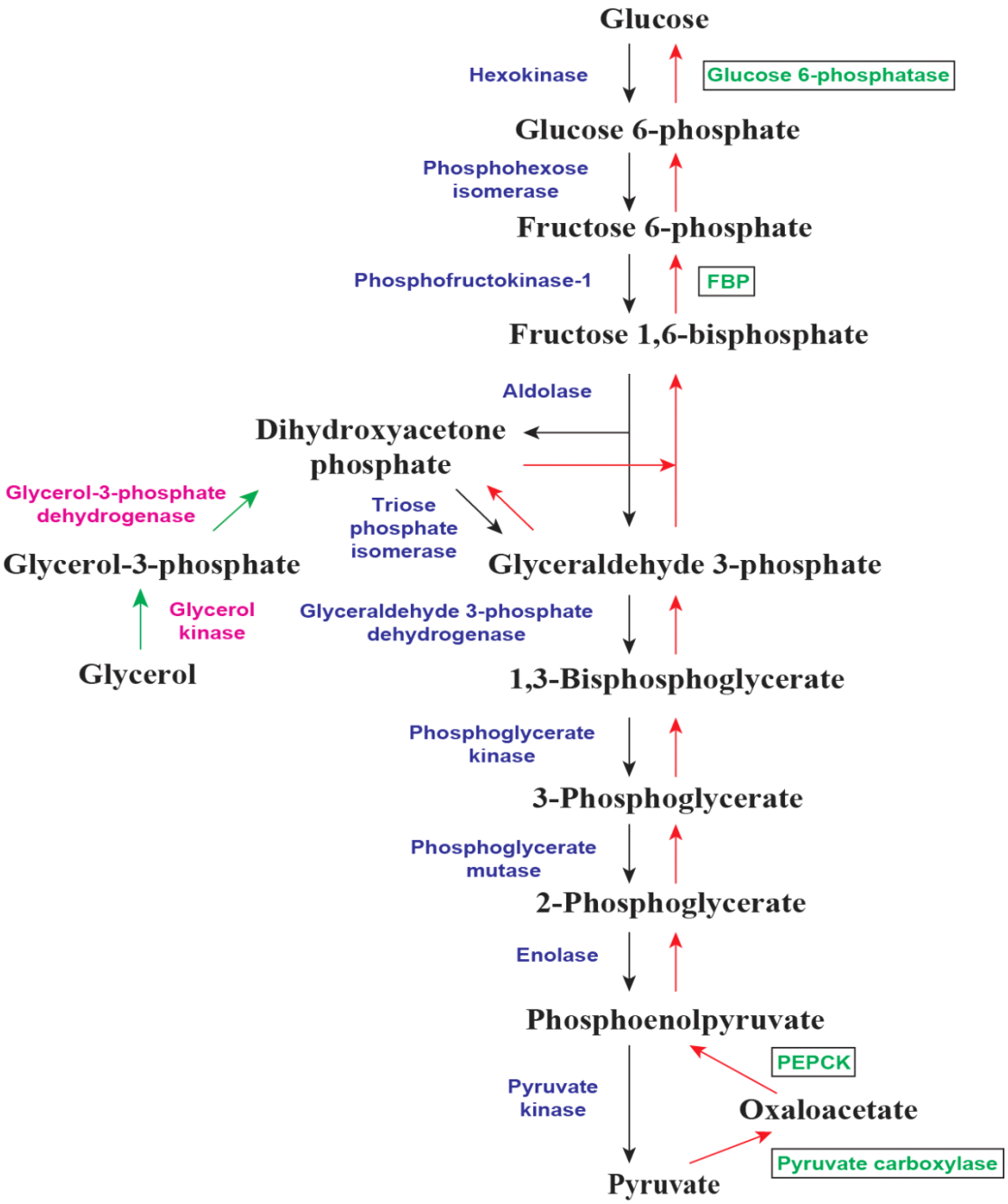
Glucose
Hexokinase
Glucose 6-phosphatase
Glucose 6-phosphate
Phosphohexose isomerase
Fructose 6-phosphate
Phosphofructokinase-1
FBP
Fructose 1,6-bisphosphate
Aldolase
Dihydroxyacetone phosphate
Glycerol-3-phosphate dehydrogenase
Triose phosphate isomerase
Glycerol-3-phosphate
Glyceraldehyde 3-phosphate
Glycerol kinase
Glycerol
Glyceraldehyde 3-phosphate dehydrogenase
1,3-Bisphosphoglycerate
Phosphoglycerate kinase
3-Phosphoglycerate
Phosphoglycerate mutase
2-Phosphoglycerate
Enolase
Phosphoenolpyruvate
PEPCK
Pyruvate kinase
Oxaloacetate
Pyruvate carboxylase
Pyruvate

required specifically for gluconeogenesis to achieve the reverse reaction at these steps. These enzymes are pyruvate carboxylase, PEPCK, FBP, and glucose 6-phosphatase (Fig. 4.1).

The AOD2 and AOD5 orthologues in *A. nidulans* have been shown to be required for the maximal expression of the PEPCK- and FBP- encoding genes when cells utilized glucose or acetate as the carbon source (Hynes *et al.* 2007). In *A. fumigatus*, loss of the AOD2 orthologue led to reduced expression PEPCK- and FBP-encoding genes (16-fold and seven-fold, respectively) when cells use glucose as the carbon source (Liu *et al.* 2010). Furthermore, using standard ChIP or ChIP-chip analyses, the AOD2 and AOD5 orthologues were found to bind the promoter of the PEPCK- and FBP-encoding genes in *S. cerevisiae* grown on glucose or ethanol, and in *A. nidulans* grown on glucose or acetate (Gasmi *et al.* 2014; Soontorngun *et al.* 2012; Soontorngun *et al.* 2007; Suzuki *et al.* 2012). In addition, binding at the promoter of *S. cerevisiae* PYC1 (pyruvate carboxylase isoform1) was found for the AOD2 and AOD5 orthologues upon a shift in carbon source from glucose to glycerol and ethanol (Gasmi *et al.* 2014; Soontorngun *et al.* 2012). No binding at the promoter of the glucose 6-phosphatase-encoding gene has been reported.

In *N. crassa*, I found that AOD2 regulated the expression of PEPCK, since the transcript levels of PEPCK were reduced in Δ*aod-2* cells which utilized acetate as the sole carbon source (Fig. 3.6C). Even when cells were grown in sucrose where PEPCK should be present at low basal levels, the expression of the PEPCK transcript was reduced significantly (about 25-fold) in Δ*aod-2* cells (Fig. 3.6C). The finding that expression of PEPCK is reduced in Δ*aod-2* cells grown in sucrose is in agreement with the data obtained from *A. fumigatus* (Liu *et al.* 2010), where levels of the transcript were reduced 16-fold when the orthologue was deleted. In *S. cerevisiae*, a

similar finding was observed, where the deletion of the *aod-2* orthologue greatly decreases the expression of PEPCK when cells were shifted from glucose to ethanol as a carbon source (Soontorngun *et al.* 2007). Surprisingly, my data suggest that the deletion of *aod-2* has no effect on the expression of the FBP gene in *N. crassa*. This is inconsistent with the findings in *A. nidulans* and *A. fumigatus*. Thus, it seems likely that other factors regulate FBP expression in *N. crassa*.

The relationship between the induction of AOX and PEPCK suggests obvious questions. What is the connection between AOX expression and gluconeogenesis? Are both genes induced under both AOX-inducing and gluconeogenesis inducing conditions? Do the two induction pathways share the same signal(s)? My results suggest that there is some "cross talk" between the signals produced in the presence of CM and those produced when glucoenogenesis is required. That is, slight increases in AOX transcripts are seen in poor carbon sources and slight increases in PEPCK transcripts are seen in CM. However, since PEPCK is induced to a higher extent in poor carbon sources, while AOX transcripts are higher in CM, this argues for different signals produced under the two conditions. These signals activate AOD2 and AOD5 to various degrees, resulting in dramatic or minor induction of the target genes.

There are two basic mechanisms by which different signals might act. First, AOD2 and/or AOD5 might bind different molecules resulting in different degrees of activation at different promoters. Second, other factors may bind a different molecule at the same promoter and work in conjunction with AOD2 and/or AOD5. Both AOD2 and AOD5 contain a PAS domain which is thought to be involved in signal transduction (Chae *et al.* 2007b). PAS domains are known to recognize a number of small molecules from ions to C6 carboxylates (Henry & Crosson 2011). It has been

reported that two glycine residues in the PAS domain of both AOD2 and AOD5 are highly conserved and amino acid substitutions at these positions resulted in reduced growth on medium containing antimycin A (Chae *et al.* 2007b). This suggests that the PAS domain in each protein is crucial for function. PAS domains are also used for protein-protein interaction. For instance, WC-1 (white collar-1) and WC-2, two transcription factors that are involved in circadian rhythms in *N. crassa*, form a heterodimer via interaction between the PAS domain in each protein (Cheng *et al.* 2002; Cheng *et al.* 2003). PAS domains are also important for forming a heterodimeric complex of the bHLH (basic helix-loop-helix)-PAS transcription factors in insects and mammals (see review Partch and Gardner (2010)). An EMSA experiment has shown that truncated recombinant AOD2 and AOD5 proteins, containing only the DNA binding domains, are able to bind the AIM sequence of the AOX promoter when added together. However, the individual proteins are unable to bind (Chae *et al.* 2007b). These data suggest that there is an *in vitro* interaction between the two truncated proteins and that the PAS domains in both proteins are not required for this interaction. However, it is conceivable that interaction between the PAS domains is required for activation. It is also conceivable that AOD2 and/or AOD5 interact with other proteins via the PAS domain.

Another possibility for the different response of PEPCK and AOX in different media would be that other transcription factors respond to the signal for the induction of AOX or gluconeogenesis, and coordinate with AOD2 and AOD5 to facilitate proper gene expression (Fig 4.2). Interplay between Rds2p, the *S. cerevisiae* AOD2 orthologue, and the additional transcription factors Cat8p and Sip4p, has been reported (Soontorngun *et al.* 2007). Cat8p and Sip4p are activated by Snf1p when cells are using non-fermentable carbon sources and they activate PEPCK transcription

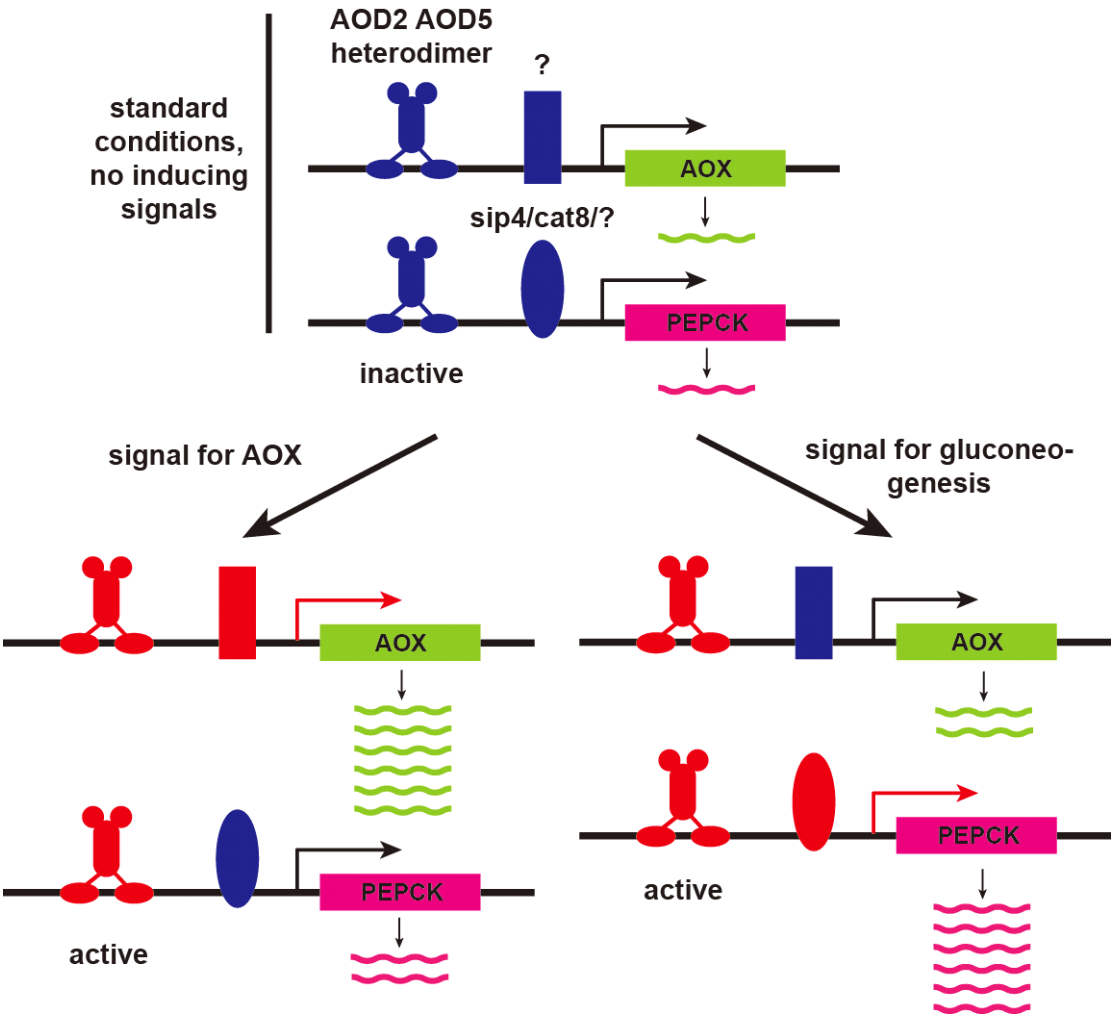

Figure 4.2. Model for regulation of the expression of AOX and PEPCK by AOD2 and AOD5. In the absence of inducing signals, the AOD2 AOD5 dimer and unknown factors (indicated by a rectangle and an oval) bind to the promoter of the AOX and PEPCK genes as shown. Under normal conditions, they are inactive and only a low level of constitutive transcription of AOX and PEPCK occurs, as indicated by the wavy lines. In the presence of inducing signals, either for AOX or gluconeogenesis, the AOD2/AOD5 dimer is activated, but the extent of the induction of transcription also depends on the unknown factors, which also respond specifically to the signal. For instance, the rectangle factor may respond only to the signal for AOX whereas the oval responds only to the signal for gluconeogenesis. Active proteins are indicated in red whereas inactive proteins are shown in blue.

by binding to the CSRE (carbon source-responsive element) of the gene's promoter (Turcotte *et al.* 2010). Deletion of CAT8 reduced the binding of Rds2p to the promoters of PEPCK and FBP (Soontorngun *et al.* 2007). An additional zinc finger transcription factor, Adr1p (alcohol dehydrogenase regulator 1) that is known to be another target of Snf1p upon utilization of ethanol, coordinates with Cat8p to induce some target genes upon glucose depletion (Kayikci & Nielsen 2015; Ratnakumar *et al.* 2009; Tachibana *et al.* 2005; Turcotte *et al.* 2010; Young *et al.* 2003). Adr1p was recently shown to share some binding targets with Rds2p, including the PEPCK promoter (Soontorngun *et al.* 2012). Thus, the activation of PEPCK in *S. cerevisiae* occurs by a complex mechanism and involves the interplay of several transcription factors. In *A. thaliana*, a number of proteins (such as ABI4 and WRKY15) that are responsible for the expression of AOX have been identified (see section 1.10.6 for details).

In *N. crassa*, only AOD2 and AOD5 have been described as transcription factors involved in AOX production. However, it is likely that other factors are involved. An additional 62 genes that are needed for maximal production of the AOX protein were identified in the *N. crassa* knock-out library screen (Nargang *et al.* 2012). The roles of the genes and their products in AOX production and whether or not they interact with AOD2 and AOD5 are not yet known. In addition, three other genes (*aod-4*, *aod-6* and *aod-7*) identified in a traditional genetic screen have been shown to have reduced transcription of AOX in response to growth in CM (Descheneau *et al.* 2005). It is not yet known if these are allelic to genes identified in the knock-out library.

I found that the expression levels of PEPCK increased when acetate and ethanol served as the carbon source (Fig. 3.6C). However, the expression of PEPCK

was not activated when glycerol was the sole carbon source. This is likely because glycerol enters the gluconeogenesis pathway downstream from the PEPCK reaction (Fig. 4.1). In support of this idea, it has previously been shown that *S. cerevisiae* (Nevoigt & Stahl 1997) and *A. nidulans* metabolize glycerol to glucose-6-phosphate in a pathway that bypasses the need for PEPCK early in the gluconeogenic pathway (Borkovich & Ebbole 2010). Glycerol is first phosphorylated to glycerol-3-phosphate by glycerol kinase, and is then further converted to dihydroxyacetone phosphate by glycerol-3-phosphate dehydrogenase. Dihydroxyacetone phosphate enters the gluconeogenic pathway and ultimately leads to the production of glucose. Consistent with my results, it was also reported that the activity of PEPCK was low in the yeast *Y. lipolytica* when grown in glucose or glycerol compared to cells grown in acetate or ethanol (Jardon *et al.* 2008).

4.4 Interpretation of ChIP-seq data

To gain a deeper understanding of the behavior of AOD2 and AOD5 in response to CM treatment, I performed ChIP-seq experiments. ChIP-seq is based on high-throughput next generation sequencing techniques. Compared to the ChIP-chip technique, it has greater coverage, lower systematic noise, higher accuracy and higher resolution properties (Park 2009). In my experiments, MACS2 called many peaks for each of the four conditions tested. There are various interpretations of these findings. First, upon inspection, many of the peaks called in each category are not robust. This is observed even among the 65 ChIP-seq peaks that have more than four-fold enrichment in each of the four experimental conditions. Thus, it is difficult to assign biological significance to all of the called peaks. The fact that many peaks were not common to all four experiments suggests that in addition to their common binding

sites, AOD2 exclusively occupies some sites without the binding of AOD5, and vice versa. Thus, even though AOD2 and AOD5 are thought to form a heterodimer at the promoter of *aod-1*, they may have additional functions in which they might act as monomers, homodimers, or in heterodimers with different transcription factors. As mentioned above, ChIP-chip studies in *S. cerevisiae* have shown that the AOD2 and AOD5 orthologues have common, as well as distinct, binding sites in cells grown both in glucose and ethanol (Gasmi *et al.* 2014; Soontorngun *et al.* 2007). A transcriptome study has shown that the AOD2 and AOD5 orthologues in the pathogen *A. fumigatus* regulate different target genes during *in vivo* infection (Pongpom *et al.* 2015). In addition, it has been shown that female fertility in the Δ*rse3* (AOD5 orthologue) mutant of *P. anserina* was virtually abolished, while fertility was unaffected in the Δ*rse2* mutant (Bovier *et al.* 2014). Taken together, these observations imply that AOD2 and AOD5 and their orthologues have both common and distinct functions.

Similar to other ChIP-seq studies (such as the ChIP-seq data from the Encyclopedia of DNA Elements project which is a broad investigation of functional elements in the human genome, see https://www.encodeproject.org/), there are differences in peak height for the regions bound by AOD2 and/or AOD5. It seems unlikely that differences in peak height are due to different cell types because I used growing mycelium, which should contain a relatively homogeneous set of nuclei. However, it is conceivable that nuclei and specific gene promoters at growing tips versus older regions of mycelium might differ in binding of the AOD2 and AOD5 proteins, due to changes in chromatin arrangement. For example, binding to a promoter that was only available in nuclei of growing tips would show up as a smaller peak relative to a promoter available for binding in all nuclei of the culture. In

addition, sites with low peak height may simply have a lower binding affinity for the proteins (Furey 2012). This could be due to a number of factors including unfavorable chromatin structure, competition between transcription factors at or near the same binding site, or influence of nucleotides surrounding the AIM (or other binding sites).

4.5 Binding sites of AOD2 and AOD5

Zn(II)Cys6 cluster transcription factors generally recognize a pair of CGG triplets as a binding element arranged as direct, inverted, or everted repeats (MacPherson *et al.* 2006). In *vitro* EMSA experiments showed that AOD2 and AOD5 bind as a heterodimer to the AIM of the *aod-1* promoter region (Chae *et al.* 2007a). Related sites have been found in the upstream region of genes regulated by the AOD2 and AOD5 orthologues in *A. nidulans* and *P. anserina* (Bovier *et al.* 2014; Suzuki *et al.* 2012), and the AOD5 orthologue in *S. cerevisiae* (Gasmi *et al.* 2014). My ChIP-seq data show that among the group of 65 peaks that are common to all four experimental conditions, 56 contain at least one such binding site (Fig. 3.10, Supplementary Fig. 3.7). Nine out of 65 peaks are devoid of the AIM sequence (Table 3.2). Furthermore, for some peaks (those associated with NCU03408, NCU04730, NCU04953, NCU05203, NCU05616, NCU06083, NCU07098, and NCU07530) that do contain one or more AIM sequences, the AIMs are not closely aligned with peak summits. The inability to identify canonical binding motifs in a proportion of peaks from a ChIP-seq experiment is not uncommon. It has been suggested that this is due to limited understanding of various aspects of DNA binding of the transcription factors (such as binding motifs other than the canonical one) or binding of the transcription factors to peak regions via additional factors (Worsley Hunt & Wasserman 2014). The possibility that AOD2 and AOD5 are able to bind non-CGG

containing motifs in the *N. crassa* genome cannot be ruled out, since some Zn(II)Cys6 transcription factors have been shown to have this capability (MacPherson *et al.* 2006). For instance, EMSA analysis showed that FacB (=AcuB, acetate non-utilising) binds to 5'-TCC/G-3' or 5'-GCC/A-3' in *A. nidulan*s (Todd *et al.* 1998), and AFLR (aflatoxin pathway specific DNA-binding protein) binds to the 5'-TCGN_5CGA-3' palindrome in *A. parasiticus* (Ehrlich *et al.* 1999). In *A. oryzae*, a microarray study revealed that the putative binding site of XlnR (xylanolytic regulator) includes 5'-GGCTAA-3', 5'-GGCTAG-3', and 5'-GGCTGA-3' (Noguchi *et al.* 2009). Moreover, EMSA and DNaseI footprinting experiments showed that, in addition to binding the CGGN_6CGG motif in the 5' upstream region of the CYC1 (cytochrome *c* 1) gene in *S. cerevisiae* (Pfeifer *et al.* 1987a), Hap1p had loose binding specificity for a CGCN_6CGC motif in the 5' upstream region of the CYC7 gene (King *et al.* 1999; Pfeifer *et al.* 1987b) and other non-CGG motifs in the 5' upstream region of the CYB2 (cytochrome *b* 2) and CTT1 (catalase T 1) genes (Lodi & Guiard 1991; Winkler *et al.* 1988). Resolution of the crystal structure of yeast Cep3p also demonstrated similarly loose binding properties, with a binding motif containing only one CCG triplet (TGTN_9CCG) (Bellizzi *et al.* 2007). For other Zn(II)Cys6 transcription factors both CGG and non-CGG motifs were predicted in the 5' upstream region of the genes that the factors regulate using various motif finders. However, these sites were not confirmed as binding sites by EMSA or ChIP experiments (Fox *et al.* 2008; Yuan *et al.* 2008). Taken together, it seems possible that AOD2 and AOD5 might also bind a "relaxed" CGG triplet or related motif.

Another possibility is that AOD2 and AOD5 might also bind an unknown protein factor(s) that directly binds DNA. One example of transcription factors that can either directly or indirectly bind DNA is the transcription factor STE12, which is

involved in regulation of mating and filamentation in *S. cerevisiae*. Upon treatment with the alpha pheromone, mating of haploid cells is induced and the Ste12p protein has been shown to directly bind to the promoter of pheromone-responsive genes (Chou *et al.* 2006; Gordan *et al.* 2009). When filamentation is induced, Ste12p associates with Tec1p, another transcription factor, to drive the expression of genes involved in filamentous growth (pseudohyphae). However, Ste12p does not directly bind the promoter of these genes but instead is recruited to the promoter by Tec1p, which directly binds DNA (Chou *et al.* 2006; Gordan *et al.* 2009).

To determine whether or not AOD2 and/or AOD5 directly bind sequences identified by ChIP-seq is challenging. It requires the availability of ChIP-seq data of other transcription factors, as well as the knowledge of the binding motif of each transcription factor. If AOD2 or AOD5 and a transcription factor "X" occupy the same site, but this site only contains the known binding motif of the factor "X" and lacks an AIM sequence, then it is possible that AOD2 or AOD5 do not directly bind the DNA but interact with the site via the factor "X". Another possible solution for finding out whether AOD2 and/or AOD5 directly bind DNA is to identify their binding partners. This could be done by IP of tagged AOD2 and/or AOD5 and then by detection of each protein that has been pulled down by AOD2 and/or AOD5 by mass spectrometry.

4.6 AIMs that are not bound by AOD2 and/or AOD5

My analysis of AIM sequences in the 65 peaks that are common to all four experiments revealed that AOD2 and AOD5 only bind to some AIM sequences under the conditions tested. One possible explanation for this could be that the flanking sequence on both sides of the bound AIMs contribute to the binding specificity. A recent study has shown that the sequence outside the binding sites of two well-studied

yeast transcription factors (Gcn4p (general control nonderepressible) and Gal4p (galactose metabolism)) affects the binding of the transcription factors (Levo *et al.* 2015). A second possibility is that the internal linker between the two CGGs of the AIM may contribute to the binding strength. However, a previous mutagenesis study found that changes in the flanking sequence or the linker had no obvious effect on the AIM sequence that is most proximal to the *aod-1* coding sequence, at least in EMSA experiments (Chae *et al.* 2007a). Conceivably, the situation may be different *in vivo*. A third possibility could be that the non-bound AIMs are occupied by nucleosomes or other proteins so that AOD2 and/or AOD5 are unable to access these sites.

4.7 Relatively long distance between peaks and genes

Among the 65 peaks, I noticed that four nicely shaped peaks (those in the 5' upstream region of NCU00794, NCU01835, NCU03257, and NCU06724 genes) that align perfectly with an AIM sequence were between 3 to 5 kb from the start codon of the nearest gene (Supplementary Fig. 3.7). Because the average intergenic distance in *N. crassa* is 1953 bp (Galagan *et al.* 2003), these peaks might represent long distance transcriptional regulation. It is not known whether these binding sites are associated with gene transcription or not since no RT-qPCR data was obtained for these genes. It is also not known how distant *N. crassa* transcription factors are capable of regulating their target genes. In *S. cerevisiae*, the upstream activation sequence (UAS) functions to regulate the expression of the downstream gene. Using a UAS containing a Gal4p binding site, it has been shown that UASs with a distance larger than 700 bp from the TATA box of the HIS3 gene are not functional (Dobi & Winston 2007). On the other hand, in metazoans, enhancers of transcription can exist from a few kb to over 100 kb away from a gene promoter (Heinz *et al.* 2015; Kim & Shiekhattar 2015; Ong &

Corces 2011). At least in terms of distance from the controlled gene, the four peaks seem to be intermediate between the UAS of *S. cerevisiae* and enhancers in metazoans.

4.8 Binding and transcriptional regulation

Among the 65 peaks that are common to all four experimental sets, the RT-qPCR data showed that the expression of 12 genes (Fig. 3.11 and NCU08947 in Fig. 3.13B) was positively regulated by AOD2 and AOD5 when cells were grown in the presence and/or absence of CM. The expression of two genes (NCU03749 and NCU06230) were negatively regulated by AOD2 and AOD5 only when cells were grown in the presence of CM, and the expression of one gene (NCU04874) was negatively regulated by AOD5 without CM (Fig. 3.12). However, there were a number of genes whose transcription was virtually unaffected by the deletion of *aod-2* or *aod-5*, even though the summit of the peaks in the 5' region of these genes (such as NCU04307 and NCU08877) aligns perfectly with AIM(s). It is of note that only two growth conditions (presence and absence of CM) were tested and it is possible that AOD2 and/or AOD5 are involved in other cell functions that respond to different signals and require additional proteins. One example of a zinc cluster transcription factor that can respond to different signals is Pdr1p, a regulator of multidrug resistance in *S. cerevisiae* (Paul & Moye-Rowley 2014). Pdr1p can function as a drug receptor. It contains a xenobiotic-binding domain that directly binds to structurally unrelated xenobiotics such as ketoconazole, rifampicin, and cycloheximide (Thakur *et al.* 2008). Binding of these drugs activates the protein and drives the expression of its target genes. It is not known whether AOD2 and AOD5 can bind to different small molecules.

The RT-qPCR data of genes from groups other than the common 65 peaks are sometimes difficult to understand. The negative regulation of NCU00628 by AOD2 (Fig. 3.15A) does not seem to coincide with its grouping in the category with significant binding of only AOD5 plus or minus CM (Table 3.3). NCU04899 was found in the same group, but its expression was enhanced by both AOD2 and AOD5 in cells grown in the presence of CM (Fig. 3.15D). Therefore, at face value, the categories do not always seem to be relevant with the results of expression obtained by RT-qPCR. There are various possible explanations for these findings. The first relates to my arbitrary cutoff point of four-fold enrichment. This could lead to omission of some peaks that may be significant. For instance, a ChIP-seq peak for the AOD2 +CM experiments is present in the 5' upstream region of NCU04899, but the fold-enrichment was only 2.7. Thus, it is possible that AOD2 binds this region when cells are grown in the presence of CM. Second, even though NCU00628 is present in the AOD5 group it does not seem to be regulated by AOD5. As mentioned above, AOD5 might control the transcription of NCU00628 under conditions other than –CM and +CM. Third, the transcriptional changes measured by RT-qPCR are relatively small (Fig. 3.15) in these two cases. It is conceivable that the differences may not be biologically relevant.

An interesting observation was made for NCU02474 (Tom5) and NCU02475 (glycine dehydrogenase). These genes are on opposite sides of a peak that is in the 5' upstream region for both genes. The summit of the peak aligns perfectly with an AIM (Supplementary Fig. 3.7). NCU02475 was found to be positively regulated by both AOD2 and AOD5 in cells grown in the presence and absence of CM (Fig. 3.11B), whereas these proteins had no effect on the expression of NCU02474 (Fig. 3.13A). However, NCU02474 expression was found to be affected by CM. This suggests

separate factors for a response to CM. It is unknown whether or not the mechanism of regulation by these putative factors is influenced by the arrangement of the two genes and the AIM binding site.

4.9 RT-qPCR validation of genes identified by ChIP-seq

In the group of 65, 34 genes were examined by RT-qPCR in wild-type, Δ*aod-2,* and Δ*aod-5* cells, each grown in the presence and absence of CM, in an attempt to validate the ChIP-seq findings. In total, 16 of the genes examined showed some effects due to loss of either or both AOD2 and AOD5, while 18 genes showed no effects. As expected, *aod-1* was found to be controlled by AOD2 and AOD5, as the absence of either protein reduced basal *aod-1* transcript levels and severely reduced *aod-1* transcript levels in cells grown in the presence of CM (Fig. 3.11A). My data also suggested that other factors may be involved in the regulation of *aod-1* transcription, since some transcript was still detected in the *aod-2 aod-5* double mutant cells (DX13) and a slight increase in the presence of CM was seen (Fig. 3.16A). Future work could be aimed at identifying these factors.

As mentioned above, in addition to *aod-1*, AOD2 is involved in the regulation of PEPCK expression. PEPCK is a critical enzyme in gluconeogenesis. It catalyzes the conversion of oxaloacetate to phosphoenolpyruvate (PEP). I found that when wild-type cells were grown in the presence of CM in sucrose-containing media, the transcript levels of PEPCK were increased about seven-fold (Fig. 3.11A). Consistent with my finding, it was reported that the transcript levels of PEPCK were increased (about seven-fold) in a wild-type *P. anserina* strain when grown in the presence of antimycin A (Bovier *et al.* 2014). The opposite result was seen in an older study in *S. cerevisiae* which showed that 24 hr after addition of CM or antimycin A to

cultures grown in the glucose-containing medium, cells exhibited 13 times lower and no PEPCK activity, respectively, when compared to cells grown without inhibitors (Wilson & Bhattacharjee 1986). On the other hand, the PEPCK activity was about two times higher in cells after 30 hr growth in ethanol when compared to cells grown in glucose medium. In *A. nidulans*, growth in the presence of CM on glucose medium induced expression of the PEPCK encoding gene, acuF, fused to a LacZ reporter gene (Suzuki *et al.* 2012). However, it should be noted that the cells used in this experiment had a malate dehydrogenase deletion background (Δmdhc) where malate, a suspected inducer for acuM and acuK, should accumulate.

Several observations in *A. nidulans* have led to the suggestion that malate is an inducer recognized by acuM and acuK. For example, induction of the PEPCK gene on poor carbon sources is dependent on acuM and acuK (Hynes *et al.* 2007). Induction of PEPCK was slightly higher in a Δmdhc strain (which is predicted to accumulate cytosolic malate) grown in acetate when compared to wild-type cells (Suzuki *et al.* 2012). Furthermore, the Δmdhc strain grown in the presence of malate exhibited a several fold induction of the PEPCK gene when compared to the growth in glucose (Suzuki *et al.* 2012). However, even if malate were the inducing molecule for PEPCK, it might not be for AOX. Malate does not accumulate in *P. anserina* when cells are grown in the presence of antimycin A (Bovier *et al.* 2014). Thus, it remains unclear how PEPCK and AOX respond to mitochondrial impairment and poor carbon sources. The difference in magnitude of response of the two genes under different conditions strongly suggests differential interpretation of non-identical signals (as discussed in section 4.3.

FBP is another important gluconeogenic enzyme that was shown to be controlled by the AOD2 and AOD5 orthologues in *A. nidulans* and *P. anserina*, and

by the AOD2 orthologue in *S. cerevisiae* (Hynes *et al.* 2007; Sellem *et al.* 2009; Soontorngun *et al.* 2007). In contrast, my RT-qPCR data indicated that neither AOD2 nor AOD5 are involved in the transcriptional regulation of FBP in *N. crassa* (Supplementary Fig. 3.9). FBP was not among the group of 65 from the ChIP-seq data. Inspection of the upstream region of the FBP gene revealed binding of small amounts of AOD2 and AOD5 when compared to the amount bound at *aod-1* (Supplementary Fig. 3.10). When FBP was induced during growth of cells on poor carbon sources, AOD2 was not required for the induction (Fig. 3.6D). This finding is unexpected since *N. crassa* and *P. anserina* are closely phylogenetically related. In *S. cerevisiae*, it has been reported that Cat8p, a Zn(II)Cys6 transcription factor, regulates the expression of FBP (Haurie *et al.* 2001). It has been shown that Sip4p binds to the CSRE in FBP's promoter as does Cat8p (Vincent & Carlson 1998). Furthermore, Rds2p also recognizes this CSRE and the binding of Rds2p to the promoter of FBP is dependent on Cat8p and Snf1p (Soontorngun *et al.* 2007). However, Cat8p and Sip4p do not appear to have orthologues in *N. crassa*, as BLASTing their protein sequences in the *N. crassa* genome database returns no similar genes. It seems likely that other factors are involved in the transcriptional regulation of FBP in *N. crassa*.

As shown in Fig. 3.11, the expression of several genes (including *aod-1* and PEPCK) is positively regulated by AOD2 and AOD5. I will describe these genes in order of their NCU numbers below. Cytochrome *c* (NCU01808) is a component of the sETC and it is upregulated in the presence of CM. The level of induction in cells lacking AOD2 or AOD5 is less than half the level in wild-type cells grown in CM (Fig. 3.11A). The cytochrome *c* protein has long been known to be elevated in mitochondria from *N. crassa* cultures grown in the presence of sETC inhibitors (Descheneau *et al.* 2005). Elevated cytochrome *c* protein was also observed in some

N. crassa mutants that had reduced cytochrome aa_3 or *b* levels (Bertrand *et al.* 1977). The regulation of cytochrome *c* has been well studied in other systems. In yeast, there are two isoforms of cytochrome *c* encoded by two genes CYC1 and CYC7. CYC1 is expressed under normoxic conditions whereas CYC7 is induced under hypoxic conditions. The upstream region of CYC1 contains two UASs which are bound by HAP1 and the HAP2/3/4/5 complex to activate the transcription of the gene (Sherman 2005). CYC7, on the other hand, is induced under hypoxia, in which heme levels are reduced and HAP1 is repressed (Zhang & Hach 1999). The low activity of HAP1 results in low expression of ROX1, which is a transcriptional repressor of CYC7 (Lowry & Zitomer 1988). Interestingly, a recent study showed that under normoxic conditions, H_2O_2 was able to target ROX1 and removed it from the CYC7 promoter, thus inducing CYC7 (Liu & Barrientos 2013). In mammals, the expression of cytochrome *c* is regulated by NRF-1 (nuclear respiratory factor 1) (Evans & Scarpulla 1990) and the cAMP response element binding protein (CREB) (Gopalakrishnan & Scarpulla 1994; Herzig *et al.* 2000). It is noteworthy that NRF-1 is a target of PGC-1α, which is a key regulator that governs mitochondrial biogenesis (Scarpulla 2011).

My RT-qPCR data revealed that the transcript for NCU03408 was induced when cells were grown in the presence of CM (Fig. 3.11A). The transcription of the gene was dependent on AOD2 and AOD5 since it was reduced in Δ*aod-2* and Δ*aod-5* cells grown in the presence (about six-fold) and absence (about three-fold) of CM (Fig. 3.11A). NCU03408 belongs to an α/β hydrolase fold superfamily, which contains members such as esterases and lipases, that have been implicated in lipid metabolism and lipid signal transduction in mammals (Lord *et al.* 2013). However, some subfamilies have diverged functions because the interactions with their binding

partners confer novel functions upon them (Lord *et al.* 2013). The canonical structure of α/β hydrolase fold proteins includes eight β strand sheets and five α helices (Marchot & Chatonnet 2012). The exact function of NCU03408 and why it is induced in the presence of CM is not known. The orthologue in *P. anserina* (Pa_6_4030) was also identified in microarray data where it showed reduced transcript levels in the Δ*rse2*, Δ*rse3*, and Δ*rse2*Δ*rse3* backgrounds (Bovier *et al.* 2014). Consistent with my observation, Pa_6_4030 was also found to be induced when cells were grown in antimycin A (Bovier *et al.* 2014), indicating that the regulation of this gene responds to mitochondrial dysfunctions. Pa_6_4030 was also found to be induced when cells were grown in acetate (Bovier *et al.* 2014). It should also be noted that although NCU03408 was found in the group of 65, it is also within the group associated with the 310 bp repeat (section 3.3.6).

5-oxoprolinase (NCU04569) is an important enzyme involved in the γ-glutamyl cycle (Fig. 4.3) and deficiency of this enzyme may lead to 5-oxoprolinuria in humans (Calpena *et al.* 2013). An important intermediate in the cycle is GSH which is a well-known thiol involved in many cellular redox reactions. The primary role of GSH is as an antioxidant to convert hydrogen peroxide to water while becoming oxidized to GSSG (oxidized form of GSH) (Ribas *et al.* 2014). GSSG can be reduced back to GSH by the GSSG reductase, a process that requires the presence of NADPH. GSSG can reversibly modify some proteins by S-glutathionylation, in which a thiol-disulfide exchange reaction occurs between GSSG and a thiol group of proteins, to activate or inactivate proteins (Dalle-Donne *et al.* 2009; Lu 2013). GSH is also involved in detoxification of xenobiotics and storage of cysteine in the cell (see reviews Lu (2009), Lu (2013), and Liu *et al.* (2014)).

In this study, I have shown that 5-oxoprolinase is induced by CM in *N.*

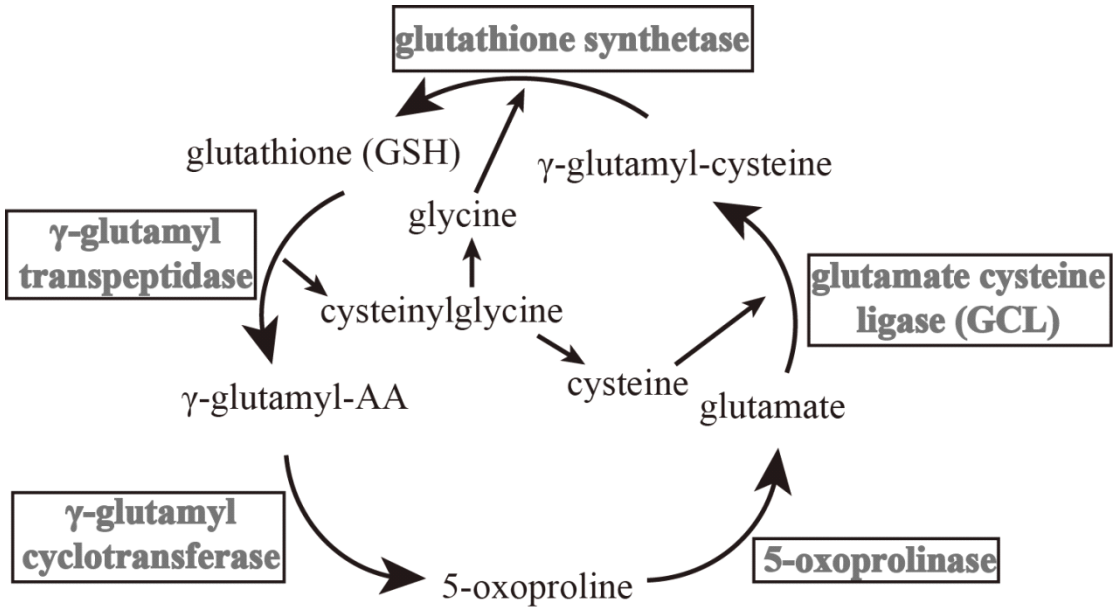

Figure 4.3. Schematic of the γ-glutamyl cycle. Enzymes are highlighted in black boxes. 5-oxoprolinase catalyzes the conversion of 5-oxoproline to glutamate. The figure was adapted from Almaghlouth *et al.* (2012). AA, amino acids.

crassa (Fig. 3.11A). This enzyme interconverts 5-oxoproline and glutamate (Fig. 4.3). In *S. cerevisiae*, overexpression of the 5-oxoprolinase encoding gene in a glutamate auxotrophic strain enabled cells to grow on medium containing 5-oxoproline as a sole nitrogen source, but normal expression of the gene resulted in virtually no growth on this medium (Kumar & Bachhawat 2010). It would be interesting to know if the induction of 5-oxoprolinase in *N. crassa* by growth in the presence of CM results in increased production of glutamate and/or GSH in cells.

In the γ-glutamyl cycle, the rate-limiting step for the synthesis of GSH is the conversion of glutamate and cysteine to γ-glutamyl-cysteine by glutamate cysteine ligase (GCL). GCL has a catalytic subunit and a modifier subunit (Lu 2013). These proteins correspond to NCU01157 and NCU04596, respectively, in *N. crassa*. Interestingly, both genes were found in the AOD5 +CM group of my ChIP-seq data at 4.2- and 4.9-fold enrichment. Peaks were also associated with NCU01157 in the AOD2 –CM and +CM experiments, but the fold-enrichment was slightly below the arbitrary cutoff of four at 3.4 and 3.6, respectively. It is not known whether the expression of the GCL encoding genes is increased under oxidative stress in *N. crassa* or whether they are regulated by AOD2 and/or AOD5.

AOD2 and AOD5 were also shown to control NCU06382 (ABC transporter). A BLAST search of the protein sequence against the *S. cerevisiae* genome database (SGD), revealed greatest similarity to the Ybt1p (previous named Bat1p (bile acid transporter 1), E value = 2.3e-147) (Fig. 4.4). Ybt1p belongs to the class C ABC (ABCC) transporters (Sasser & Fratti 2014) and has been shown to be required for importing bile acids into *S. cerevisiae* isolated vacuolar fractions in an ATP-dependent manner (Ortiz *et al.* 1997). It has also been suggested to play a role in the modulation of phospholipid homeostasis in the vacuolar membrane

Figure 4.4. Alignment of human ABCC1, *S. cerevisiae* Ybt1p, and *N. crassa* NCU06382 protein sequences. The protein sequence of human ABCC1 was retrieved from the UniProt database, Ybt1p from the SGD, and NCU06382 from the FungiDB database. Alignment was performed using the Clustal Omega program (Sievers *et al.* 2011). Asterisks, colons, or periods at the bottom of the alignment indicate fully, highly, or weakly conserved amino acids, respectively, based on the calculations in the Clustal Omega program. Amino acids with one of the three marks are also shown in grey. Red and blue bars on the top indicate the sequences of transmembrane helices and cytoplasmic nucleotide-binding domains of the human ABCC1 protein, respectively. The sequences of these domains were obtained from the UniProt database.

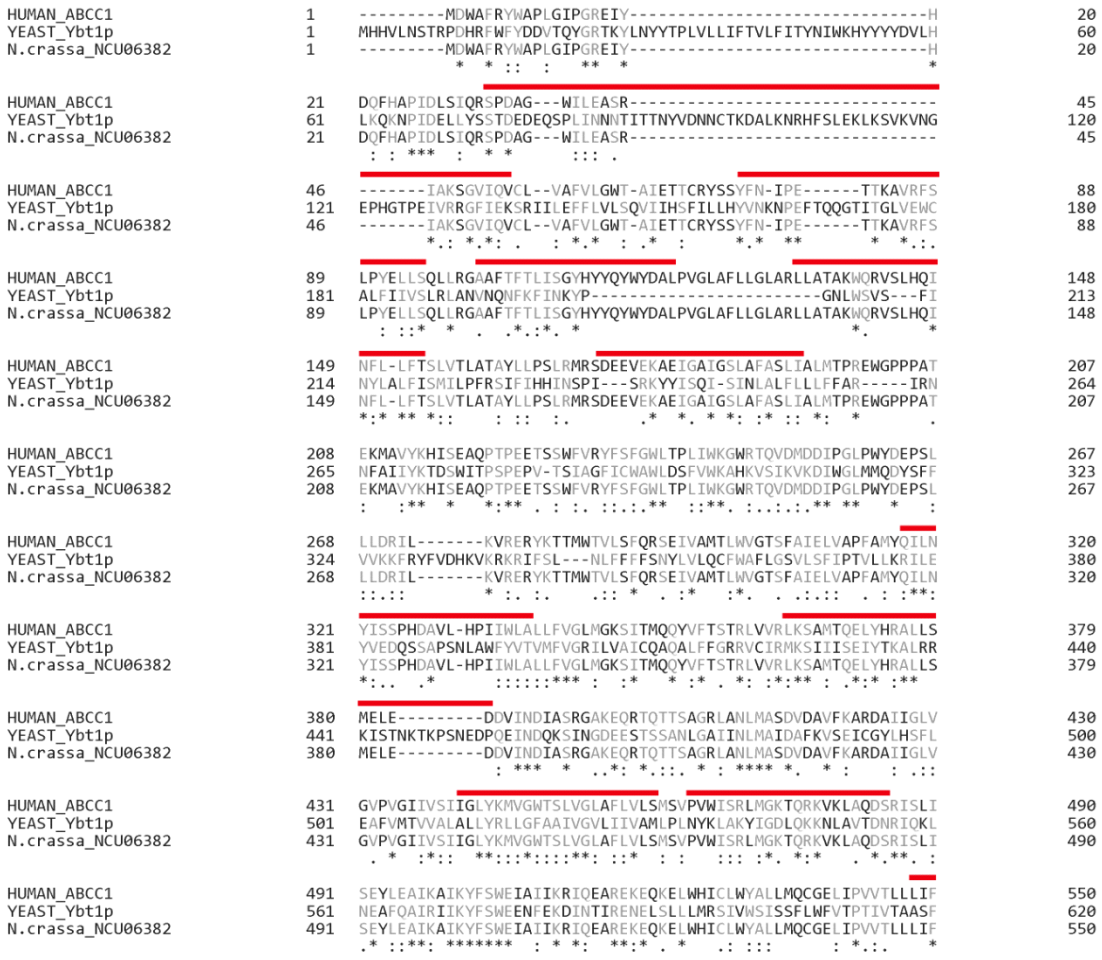

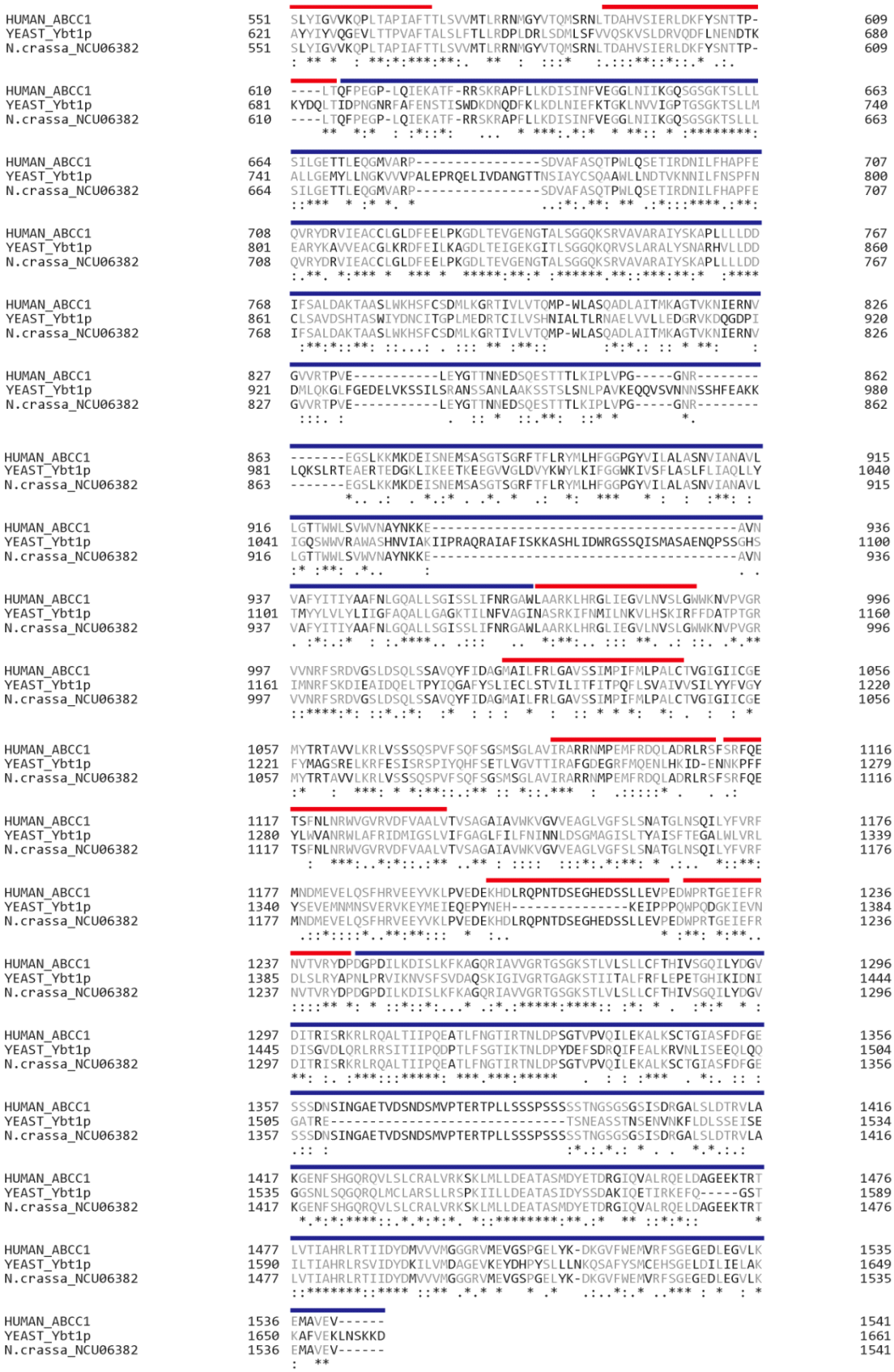
HUMAN_ABCC1 551 SLYIGVVKQPLTAPIAFTTLSVVMTLRRNMGYVTQMSRNLTDAHVSIERLDKFYSNTTP- 609
YEAST_Ybt1p 621 AYYIYVQGEVLTTPVAFTALSLFTLLRDPLDRLSDMLSFVVQSKVSLDRVQDFLNENDTK 680
N.crassa_NCU06382 551 SLYIGVVKQPLTAPIAFTTLSVVMTLRRNMGYVTQMSRNLTDAHVSIERLDKFYSNTTP- 609
HUMAN_ABCC1 610 ----LTQFPEGP-LQIEKATF-RRSKRAPFLLKDISINFVEGGLNIIKGQSGSGKTSLLL 663
YEAST_Ybt1p 681 KYDQLTIDPNGNRFAFENSTISWDKDNQDFKLKDLNIEFKTGKLNVVIGPTGSGKTSLLM 740
N.crassa_NCU06382 610 ----LTQFPEGP-LQIEKATF-RRSKRAPFLLKDISINFVEGGLNIIKGQSGSGKTSLLL 663
HUMAN_ABCC1 664 SILGETTLEQGMVARP----------SDVAFASQTPWLQSETIRDNILFHAPFE 707
YEAST_Ybt1p 741 ALLGEMYLLNGKVVVPALEPRQELIVDANGTTNSIAYCSQAAWLLNDTVKNNILFNSPFN 800
N.crassa_NCU06382 664 SILGETTLEQGMVARP----------SDVAFASQTPWLQSETIRDNILFHAPFE 707
HUMAN_ABCC1 708 QVRYDRVIEACCLGLDFEELPKGDLTEVGENGTALSGGQKSRVAVARAIYSKAPLLLLDD 767
YEAST_Ybt1p 801 EARYKAVVEACGLKRDFEILKAGDLTEIGEKGITLSGGQKQRVSLARALYSNARHVLLDD 860
N.crassa_NCU06382 708 QVRYDRVIEACCLGLDFEELPKGDLTEVGENGTALSGGQKSRVAVARAIYSKAPLLLLDD 767
HUMAN_ABCC1 768 IFSALDAKTAASLWKHSFCSDMLKGRTIVLVTQMP-WLASQADLAITMKAGTVKNIERNV 826
YEAST_Ybt1p 861 CLSAVDSHTASWIYDNCITGPLMEDRTCILVSHNIALTLRNAELVVLLEDGRVKDQGDPI 920
N.crassa_NCU06382 768 IFSALDAKTAASLWKHSFCSDMLKGRTIVLVTQMP-WLASQADLAITMKAGTVKNIERNV 826
HUMAN_ABCC1 827 GVVRTPVE-----------LEYGTTNNEDSQESTTTLKIPLVPG-----GNR-------- 862
YEAST_Ybt1p 921 DMLQKGLFGEDELVKSSILSRANSSANLAAKSSTSLSNLPAVKEQQVSVNNNSSHFEAKK 980
N.crassa_NCU06382 827 GVVRTPVE-----------LEYGTTNNEDSQESTTTLKIPLVPG-----GNR-------- 862
HUMAN_ABCC1 863 -------EGSLKKMKDEISNEMSASGTSGRFTFLRYMLHFGGPGYVILALASNVIANAVL 915
YEAST_Ybt1p 981 LQKSLRTEAERTEDGKLIKEETKEEGVVGLDVYKWYLKIFGGWKIVSFLASLFLIAQLLY 1040
N.crassa_NCU06382 863 -------EGSLKKMKDEISNEMSASGTSGRFTFLRYMLHFGGPGYVILALASNVIANAVL 915
HUMAN_ABCC1 916 LGTTWWLSVWVNAYNKKE---------------------------------------AVN 936
YEAST_Ybt1p 1041 IGQSWWVRAWASHNVIAKIIPRAQRAIAFISKKASHLIDWRGSSQISMASAENQPSSGHS 1100
N.crassa_NCU06382 916 LGTTWWLSVWVNAYNKKE---------------------------------------AVN 936
HUMAN_ABCC1 937 VAFYITIYAAFNLGQALLSGISSLIFNRGAWLAARKLHRGLIEGVLNVSLGWWKNVPVGR 996
YEAST_Ybt1p 1101 TMYYLVLYLIIGFAQALLGAGKTILNFVAGINASRKIFNMILNKVLHSKIRFFDATPTGR 1160
N.crassa_NCU06382 937 VAFYITIYAAFNLGQALLSGISSLIFNRGAWLAARKLHRGLIEGVLNVSLGWWKNVPVGR 996
HUMAN_ABCC1 997 VVNRFSRDVGSLDSQLSSAVQYFIDAGMAILFRLGAVSSIMPIFMLPALCTVGIGIICGE 1056
YEAST_Ybt1p 1161 IMNRFSKDIEAIDQELTPYIQGAFYSLIECLSTVILITFITPQFLSVAIVVSILYYFVGY 1220
N.crassa_NCU06382 997 VVNRFSRDVGSLDSQLSSAVQYFIDAGMAILFRLGAVSSIMPIFMLPALCTVGIGIICGE 1056
HUMAN_ABCC1 1057 MYTRTAVVLKRLVSSSQSPVFSQFSGSMSGLAVIRARRNMPEMFRDQLADRLRSFSRFQE 1116
YEAST_Ybt1p 1221 FYMAGSRELKRFESISRSPIYQHFSETLVGVTTIRAFGDEGRFMQENLHKID-ENNKPFF 1279
N.crassa_NCU06382 1057 MYTRTAVVLKRLVSSSQSPVFSQFSGSMSGLAVIRARRNMPEMFRDQLADRLRSFSRFQE 1116
HUMAN_ABCC1 1117 TSFNLNRWVGVRVDFVAALVTVSAGAIAVWKVGVVEAGLVGFSLSNATGLNSQILYFVRF 1176
YEAST_Ybt1p 1280 YLWVANRWLAFRIDMIGSLVIFGAGLFILFNINNLDSGMAGISLTYAISFTEGALWLVRL 1339
N.crassa_NCU06382 1117 TSFNLNRWVGVRVDFVAALVTVSAGAIAVWKVGVVEAGLVGFSLSNATGLNSQILYFVRF 1176
HUMAN_ABCC1 1177 MNDMEVELQSFHRVEEYVKLPVEDEKHDLRQPNTDSEGHEDSSLLEVPEDWPRTGEIEFR 1236
YEAST_Ybt1p 1340 YSEVEMNMNSVERVKEYMEIEQEPYNEH----------KEIPPPQWPQDGKIEVN 1384
N.crassa_NCU06382 1177 MNDMEVELQSFHRVEEYVKLPVEDEKHDLRQPNTDSEGHEDSSLLEVPEDWPRTGEIEFR 1236
HUMAN_ABCC1 1237 NVTVRYDPDGPDILKDISLKFKAGQRIAVVGRTGSGKSTLVLSLLCFTHIVSGQILYDGV 1296
YEAST_Ybt1p 1385 DLSLRYAPNLPRVIKNVSFSVDAQSKIGIVGRTGAGKSTIITALFRFLEPETGHIKIDNI 1444
N.crassa_NCU06382 1237 NVTVRYDPDGPDILKDISLKFKAGQRIAVVGRTGSGKSTLVLSLLCFTHIVSGQILYDGV 1296
HUMAN_ABCC1 1297 DITRISRKRLRQALTIIPQEATLFNGTIRTNLDPSGTVPVQILEKALKSCTGIASFDFGE 1356
YEAST_Ybt1p 1445 DISGVDLQRLRRSITIIPQDPTLFSGTIKTNLDPYDEFSDRQIFEALKRVNLISEEQLQQ 1504
N.crassa_NCU06382 1297 DITRISRKRLRQALTIIPQEATLFNGTIRTNLDPSGTVPVQILEKALKSCTGIASFDFGE 1356
HUMAN_ABCC1 1357 SSSDNSINGAETVDSNDSMVPTERTPLLSSSPSSSSTNGSGSGSISDRGALSLDTRVLA 1416
YEAST_Ybt1p 1505 GATRE-------------------------------TSNEASSTNSENVNKFLDLSSEISE 1534
N.crassa_NCU06382 1357 SSSDNSINGAETVDSNDSMVPTERTPLLSSSPSSSSTNGSGSGSISDRGALSLDTRVLA 1416
HUMAN_ABCC1 1417 KGENFSHGQRQVLSLCRALVRKSKLMLLDEATASMDYETDRGIQVALRQELDAGEEKTRT 1476
YEAST_Ybt1p 1535 GGSNLSQGQRQLMCLARSLLRSPKIILLDEATASIDYSSDAKIQETIRKEFQ-----GST 1589
N.crassa_NCU06382 1417 KGENFSHGQRQVLSLCRALVRKSKLMLLDEATASMDYETDRGIQVALRQELDAGEEKTRT 1476
HUMAN_ABCC1 1477 LVTIAHRLRTIIDYDMVVVMGGGRVMEVGSPGELYK-DKGVFWEMVRFSGEGEDLEGVLK 1535
YEAST_Ybt1p 1590 ILTIAHRLRSVIDYDKILVMDAGEVKEYDHPYSLLLNKQSAFYSMCEHSGELDILIELAK 1649
N.crassa_NCU06382 1477 LVTIAHRLRTIIDYDMVVVMGGGRVMEVGSPGELYK-DKGVFWEMVRFSGEGEDLEGVLK 1535
HUMAN_ABCC1 1536 EMAVEV------ 1541
YEAST_Ybt1p 1650 KAFVEKLNSKKD 1661
N.crassa_NCU06382 1536 EMAVEV------ 1541

(Gulshan & Moye-Rowley 2011), and to be involved in membrane fusion of vacuoles (Sasser *et al.* 2012). Interestingly, another member of the ABCC transporters, Ycf1p (yeast cadmium factor 1), which is also similar to NCU06382 (E value = 4.4e-110), has been shown to transport glutathione S-conjugates into vacuoles for detoxification purposes (Li *et al.* 1996). It also maintains the cytosolic GSSG concentration by importing excess GSSG into vacuoles when glutathione reductase, an enzyme that reduces GSSG in the cytosol, is absent (Morgan *et al.* 2013). In fact, it has been suggested that YCF1, YBT1, as well as BPT1 (bile pigment transporter 1), another member of the ABCC group, have overlapping functions in transporting glutathione S-conjugates (Paumi *et al.* 2009). However, neither these genes, nor other members in the ABCC were found in the ChIP-chip studies in *S. cerevisiae* that examined the genome-wide binding of Rds2p and Ert1p upon medium shift from glucose to ethanol (Gasmi *et al.* 2014; Soontorngun *et al.* 2007).

The ABCC transporters in yeast belong to the MRP/CFTR family (multidrug resistance-associated protein/cystic fibrosis transmembrane conductance regulator) in mammals (Paumi *et al.* 2009). This protein family contains nine MRPs that are composed of two cytoplasmic nucleotide-binding domains and various numbers of plasma membrane spanning domains (Chen & Tiwari 2011; Keppler 2011; Sodani *et al.* 2012). Some of the nine MRPs serve as an ATP-dependent efflux pump to export amphiphilic organic compounds in a glutathione-dependent manner. A BLAST search with NCU06352 against the *Homo sapiens* reference protein database showed that NCU06382 is most similar to MRP1 (also named ABCC1, E value = 2e-138) (Fig. 4.4). This protein has a broad range of substrates including glutathione and GSSG (Keppler 2011; Sodani *et al.* 2012). It also exports glutathione to the outside of the cell. This process is thought to be triggered by the presence of xenobiotics. However,

the binding affinity for the GSH is very low and the biological significance of efflux of GSH by MRP1 is not well understood (Cole 2014). However, the binding affinity for GSSG is high and it has been suggested that the export of GSSG by MRP1 can lower the levels of GSSG in the cell (Cole 2014). Nothing is known about the role of NCU06382 in *N. crassa*. It would be interesting to determine its subcellular localization and whether or not it is involved in a response to oxidative stress.

Another gene dependent on AOD2 and AOD5 for expression is NCU08674 (pentatricopeptide repeat protein) (Fig. 3.11A). Pentatricopeptide repeat proteins harbor 35-amino-acid repeats and these repeats can be present up to 30 times in tandem (Lightowlers & Chrzanowska-Lightowlers 2013; Schmitz-Linneweber & Small 2008). These proteins are typically found in land plants, but a few are present in fungi and humans. They appear to only localize to chloroplasts or mitochondria. The key molecular function of these proteins is in RNA metabolic processes such as RNA stabilization, RNA editing, or RNA cleavage (Barkan & Small 2014; Schmitz-Linneweber & Small 2008). A recent investigation revealed that the amount of Complexes I, III, and IV was greatly reduced in an *N. crassa* NCU08674 deletion mutant (Solotoff *et al.* 2015). It is possible that the absence of NCU08674 results in degradation of the mitochondrial encoded transcripts for proteins of these complexes in mitochondria. Conceivably, the induction of NCU08674 in the presence of CM observed in this study may enhance the stability of transcripts when the mitochondrial protein translation system is compromised. The expression of NCU08674 appears to be dependent on AOD2 and AOD5, supporting a role for AOD2 and AOD5 in regulation of energy homeostasis.

Four genes involved in malate metabolism were identified in the ChIP-seq analysis. Two were found in the group of 65 and two were in other groups examined.

Examination of expression by RT-qPCR showed that AOD2 and AOD5 may be required for maximal expression of two of these genes: NCU03651 (NADP-dependent malic enzyme) and NCU10007 (malate synthase). The expression of NCU03651 is reduced about three-fold in Δ*aod-2* and Δ*aod-5* cells grown in the absence of CM, and about seven-fold when grown in the presence of CM, whereas for NCU10007, the expression is reduced about four-fold in the absence of CM and 2.5-fold in the presence of CM (Fig. 3.11). For NCU04899 (malate dehydrogenase with a mitochondrial target signal), the differences in expression are only 1.6- to two-fold in Δ*aod-2* and Δ*aod-5* cells, respectively, when grown in the presence of CM as compared to wild-type cells (Fig. 3.15D), thus it is difficult to conclude with certainty that AOD2 and AOD5 are required for induction of NCU04899 under the conditions tested. Furthermore, AOD2 and AOD5 were not required for the expression of NCU06211 (cytosolic malate dehydrogenase) (Supplementary Fig. 3.9) under the condition tested. Malate has been suggested as the inducer of the AOD2 and AOD5 orthologues in *A. nidulans* (section 1.10.9) (Suzuki *et al.* 2012). However, an investigation of the *P. anserina* metabolome found that the level of malate was only increased 1.6-fold when cells were grown in the presence of antimycin A for 48 hr. It seems unlikely that a less than two-fold change in malate concentration could account for activation of the AOD2 and AOD5 orthologues, but the possibility cannot be eliminated. It is also possible that measurement of the level of malate after 48 hr does not reflect a possible greater early accumulation that results in induction.

There is considerable evidence that supports a close relationship between mitochondrial dysfunction and alterations in metabolism. For instance, inhibition of OXPHOS by oligomycin was found to enhance glycolysis and slow down the TCA cycle in human cells (Yadava *et al.* 2013). A Complex III deficiency in yeast was

shown to accelerate glycolysis as well as protein catabolism (Marin-Buera *et al.* 2014). Based on my FunCat analysis there is an enrichment for genes, whose promoter is bound by AOD2 and/or AOD5, that are involved in metabolism (section 3.3.5). Thus, AOD2 and/or AOD5 may be involved in adjusting general metabolism under specific conditions.

The orthologue of NCU10051 (flavohemoglobin) was reported to be downregulated in the Δ*rse2* and Δ*rse3* deletion strains (about three-fold) in *P. anserina* (Bovier *et al.* 2014). However, the expression of NCU10051 was shown to be only slightly affected by the loss of AOD2 or AOD5 when cells were grown in the presence of CM (Supplementary Fig. 3.11). Flavohemoglobin contains NO dioxygenase activity that catalyzes the conversion of NO to nitrate (Bonamore & Boffi 2008; Gardner 2012). In fungi, the source of NO is poorly understood, but it plays a role in fungal germination and development of sexual and asexual spores (Arasimowicz-Jelonek & Floryszak-Wieczorek 2014). NO can diffuse to mitochondria where it competes with oxygen for the binding of Complex IV and thus inhibits respiration (see review Figueira *et al.* (2013)). However, the binding is reversible and the NO concentration is regulated in order not to inhibit respiration completely under normal conditions (Taylor & Moncada 2010).

Peaks were found in the 5' upstream region of NCU10051 in the ChIP-seq experiments. However, the fold-enrichment was more than four-fold only in the AOD5 +CM experiment, while the others ranged from 2.1- to 3.5-fold. RT-qPCR data indicated that the transcript levels were slightly increased (1.9-fold) in the wild-type +CM, but the levels were even higher in the absence of AOD2 (3.5-fold) or AOD5 (3.9-fold) when compared to the wild-type –CM control (Supplementary Fig. 3.11). In *P. anserina*, a 250-fold increase in flavohemoglobin transcripts was observed when

wild-type cells were grown in the presence of antimycin A (Bovier *et al.* 2014). The increase was at least partially dependent on the AOD2 and AOD5 orthologues since only a 20-fold increase was seen in the Δ*rse2*Δ*rse3* mutant grown under the same conditions. Thus, the role of AOD2 and AOD5 appear to be opposite in the two organisms.

4.10 Genes affected by CM

My RT-qPCR data clearly showed that CM affects the expression of a number of genes (Fig. 3.11A and 3.13). Interestingly, all of these genes were associated with ChIP-seq peaks, but not all were found to be controlled by AOD2 and AOD5 under the conditions tested. CM affects mitochondrial protein translation by binding to the 16S rRNA and preventing peptidyl transferase from forming peptide bonds. In this study, several transcripts from nuclear genes encoding mitochondrial proteins were found to be induced by CM. Some are components of the ETC and OXPHOS systems, such as NCU01808 (cytochrome *c*), NCU02514 (ATPase subunit α), NCU07953 (*aod-1*), and NCU08947 (Complex III subunit 8). In addition, NCU02623, which was found in the group of 5- 5+, is a hypothetical protein containing a mitochondrial hypoxia responsive domain. This protein might also be considered an OXPHOS related protein because it has similarity to the Rcf2p (respiratory supercomplex factor 2, E value = 2.5e-8) of *S. cerevisiae*. Rcf2p and Rcf1p are members of the conserved hypoxia-induced gene 1 (HIG1) protein family. They have been shown to mediate the formation of the Complex III-Complex IV supercomplex by independent association with both complexes (Chen *et al.* 2012; Strogolova *et al.* 2012; Vukotic *et al.* 2012). Deletion of RCF1 has been shown to decrease the stability of respiratory complexes and elevate mitochondrial oxidative

stress (Chen *et al.* 2012). HIG2A, the mammalian homologue of RCF1, was also shown to organize respiratory complexes (Chen *et al.* 2012). It is conceivable that in the presence of CM, NCU02623 is induced in response to the lower levels of respiratory supercomplexes formed and/or to minimize ROS production.

In addition to components involved in OXPHOS, CM affects the expression of Tom5, a component of the TOM complex (Dietmeier *et al.* 1997). In agreement with this finding, a transcriptomic analysis of *Arabidopsis* cell cultures treated with rotenone has shown that some genes encoding components of the mitochondrial import machinery (such as Tom40, Tom7, and Tim23) were induced (Lister *et al.* 2004). Whether other components of the mitochondrial import machinery are induced by CM in *N. crassa* is not known. If the protein levels of nuclear-encoded OXPHOS components of the sETC were increased by growth of cells in CM, it is conceivable that increases in mitochondrial protein import might also be required. It has been suggested that impaired mitochondrial protein translation would lead to malfunction of the sETC and hence reduced membrane potential (Battersby & Richter 2013). Reduced membrane potential is known to inhibit the transport of presequence-containing proteins across the MIM (Harbauer *et al.* 2014). It is possible that the cell can sense the efficiency of mitochondrial protein import and induce genes encoding components of the mitochondrial import machinery. It would be of interest to investigate the rate of mitochondrial protein import in *N. crassa* upon CM treatment and whether the transcripts of other components of the mitochondrial import machinery are increased.

The NCU07678 (hypothetical protein), NCU08946 (hypothetical protein), and NCU11414 (plasma membrane zinc ion transporter) found in the group of 65 were also found to be induced in the presence of CM (Fig. 3.13A). Loss of AOD2 or

AOD5 did not affect their expression greatly. The function of NCU07678 is not known and it has no apparent orthologue in *S. cerevisiae*. NCU08946 is similar to PHB1 (E value = 2.1e-101) and PHB2 (E value = 9.6e-74) in *S. cerevisiae*. The products of PHB1 and PHB2 form the prohibitin complex that exists as a large ring structure in the MIM (Tatsuta *et al.* 2005). Prohibitin was originally identified as an inhibitor of cell proliferation when its transcript was microinjected into human fibroblasts (McClung *et al.* 1989). It has now been shown to be involved in multiple cell processes including mitochondrial dynamics and cristae formation (Artal-Sanz & Tavernarakis 2009). It also functions as a chaperone in the MIM to stabilize newly produced proteins in the OXPHOS system (Artal-Sanz & Tavernarakis 2009; Theiss & Sitaraman 2011). It has been shown that knockdown of prohibitin increased mitochondrial ROS levels in mice endothelial cells and this was due to reduced Complex I, but not Complex III activity (Schleicher *et al.* 2008). Similarly, knockdown of prohibitin increased human HK-2 cells (an immortalized proximal tubule epithelial cell line) sensitivity to H_2O_2, while overexpression prevented cells from undergoing H_2O_2-induced apoptosis (Ye *et al.* 2015). Therefore, it is conceivable that induction of NCU08946 can protect cells against possible oxidative stress caused by treatment of CM in *N. crassa*.

NCU11414 (plasma membrane zinc ion transporter) is similar to ZRT1 (zinc-regulated transporter 1, E value = 1.6e-46) and ZRT2 (E value = 7.5e-39) in *S. cerevisiae*. They are responsible for zinc ion uptake (Zhao & Eide 1996a, 1996b). ZRT1 is greatly induced and the activity of the protein is increased when the supply of zinc is limited, whereas the activity of Zrt2p does not seem to be controlled by the concentration of zinc (Zhao & Eide 1996a). The induction of NCU11414 by CM is not likely due to limitation of zinc ions, since the concentration of zinc is presumably

unchanged in the –CM and +CM media. It is not known whether mitochondrial dysfunctions caused by treatment of CM would affect the intracellular zinc pool or not.

4.11 Functional categories of AOD2 and AOD5

I have functionally categorized genes identified in the ChIP-seq data using FunCat. These genes mainly clustered in the metabolism and energy categories, suggesting that AOD2 and AOD5 might be involved in several important cell processes and might serve to coordinate metabolic process and energy production. In addition, 'biosynthesis of glutamate' and 'degradation of glycine' are categories that are overrepresented in the 98 genes that belong to the group of 65. The 5-oxoprolinase in the 'biosynthesis of glutamate' category, as well as the glycine dehydrogenase and glycine cleavage system H protein in the 'degradation of glycine' category, were examined by RT-qPCR in this study. Only the expression of 5-oxoprolinase and glycine dehydrogenase were shown to be regulated by AOD2 and AOD5 (Fig. 3.11). As discussed in section 1.8, mutants of the RTG pathway in *S. cerevisiae* are glutamate auxotrophs. Thus, at least in this context, there may be a relationship between the roles of AOD2 and AOD5 and those of the RTGs in yeast. Of the three yeast RTG proteins, only RTG2 has an orthologue in *N. crassa* (Chae & Nargang 2009). However, deletion of RTG2 in *N. crassa* does not affect the induction of AOX by growth in the presence of CM nor does it have an effect on growth under low nitrogen conditions (Chae & Nargang 2009), a finding that is inconsistent with the data in *S. cerevisiae*, where *rtg2* mutant cells are auxotrophic for glutamate (Liao & Butow 1993). Therefore, it is not likely that AOD2 and AOD5 regulate the biosynthesis of glutamate via a connection with RTG2 in *N. crassa*. It should be noted

that *aod-2* and *aod-5* mutants are not auxotrophic for glutamate. Furthermore, no reports have demonstrated the involvement of RDS2 and ERT1 (the *S. cerevisiae* AOD2 and AOD5 orthologues) in glutamate metabolism in *S. cerevisiae*.

As discussed in section 4.9, the synthesis of glutathione requires glutamate, cysteine, and glycine as well as two enzymes, GCL and glutathione synthetase (Fig. 4.3). It is therefore possible that effects on the metabolism of glutamate and glycine would ultimately lead to effects on glutathione synthesis. Three genes (NCU02475, NCU06424, and NCU08877) found in the group of 65 are overrepresented in the 'degradation of glycine' category. They encode three of the four enzymes involved in the glycine cleavage system (Kikuchi *et al.* 2008). This system functions together with serine hydroxymethyltransferase to reversibly convert glycine to serine in metazoans (Wang *et al.* 2013). The system is also known as glycine synthase when it runs in reverse to make glycine. Therefore, it is conceivable that when the cell requires more glutathione, the system utilizes serine for glycine synthesis to supply one of the substrates for production of glutathione (Wang *et al.* 2013).

4.12 The additional AOD2 binding motif

The 310 bp repeat unit containing the additional AOD2 binding motif occurs at 11 loci in the *N. crassa* genome. All but one of these is bound by AOD2 under the conditions of my ChIP-seq experiments (Table 3.4). It is conceivable that some factor such as chromatin structure might prevent AOD2 binding at the lone unbound site. For the ten loci that are bound by AOD2, one locus displays a ChIP-seq peak (NCU01957/NCU01958) that is not associated with any genes in the correct orientation relative to the peak (Fig. 3.19A). This suggests that AOD2 binding to this locus does not lead to transcriptional regulation of a gene. Various questions arise

regarding the binding motif. It would be of interest to know if AOD2 binds to the motif by itself or if it requires other partners for the binding. It is of note that some of the binding sites are also associated with small amounts of AOD5 (see below).

RT-qPCR data was obtained for eight of the 14 genes associated with the repeated region peaks in the correct orientation. Three of the genes showed no dependence on AOD2 or AOD5 and no effect due to growth in CM. Only the expression of NCU02128 was found to be dependent on AOD2 and not AOD5. Its transcript levels were reduced more than two-fold in the Δ*aod-2* cells grown in the absence of CM (Fig. 3.15C). The expression of NCU03408 was affected by both AOD2 and AOD5. The transcript levels were reduced three-fold in the Δ*aod-2* and Δ*aod-5* cells grown in the absence of CM, and six-fold in the presence of CM (Fig. 3.11A). Unexpectedly, the transcription of NCU04392 and NCU09144 did not appear to be affected by AOD2 but were affected by AOD5, as their expression in the Δ*aod-5* cells grown in the absence of CM was increased greater than two-fold (Fig. 3.15B). The ChIP-seq data do show that some of these regions were also bound by small amounts of AOD5, such as the regions between NCU01321/NCU01322, NCU03408/NCU03409, NCU04986/NCU11067, NCU05202/NCU05203, and NCU09144. It is not clear what the role of weak binding of AOD5 in these regions is. My RT-qPCR data showed that AOD5 is only involved in the regulation of the expression of NCU03408 and NCU09144. The expression of NCU01321, NCU01322, NCU04986, and NCU11067 has not been examined. The regions between NCU03408/NCU03409 and NCU05202/NCU05203 were also found to have AIM sequences, but only the two AIM sequences in the NCU03408/NCU03409 region aligned with the AOD5 peak summit and these did not align with the double AOD2 summits. The AIM sequences are located about 270 bp from the repeat region

of the AOD2 binding motif. Therefore, it is not known whether the AOD5 binding at the region is biologically significant or whether AOD2 and AOD5 form a heterodimer at the region.

4.13 Perspective

This study has increased our understanding of how AOD2 and AOD5 behave *in vivo*. It has been shown that the two proteins are involved in the regulation of many more genes than simply *aod-1*. They appear to be involved in various aspects of energy production and metabolism. Good evidence has also been obtained that the proteins can respond differently to different signals. The latter may require additional proteins such as other transcription factors. This study has also revealed an additional AOD2 binding site unexpectedly associated with a region that is repeated in the genome. Unfortunately, the significance of this is not apparent.

Major questions that persist are the nature of the signal(s) produced in compromised mitochondria and how this signal(s) acts to induce AOX and the other genes controlled by AOD2 and AOD5. The best approach towards exploring the signaling pathway might be to find out how AOD2 and AOD5 are activated when cells are grown in the presence of CM. It is not yet known whether AOD2 and AOD5 are activated by covalent post-translational modifications such as phosphorylation, or by binding of other proteins or small molecules. My phos-tag SDS-PAGE data is preliminary and conflicting and more work is required to elucidate the phosphorylation status of AOD2 and AOD5 under AOX inducing and non-inducing conditions. For instance, Western blots using antibodies against phosphoserine/threonine/tyrosine could be performed to detect changes in phosphorylation status of purified AOD2 and/or AOD5 in the presence and absence of

CM. To find out whether AOD2 and AOD5 are bound by other proteins, a pull-down experiment is needed to IP AOD2 and AOD5 as well as any possible binding partners so that they could be identified by mass spectrometry. Such experiments could be done under different conditions, such as growth in the presence of CM or in poor carbon sources, to determine if the binding partners change. The challenge for this type of experiment would be the yield of immunoprecipitated AOD2 or AOD5 since their abundance seems to be low.

As discussed in section 4.11, genes for the synthesis of glutamate and glycine were identified in the group of 65 of the ChIP-seq study. The use of these two amino acids in the biosynthesis of glutathione may point to an involvement of ROS as possible signaling molecules for activation of AOD2 and/or AOD5, since glutathione is used in defence against ROS (Ribas *et al.* 2014). However, there is no direct evidence supporting this possibility for *N. crassa*.

In this study, I did not test the hypothesis of whether malate is the activator of AOD2 and AOD5, as proposed by Suzuki *et al.* (2012). They deleted the cytosolic isoform of malate dehydrogenase in *A. nidulans* and assumed that cytosolic malate accumulated in the deletion strain. They found that the expression of PEPCK was greatly increased in the deletion strain when cells were grown in poor carbon sources. I have done initial work attempting to knock out the NCU06211 gene in an *N. crassa* strain, which encodes the cytosolic isoform of malate dehydrogenase. Future work would include confirmation of the deletion strain and determination of whether AOX is induced when NCU06211 is deleted under normal growth conditions. It should also be noted that although not identified in the FunCat analysis, two genes associated with malate metabolism were included in the group of 65 peak sets (NCU03651, malic enzyme and NCU10007, malate synthase) and two others (NCU04899, mitochondrial

malate dehydrogenase and NCU06211, cytosolic malate dehydrogenase) appeared among the group with robust peak sets that did not fall within the group of 65. NCU03651, and NCU10007 showed no response to CM, but AOD2 and AOD5 were required for their expression both with and without CM in the growth medium. On the other hand, NCU04899 showed a response to CM which required the presence of AOD2 and AOD5. Thus, it is conceivable that malate might somehow be involved in the system.

Of all the genes that were found in the various ChIP-seq data sets, only 53 genes were further investigated using RT-qPCR. It would be of interest to know whether the expression of the remaining genes is regulated by AOD2 and/or AOD5. Furthermore, because I only measured the transcription of the 53 genes when cells were grown in the presence and absence of CM, it would be of interest to determine whether the expression of the 53 genes is altered when cells are grown in different carbon sources or different inhibitors of the OXPHOS system and whether any alterations are dependent on AOD2 and/or AOD5. The best way to achieve this would be through RNA-seq experiments that could be compared to the ChIP-seq data. Adrien Beau Desaulniers and I have isolated total RNAs from wild-type cultures grown in the presence and absence of CM and RNA-seq was performed once by Delta Genomics. However, more biological replicates are needed to obtain reliable data for future analysis.

For the 310 bp repeat sequences, it would be of interest to determine whether the sequences are bona fide AOD2 binding sites or not. To address the question, EMSA could be done using DNA fragments that contain one of the 14 bp highly conserved regions (Fig. 3.18). These regions align with the bimodal summits of the ChIP-seq peaks. If binding was observed, the effect of mutations in the 14 bp

sequence and the surrounding sequence could be investigated. Furthermore, because some of the repeat sequences are associated with variable amounts of AOD5 binding, it would be of interest to know whether AOD2 and AOD5 act as a heterodimer at these sequences or if AOD2 can bind on its own. Six genes that are in correct orientation relative to the ChIP-seq peak sets surrounding the repeat sequences were not examined by RT-qPCR for expression. Information on their expression would be helpful to obtain a comprehensive understanding of the role that AOD2 and/or AOD5 play in these regions.

4.14 Summary

This study revealed that AOD2 and AOD5, two Zn(II)Cys6 transcription factors of *N. crassa*, constitutively localize to the nucleus under both AOX inducing and non-inducing conditions. They form a heterodimer *in vivo* and synergistically bind to the 5' upstream region of a number of genes such as NCU07953 (*aod-1*) and NCU09873 (PEPCK) under AOX inducing and non-inducing conditions. It appears that AOD2 and AOD5 bind to the AIM sequences but exceptions were also seen. Of the genes that are bound by AOD2 and AOD5, a high proportion of them are involved either in amino acid metabolism or in energy production, suggesting a regulatory role of AOD2 and AOD5 in these cell functions. For the genes that bound AOD2 and AOD5 in their 5' upstream regions, I was able to show that the transcription of some was regulated by AOD2 and AOD5 under both AOX inducing and non-inducing conditions. In addition, I also confirmed that similar to their orthologues in some other fungi species, AOD2 and AOD5 are involved in gluconeogenesis. The exact mechanism by which AOD2 and AOD5 regulate different cell functions is unknown. This study has shown that they are able to function differently in response to different

conditions and may coordinate with other transcription factors to achieve different regulatory effects.

The origin of the 310 bp repeat regions and the relevance of AOD2 binding within them, are not apparent. BLAST searches of other Neurospora species (data not shown) available at fungiDB (http://fungidb.org/fungidb/) revealed that *N. tetrasperma* contained four sequences with high identity to the entire 310 bp region. *N. discreta* had no sites related to the entire 310 bp sequence but did have two smaller sites with high similarity to portions of the inverted repeat region. This suggests that the sequence may have originated in an ancestral species, but is only being maintained in *N. crassa*. A consensus sequence was identified at the summit of the AOD2 binding sites, but further work is required to determine if it is actually a binding site for the protein.

References

Abrahams, J. P., Leslie, A. G., Lutter, R., & Walker, J. E. (1994). Structure at 2.8 A resolution of F1-ATPase from bovine heart mitochondria. *Nature,* **370** (6491): 621-628.

Acin-Perez, R., & Enriquez, J. A. (2014). The function of the respiratory supercomplexes: the plasticity model. *Biochim. Biophys. Acta.,* **1837** (4): 444-450.

Akhter, S., McDade, H. C., Gorlach, J. M., Heinrich, G., Cox, G. M., & Perfect, J. R. (2003). Role of Alternative oxidase gene in pathogenesis of *Cryptococcus neoformans*. *Infect. Immun.,* **71** (10): 5794-5802.

Akram, M. (2014). Citric acid cycle and role of its intermediates in metabolism. *Cell Biochem. Biophys.,* **68** (3): 475-478.

Albury, M. S., Affourtit, C., Crichton, P. G., & Moore, A. L. (2002). Structure of the plant alternative oxidase. Site-directed mutagenesis provides new information on the active site and membrane topology. *J. Biol. Chem.,* **277** (2): 1190-1194.

Albury, M. S., Elliott, C., & Moore, A. L. (2009). Towards a structural elucidation of the alternative oxidase in plants. *Physiol. Plant,* **137** (4): 316-327.

Aldridge, J. E., Horibe, T., & Hoogenraad, N. J. (2007). Discovery of genes activated by the mitochondrial unfolded protein response (mtUPR) and cognate promoter elements. *PloS One,* **2** (9): e874.

Alkhaja, A. K., Jans, D. C., Nikolov, M., Vukotic, M., Lytovchenko, O., Ludewig, F., Schliebs, W., Riedel, D., Urlaub, H., Jakobs, S., & Deckers, M. (2012). MINOS1 is a conserved component of mitofilin complexes and required for mitochondrial function and cristae organization. *Mol. Biol. Cell,* **23** (2): 247-257.

Almaghlouth, I. A., Mohamed, J. Y., Al-Amoudi, M., Al-Ahaidib, L., Al-Odaib, A., & Alkuraya, F. S. (2012). 5-Oxoprolinase deficiency: report of the first human OPLAH mutation. *Clin. Genet.,* **82** (2): 193-196.

Althoff, T., Mills, D. J., Popot, J. L., & Kuhlbrandt, W. (2011). Arrangement of electron transport chain components in bovine mitochondrial supercomplex I1III2IV1. *EMBO J.,* **30** (22): 4652-4664.

Amirsadeghi, S., Robson, C. A., McDonald, A. E., & Vanlerberghe, G. C. (2006). Changes in plant mitochondrial electron transport alter cellular levels of reactive oxygen species and susceptibility to cell death signaling molecules. *Plant Cell Physiol.,* **47** (11): 1509-1519.

Anderson, S., Bankier, A. T., Barrell, B. G., de Bruijn, M. H., Coulson, A. R., Drouin, J., Eperon, I. C., Nierlich, D. P., Roe, B. A., Sanger, F., Schreier, P. H., Smith, A. J., Staden, R., & Young, I. G. (1981). Sequence and organization of the human mitochondrial genome. *Nature,* **290** (5806): 457-465.

Andersson, M. E., & Nordlund, P. (1999). A revised model of the active site of alternative oxidase. *FEBS Lett.,* **449** (1): 17-22.

Anton, F., Fres, J. M., Schauss, A., Pinson, B., Praefcke, G. J., Langer, T., & Escobar-Henriques, M. (2011). Ugo1 and Mdm30 act sequentially during Fzo1-mediated mitochondrial outer membrane fusion. *J. Cell Sci.,* **124** (Pt 7): 1126-1135.

Aramayo, R., & Selker, E. U. (2013). *Neurospora crassa*, a model system for epigenetics research. *Cold Spring Harb. Perspect. Biol.,* **5** (10): a017921.

Arasimowicz-Jelonek, M., & Floryszak-Wieczorek, J. (2014). Nitric oxide: an effective weapon of the plant or the pathogen? *Mol. Plant Pathol.,* **15** (4): 406-416.

Archibald, J. M. (2015). Endosymbiosis and eukaryotic cell evolution. *Curr. Biol.,* **25** (19): R911-921.

Arnold, I., Pfeiffer, K., Neupert, W., Stuart, R. A., & Schagger, H. (1998). Yeast mitochondrial F1F0-ATP synthase exists as a dimer: identification of three dimer-specific subunits. *EMBO J.,* **17** (24): 7170-7178.

Artal-Sanz, M., & Tavernarakis, N. (2009). Prohibitin and mitochondrial biology. *Trends Endocrinol. Metab.,* **20** (8): 394-401.

Atteia, A., van Lis, R., van Hellemond, J. J., Tielens, A. G., Martin, W., & Henze, K. (2004). Identification of prokaryotic homologues indicates an endosymbiotic origin for the alternative oxidases of mitochondria (AOX) and chloroplasts (PTOX). *Gene,* **330**: 143-148.

Baker, B. M., Nargund, A. M., Sun, T., & Haynes, C. M. (2012). Protective coupling of mitochondrial function and protein synthesis via the eIF2alpha kinase GCN-2. *PLoS Genet.,* **8** (6): e1002760.

Barkan, A., & Small, I. (2014). Pentatricopeptide repeat proteins in plants. *Annu. Rev. Plant Biol.,* **65**: 415-442.

Barros, M. H., Bandy, B., Tahara, E. B., & Kowaltowski, A. J. (2004). Higher respiratory activity decreases mitochondrial reactive oxygen release and increases life span in *Saccharomyces cerevisiae*. *J. Biol. Chem.,* **279** (48): 49883-49888.

Battersby, B. J., & Richter, U. (2013). Why translation counts for mitochondria - retrograde signalling links mitochondrial protein synthesis to mitochondrial biogenesis and cell proliferation. *J. Cell Sci.,* **126** (Pt 19): 4331-4338.

Becker, T., Bottinger, L., & Pfanner, N. (2012). Mitochondrial protein import: from transport pathways to an integrated network. *Trends Biochem. Sci.,* **37** (3): 85-91.

Becker, T., Pfannschmidt, S., Guiard, B., Stojanovski, D., Milenkovic, D., Kutik, S., Pfanner, N., Meisinger, C., & Wiedemann, N. (2008). Biogenesis of the mitochondrial TOM complex: Mim1 promotes insertion and assembly of signal-anchored receptors. *J. Biol. Chem.,* **283** (1): 120-127.

Becker, T., Wenz, L. S., Kruger, V., Lehmann, W., Muller, J. M., Goroncy, L., Zufall, N., Lithgow, T., Guiard, B., Chacinska, A., Wagner, R., Meisinger, C., & Pfanner, N. (2011). The mitochondrial import protein Mim1 promotes biogenesis of multispanning outer membrane proteins. *J. Cell. Biol.,* **194** (3): 387-395.

Bellizzi, J. J., 3rd, Sorger, P. K., & Harrison, S. C. (2007). Crystal structure of the yeast inner kinetochore subunit Cep3p. *Structure,* **15** (11): 1422-1430.

Benedetti, C., Haynes, C. M., Yang, Y., Harding, H. P., & Ron, D. (2006). Ubiquitin-like protein 5 positively regulates chaperone gene expression in the mitochondrial unfolded protein response. *Genetics,* **174** (1): 229-239.

Bennett, C. F., Vander Wende, H., Simko, M., Klum, S., Barfield, S., Choi, H., Pineda, V. V., & Kaeberlein, M. (2014). Activation of the mitochondrial unfolded protein response does not predict longevity in *Caenorhabditis elegans*. *Nat. Commun.,* **5**: 3483.

Berry, E. A., Huang, L. S., Lee, D. W., Daldal, F., Nagai, K., & Minagawa, N. (2010). Ascochlorin is a novel, specific inhibitor of the mitochondrial cytochrome bc1 complex. *Biochim. Biophys. Acta.,* **1797** (3): 360-370.

Berthold, D. A., Andersson, M. E., & Nordlund, P. (2000). New insight into the structure and function of the alternative oxidase. *Biochim. Biophys. Acta.,* **1460** (2-3): 241-254.

Bertrand, H., Argan, C. A., & Szakacs, N. A. (1983). K. Wolf Schweyen, F. Kaudewitz, eds. Genetic control of the biogenesis of cyanide insensitive respiration in *Neurospora crassa*. Berlin: Walter de Gruyter.

Bertrand, H., Nargang, F. E., Collins, R. A., & Zagozeski, C. A. (1977). Nuclear cytochrome-deficient mutants of *Neurospora crassa*: isolation, characterization, and genetic mapping. *Mol. Gen. Genet.,* **153** (3): 247-257.

Blaza, J. N., Serreli, R., Jones, A. J., Mohammed, K., & Hirst, J. (2014). Kinetic evidence against partitioning of the ubiquinone pool and the catalytic relevance of respiratory-chain supercomplexes. *Proc. Natl. Acad. Sci. U S A,* **111** (44): 15735-15740.

Boivin, B., Yang, M., & Tonks, N. K. (2010). Targeting the reversibly oxidized protein tyrosine phosphatase superfamily. *Sci. Signal.,* **3** (137): pl2.

Bonamore, A., & Boffi, A. (2008). Flavohemoglobin: structure and reactivity. *IUBMB Life,* **60** (1): 19-28.

Borecky, J., Nogueira, F. T., de Oliveira, K. A., Maia, I. G., Vercesi, A. E., & Arruda, P. (2006). The plant energy-dissipating mitochondrial systems: depicting the genomic structure and the expression profiles of the gene families of uncoupling protein and alternative oxidase in monocots and dicots. *J. Exp. Bot.,* **57** (4): 849-864.

Borghouts, C., Werner, A., Elthon, T., & Osiewacz, H. D. (2001). Copper-modulated gene expression and senescence in the filamentous fungus *Podospora anserina*. *Mol. Cell Biol.,* **21** (2): 390-399.

Borkovich, K., & Ebbole, D. J. (2010). Cellular and Molecular Biology of Filamentous Fungi. Washington, DC: ASM Press.

Botelho, S. C., Osterberg, M., Reichert, A. S., Yamano, K., Bjorkholm, P., Endo, T., von Heijne, G., & Kim, H. (2011). TIM23-mediated insertion of transmembrane alpha-helices into the mitochondrial inner membrane. *EMBO J.,* **30** (6): 1003-1011.

Bovier, E., Sellem, C. H., Humbert, A., & Sainsard-Chanet, A. (2014). Genetic and functional investigation of Zn(2)Cys(6) transcription factors RSE2 and RSE3 in *Podospora anserina*. *Eukaryot. Cell,* **13** (1): 53-65.

Brand, M. D. (2010). The sites and topology of mitochondrial superoxide production. *Exp. Gerontol.,* **45** (7-8): 466-472.

Brindefalk, B., Ettema, T. J., Viklund, J., Thollesson, M., & Andersson, S. G. (2011). A phylometagenomic exploration of oceanic alphaproteobacteria reveals mitochondrial relatives unrelated to the SAR11 clade. *PloS One,* **6** (9): e24457.

Brunner, S., Everard-Gigot, V., & Stuart, R. A. (2002). Subunit e of the yeast F1Fo-ATP synthase forms homodimers. *J. Biol. Chem.,* **277** (50): 48484-48489.

Burger, G., Gray, M. W., Forget, L., & Lang, B. F. (2013). Strikingly bacteria-like and gene-rich mitochondrial genomes throughout jakobid protists. *Genome Biol. Evol.,* **5** (2): 418-438.

Burte, F., Carelli, V., Chinnery, P. F., & Yu-Wai-Man, P. (2015). Disturbed mitochondrial dynamics and neurodegenerative disorders. *Nat. Rev. Neurol.,* **11** (1): 11-24.

Cabezas-Opazo, F. A., Vergara-Pulgar, K., Perez, M. J., Jara, C., Osorio-Fuentealba, C., & Quintanilla, R. A. (2015). Mitochondrial Dysfunction Contributes to the Pathogenesis of Alzheimer's Disease. *Oxid. Med. Cell. Longev.,* **2015**: 509654.

Cadenas, E. (2004). Mitochondrial free radical production and cell signaling. *Mol. Aspects Med.,* **25** (1-2): 17-26.

Cadenas, E., & Davies, K. J. (2000). Mitochondrial free radical generation, oxidative stress, and aging. *Free Radic. Biol. Med.,* **29** (3-4): 222-230.

Cai, S., Han, H. J., & Kohwi-Shigematsu, T. (2003). Tissue-specific nuclear architecture and gene expression regulated by SATB1. *Nat. Genet.,* **34** (1): 42-51.

Calpena, E., Casado, M., Martinez-Rubio, D., Nascimento, A., Colomer, J., Gargallo, E., Garcia-Cazorla, A., Palau, F., Artuch, R., & Espinos, C. (2013). 5-Oxoprolinuria in Heterozygous Patients for 5-Oxoprolinase (OPLAH) Missense Changes. *JIMD Rep.,* **7**: 123-128.

Calvo, S. E., & Mootha, V. K. (2010). The mitochondrial proteome and human disease. *Annu. Rev. Genomics Hum. Genet.,* **11**: 25-44.

Cannino, G., El-Khoury, R., Pirinen, M., Hutz, B., Rustin, P., Jacobs, H. T., & Dufour, E. (2012). Glucose modulates respiratory complex I activity in response to acute mitochondrial dysfunction. *J. Biol. Chem.,* **287** (46): 38729-38740.

Carling, D., & Viollet, B. (2015). Beyond energy homeostasis: the expanding role of AMP-activated protein kinase in regulating metabolism. *Cell Metab.,* **21** (6): 799-804.

Carol, P., Stevenson, D., Bisanz, C., Breitenbach, J., Sandmann, G., Mache, R., Coupland, G., & Kuntz, M. (1999). Mutations in the Arabidopsis gene IMMUTANS cause a variegated phenotype by inactivating a chloroplast terminal oxidase associated with phytoene desaturation. *Plant Cell,* **11** (1): 57-68.

Carri, M. T., Valle, C., Bozzo, F., & Cozzolino, M. (2015). Oxidative stress and mitochondrial damage: importance in non-SOD1 ALS. *Front. Cell. Neurosci.,* **9**: 41.

Carroll, J., Fearnley, I. M., Skehel, J. M., Shannon, R. J., Hirst, J., & Walker, J. E. (2006). Bovine complex I is a complex of 45 different subunits. *J. Biol. Chem.,* **281** (43): 32724-32727.

Cavalcanti, J. H., Oliveira, G. M., Saraiva, K. D., Torquato, J. P., Maia, I. G., de Melo, D. F., & Costa, J. H. (2013). Identification of duplicated and stress-inducible Aox2b gene co-expressed with Aox1 in species of the Medicago genus reveals a regulation linked to gene rearrangement in leguminous genomes. *J. Plant Physiol.,* **170** (18): 1609-1619.

Cedergren, R., Gray, M. W., Abel, Y., & Sankoff, D. (1988). The evolutionary relationships among known life forms. *J. Mol. Evol.,* **28** (1-2): 98-112.

Chacinska, A., Koehler, C. M., Milenkovic, D., Lithgow, T., & Pfanner, N. (2009). Importing mitochondrial proteins: machineries and mechanisms. *Cell,* **138** (4): 628-644.

Chacinska, A., Pfannschmidt, S., Wiedemann, N., Kozjak, V., Sanjuan Szklarz, L. K., Schulze-Specking, A., Truscott, K. N., Guiard, B., Meisinger, C., & Pfanner, N. (2004). Essential role of Mia40 in import and assembly of mitochondrial intermembrane space proteins. *EMBO J.,* **23** (19): 3735-3746.

Chae, M. S., Lin, C. C., Kessler, K. E., Nargang, C. E., Tanton, L. L., Hahn, L. B., & Nargang, F. E. (2007a). Identification of an alternative oxidase induction motif in the promoter region of the aod-1 gene in *Neurospora crassa*. *Genetics,* **175** (4): 1597-1606.

Chae, M. S., Nargang, C. E., Cleary, I. A., Lin, C. C., Todd, A. T., & Nargang, F. E. (2007b). Two zinc-cluster transcription factors control induction of alternative oxidase in *Neurospora crassa*. *Genetics,* **177** (4): 1997-2006.

Chae, M. S., & Nargang, F. E. (2009). Investigation of regulatory factors required for alternative oxidase production in *Neurospora crassa*. *Physiol. Plant,* **137** (4): 407-418.

Chan, D. C. (2012). Fusion and fission: interlinked processes critical for mitochondrial health. *Annu. Rev. Genet.,* **46**: 265-287.

Chang, H. W., Shtessel, L., & Lee, S. S. (2015). Collaboration between mitochondria and the nucleus is key to long life in Caenorhabditis elegans. *Free Radic. Biol. Med.,* **78**: 168-178.

Chaturvedi, R. K., & Flint Beal, M. (2013). Mitochondrial diseases of the brain. *Free Radic. Biol. Med.,* **63**: 1-29.

Chaudhuri, M., Ott, R. D., & Hill, G. C. (2006). Trypanosome alternative oxidase: from molecule to function. *Trends Parasitol.,* **22** (10): 484-491.

Chaudhuri, M., Ott, R. D., Saha, L., Williams, S., & Hill, G. C. (2005). The trypanosome alternative oxidase exists as a monomer in *Trypanosoma brucei* mitochondria. *Parasitol. Res.,* **96** (3): 178-183.

Chen, C., & Noble, S. M. (2012). Post-transcriptional regulation of the Sef1 transcription factor controls the virulence of *Candida albicans* in its mammalian host. *PLoS pathog.,* **8** (11): e1002956.

Chen, L., Winger, A. J., & Knowlton, A. A. (2014a). Mitochondrial dynamic changes in health and genetic diseases. *Mol. Biol. Rep.,* **41** (11): 7053-7062.

Chen, Y. C., Taylor, E. B., Dephoure, N., Heo, J. M., Tonhato, A., Papandreou, I., Nath, N., Denko, N. C., Gygi, S. P., & Rutter, J. (2012). Identification of a protein mediating respiratory supercomplex stability. *Cell Metab.,* **15** (3): 348-360.

Chen, Z., Qi, Y., French, S., Zhang, G., Garcia, R. C., Balaban, R., & Xu, H. (2014b). Genetic mosaic analysis of a deleterious mitochondrial DNA mutation in Drosophila reveals novel aspects of mitochondrial regulation and function. *Mol. Biol. Cell*, **26** (4):674-84.

Chen, Z. S., & Tiwari, A. K. (2011). Multidrug resistance proteins (MRPs/ABCCs) in cancer chemotherapy and genetic diseases. *FEBS J.,* **278** (18): 3226-3245.

Cheng, P., Yang, Y., Gardner, K. H., & Liu, Y. (2002). PAS domain-mediated WC-1/WC-2 interaction is essential for maintaining the steady-state level of WC-1 and the function of both proteins in circadian clock and light responses of Neurospora. *Mol. Cell. Biol.,* **22** (2): 517-524.

Cheng, P., Yang, Y., Wang, L., He, Q., & Liu, Y. (2003). WHITE COLLAR-1, a multifunctional neurospora protein involved in the circadian feedback loops, light sensing, and transcription repression of wc-2. *J. Biol. Chem.,* **278** (6): 3801-3808.

Chou, S., Lane, S., & Liu, H. (2006). Regulation of mating and filamentation genes by two distinct Ste12 complexes in *Saccharomyces cerevisiae*. *Mol. Cell. Biol.,* **26** (13): 4794-4805.

Chovancova, E., Pavelka, A., Benes, P., Strnad, O., Brezovsky, J., Kozlikova, B., Gora, A., Sustr, V., Klvana, M., Medek, P., Biedermannova, L., Sochor, J., & Damborsky, J. (2012). CAVER 3.0: a tool for the analysis of transport pathways in dynamic protein structures. *PLoS Comput. Biol.,* **8** (10): e1002708.

Clifton, R., Lister, R., Parker, K. L., Sappl, P. G., Elhafez, D., Millar, A. H., Day, D. A., & Whelan, J. (2005). Stress-induced co-expression of alternative respiratory chain components in *Arabidopsis thaliana*. *Plant Mol. Biol.,* **58** (2): 193-212.

Cohen, M. M., Amiott, E. A., Day, A. R., Leboucher, G. P., Pryce, E. N., Glickman, M. H., McCaffery, J. M., Shaw, J. M., & Weissman, A. M. (2011). Sequential requirements for the GTPase domain of the mitofusin Fzo1 and the ubiquitin ligase SCFMdm30 in mitochondrial outer membrane fusion. *J. Cell Sci.,* **124** (Pt 9): 1403-1410.

Cole, S. P. (2014). Multidrug resistance protein 1 (MRP1, ABCC1), a "multitasking" ATP-binding cassette (ABC) transporter. *The J. Biol. Chem.,* **289** (45): 30880-30888.

Conrad, M., Schothorst, J., Kankipati, H. N., Van Zeebroeck, G., Rubio-Texeira, M., & Thevelein, J. M. (2014). Nutrient sensing and signaling in the yeast *Saccharomyces cerevisiae*. *FEMS Microbiol. Rev.,* **38** (2): 254-299.

Considine, M. J., Holtzapffel, R. C., Day, D. A., Whelan, J., & Millar, A. H. (2002). Molecular distinction between alternative oxidase from monocots and dicots. *Plant Physiol.,* **129** (3): 949-953.

Copeland, J. M., Cho, J., Lo, T., Jr., Hur, J. H., Bahadorani, S., Arabyan, T., Rabie, J., Soh, J., & Walker, D. W. (2009). Extension of Drosophila life span by RNAi of the mitochondrial respiratory chain. *Curr. Biol.,* **19** (19): 1591-1598.

Copeland, W. C. (2012). Defects in mitochondrial DNA replication and human disease. *Crit. Rev. Biochem. Mol. Biol.,* **47** (1): 64-74.

Copeland, W. C. (2014). Defects of mitochondrial DNA replication. *J. Child Neurol.,* **29** (9): 1216-1224.

Costa, J. H., McDonald, A. E., Arnholdt-Schmitt, B., & Fernandes de Melo, D. (2014). A classification scheme for alternative oxidases reveals the taxonomic distribution and evolutionary history of the enzyme in angiosperms. *Mitochondrion,* **19 Pt B**: 172-183.

Costa, J. H., Mota, E. F., Cambursano, M. V., Lauxmann, M. A., de Oliveira, L. M., Silva Lima Mda, G., Orellano, E. G., & Fernandes de Melo, D. (2010). Stress-induced co-expression of two alternative oxidase (VuAox1 and 2b) genes in Vigna unguiculata. *J. Plant Physiol.,* **167** (7): 561-570.

Cozzolino, M., Rossi, S., Mirra, A., & Carri, M. T. (2015). Mitochondrial dynamism and the pathogenesis of Amyotrophic Lateral Sclerosis. *Front. Cell. Neurosci.,* **9**: 31.

Crozet, P., Margalha, L., Confraria, A., Rodrigues, A., Martinho, C., Adamo, M., Elias, C. A., & Baena-Gonzalez, E. (2014). Mechanisms of regulation of SNF1/AMPK/SnRK1 protein kinases. *Front. Plant Sci.,* **5**: 190.

Cruciat, C. M., Brunner, S., Baumann, F., Neupert, W., & Stuart, R. A. (2000). The

cytochrome bc1 and cytochrome c oxidase complexes associate to form a single supracomplex in yeast mitochondria. *J. Biol. Chem.,* **275** (24): 18093-18098.

Cvetkovska, M., Dahal, K., Alber, N. A., Jin, C., Cheung, M., & Vanlerberghe, G. C. (2014). Knockdown of mitochondrial alternative oxidase induces the 'stress state' of signaling molecule pools in Nicotiana tabacum, with implications for stomatal function. *New Phytol.,* **203** (2): 449-461.

Cvetkovska, M., & Vanlerberghe, G. C. (2012). Alternative oxidase modulates leaf mitochondrial concentrations of superoxide and nitric oxide. *New Phytol.,* **195** (1): 32-39.

Cvetkovska, M., & Vanlerberghe, G. C. (2013). Alternative oxidase impacts the plant response to biotic stress by influencing the mitochondrial generation of reactive oxygen species. *Plant Cell Environ.,* **36** (3): 721-732.

Dalle-Donne, I., Rossi, R., Colombo, G., Giustarini, D., & Milzani, A. (2009). Protein S-glutathionylation: a regulatory device from bacteria to humans. *Trends Biochem. Sci.,* **34** (2): 85-96.

D'Autreaux, B., & Toledano, M. B. (2007). ROS as signalling molecules: mechanisms that generate specificity in ROS homeostasis. *Nat. Rev. Mol. Cell Biol.,* **8** (10): 813-824.

Dassa, E. P., Dufour, E., Goncalves, S., Jacobs, H. T., & Rustin, P. (2009a). The alternative oxidase, a tool for compensating cytochrome c oxidase deficiency in human cells. *Physiol. Plant,* **137** (4): 427-434.

Dassa, E. P., Dufour, E., Goncalves, S., Paupe, V., Hakkaart, G. A., Jacobs, H. T., & Rustin, P. (2009b). Expression of the alternative oxidase complements cytochrome c oxidase deficiency in human cells. *EMBO Mol. Med.,* **1** (1): 30-36.

Davies, K. M., Anselmi, C., Wittig, I., Faraldo-Gomez, J. D., & Kuhlbrandt, W. (2012). Structure of the yeast F1Fo-ATP synthase dimer and its role in shaping the mitochondrial cristae. *Proc. Natl. Acad. Sci. U S A,* **109** (34): 13602-13607.

Davis, I. R. H. (2000). Neurospora : Contributions of a Model Organism: Contributions of a Model Organism. Oxford University Press, USA

Davis, R. H., & De Serres, F. J. (1970). Genetic and microbiological research techniques for *Neurospora crassa*. *Methods Enzymol.,* **17**: 79-143.

De Clercq, I., Vermeirssen, V., Van Aken, O., Vandepoele, K., Murcha, M. W., Law, S. R., Inze, A., Ng, S., Ivanova, A., Rombaut, D., van de Cotte, B., Jaspers, P., Van de

Peer, Y., Kangasjarvi, J., Whelan, J., & Van Breusegem, F. (2013). The membrane-bound NAC transcription factor ANAC013 functions in mitochondrial retrograde regulation of the oxidative stress response in Arabidopsis. *Plant Cell,* **25** (9): 3472-3490.

Descheneau, A. T., Cleary, I. A., & Nargang, F. E. (2005). Genetic evidence for a regulatory pathway controlling alternative oxidase production in *Neurospora crassa*. *Genetics,* **169** (1): 123-135.

Dickson, V. K., Silvester, J. A., Fearnley, I. M., Leslie, A. G., & Walker, J. E. (2006). On the structure of the stator of the mitochondrial ATP synthase. *EMBO J.,* **25** (12): 2911-2918.

Dietmeier, K., Honlinger, A., Bomer, U., Dekker, P. J., Eckerskorn, C., Lottspeich, F., Kubrich, M., & Pfanner, N. (1997). Tom5 functionally links mitochondrial preprotein receptors to the general import pore. *Nature,* **388** (6638): 195-200.

Diezmann, S., & Dietrich, F. S. (2011). Oxidative stress survival in a clinical Saccharomyces cerevisiae isolate is influenced by a major quantitative trait nucleotide. *Genetics,* **188** (3): 709-722.

Dillin, A., Hsu, A. L., Arantes-Oliveira, N., Lehrer-Graiwer, J., Hsin, H., Fraser, A. G., Kamath, R. S., Ahringer, J., & Kenyon, C. (2002). Rates of behavior and aging specified by mitochondrial function during development. *Science,* **298** (5602): 2398-2401.

Dilova, I., Aronova, S., Chen, J. C., & Powers, T. (2004). Tor signaling and nutrient-based signals converge on Mks1p phosphorylation to regulate expression of Rtg1.Rtg3p-dependent target genes. *J. Biol. Chem.,* **279** (45): 46527-46535.

Dilova, I., Chen, C. Y., & Powers, T. (2002). Mks1 in concert with TOR signaling negatively regulates RTG target gene expression in *S. cerevisiae*. *Curr. Biol.,* **12** (5): 389-395.

Djajanegara, I., Finnegan, P. M., Mathieu, C., McCabe, T., Whelan, J., & Day, D. A. (2002). Regulation of alternative oxidase gene expression in soybean. *Plant Mol. Biol.,* **50** (4-5): 735-742.

Dobi, K. C., & Winston, F. (2007). Analysis of transcriptional activation at a distance in *Saccharomyces cerevisiae*. *Mol. Cell. Biol.,* **27** (15): 5575-5586.

Dobreva, G., Dambacher, J., & Grosschedl, R. (2003). SUMO modification of a novel MAR-binding protein, SATB2, modulates immunoglobulin mu gene expression. *Genes Dev.,* **17** (24): 3048-3061.

Dojcinovic, D., Krosting, J., Harris, A. J., Wagner, D. J., & Rhoads, D. M. (2005). Identification of a region of the Arabidopsis AtAOX1a promoter necessary for mitochondrial retrograde regulation of expression. *Plant Mol. Biol.,* **58** (2): 159-175.

Dudek, J., Rehling, P., & van der Laan, M. (2013). Mitochondrial protein import: common principles and physiological networks. *Biochim. Biophys. Acta.,* **1833** (2): 274-285.

Dudkina, N. V., Kudryashev, M., Stahlberg, H., & Boekema, E. J. (2011). Interaction of complexes I, III, and IV within the bovine respirasome by single particle cryoelectron tomography. *Proc. Natl. Acad. Sci. U S A,* **108** (37): 15196-15200.

Durcan, T. M., & Fon, E. A. (2015). The three 'P's of mitophagy: PARKIN, PINK1, and post-translational modifications. *Genes Dev.,* **29** (10): 989-999.

Ederli, L., Morettini, R., Borgogni, A., Wasternack, C., Miersch, O., Reale, L., Ferranti, F., Tosti, N., & Pasqualini, S. (2006). Interaction between nitric oxide and ethylene in the induction of alternative oxidase in ozone-treated tobacco plants. *Plant Physiol.,* **142** (2): 595-608.

Ehrlich, K. C., Montalbano, B. G., & Cary, J. W. (1999). Binding of the C6-zinc cluster protein, AFLR, to the promoters of aflatoxin pathway biosynthesis genes in *Aspergillus parasiticus*. *Gene,* **230** (2): 249-257.

El-Khoury, R., Dufour, E., Rak, M., Ramanantsoa, N., Grandchamp, N., Csaba, Z., Duvillie, B., Benit, P., Gallego, J., Gressens, P., Sarkis, C., Jacobs, H. T., & Rustin, P. (2013). Alternative oxidase expression in the mouse enables bypassing cytochrome c oxidase blockade and limits mitochondrial ROS overproduction. *PLoS Genet.,* **9** (1): e1003182.

Embley, T. M., & Williams, T. A. (2015). Evolution: Steps on the road to eukaryotes. *Nature,* **521** (7551): 169-170.

Epstein, C. B., Waddle, J. A., Hale, W. t., Dave, V., Thornton, J., Macatee, T. L., Garner, H. R., & Butow, R. A. (2001). Genome-wide responses to mitochondrial dysfunction. *Mol. Biol. Cell,* **12** (2): 297-308.

Escobar-Henriques, M., & Anton, F. (2013). Mechanistic perspective of mitochondrial fusion: tubulation vs. fragmentation. *Biochim. Biophys. Acta.,* **1833** (1): 162-175.

Esser, C., Ahmadinejad, N., Wiegand, C., Rotte, C., Sebastiani, F., Gelius-Dietrich, G., Henze, K., Kretschmann, E., Richly, E., Leister, D., Bryant, D., Steel, M. A., Lockhart, P. J., Penny, D., & Martin, W. (2004). A genome phylogeny for mitochondria among alpha-proteobacteria and a predominantly eubacterial ancestry of yeast nuclear genes.

Mol. Biol. Evol., **21** (9): 1643-1660.

Esser, L., Elberry, M., Zhou, F., Yu, C. A., Yu, L., & Xia, D. (2008). Inhibitor-complexed structures of the cytochrome bc1 from the photosynthetic bacterium *Rhodobacter sphaeroides*. *J. Biol. Chem.,* **283** (5): 2846-2857.

Eubel, H., Jansch, L., & Braun, H. P. (2003). New insights into the respiratory chain of plant mitochondria. Supercomplexes and a unique composition of complex II. *Plant Physiol.,* **133** (1): 274-286.

Evans, M. J., & Scarpulla, R. C. (1990). NRF-1: a trans-activator of nuclear-encoded respiratory genes in animal cells. *Genes Dev.,* **4** (6): 1023-1034.

Feng, H., Guan, D., Sun, K., Wang, Y., Zhang, T., & Wang, R. (2013). Expression and signal regulation of the alternative oxidase genes under abiotic stresses. *Acta. Biochim. Biophys. Sin.,* **45** (12): 985-994.

Feng, H., Wang, Y., Li, H., Wang, R., Sun, K., & Jia, L. (2010). Salt stress-induced expression of rice AOX1a is mediated through an accumulation of hydrogen peroxide. *Biologia,* **65** (5): 868-873.

Fernandez-Ayala, D. J., Sanz, A., Vartiainen, S., Kemppainen, K. K., Babusiak, M., Mustalahti, E., Costa, R., Tuomela, T., Zeviani, M., Chung, J., O'Dell, K. M., Rustin, P., & Jacobs, H. T. (2009). Expression of the *Ciona intestinalis* alternative oxidase (AOX) in Drosophila complements defects in mitochondrial oxidative phosphorylation. *Cell Metab.,* **9** (5): 449-460.

Figueira, T. R., Barros, M. H., Camargo, A. A., Castilho, R. F., Ferreira, J. C., Kowaltowski, A. J., Sluse, F. E., Souza-Pinto, N. C., & Vercesi, A. E. (2013). Mitochondria as a source of reactive oxygen and nitrogen species: from molecular mechanisms to human health. *Antioxid. Redox Signal.,* **18** (16): 2029-2074.

Finkel, T. (2012). Signal transduction by mitochondrial oxidants. *J. Biol. Chem.,* **287** (7): 4434-4440.

Finnegan, P. M., Umbach, A. L., & Wilce, J. A. (2003). Prokaryotic origins for the mitochondrial alternative oxidase and plastid terminal oxidase nuclear genes. *FEBS Lett.,* **555** (3): 425-430.

Fitzpatrick, D. A., Creevey, C. J., & McInerney, J. O. (2006). Genome phylogenies indicate a meaningful alpha-proteobacterial phylogeny and support a grouping of the mitochondria with the Rickettsiales. *Mol. Biol. Evol.,* **23** (1): 74-85.

Fox, E. M., Gardiner, D. M., Keller, N. P., & Howlett, B. J. (2008). A Zn(II)2Cys6

DNA binding protein regulates the sirodesmin PL biosynthetic gene cluster in *Leptosphaeria maculans*. *Fungal Genet. Biol.,* **45** (5): 671-682.

Frederico, A. M., Zavattieri, M. A., Campos, M. D., Cardoso, H. G., McDonald, A. E., & Arnholdt-Schmitt, B. (2009). The gymnosperm Pinus pinea contains both AOX gene subfamilies, AOX1 and AOX2. *Physiol. Plant,* **137** (4): 566-577.

Friedman, J. R., Lackner, L. L., West, M., DiBenedetto, J. R., Nunnari, J., & Voeltz, G. K. (2011). ER tubules mark sites of mitochondrial division. *Science,* **334** (6054): 358-362.

Fukai, T., & Ushio-Fukai, M. (2011). Superoxide dismutases: role in redox signaling, vascular function, and diseases. *Antioxid. Redox Signal.,* **15** (6): 1583-1606.

Furey, T. S. (2012). ChIP-seq and beyond: new and improved methodologies to detect and characterize protein-DNA interactions. *Nat. Rev. Genet.,* **13** (12): 840-852.

Furukawa, M., & Xiong, Y. (2005). BTB protein Keap1 targets antioxidant transcription factor Nrf2 for ubiquitination by the Cullin 3-Roc1 ligase. *Mol. Cell Biol.,* **25** (1): 162-171.

Galagan, J. E., Calvo, S. E., Borkovich, K. A., Selker, E. U., Read, N. D., Jaffe, D., FitzHugh, W., Ma, L. J., Smirnov, S., Purcell, S., Rehman, B., Elkins, T., Engels, R., Wang, S., Nielsen, C. B., Butler, J., Endrizzi, M., Qui, D., Ianakiev, P., Bell-Pedersen, D., Nelson, M. A., Werner-Washburne, M., Selitrennikoff, C. P., Kinsey, J. A., Braun, E. L., Zelter, A., Schulte, U., Kothe, G. O., Jedd, G., Mewes, W., Staben, C., Marcotte, E., Greenberg, D., Roy, A., Foley, K., Naylor, J., Stange-Thomann, N., Barrett, R., Gnerre, S., Kamal, M., Kamvysselis, M., Mauceli, E., Bielke, C., Rudd, S., Frishman, D., Krystofova, S., Rasmussen, C., Metzenberg, R. L., Perkins, D. D., Kroken, S., Cogoni, C., Macino, G., Catcheside, D., Li, W., Pratt, R. J., Osmani, S. A., DeSouza, C. P., Glass, L., Orbach, M. J., Berglund, J. A., Voelker, R., Yarden, O., Plamann, M., Seiler, S., Dunlap, J., Radford, A., Aramayo, R., Natvig, D. O., Alex, L. A., Mannhaupt, G., Ebbole, D. J., Freitag, M., Paulsen, I., Sachs, M. S., Lander, E. S., Nusbaum, C., & Birren, B. (2003). The genome sequence of the filamentous fungus *Neurospora crassa*. *Nature,* **422** (6934): 859-868.

Gandre-Babbe, S., & van der Bliek, A. M. (2008). The novel tail-anchored membrane protein Mff controls mitochondrial and peroxisomal fission in mammalian cells. *Mol. Biol. Cell,* **19** (6): 2402-2412.

Gao, X., Wen, X., Yu, C., Esser, L., Tsao, S., Quinn, B., Zhang, L., Yu, L., & Xia, D. (2002). The crystal structure of mitochondrial cytochrome bc1 in complex with famoxadone: the role of aromatic-aromatic interaction in inhibition. *Biochemistry,* **41** (39): 11692-11702.

Gardner, P. R. (2012). Hemoglobin: a nitric-oxide dioxygenase. *Scientifica,* **2012**: 683729.

Gasmi, N., Jacques, P. E., Klimova, N., Guo, X., Ricciardi, A., Robert, F., & Turcotte, B. (2014). The switch from fermentation to respiration in *Saccharomyces cerevisiae* is regulated by the Ert1 transcriptional activator/repressor. *Genetics,* **198** (2): 547-560.

Gebert, N., Gebert, M., Oeljeklaus, S., von der Malsburg, K., Stroud, D. A., Kulawiak, B., Wirth, C., Zahedi, R. P., Dolezal, P., Wiese, S., Simon, O., Schulze-Specking, A., Truscott, K. N., Sickmann, A., Rehling, P., Guiard, B., Hunte, C., Warscheid, B., van der Laan, M., Pfanner, N., & Wiedemann, N. (2011). Dual function of Sdh3 in the respiratory chain and TIM22 protein translocase of the mitochondrial inner membrane. *Mol. Cell,* **44** (5): 811-818.

Georgiades, K., Madoui, M. A., Le, P., Robert, C., & Raoult, D. (2011). Phylogenomic analysis of Odyssella thessalonicensis fortifies the common origin of Rickettsiales, *Pelagibacter ubique* and *Reclimonas americana* mitochondrion. *PloS One,* **6** (9): e24857.

Gessmann, D., Flinner, N., Pfannstiel, J., Schlosinger, A., Schleiff, E., Nussberger, S., & Mirus, O. (2011). Structural elements of the mitochondrial preprotein-conducting channel Tom40 dissolved by bioinformatics and mass spectrometry. *Biochim. Biophys. Acta.,* **1807** (12): 1647-1657.

Ghelli, A., Tropeano, C. V., Calvaruso, M. A., Marchesini, A., Iommarini, L., Porcelli, A. M., Zanna, C., De Nardo, V., Martinuzzi, A., Wibrand, F., Vissing, J., Kurelac, I., Gasparre, G., Selamoglu, N., Daldal, F., & Rugolo, M. (2013). The cytochrome b p.278Y>C mutation causative of a multisystem disorder enhances superoxide production and alters supramolecular interactions of respiratory chain complexes. *Hum. Mol. Genet.,* **22** (11): 2141-2151.

Ghillebert, R., Swinnen, E., Wen, J., Vandesteene, L., Ramon, M., Norga, K., Rolland, F., & Winderickx, J. (2011). The AMPK/SNF1/SnRK1 fuel gauge and energy regulator: structure, function and regulation. *FEBS J.,* **278** (21): 3978-3990.

Giannattasio, S., Liu, Z., Thornton, J., & Butow, R. A. (2005). Retrograde response to mitochondrial dysfunction is separable from TOR1/2 regulation of retrograde gene expression. *J. Biol. Chem.,* **280** (52): 42528-42535.

Gibbons, C., Montgomery, M. G., Leslie, A. G., & Walker, J. E. (2000). The structure of the central stalk in bovine F(1)-ATPase at 2.4 A resolution. *Nat. Struct. Biol.,* **7** (11): 1055-1061.

Giraud, E., Ho, L. H., Clifton, R., Carroll, A., Estavillo, G., Tan, Y. F., Howell, K. A.,

Ivanova, A., Pogson, B. J., Millar, A. H., & Whelan, J. (2008). The absence of ALTERNATIVE OXIDASE1a in Arabidopsis results in acute sensitivity to combined light and drought stress. *Plant Physiol.,* **147** (2): 595-610.

Giraud, E., Van Aken, O., Ho, L. H., & Whelan, J. (2009). The transcription factor ABI4 is a regulator of mitochondrial retrograde expression of ALTERNATIVE OXIDASE1a. *Plant Physiol.,* **150** (3): 1286-1296.

Gladyshev, E., & Kleckner, N. (2014). Direct recognition of homology between double helices of DNA in *Neurospora crassa*. *Nat. Commun.,* **5**: 3509.

Gopalakrishnan, L., & Scarpulla, R. C. (1994). Differential regulation of respiratory chain subunits by a CREB-dependent signal transduction pathway. Role of cyclic AMP in cytochrome c and COXIV gene expression. *J. Biol. Chem.,* **269** (1): 105-113.

Gordan, R., Hartemink, A. J., & Bulyk, M. L. (2009). Distinguishing direct versus indirect transcription factor-DNA interactions. *Genome Res.,* **19** (11): 2090-2100.

Grant, N., Onda, Y., Kakizaki, Y., Ito, K., Watling, J., & Robinson, S. (2009). Two cys or not two cys? That is the question; alternative oxidase in the thermogenic plant sacred Lotus. *Plant Physiol.,* **150** (2): 987-995.

Grant, N. M., Miller, R. E., Watling, J. R., & Robinson, S. A. (2008). Synchronicity of thermogenic activity, alternative pathway respiratory flux, AOX protein content, and carbohydrates in receptacle tissues of sacred lotus during floral development. *J. Exp. Bot.,* **59** (3): 705-714.

Gray, M. W. (2015). Mosaic nature of the mitochondrial proteome: Implications for the origin and evolution of mitochondria. *Proc. Natl. Acad. Sci. U S A,* **112** (33): 10133-10138.

Gray, M. W., Sankoff, D., & Cedergren, R. J. (1984). On the evolutionary descent of organisms and organelles: a global phylogeny based on a highly conserved structural core in small subunit ribosomal RNA. *Nucleic. Acids Res.,* **12** (14): 5837-5852.

Gregersen, N., Hansen, J., & Palmfeldt, J. (2012). Mitochondrial proteomics--a tool for the study of metabolic disorders. *J. Inherit. Metab. Dis.,* **35** (4): 715-726.

Gulshan, K., & Moye-Rowley, W. S. (2011). Vacuolar import of phosphatidylcholine requires the ATP-binding cassette transporter Ybt1. *Traffic,* **12** (9): 1257-1268.

Guo, J., Huang, G., Cha, J., & Liu, Y. (2010). Biochemical methods used to study the gene expression and protein complexes in the filamentous fungus *Neurospora crassa*. *Methods Mol. Biol.,* **638**: 189-200.

Gupta, K. J., Fernie, A. R., Kaiser, W. M., & van Dongen, J. T. (2011). On the origins of nitric oxide. *Trends Plant Sci.,* **16** (3): 160-168.

Hakkaart, G. A., Dassa, E. P., Jacobs, H. T., & Rustin, P. (2006). Allotopic expression of a mitochondrial alternative oxidase confers cyanide resistance to human cell respiration. *EMBO Rep.,* **7** (3): 341-345.

Hamilton, B., Dong, Y., Shindo, M., Liu, W., Odell, I., Ruvkun, G., & Lee, S. S. (2005). A systematic RNAi screen for longevity genes in C. elegans. *Genes Dev.,* **19** (13): 1544-1555.

Han, D., Antunes, F., Canali, R., Rettori, D., & Cadenas, E. (2003). Voltage-dependent anion channels control the release of the superoxide anion from mitochondria to cytosol. *J. Biol. Chem.,* **278** (8): 5557-5563.

Hanqing, F., Kun, S., Mingquan, L., Hongyu, L., Xin, L., Yan, L., & Yifeng, W. (2010). The expression, function and regulation of mitochondrial alternative oxidase under biotic stresses. *Mol. Plant Pathol.,* **11** (3): 429-440.

Harbauer, A. B., Zahedi, R. P., Sickmann, A., Pfanner, N., & Meisinger, C. (2014). The protein import machinery of mitochondria-a regulatory hub in metabolism, stress, and disease. *Cell Metab.,* **19** (3): 357-372.

Hardie, D. G. (2015). AMPK: positive and negative regulation, and its role in whole-body energy homeostasis. *Curr. Opin. Cell Biol.,* **33**: 1-7.

Hardie, D. G., Ross, F. A., & Hawley, S. A. (2012). AMPK: a nutrient and energy sensor that maintains energy homeostasis. *Nat. Rev. Mol. Cell Biol.,* **13** (4): 251-262.

Harner, M., Korner, C., Walther, D., Mokranjac, D., Kaesmacher, J., Welsch, U., Griffith, J., Mann, M., Reggiori, F., & Neupert, W. (2011). The mitochondrial contact site complex, a determinant of mitochondrial architecture. *EMBO J.,* **30** (21): 4356-4370.

Hashim, Z., Mukai, Y., Bamba, T., & Fukusaki, E. (2014). Metabolic profiling of retrograde pathway transcription factors rtg1 and rtg3 knockout yeast. *Metabolites,* **4** (3): 580-598.

Haurie, V., Perrot, M., Mini, T., Jeno, P., Sagliocco, F., & Boucherie, H. (2001). The transcriptional activator Cat8p provides a major contribution to the reprogramming of carbon metabolism during the diauxic shift in *Saccharomyces cerevisiae*. *J. Biol. Chem.,* **276** (1): 76-85.

Haynes, C. M., Petrova, K., Benedetti, C., Yang, Y., & Ron, D. (2007). ClpP mediates

activation of a mitochondrial unfolded protein response in *C. elegans*. *Dev. Cell,* **13** (4): 467-480.

Haynes, C. M., Yang, Y., Blais, S. P., Neubert, T. A., & Ron, D. (2010). The matrix peptide exporter HAF-1 signals a mitochondrial UPR by activating the transcription factor ZC376.7 in C. elegans. *Mol. Cell,* **37** (4): 529-540.

Hedbacker, K., & Carlson, M. (2008). SNF1/AMPK pathways in yeast. *Front. Biosci.,* **13**: 2408-2420.

Heinemeyer, J., Braun, H. P., Boekema, E. J., & Kouril, R. (2007). A structural model of the cytochrome C reductase/oxidase supercomplex from yeast mitochondria. *J. Biol. Chem.,* **282** (16): 12240-12248.

Heinz, S., Romanoski, C. E., Benner, C., & Glass, C. K. (2015). The selection and function of cell type-specific enhancers. *Nat. Rev. Mol. Cell Biol.,* **16** (3): 144-154.

Hell, K. (2008). The Erv1-Mia40 disulfide relay system in the intermembrane space of mitochondria. *Biochim. Biophys. Acta.,* **1783** (4): 601-609.

Hennon, S. W., Soman, R., Zhu, L., & Dalbey, R. E. (2015). YidC/Alb3/Oxa1 Family of Insertases. *J. Biol. Chem.,* **290** (24): 14866-14874.

Henry, J. T., & Crosson, S. (2011). Ligand-binding PAS domains in a genomic, cellular, and structural context. *Annu. Rev. Microbiol.,* **65**: 261-286.

Herzig, R. P., Scacco, S., & Scarpulla, R. C. (2000). Sequential serum-dependent activation of CREB and NRF-1 leads to enhanced mitochondrial respiration through the induction of cytochrome c. *J. Biol. Chem.,* **275** (17): 13134-13141.

Hill, B. G., Dranka, B. P., Bailey, S. M., Lancaster, J. R., Jr., & Darley-Usmar, V. M. (2010). What part of NO don't you understand? Some answers to the cardinal questions in nitric oxide biology. *J. Biol. Chem.,* **285** (26): 19699-19704.

Hirst, J. (2011). Why does mitochondrial complex I have so many subunits? *Biochem. J.,* **437** (2): e1-3.

Hirst, J. (2013). Mitochondrial complex I. *Annu. Rev. Biochem.,* **82**: 551-575.

Ho, L. H., Giraud, E., Lister, R., Thirkettle-Watts, D., Low, J., Clifton, R., Howell, K. A., Carrie, C., Donald, T., & Whelan, J. (2007). Characterization of the regulatory and expression context of an alternative oxidase gene provides insights into cyanide-insensitive respiration during growth and development. *Plant Physiol.,* **143** (4): 1519-1533.

Ho, L. H., Giraud, E., Uggalla, V., Lister, R., Clifton, R., Glen, A., Thirkettle-Watts, D., Van Aken, O., & Whelan, J. (2008). Identification of regulatory pathways controlling gene expression of stress-responsive mitochondrial proteins in Arabidopsis. *Plant Physiol.,* **147** (4): 1858-1873.

Holmstrom, K. M., & Finkel, T. (2014). Cellular mechanisms and physiological consequences of redox-dependent signalling. *Nat. Rev. Mol. Cell Biol.,* **15** (6): 411-421.

Holtzapffel, R. C., Castelli, J., Finnegan, P. M., Millar, A. H., Whelan, J., & Day, D. A. (2003). A tomato alternative oxidase protein with altered regulatory properties. *Biochim. Biophys. Acta.,* **1606** (1-3): 153-162.

Honda, Y., Hattori, T., & Kirimura, K. (2012). Visual expression analysis of the responses of the alternative oxidase gene (aox1) to heat shock, oxidative, and osmotic stresses in conidia of citric acid-producing *Aspergillus niger*. *J. Biosci. Bioeng.,* **113** (3): 338-342.

Hoppins, S. C., Go, N. E., Klein, A., Schmitt, S., Neupert, W., Rapaport, D., & Nargang, F. E. (2007). Alternative splicing gives rise to different isoforms of the *Neurospora crassa* Tob55 protein that vary in their ability to insert beta-barrel proteins into the outer mitochondrial membrane. *Genetics,* **177** (1): 137-149.

Hoppins, S., Collins, S. R., Cassidy-Stone, A., Hummel, E., Devay, R. M., Lackner, L. L., Westermann, B., Schuldiner, M., Weissman, J. S., & Nunnari, J. (2011). A mitochondrial-focused genetic interaction map reveals a scaffold-like complex required for inner membrane organization in mitochondria. *J. Cell. Biol.,* **195** (2): 323-340.

Horibe, T., & Hoogenraad, N. J. (2007). The chop gene contains an element for the positive regulation of the mitochondrial unfolded protein response. *PloS One,* **2** (9): e835.

Horvath, S. E., Rampelt, H., Oeljeklaus, S., Warscheid, B., van der Laan, M., & Pfanner, N. (2015). Role of membrane contact sites in protein import into mitochondria. *Protein Sci.,* **24** (3): 277-297.

Huang, L. S., Cobessi, D., Tung, E. Y., & Berry, E. A. (2005). Binding of the respiratory chain inhibitor antimycin to the mitochondrial bc1 complex: a new crystal structure reveals an altered intramolecular hydrogen-bonding pattern. *J. Mol. Biol.,* **351** (3): 573-597.

Huang, L. S., Sun, G., Cobessi, D., Wang, A. C., Shen, J. T., Tung, E. Y., Anderson, V. E., & Berry, E. A. (2006). 3-nitropropionic acid is a suicide inhibitor of mitochondrial

respiration that, upon oxidation by complex II, forms a covalent adduct with a catalytic base arginine in the active site of the enzyme. *J. Biol. Chem.,* **281** (9): 5965-5972.

Huang, X., von Rad, U., & Durner, J. (2002). Nitric oxide induces transcriptional activation of the nitric oxide-tolerant alternative oxidase in Arabidopsis suspension cells. *Planta,* **215** (6): 914-923.

Huh, W. K., & Kang, S. O. (1999). Molecular cloning and functional expression of alternative oxidase from *Candida albicans*. *J. Bacteriol.,* **181** (13): 4098-4102.

Huh, W. K., & Kang, S. O. (2001). Characterization of the gene family encoding alternative oxidase from *Candida albicans*. *Biochem. J.,* **356** (Pt 2): 595-604.

Humphrey, D. M., Parsons, R. B., Ludlow, Z. N., Riemensperger, T., Esposito, G., Verstreken, P., Jacobs, H. T., Birman, S., & Hirth, F. (2012). Alternative oxidase rescues mitochondria-mediated dopaminergic cell loss in Drosophila. *Hum. Mol. Genet.,* **21** (12): 2698-2712.

Hunte, C., Koepke, J., Lange, C., Rossmanith, T., & Michel, H. (2000). Structure at 2.3 A resolution of the cytochrome bc(1) complex from the yeast *Saccharomyces cerevisiae* co-crystallized with an antibody Fv fragment. *Structure,* **8** (6): 669-684.

Hunte, C., Zickermann, V., & Brandt, U. (2010). Functional modules and structural basis of conformational coupling in mitochondrial complex I. *Science,* **329** (5990): 448-451.

Hynes, M. J., Szewczyk, E., Murray, S. L., Suzuki, Y., Davis, M. A., & Sealy-Lewis, H. M. (2007). Transcriptional control of gluconeogenesis in *Aspergillus nidulans*. *Genetics,* **176** (1): 139-150.

Ieva, R., Schrempp, S. G., Opalinski, L., Wollweber, F., Hoss, P., Heisswolf, A. K., Gebert, M., Zhang, Y., Guiard, B., Rospert, S., Becker, T., Chacinska, A., Pfanner, N., & van der Laan, M. (2014). Mgr2 functions as lateral gatekeeper for preprotein sorting in the mitochondrial inner membrane. *Mol. Cell,* **56** (5): 641-652.

Igamberdiev, A. U., Ratcliffe, R. G., & Gupta, K. J. (2014). Plant mitochondria: source and target for nitric oxide. *Mitochondrion,* **19 Pt B**: 329-333.

Ivanova, A., Law, S. R., Narsai, R., Duncan, O., Lee, J. H., Zhang, B., Van Aken, O., Radomiljac, J. D., van der Merwe, M., Yi, K., & Whelan, J. (2014). A functional antagonistic relationship between auxin and mitochondrial retrograde signaling regulates alternative oxidase1a expression in Arabidopsis. *Plant Physiol.,* **165** (3): 1233-1254.

Iwata, S., Lee, J. W., Okada, K., Lee, J. K., Iwata, M., Rasmussen, B., Link, T. A., Ramaswamy, S., & Jap, B. K. (1998). Complete structure of the 11-subunit bovine mitochondrial cytochrome bc1 complex. *Science,* **281** (5373): 64-71.

Iwata, S., Ostermeier, C., Ludwig, B., & Michel, H. (1995). Structure at 2.8 A resolution of cytochrome c oxidase from *Paracoccus denitrificans*. *Nature,* **376** (6542): 660-669.

Jardon, R., Gancedo, C., & Flores, C. L. (2008). The gluconeogenic enzyme fructose-1,6-bisphosphatase is dispensable for growth of the yeast *Yarrowia lipolytica* in gluconeogenic substrates. *Eukaryot. Cell,* **7** (10): 1742-1749.

Jia, Y., Rothermel, B., Thornton, J., & Butow, R. A. (1997). A basic helix-loop-helix-leucine zipper transcription complex in yeast functions in a signaling pathway from mitochondria to the nucleus. *Mol. Cell Biol.,* **17** (3): 1110-1117.

Johnson, W. E., Li, W., Meyer, C. A., Gottardo, R., Carroll, J. S., Brown, M., & Liu, X. S. (2006). Model-based analysis of tiling-arrays for ChIP-chip. *Proc. Natl. Acad. Sci. U S A*, **103** (33): 12457-12462.

Jovaisaite, V., Mouchiroud, L., & Auwerx, J. (2014). The mitochondrial unfolded protein response, a conserved stress response pathway with implications in health and disease. *J. Exp. Biol.,* **217** (Pt 1): 137-143.

Karisch, R., Fernandez, M., Taylor, P., Virtanen, C., St-Germain, J. R., Jin, L. L., Harris, I. S., Mori, J., Mak, T. W., Senis, Y. A., Ostman, A., Moran, M. F., & Neel, B. G. (2011). Global proteomic assessment of the classical protein-tyrosine phosphatome and "Redoxome". *Cell,* **146** (5): 826-840.

Karpova, O. V., Kuzmin, E. V., Elthon, T. E., & Newton, K. J. (2002). Differential expression of alternative oxidase genes in maize mitochondrial mutants. *Plant Cell,* **14** (12): 3271-3284.

Kayikci, O., & Nielsen, J. (2015). Glucose repression in *Saccharomyces cerevisiae*. *FEMS Yeast Res.,* **15** (6).

Kazlauskaite, A., & Muqit, M. M. (2015). PINK1 and Parkin - mitochondrial interplay between phosphorylation and ubiquitylation in Parkinson's disease. *FEBS J.,* **282** (2): 215-223.

Kemppainen, K. K., Kemppainen, E., & Jacobs, H. T. (2014a). The alternative oxidase AOX does not rescue the phenotype of tko25t mutant flies. *G3,* **4** (10): 2013-2021.

Kemppainen, K. K., Rinne, J., Sriram, A., Lakanmaa, M., Zeb, A., Tuomela, T., Popplestone, A., Singh, S., Sanz, A., Rustin, P., & Jacobs, H. T. (2014b). Expression of alternative oxidase in Drosophila ameliorates diverse phenotypes due to cytochrome oxidase deficiency. *Hum. Mol. Genet.,* **23** (8): 2078-2093.

Keppler, D. (2011). Multidrug resistance proteins (MRPs, ABCCs): importance for pathophysiology and drug therapy. *Handb. Exp. Pharmacol.,* (201): 299-323.

Kern, A., Hartner, F. S., Freigassner, M., Spielhofer, J., Rumpf, C., Leitner, L., Frohlich, K. U., & Glieder, A. (2007). *Pichia pastoris* "just in time" alternative respiration. *Microbiology,* **153** (Pt 4): 1250-1260.

Kikuchi, G., Motokawa, Y., Yoshida, T., & Hiraga, K. (2008). Glycine cleavage system: reaction mechanism, physiological significance, and hyperglycinemia. *Proc. Jpn. Acad. Ser. B Phys. Biol. Sci.,* **84** (7): 246-263.

Kim, T. K., & Shiekhattar, R. (2015). Architectural and functional commonalities between enhancers and promoters. *Cell,* **162** (5): 948-959.

King, D. A., Zhang, L., Guarente, L., & Marmorstein, R. (1999). Structure of a HAP1-DNA complex reveals dramatically asymmetric DNA binding by a homodimeric protein. *Nat. Struct. Biol.,* **6** (1): 64-71.

Kinoshita, E., Kinoshita-Kikuta, E., & Koike, T. (2009). Separation and detection of large phosphoproteins using Phos-tag SDS-PAGE. *Nat. Protoc.,* **4** (10): 1513-1521.

Kirchman, P. A., Kim, S., Lai, C. Y., & Jazwinski, S. M. (1999). Interorganelle signaling is a determinant of longevity in *Saccharomyces cerevisiae*. *Genetics,* **152** (1): 179-190.

Kirkpatrick, C. R., & Schimmel, P. (1995). Detection of leucine-independent DNA site occupancy of the yeast Leu3p transcriptional activator *in vivo*. *Mol. Cell. Biol.,* **15** (8): 4021-4030.

Klein, A., Israel, L., Lackey, S. W., Nargang, F. E., Imhof, A., Baumeister, W., Neupert, W., & Thomas, D. R. (2012). Characterization of the insertase for beta-barrel proteins of the outer mitochondrial membrane. *J. Cell. Biol.,* **199** (4): 599-611.

Kmita, K., & Zickermann, V. (2013). Accessory subunits of mitochondrial complex I. *Biochem. Soc. Trans.,* **41** (5): 1272-1279.

Komeili, A., Wedaman, K. P., O'Shea, E. K., & Powers, T. (2000). Mechanism of metabolic control. Target of rapamycin signaling links nitrogen quality to the activity of the Rtg1 and Rtg3 transcription factors. *J. Cell. Biol.,* **151** (4): 863-878.

Koonin, E. V. (2015). Archaeal ancestors of eukaryotes: not so elusive any more. *BMC Biol.,* **13**: 84.

Kornmann, B., Currie, E., Collins, S. R., Schuldiner, M., Nunnari, J., Weissman, J. S., & Walter, P. (2009). An ER-mitochondria tethering complex revealed by a synthetic biology screen. *Science,* **325** (5939): 477-481.

Kornmann, B., Osman, C., & Walter, P. (2011). The conserved GTPase Gem1 regulates endoplasmic reticulum-mitochondria connections. *Proc. Natl. Acad. Sci. U S A,* **108** (34): 14151-14156.

Kornmann, B., & Walter, P. (2010). ERMES-mediated ER-mitochondria contacts: molecular hubs for the regulation of mitochondrial biology. *J. Cell Sci.,* **123** (Pt 9): 1389-1393.

Koussevitzky, S., Nott, A., Mockler, T. C., Hong, F., Sachetto-Martins, G., Surpin, M., Lim, J., Mittler, R., & Chory, J. (2007). Signals from chloroplasts converge to regulate nuclear gene expression. *Science,* **316** (5825): 715-719.

Kuhlbrandt, W. (2015). Structure and function of mitochondrial membrane protein complexes. *BMC Biol.,* **13**: 89.

Kujoth, G. C., Hiona, A., Pugh, T. D., Someya, S., Panzer, K., Wohlgemuth, S. E., Hofer, T., Seo, A. Y., Sullivan, R., Jobling, W. A., Morrow, J. D., Van Remmen, H., Sedivy, J. M., Yamasoba, T., Tanokura, M., Weindruch, R., Leeuwenburgh, C., & Prolla, T. A. (2005). Mitochondrial DNA mutations, oxidative stress, and apoptosis in mammalian aging. *Science,* **309** (5733): 481-484.

Kumar, A., & Bachhawat, A. K. (2010). OXP1/YKL215c encodes an ATP-dependent 5-oxoprolinase in *Saccharomyces cerevisiae*: functional characterization, domain structure and identification of actin-like ATP-binding motifs in eukaryotic 5-oxoprolinases. *FEMS Yeast Res.,* **10** (4): 394-401.

Kuras, L., & Struhl, K. (1999). Binding of TBP to promoters *in vivo* is stimulated by activators and requires Pol II holoenzyme. *Nature,* **399** (6736): 609-613.

Kutik, S., Stojanovski, D., Becker, L., Becker, T., Meinecke, M., Kruger, V., Prinz, C., Meisinger, C., Guiard, B., Wagner, R., Pfanner, N., & Wiedemann, N. (2008). Dissecting membrane insertion of mitochondrial beta-barrel proteins. *Cell,* **132** (6): 1011-1024.

Labbe, K., Murley, A., & Nunnari, J. (2014). Determinants and functions of mitochondrial behavior. *Annu. Rev. Cell Dev. Biol.,* **30**: 357-391.

Lackey, S. W., Taylor, R. D., Go, N. E., Wong, A., Sherman, E. L., & Nargang, F. E. (2014). Evidence supporting the 19 beta-strand model for Tom40 from cysteine scanning and protease site accessibility studies. *J. Biol. Chem.,* **289** (31): 21640-21650.

Laemmli, U. K. (1970). Cleavage of structural proteins during the assembly of the head of bacteriophage T4. *Nature,* **227** (5259): 680-685.

Lake, J. A., Henderson, E., Oakes, M., & Clark, M. W. (1984). Eocytes: a new ribosome structure indicates a kingdom with a close relationship to eukaryotes. *Proc. Natl. Acad. Sci. U S A,* **81** (12): 3786-3790.

Lambowitz, A. M. (1979). Preparation and analysis of mitochondrial ribosomes. *Methods Enzymol.,* **59**: 421-433.

Lang, A., John Peter, A. T., & Kornmann, B. (2015). ER-mitochondria contact sites in yeast: beyond the myths of ERMES. *Curr. Opin. Cell Biol.,* **35**: 7-12.

Lapuente-Brun, E., Moreno-Loshuertos, R., Acin-Perez, R., Latorre-Pellicer, A., Colas, C., Balsa, E., Perales-Clemente, E., Quiros, P. M., Calvo, E., Rodriguez-Hernandez, M. A., Navas, P., Cruz, R., Carracedo, A., Lopez-Otin, C., Perez-Martos, A., Fernandez-Silva, P., Fernandez-Vizarra, E., & Enriquez, J. A. (2013). Supercomplex assembly determines electron flux in the mitochondrial electron transport chain. *Science,* **340** (6140): 1567-1570.

Larkin, M. A., Blackshields, G., Brown, N. P., Chenna, R., McGettigan, P. A., McWilliam, H., Valentin, F., Wallace, I. M., Wilm, A., Lopez, R., Thompson, J. D., Gibson, T. J., & Higgins, D. G. (2007). Clustal W and Clustal X version 2.0. *Bioinformatics,* **23** (21): 2947-2948.

Lee, S. S., Lee, R. Y., Fraser, A. G., Kamath, R. S., Ahringer, J., & Ruvkun, G. (2003). A systematic RNAi screen identifies a critical role for mitochondria in *C. elegans* longevity. *Nat. Genet.,* **33** (1): 40-48.

Leon, P., Gregorio, J., & Cordoba, E. (2012). ABI4 and its role in chloroplast retrograde communication. *Front Plant Sci.,* **3**: 304.

Levo, M., Zalckvar, E., Sharon, E., Dantas Machado, A. C., Kalma, Y., Lotam-Pompan, M., Weinberger, A., Yakhini, Z., Rohs, R., & Segal, E. (2015). Unraveling determinants of transcription factor binding outside the core binding site. *Genome Res.,* **25** (7): 1018-1029.

Li, Q., Ritzel, R. G., McLean, L. L., McIntosh, L., Ko, T., Bertrand, H., & Nargang, F. E. (1996). Cloning and analysis of the alternative oxidase gene of *Neurospora crassa*.

Genetics, **142** (1): 129-140.

Li, Z. S., Szczypka, M., Lu, Y. P., Thiele, D. J., & Rea, P. A. (1996). The yeast cadmium factor protein (YCF1) is a vacuolar glutathione S-conjugate pump. *J. Biol. Chem.,* **271** (11): 6509-6517.

Li, Z., & Xing, D. (2011). Mechanistic study of mitochondria-dependent programmed cell death induced by aluminium phytotoxicity using fluorescence techniques. *J. Exp. Bot.,* **62** (1): 331-343.

Liao, X., & Butow, R. A. (1993). RTG1 and RTG2: two yeast genes required for a novel path of communication from mitochondria to the nucleus. *Cell,* **72** (1): 61-71.

Liao, X. S., Small, W. C., Srere, P. A., & Butow, R. A. (1991). Intramitochondrial functions regulate nonmitochondrial citrate synthase (CIT2) expression in Saccharomyces cerevisiae. *Mol. Cell Biol.,* **11** (1): 38-46.

Lightowlers, R. N., & Chrzanowska-Lightowlers, Z. M. (2013). Human pentatricopeptide proteins: only a few and what do they do? *RNA Biol.,* **10** (9): 1433-1438.

Lister, R., Chew, O., Lee, M. N., Heazlewood, J. L., Clifton, R., Parker, K. L., Millar, A. H., & Whelan, J. (2004). A transcriptomic and proteomic characterization of the Arabidopsis mitochondrial protein import apparatus and its response to mitochondrial dysfunction. *Plant Physiol.,* **134** (2): 777-789.

Liu, H., Gravelat, F. N., Chiang, L. Y., Chen, D., Vanier, G., Ejzykowicz, D. E., Ibrahim, A. S., Nierman, W. C., Sheppard, D. C., & Filler, S. G. (2010). *Aspergillus fumigatus* AcuM regulates both iron acquisition and gluconeogenesis. *Mol. Microbiol.,* **78** (4): 1038-1054.

Liu, J., & Barrientos, A. (2013). Transcriptional regulation of yeast oxidative phosphorylation hypoxic genes by oxidative stress. *Antioxid. Redox Signal.,* **19** (16): 1916-1927.

Liu, Y., Hyde, A. S., Simpson, M. A., & Barycki, J. J. (2014). Emerging regulatory paradigms in glutathione metabolism. *Adv. Cancer Res.,* **122**: 69-101.

Liu, Z., & Butow, R. A. (1999). A transcriptional switch in the expression of yeast tricarboxylic acid cycle genes in response to a reduction or loss of respiratory function. *Mol. Cell Biol.,* **19** (10): 6720-6728.

Liu, Z., Sekito, T., Epstein, C. B., & Butow, R. A. (2001). RTG-dependent mitochondria to nucleus signaling is negatively regulated by the seven WD-repeat

protein Lst8p. *EMBO J.,* **20** (24): 7209-7219.

Liu, Z., Sekito, T., Špírek, M., Thornton, J., & Butow, R. A. (2003). Retrograde signaling is regulated by the dynamic interaction between Rtg2p and Mks1p. *Mol. Cell,* **12** (2): 401-411.

Liu, Z., Spirek, M., Thornton, J., & Butow, R. A. (2005). A novel degron-mediated degradation of the RTG pathway regulator, Mks1p, by SCFGrr1. *Mol. Biol. Cell,* **16** (10): 4893-4904.

Lodi, T., & Guiard, B. (1991). Complex transcriptional regulation of the *Saccharomyces cerevisiae* CYB2 gene encoding cytochrome b2: CYP1(HAP1) activator binds to the CYB2 upstream activation site UAS1-B2. *Mol. Cell. Biol.,* **11** (7): 3762-3772.

Loewith, R., & Hall, M. N. (2011). Target of rapamycin (TOR) in nutrient signaling and growth control. *Genetics,* **189** (4): 1177-1201.

Longen, S., Woellhaf, M. W., Petrungaro, C., Riemer, J., & Herrmann, J. M. (2014). The disulfide relay of the intermembrane space oxidizes the ribosomal subunit mrp10 on its transit into the mitochondrial matrix. *Dev. Cell,* **28** (1): 30-42.

Longo, V. D., Shadel, G. S., Kaeberlein, M., & Kennedy, B. (2012). Replicative and chronological aging in *Saccharomyces cerevisiae*. *Cell Metab.,* **16** (1): 18-31.

Lord, C. C., Thomas, G., & Brown, J. M. (2013). Mammalian alpha beta hydrolase domain (ABHD) proteins: Lipid metabolizing enzymes at the interface of cell signaling and energy metabolism. *Biochim. Biophys. Acta.,* **1831** (4): 792-802.

Lowry, C. V., & Zitomer, R. S. (1988). ROX1 encodes a heme-induced repression factor regulating ANB1 and CYC7 of *Saccharomyces cerevisiae*. *Mol. Cell. Biol.,* **8** (11): 4651-4658.

Lu, S. C. (2009). Regulation of glutathione synthesis. *Mol. Aspects Med.,* **30** (1-2): 42-59.

Lu, S. C. (2013). Glutathione synthesis. *Biochim. Biophys. Acta.,* **1830** (5): 3143-3153.

MacPherson, S., Larochelle, M., & Turcotte, B. (2006). A fungal family of transcriptional regulators: the zinc cluster proteins. *Microbiol. Mol. Biol. Rev.,* **70** (3): 583-604.

Mager, F., Gessmann, D., Nussberger, S., & Zeth, K. (2011). Functional refolding and

characterization of two Tom40 isoforms from human mitochondria. *J. Membr. Biol.,* **242** (1): 11-21.

Magnani, T., Soriani, F. M., Martins Vde, P., Policarpo, A. C., Sorgi, C. A., Faccioli, L. H., Curti, C., & Uyemura, S. A. (2008). Silencing of mitochondrial alternative oxidase gene of *Aspergillus fumigatus* enhances reactive oxygen species production and killing of the fungus by macrophages. *J. Bioenerg. Biomembr.,* **40** (6): 631-636.

Magnani, T., Soriani, F. M., Martins, V. P., Nascimento, A. M., Tudella, V. G., Curti, C., & Uyemura, S. A. (2007). Cloning and functional expression of the mitochondrial alternative oxidase of *Aspergillus fumigatus* and its induction by oxidative stress. *FEMS Microbiol. Lett.,* **271** (2): 230-238.

Malhotra, K., Sathappa, M., Landin, J. S., Johnson, A. E., & Alder, N. N. (2013). Structural changes in the mitochondrial Tim23 channel are coupled to the proton-motive force. *Nat. Struct. Mol. Biol.,* **20** (8): 965-972.

Maranzana, E., Barbero, G., Falasca, A. I., Lenaz, G., & Genova, M. L. (2013). Mitochondrial respiratory supercomplex association limits production of reactive oxygen species from complex I. *Antioxid. Redox Signal.,* **19** (13): 1469-1480.

Marchot, P., & Chatonnet, A. (2012). Enzymatic activity and protein interactions in alpha/beta hydrolase fold proteins: moonlighting versus promiscuity. *Protein Pept. Lett.,* **19** (2): 132-143.

Margulis, L. (1970). Origin of Eukaryotic Cells. New Haven, CT: Yale University Press

Marin-Buera, L., Garcia-Bartolome, A., Moran, M., Lopez-Bernardo, E., Cadenas, S., Hidalgo, B., Sanchez, R., Seneca, S., Arenas, J., Martin, M. A., & Ugalde, C. (2014). Differential proteomic profiling unveils new molecular mechanisms associated with mitochondrial complex III deficiency. *J. Proteomics,* **113C**: 38-56.

Martinez-Caballero, S., Grigoriev, S. M., Herrmann, J. M., Campo, M. L., & Kinnally, K. W. (2007). Tim17p regulates the twin pore structure and voltage gating of the mitochondrial protein import complex TIM23. *J. Biol. Chem.,* **282** (6): 3584-3593.

Martins, V. P., Dinamarco, T. M., Soriani, F. M., Tudella, V. G., Oliveira, S. C., Goldman, G. H., Curti, C., & Uyemura, S. A. (2011). Involvement of an alternative oxidase in oxidative stress and mycelium-to-yeast differentiation in *Paracoccidioides brasiliensis*. *Eukaryot. Cell,* **10** (2): 237-248.

Martyanov, V., & Gross, R. H. (2011). Using SCOPE to identify potential regulatory motifs in coregulated genes. *J. Vis. Exp.,* (51).

Maxwell, D. P., Nickels, R., & McIntosh, L. (2002). Evidence of mitochondrial involvement in the transduction of signals required for the induction of genes associated with pathogen attack and senescence. *Plant J.,* **29** (3): 269-279.

McClung, J. K., Danner, D. B., Stewart, D. A., Smith, J. R., Schneider, E. L., Lumpkin, C. K., Dell'Orco, R. T., & Nuell, M. J. (1989). Isolation of a cDNA that hybrid selects antiproliferative mRNA from rat liver. *Biochem. Biophys. Res. Commun.,* **164** (3): 1316-1322.

McDonald, A., & Vanlerberghe, G. (2004). Branched mitochondrial electron transport in the Animalia: presence of alternative oxidase in several animal phyla. *IUBMB Life,* **56** (6): 333-341.

McDonald, A. E. (2008). Alternative oxidase: an inter-kingdom perspective on the function and regulation of this broadly distributed 'cyanide-resistant' terminal oxidase. *Funct. Plant Biol.,* **35** (7): 535-552.

McDonald, A. E., Amirsadeghi, S., & Vanlerberghe, G. C. (2003). Prokaryotic orthologues of mitochondrial alternative oxidase and plastid terminal oxidase. *Plant Mol. Biol.,* **53** (6): 865-876.

McDonald, A. E., Ivanov, A. G., Bode, R., Maxwell, D. P., Rodermel, S. R., & Huner, N. P. (2011). Flexibility in photosynthetic electron transport: the physiological role of plastoquinol terminal oxidase (PTOX). *Biochim. Biophys. Acta.,* **1807** (8): 954-967.

McDonald, A. E., & Vanlerberghe, G. C. (2005). Alternative oxidase and plastoquinol terminal oxidase in marine prokaryotes of the Sargasso Sea. *Gene,* **349**: 15-24.

McDonald, A. E., & Vanlerberghe, G. C. (2006). Origins, evolutionary history, and taxonomic distribution of alternative oxidase and plastoquinol terminal oxidase. *Comp. Biochem. Physiol. Part D Genomics Proteomics,* **1** (3): 357-364.

McDonald, A. E., Vanlerberghe, G. C., & Staples, J. F. (2009). Alternative oxidase in animals: unique characteristics and taxonomic distribution. *J. Exp. Biol.,* **212** (Pt 16): 2627-2634.

Medentsev, A. G., & Akimenko, V. K. (1999). Development and activation of cyanide-resistant respiration in the yeast *Yarrowia lipolytica*. *Biochemistry,* **64** (8): 945-951.

Meeuse, B. J. D. (1975). Thermogenic Respiration in Aroids. *Annu. Rev. Plant Physiol.,* **26** (1): 117-126.

Michel, A. H., & Kornmann, B. (2012). The ERMES complex and ER-mitochondria

connections. *Biochem. Soc. Trans.,* **40** (2): 445-450.

Milenkovic, D., Ramming, T., Muller, J. M., Wenz, L. S., Gebert, N., Schulze-Specking, A., Stojanovski, D., Rospert, S., & Chacinska, A. (2009). Identification of the signal directing Tim9 and Tim10 into the intermembrane space of mitochondria. *Mol. Biol. Cell,* **20** (10): 2530-2539.

Millar, A. H., Wiskich, J. T., Whelan, J., & Day, D. A. (1993). Organic acid activation of the alternative oxidase of plant mitochondria. *FEBS Lett.,* **329** (3): 259-262.

Millenaar, F. F., Gonzalez-Meler, M. A., Siedow, J. N., Wagner, A. M., & Lambers, H. (2002). Role of sugars and organic acids in regulating the concentration and activity of the alternative oxidase in *Poa annua* roots. *J. Exp. Bot.,* **53** (371): 1081-1088.

Millenaar, F. F. a. L., H. (2003). The alternative oxidase: *in vivo* regulation and function. *Plant Biol.,* **5**: 2-15.

Minagawa, N., Koga, S., Nakano, M., Sakajo, S., & Yoshimoto, A. (1992). Possible involvement of superoxide anion in the induction of cyanide-resistant respiration in Hansenula anomala. *FEBS Lett.,* **302** (3): 217-219.

Minagawa, N., Sakajo, S., Komiyama, T., & Yoshimoto, A. (1990). Essential role of ferrous iron in cyanide-resistant respiration in *Hansenula anomala*. *FEBS Lett.,* **267** (1): 114-116.

Mishra, P., & Chan, D. C. (2016). Metabolic regulation of mitochondrial dynamics. *J. Cell. Biol.*, 212 (4): 379-387.

Mokranjac, D., & Neupert, W. (2010). The many faces of the mitochondrial TIM23 complex. *Biochim. Biophys. Acta.,* **1797** (6-7): 1045-1054.

Moore, A. L., Shiba, T., Young, L., Harada, S., Kita, K., & Ito, K. (2013). Unraveling the heater: new insights into the structure of the alternative oxidase. *Annu. Rev. Plant Biol.,* **64**: 637-663.

Moparthi, V. K., Kumar, B., Al-Eryani, Y., Sperling, E., Gorecki, K., Drakenberg, T., & Hagerhall, C. (2014). Functional role of the MrpA- and MrpD-homologous protein subunits in enzyme complexes evolutionary related to respiratory chain complex I. *Biochim. Biophys. Acta.,* **1837** (1): 178-185.

Moparthi, V. K., Kumar, B., Mathiesen, C., & Hagerhall, C. (2011). Homologous protein subunits from Escherichia coli NADH:quinone oxidoreductase can functionally replace MrpA and MrpD in Bacillus subtilis. *Biochim. Biophys. Acta.,* **1807** (4): 427-436.

Morgan, B., Ezerina, D., Amoako, T. N., Riemer, J., Seedorf, M., & Dick, T. P. (2013). Multiple glutathione disulfide removal pathways mediate cytosolic redox homeostasis. *Nat. Chem. Biol.,* **9** (2): 119-125.

Morschhauser, J., Barker, K. S., Liu, T. T., Bla, B. W. J., Homayouni, R., & Rogers, P. D. (2007). The transcription factor Mrr1p controls expression of the MDR1 efflux pump and mediates multidrug resistance in Candida albicans. *PLoS Pathog.,* **3** (11): e164.

Mossmann, D., Meisinger, C., & Vogtle, F. N. (2012). Processing of mitochondrial presequences. *Biochim. Biophys. Acta.,* **1819** (9-10): 1098-1106.

Mozdy, A. D., McCaffery, J. M., & Shaw, J. M. (2000). Dnm1p GTPase-mediated mitochondrial fission is a multi-step process requiring the novel integral membrane component Fis1p. *J. Cell. Biol.,* **151** (2): 367-380.

Nakamura, K., Sakamoto, K., Kido, Y., Fujimoto, Y., Suzuki, T., Suzuki, M., Yabu, Y., Ohta, N., Tsuda, A., Onuma, M., & Kita, K. (2005). Mutational analysis of the *Trypanosoma vivax* alternative oxidase: the E(X)6Y motif is conserved in both mitochondrial alternative oxidase and plastid terminal oxidase and is indispensable for enzyme activity. *Biochem. Biophys. Res. Commun.,* **334** (2): 593-600.

Nargang, F. E., Adames, K., Rub, C., Cheung, S., Easton, N., Nargang, C. E., & Chae, M. S. (2012). Identification of genes required for alternative oxidase production in the *Neurospora crassa* gene knockout library. *G3,* **2** (11): 1345-1356.

Nargang, F. E., & Rapaport, D. (2007). *Neurospora crassa* as a model organism for mitochondrial biogenesis. *Methods Mol. Biol.,* **372**: 107-123.

Nargund, A. M., Pellegrino, M. W., Fiorese, C. J., Baker, B. M., & Haynes, C. M. (2012). Mitochondrial import efficiency of ATFS-1 regulates mitochondrial UPR activation. *Science,* **337** (6094): 587-590.

Neimanis, K., Staples, J. F., Huner, N. P., & McDonald, A. E. (2013). Identification, expression, and taxonomic distribution of alternative oxidases in non-angiosperm plants. *Gene,* **526** (2): 275-286.

Nelson, D. L., & Cox, M. M. (2013). Lehninger Principles of Biochemistry. New York: W.H. Freeman.

Neupert, W. (2015). A perspective on transport of proteins into mitochondria: a myriad of open questions. *J. Mol. Biol.,* **427** (6 Pt A): 1135-1158.

Nevoigt, E., & Stahl, U. (1997). Osmoregulation and glycerol metabolism in the yeast

Saccharomyces cerevisiae. *FEMS Microbiol. Rev.,* **21** (3): 231-241.

Ng, S., Giraud, E., Duncan, O., Law, S. R., Wang, Y., Xu, L., Narsai, R., Carrie, C., Walker, H., Day, D. A., Blanco, N. E., Strand, A., Whelan, J., & Ivanova, A. (2013a). Cyclin-dependent kinase E1 (CDKE1) provides a cellular switch in plants between growth and stress responses. *J. Biol. Chem.,* **288** (5): 3449-3459.

Ng, S., Ivanova, A., Duncan, O., Law, S. R., Van Aken, O., De Clercq, I., Wang, Y., Carrie, C., Xu, L., Kmiec, B., Walker, H., Van Breusegem, F., Whelan, J., & Giraud, E. (2013b). A membrane-bound NAC transcription factor, ANAC017, mediates mitochondrial retrograde signaling in Arabidopsis. *Plant Cell,* **25** (9): 3450-3471.

Noguchi, Y., Sano, M., Kanamaru, K., Ko, T., Takeuchi, M., Kato, M., & Kobayashi, T. (2009). Genes regulated by AoXlnR, the xylanolytic and cellulolytic transcriptional regulator, in *Aspergillus oryzae*. *Appl. Microbiol. Biotechnol.,* **85** (1): 141-154.

Olsen, A. N., Ernst, H. A., Leggio, L. L., & Skriver, K. (2005). NAC transcription factors: structurally distinct, functionally diverse. *Trends Plant Sci.,* **10** (2): 79-87.

Ong, C. T., & Corces, V. G. (2011). Enhancer function: new insights into the regulation of tissue-specific gene expression. *Nat. Rev. Genet.,* **12** (4): 283-293.

Ortiz, D. F., St Pierre, M. V., Abdulmessih, A., & Arias, I. M. (1997). A yeast ATP-binding cassette-type protein mediating ATP-dependent bile acid transport. *J. Biol. Chem.,* **272** (24): 15358-15365.

Ostermeier, C., Harrenga, A., Ermler, U., & Michel, H. (1997). Structure at 2.7 A resolution of the *Paracoccus denitrificans* two-subunit cytochrome c oxidase complexed with an antibody FV fragment. *Proc. Natl. Acad. Sci. U S A,* **94** (20): 10547-10553.

Palmer, C. S., Osellame, L. D., Laine, D., Koutsopoulos, O. S., Frazier, A. E., & Ryan, M. T. (2011). MiD49 and MiD51, new components of the mitochondrial fission machinery. *EMBO Rep.,* **12** (6): 565-573.

Papa, L., & Germain, D. (2011). Estrogen receptor mediates a distinct mitochondrial unfolded protein response. *J. Cell Sci.,* **124** (Pt 9): 1396-1402.

Papic, D., Krumpe, K., Dukanovic, J., Dimmer, K. S., & Rapaport, D. (2011). Multispan mitochondrial outer membrane protein Ugo1 follows a unique Mim1-dependent import pathway. *J. Cell. Biol.,* **194** (3): 397-405.

Park, P. J. (2009). ChIP-seq: advantages and challenges of a maturing technology. *Nat. Rev. Genet.,* **10** (10): 669-680.

Partch, C. L., & Gardner, K. H. (2010). Coactivator recruitment: a new role for PAS domains in transcriptional regulation by the bHLH-PAS family. *J. Cell. Physiol.,* **223** (3): 553-557.

Pasqualini, S., Paolocci, F., Borgogni, A., Morettini, R., & Ederli, L. (2007). The overexpression of an alternative oxidase gene triggers ozone sensitivity in tobacco plants. *Plant Cell Environ.,* **30** (12): 1545-1556.

Paul, S., & Moye-Rowley, W. S. (2014). Multidrug resistance in fungi: regulation of transporter-encoding gene expression. *Front. Physiol.,* **5**: 143.

Paumi, C. M., Chuk, M., Snider, J., Stagljar, I., & Michaelis, S. (2009). ABC transporters in *Saccharomyces cerevisiae* and their interactors: new technology advances the biology of the ABCC (MRP) subfamily. *Microbiol. Mol. Biol. Rev.,* **73** (4): 577-593.

Payne, B. A., & Chinnery, P. F. (2015). Mitochondrial dysfunction in aging: Much progress but many unresolved questions. *Biochim. Biophys. Acta.,* **1847** (11): 1347-1353.

Pfanner, N., van der Laan, M., Amati, P., Capaldi, R. A., Caudy, A. A., Chacinska, A., Darshi, M., Deckers, M., Hoppins, S., Icho, T., Jakobs, S., Ji, J., Kozjak-Pavlovic, V., Meisinger, C., Odgren, P. R., Park, S. K., Rehling, P., Reichert, A. S., Sheikh, M. S., Taylor, S. S., Tsuchida, N., van der Bliek, A. M., van der Klei, I. J., Weissman, J. S., Westermann, B., Zha, J., Neupert, W., & Nunnari, J. (2014). Uniform nomenclature for the mitochondrial contact site and cristae organizing system. *J. Cell. Biol.,* **204** (7): 1083-1086.

Pfeifer, K., Arcangioli, B., & Guarente, L. (1987a). Yeast HAP1 activator competes with the factor RC2 for binding to the upstream activation site UAS1 of the CYC1 gene. *Cell,* **49** (1): 9-18.

Pfeifer, K., Prezant, T., & Guarente, L. (1987b). Yeast HAP1 activator binds to two upstream activation sites of different sequence. *Cell,* **49** (1): 19-27.

Pickrell, A. M., & Youle, R. J. (2015). The roles of PINK1, parkin, and mitochondrial fidelity in Parkinson's disease. *Neuron,* **85** (2): 257-273.

Pinto, M., & Moraes, C. T. (2014). Mitochondrial genome changes and neurodegenerative diseases. *Biochim. Biophys. Acta.,* **1842** (8): 1198-1207.

Polge, C., & Thomas, M. (2007). SNF1/AMPK/SnRK1 kinases, global regulators at the heart of energy control? *Trends Plant Sci.,* **12** (1): 20-28.

Polidoros, A. N., Mylona, P. V., Pasentsis, K., Scandalios, J. G., & Tsaftaris, A. S. (2005). The maize alternative oxidase 1a (Aox1a) gene is regulated by signals related to oxidative stress. *Redox Rep.,* **10** (2): 71-78.

Pongpom, M., Liu, H., Xu, W., Snarr, B. D., Sheppard, D. C., Mitchell, A. P., & Filler, S. G. (2015). Divergent targets of *Aspergillus fumigatus* AcuK and AcuM transcription factors during growth *in vitro* versus invasive disease. *Infect. Immun.,* **83** (3): 923-933.

Popov-Celeketic, D., Waegemann, K., Mapa, K., Neupert, W., & Mokranjac, D. (2011). Role of the import motor in insertion of transmembrane segments by the mitochondrial TIM23 complex. *EMBO Rep.,* **12** (6): 542-548.

Porras, C. A., & Bai, Y. (2015). Respiratory supercomplexes: plasticity and implications. *Front. Biosci.,* **20**: 621-634.

Priebe, S., Kreisel, C., Horn, F., Guthke, R., & Linde, J. (2015). FungiFun2: a comprehensive online resource for systematic analysis of gene lists from fungal species. *Bioinformatics,* **31** (3): 445-446.

Pusztahelyi, T., Klement, E., Szajli, E., Klem, J., Miskei, M., Karanyi, Z., Emri, T., Kovacs, S., Orosz, G., Kovacs, K. L., Medzihradszky, K. F., Prade, R. A., & Pocsi, I. (2011). Comparison of transcriptional and translational changes caused by long-term menadione exposure in *Aspergillus nidulans*. *Fungal Genet. Biol.,* **48** (2): 92-103.

Qiu, J., Wenz, L. S., Zerbes, R. M., Oeljeklaus, S., Bohnert, M., Stroud, D. A., Wirth, C., Ellenrieder, L., Thornton, N., Kutik, S., Wiese, S., Schulze-Specking, A., Zufall, N., Chacinska, A., Guiard, B., Hunte, C., Warscheid, B., van der Laan, M., Pfanner, N., Wiedemann, N., & Becker, T. (2013). Coupling of mitochondrial import and export translocases by receptor-mediated supercomplex formation. *Cell,* **154** (3): 596-608.

Quinlan, C. L., Treberg, J. R., Perevoshchikova, I. V., Orr, A. L., & Brand, M. D. (2012). Native rates of superoxide production from multiple sites in isolated mitochondria measured using endogenous reporters. *Free Radic. Biol. Med.,* **53** (9): 1807-1817.

Rastogi, V. K., & Girvin, M. E. (1999). Structural changes linked to proton translocation by subunit c of the ATP synthase. *Nature,* **402** (6759): 263-268.

Rath, E., Berger, E., Messlik, A., Nunes, T., Liu, B., Kim, S. C., Hoogenraad, N., Sans, M., Sartor, R. B., & Haller, D. (2012). Induction of dsRNA-activated protein kinase links mitochondrial unfolded protein response to the pathogenesis of intestinal inflammation. *Gut,* **61** (9): 1269-1278.

Ratnakumar, S., Kacherovsky, N., Arms, E., & Young, E. T. (2009). Snf1 controls the activity of adr1 through dephosphorylation of Ser230. *Genetics,* **182** (3): 735-745.

Reczek, C. R., & Chandel, N. S. (2015). ROS-dependent signal transduction. *Curr. Opin. Cell Biol.,* **33**: 8-13.

Rees, D. M., Leslie, A. G., & Walker, J. E. (2009). The structure of the membrane extrinsic region of bovine ATP synthase. *Proc. Natl. Acad. Sci. U S A,* **106** (51): 21597-21601.

Reichert, A. S., & Neupert, W. (2002). Contact sites between the outer and inner membrane of mitochondria—role in protein transport. *Biochim. Biophys. Acta.,* **1592** (1): 41-49.

Rhoads, D. M., & McIntosh, L. (1991). Isolation and characterization of a cDNA clone encoding an alternative oxidase protein of *Sauromatum guttatum* (Schott). *Proc. Natl. Acad. Sci. U S A,* **88** (6): 2122-2126.

Rhoads, D. M., & McIntosh, L. (1993). Cytochrome and alternative pathway respiration in tobacco (effects of salicylic acid). *Plant Physiol.,* **103** (3): 877-883.

Rhoads, D. M., & Subbaiah, C. C. (2007). Mitochondrial retrograde regulation in plants. *Mitochondrion,* **7** (3): 177-194.

Rhoads, D. M., Umbach, A. L., Sweet, C. R., Lennon, A. M., Rauch, G. S., & Siedow, J. N. (1998). Regulation of the cyanide-resistant alternative oxidase of plant mitochondria. Identification of the cysteine residue involved in alpha-keto acid stimulation and intersubunit disulfide bond formation. *J. Biol. Chem.,* **273** (46): 30750-30756.

Ribas, V., Garcia-Ruiz, C., & Fernandez-Checa, J. C. (2014). Glutathione and mitochondria. *Front. Pharmacol.,* **5**: 151.

Richardson, B. G., Jain, A. D., Speltz, T. E., & Moore, T. W. (2015). Non-electrophilic modulators of the canonical Keap1/Nrf2 pathway. *Bioorg. Med. Chem. Lett.,* **25** (11): 2261-2268.

Riemer, J., Fischer, M., & Herrmann, J. M. (2011). Oxidation-driven protein import into mitochondria: Insights and blind spots. *Biochim. Biophys. Acta.,* **1808** (3): 981-989.

Robson, C. A., & Vanlerberghe, G. C. (2002). Transgenic plant cells lacking mitochondrial alternative oxidase have increased susceptibility to mitochondria-dependent and -independent pathways of programmed cell death. *Plant*

Physiol., **129** (4): 1908-1920.

Rogov, A. G., Sukhanova, E. I., Uralskaya, L. A., Aliverdieva, D. A., & Zvyagilskaya, R. A. (2014). Alternative oxidase: distribution, induction, properties, structure, regulation, and functions. *Biochemistry,* **79** (13): 1615-1634.

Ross, D., Thor, H., Orrenius, S., & Moldeus, P. (1985). Interaction of menadione (2-methyl-1,4-naphthoquinone) with glutathione. *Chem. Biol. Interact.,* **55** (1-2): 177-184.

Rothermel, B. A., Thornton, J. L., & Butow, R. A. (1997). Rtg3p, a basic helix-loop-helix/leucine zipper protein that functions in mitochondrial-induced changes in gene expression, contains independent activation domains. *J. Biol. Chem.,* **272** (32): 19801-19807.

Ruepp, A., Zollner, A., Maier, D., Albermann, K., Hani, J., Mokrejs, M., Tetko, I., Guldener, U., Mannhaupt, G., Munsterkotter, M., & Mewes, H. W. (2004). The FunCat, a functional annotation scheme for systematic classification of proteins from whole genomes. *Nucleic Acids Res.,* **32** (18): 5539-5545.

Ruiz-Roig, C., Noriega, N., Duch, A., Posas, F., & de Nadal, E. (2012). The Hog1 SAPK controls the Rtg1/Rtg3 transcriptional complex activity by multiple regulatory mechanisms. *Mol. Biol. Cell,* **23** (21): 4286-4296.

Ruiz, O. H., Gonzalez, A., Almeida, A. J., Tamayo, D., Garcia, A. M., Restrepo, A., & McEwen, J. G. (2011). Alternative oxidase mediates pathogen resistance in Paracoccidioides brasiliensis infection. *PLoS Negl. Trop. Dis.,* **5** (10): e1353.

Rushton, D. L., Tripathi, P., Rabara, R. C., Lin, J., Ringler, P., Boken, A. K., Langum, T. J., Smidt, L., Boomsma, D. D., Emme, N. J., Chen, X., Finer, J. J., Shen, Q. J., & Rushton, P. J. (2012). WRKY transcription factors: key components in abscisic acid signalling. *Plant Biotechnol. J.,* **10** (1): 2-11.

Rushton, P. J., Somssich, I. E., Ringler, P., & Shen, Q. J. (2010). WRKY transcription factors. *Trends Plant Sci.,* **15** (5): 247-258.

Sabapathy, K. (2012). Role of the JNK pathway in human diseases. *Prog. Mol. Biol. Transl. Sci.,* **106**: 145-169.

Sahu, U., Krishna Rao, K., & Rangarajan, P. N. (2014). Trm1p, a Zn(II)(2)Cys(6)-type transcription factor, is essential for the transcriptional activation of genes of methanol utilization pathway, in *Pichia pastoris*. *Biochem. Biophys. Res. Commun.,* **451** (1): 158-164.

Saimoto, H., Kido, Y., Haga, Y., Sakamoto, K., & Kita, K. (2013). Pharmacophore identification of ascofuranone, potent inhibitor of cyanide-insensitive alternative oxidase of *Trypanosoma brucei*. *J. Biochem.,* **153** (3): 267-273.

Saisho, D., Nakazono, M., Tsutsumi, N., & Hirai, A. (2001). ATP synthesis inhibitors as well as respiratory inhibitors increase steady-state level of alternative oxidase mRNA in *Arabidopsis thaliana*. *J. Plant Physiol.,* **158** (2): 241-245.

Saisho, D., Nambara, E., Naito, S., Tsutsumi, N., Hirai, A., & Nakazono, M. (1997). Characterization of the gene family for alternative oxidase from *Arabidopsis thaliana*. *Plant Mol. Biol.,* **35** (5): 585-596.

Saller, M. J., Wu, Z. C., de Keyzer, J., & Driessen, A. J. (2012). The YidC/Oxa1/Alb3 protein family: common principles and distinct features. *Biol. Chem.,* **393** (11): 1279-1290.

Sambrook, J., & Russell, D. W. (2001). Molecular Cloning: A Laboratory Manual. New York: Cold Spring Harbor Laboratory Press.

Sapp, J., Carrapico, F., & Zolotonosov, M. (2002). Symbiogenesis: the hidden face of Constantin Merezhkowsky. *Hist. Philos. Life Sci.,* **24** (3-4): 413-440.

Sarewicz, M., & Osyczka, A. (2015). Electronic connection between the quinone and cytochrome c redox pools and its role in regulation of mitochondrial electron transport and redox signaling. *Physiol. Rev.,* **95** (1): 219-243.

Sarzi, E., Goffart, S., Serre, V., Chretien, D., Slama, A., Munnich, A., Spelbrink, J. N., & Rotig, A. (2007). Twinkle helicase (PEO1) gene mutation causes mitochondrial DNA depletion. *Ann. Neurol.,* **62** (6): 579-587.

Sasser, T. L., & Fratti, R. A. (2014). Class C ABC transporters and vacuole fusion. *Cell. Logist.,* **4** (3): e943588.

Sasser, T. L., Padolina, M., & Fratti, R. A. (2012). The yeast vacuolar ABC transporter Ybt1p regulates membrane fusion through Ca2+ transport modulation. *Biochem. J.,* **448** (3): 365-372.

Saw, J. H., Spang, A., Zaremba-Niedzwiedzka, K., Juzokaite, L., Dodsworth, J. A., Murugapiran, S. K., Colman, D. R., Takacs-Vesbach, C., Hedlund, B. P., Guy, L., & Ettema, T. J. (2015). Exploring microbial dark matter to resolve the deep archaeal ancestry of eukaryotes. *Philos. Trans. R. Soc. Lond. B. Biol. Sci.,* **370** (1678): 20140328.

Scarpulla, R. C. (2011). Metabolic control of mitochondrial biogenesis through the

PGC-1 family regulatory network. *Biochim. Biophys. Acta.,* **1813** (7): 1269-1278.

Schagger, H., & Pfeiffer, K. (2000). Supercomplexes in the respiratory chains of yeast and mammalian mitochondria. *EMBO J.,* **19** (8): 1777-1783.

Schieber, M., & Chandel, N. S. (2014). ROS function in redox signaling and oxidative stress. *Curr. Biol.,* **24** (10): R453-462.

Schjerling, P., & Holmberg, S. (1996). Comparative amino acid sequence analysis of the C6 zinc cluster family of transcriptional regulators. *Nucleic. Acids Res.,* **24** (23): 4599-4607.

Schleicher, M., Shepherd, B. R., Suarez, Y., Fernandez-Hernando, C., Yu, J., Pan, Y., Acevedo, L. M., Shadel, G. S., & Sessa, W. C. (2008). Prohibitin-1 maintains the angiogenic capacity of endothelial cells by regulating mitochondrial function and senescence. *J. Cell Biol.,* **180** (1): 101-112.

Schmidt, O., Pfanner, N., & Meisinger, C. (2010). Mitochondrial protein import: from proteomics to functional mechanisms. *Nat. Rev. Mol. Cell Biol.,* **11** (9): 655-667.

Schmitz-Linneweber, C., & Small, I. (2008). Pentatricopeptide repeat proteins: a socket set for organelle gene expression. *Trends Plant Sci.,* **13** (12): 663-670.

Schon, E. A., DiMauro, S., & Hirano, M. (2012). Human mitochondrial DNA: roles of inherited and somatic mutations. *Nat. Rev. Genet.,* **13** (12): 878-890.

Schonbaum, G. R., Bonner, W. D., Jr., Storey, B. T., & Bahr, J. T. (1971). Specific inhibition of the cyanide-insensitive respiratory pathway in plant mitochondria by hydroxamic acids. *Plant Physiol.,* **47** (1): 124-128.

Schubert, S., Barker, K. S., Znaidi, S., Schneider, S., Dierolf, F., Dunkel, N., Aid, M., Boucher, G., Rogers, P. D., Raymond, M., & Morschhauser, J. (2011). Regulation of efflux pump expression and drug resistance by the transcription factors Mrr1, Upc2, and Cap1 in *Candida albicans*. *Antimicrob. Agents. Chemother.,* **55** (5): 2212-2223.

Schulz, C., Schendzielorz, A., & Rehling, P. (2015). Unlocking the presequence import pathway. *Trends Cell Biol.,* **25** (5): 265-275.

Sekito, T., Liu, Z., Thornton, J., & Butow, R. A. (2002). RTG-dependent mitochondria-to-nucleus signaling is regulated by MKS1 and is linked to formation of yeast prion [URE3]. *Mol. Biol. Cell,* **13** (3): 795-804.

Sekito, T., Thornton, J., & Butow, R. A. (2000). Mitochondria-to-nuclear signaling is regulated by the subcellular localization of the transcription factors Rtg1p and Rtg3p.

Mol. Biol. Cell, **11** (6): 2103-2115.

Selker, E. U. (1990). Premeiotic instability of repeated sequences in *Neurospora crassa*. *Annu. Rev. Genet.,* **24**: 579-613.

Sellem, C. H., Bovier, E., Lorin, S., & Sainsard-Chanet, A. (2009). Mutations in two zinc-cluster proteins activate alternative respiratory and gluconeogenic pathways and restore senescence in long-lived respiratory mutants of *Podospora anserina*. *Genetics,* **182** (1): 69-78.

Sena, L. A., & Chandel, N. S. (2012). Physiological roles of mitochondrial reactive oxygen species. *Mol. Cell,* **48** (2): 158-167.

Sesaki, H., & Jensen, R. E. (2001). UGO1 encodes an outer membrane protein required for mitochondrial fusion. *J. Cell. Biol.,* **152** (6): 1123-1134.

Shadel, G. S., & Horvath, T. L. (2015). Mitochondrial ROS signaling in organismal homeostasis. *Cell,* **163** (3): 560-569.

Sherman, F. (2005). The importance of mutation, then and now: studies with yeast cytochrome c. *Mutat. Res.,* **589** (1): 1-16.

Shiba, T., Kido, Y., Sakamoto, K., Inaoka, D. K., Tsuge, C., Tatsumi, R., Takahashi, G., Balogun, E. O., Nara, T., Aoki, T., Honma, T., Tanaka, A., Inoue, M., Matsuoka, S., Saimoto, H., Moore, A. L., Harada, S., & Kita, K. (2013). Structure of the trypanosome cyanide-insensitive alternative oxidase. *Proc. Natl. Acad. Sci. U S A,* **110** (12): 4580-4585.

Shiota, T., Imai, K., Qiu, J., Hewitt, V. L., Tan, K., Shen, H. H., Sakiyama, N., Fukasawa, Y., Hayat, S., Kamiya, M., Elofsson, A., Tomii, K., Horton, P., Wiedemann, N., Pfanner, N., Lithgow, T., & Endo, T. (2015). Molecular architecture of the active mitochondrial protein gate. *Science,* **349** (6255): 1544-1548.

Sideris, D. P., Petrakis, N., Katrakili, N., Mikropoulou, D., Gallo, A., Ciofi-Baffoni, S., Banci, L., Bertini, I., & Tokatlidis, K. (2009). A novel intermembrane space-targeting signal docks cysteines onto Mia40 during mitochondrial oxidative folding. *J. Cell. Biol.,* **187** (7): 1007-1022.

Siedow, J. N., & Bickett, D. M. (1981). Structural features required for inhibition of cyanide-insensitive electron transfer by propyl gallate. *Arch. Biochem. Biophys.,* **207** (1): 32-39.

Sievers, F., Wilm, A., Dineen, D., Gibson, T. J., Karplus, K., Li, W., Lopez, R., McWilliam, H., Remmert, M., Soding, J., Thompson, J. D., & Higgins, D. G. (2011).

Fast, scalable generation of high-quality protein multiple sequence alignments using Clustal Omega. *Mol. Syst. Biol.,* **7**: 539.

Smith, K. M., Phatale, P. A., Sullivan, C. M., Pomraning, K. R., & Freitag, M. (2011). Heterochromatin is required for normal distribution of *Neurospora crassa* CenH3. *Mol. Cell. Biol.,* **31** (12): 2528-2542.

Sodani, K., Patel, A., Kathawala, R. J., & Chen, Z. S. (2012). Multidrug resistance associated proteins in multidrug resistance. *Chin. J. Cancer,* **31** (2): 58-72.

Solotoff, V., Moseler, R., & Schulte, U. (2015). Two pentatricopeptide repeat domain proteins are required for the synthesis of respiratory complex I. *Curr. Genet.,* **61** (1): 19-29.

Song, J. S., Johnson, W. E., Zhu, X., Zhang, X., Li, W., Manrai, A. K., Liu, J. S., Chen, R., & Liu, X. S. (2007). Model-based analysis of two-color arrays (MA2C). *Genome Biol.*, **8** (8): R178.

Soontorngun, N., Baramee, S., Tangsombatvichit, C., Thepnok, P., Cheevadhanarak, S., Robert, F., & Turcotte, B. (2012). Genome-wide location analysis reveals an important overlap between the targets of the yeast transcriptional regulators Rds2 and Adr1. *Biochem. Biophys. Res. Commun.,* **423** (4): 632-637.

Soontorngun, N., Larochelle, M., Drouin, S., Robert, F., & Turcotte, B. (2007). Regulation of gluconeogenesis in *Saccharomyces cerevisiae* is mediated by activator and repressor functions of Rds2. *Mol. Cell. Biol.,* **27** (22): 7895-7905.

Spang, A., Saw, J. H., Jorgensen, S. L., Zaremba-Niedzwiedzka, K., Martijn, J., Lind, A. E., van Eijk, R., Schleper, C., Guy, L., & Ettema, T. J. (2015). Complex archaea that bridge the gap between prokaryotes and eukaryotes. *Nature,* **521** (7551): 173-179.

Staben, C., Jensen, B., Singer, M., Pollock, J., Schechtman, M., Kinsey, J., & Selker, E. (1989). Use of a bacterial Hygromycin B resistance gene as a dominant selectable marker in *Neurospora crassa* transformation. *Fungal Genet. Newsl.,* **36**: 79-81.

Stajich, J. E., Harris, T., Brunk, B. P., Brestelli, J., Fischer, S., Harb, O. S., Kissinger, J. C., Li, W., Nayak, V., Pinney, D. F., Stoeckert, C. J., Jr., & Roos, D. S. (2012). FungiDB: an integrated functional genomics database for fungi. *Nucleic Acids Res.,* **40** (Database issue): D675-681.

Stein, L. D., Mungall, C., Shu, S., Caudy, M., Mangone, M., Day, A., Nickerson, E., Stajich, J. E., Harris, T. W., Arva, A., & Lewis, S. (2002). The generic genome browser: a building block for a model organism system database. *Genome Res.,* **12** (10): 1599-1610.

Stenmark, P., & Nordlund, P. (2003). A prokaryotic alternative oxidase present in the bacterium *Novosphingobium aromaticivorans*. *FEBS Lett.,* **552** (2-3): 189-192.

Stock, D., Leslie, A. G., & Walker, J. E. (1999). Molecular architecture of the rotary motor in ATP synthase. *Science,* **286** (5445): 1700-1705.

Strauss, M., Hofhaus, G., Schroder, R. R., & Kuhlbrandt, W. (2008). Dimer ribbons of ATP synthase shape the inner mitochondrial membrane. *EMBO J.,* **27** (7): 1154-1160.

Strogolova, V., Furness, A., Robb-McGrath, M., Garlich, J., & Stuart, R. A. (2012). Rcf1 and Rcf2, members of the hypoxia-induced gene 1 protein family, are critical components of the mitochondrial cytochrome bc1-cytochrome c oxidase supercomplex. *Mol. Cell. Biol.* **32** (8): 1363-1373.

Stumpf, J. D., & Copeland, W. C. (2011). Mitochondrial DNA replication and disease: insights from DNA polymerase gamma mutations. *Cell Mol. Life Sci.,* **68** (2): 219-233.

Stumpf, J. D., Saneto, R. P., & Copeland, W. C. (2013). Clinical and molecular features of POLG-related mitochondrial disease. *Cold Spring Harb. Perspect. Biol. ,* **5** (4): a011395.

Sun, F., Huo, X., Zhai, Y., Wang, A., Xu, J., Su, D., Bartlam, M., & Rao, Z. (2005). Crystal structure of mitochondrial respiratory membrane protein complex II. *Cell,* **121** (7): 1043-1057.

Sun, F., Zhou, Q., Pang, X., Xu, Y., & Rao, Z. (2013). Revealing various coupling of electron transfer and proton pumping in mitochondrial respiratory chain. *Curr. Opin. Struct. Biol.,* **23** (4): 526-538.

Suzuki, Y., Murray, S. L., Wong, K. H., Davis, M. A., & Hynes, M. J. (2012). Reprogramming of carbon metabolism by the transcriptional activators AcuK and AcuM in *Aspergillus nidulans*. *Mol. Microbiol.,* **84** (5): 942-964.

Svensson-Ek, M., Abramson, J., Larsson, G., Tornroth, S., Brzezinski, P., & Iwata, S. (2002). The X-ray crystal structures of wild-type and EQ(I-286) mutant cytochrome c oxidases from *Rhodobacter sphaeroides*. *J. Mol. Biol.,* **321** (2): 329-339.

Swierczek, M., Cieluch, E., Sarewicz, M., Borek, A., Moser, C. C., Dutton, P. L., & Osyczka, A. (2010). An electronic bus bar lies in the core of cytochrome bc1. *Science,* **329** (5990): 451-454.

Tachibana, C., Yoo, J. Y., Tagne, J. B., Kacherovsky, N., Lee, T. I., & Young, E. T. (2005). Combined global localization analysis and transcriptome data identify genes

that are directly coregulated by Adr1 and Cat8. *Mol. Cell. Biol.,* **25** (6): 2138-2146.

Talbot, K. J., & Russell, P. J. (1982). Nuclear buoyant density determination and the purification and characterization of wild-type neurospora nuclei using percoll density gradients. *Plant Physiol.,* **70** (3): 704-708.

Tanton, L. L., Nargang, C. E., Kessler, K. E., Li, Q., & Nargang, F. E. (2003). Alternative oxidase expression in *Neurospora crassa*. *Fungal Genet. Biol.,* **39** (2): 176-190.

Tatsuta, T. (2009). Protein quality control in mitochondria. *J. Biochem.,* **146** (4): 455-461.

Tatsuta, T., Model, K., & Langer, T. (2005). Formation of membrane-bound ring complexes by prohibitins in mitochondria. *Mol. Biol. Cell,* **16** (1): 248-259.

Taylor, C. T., & Moncada, S. (2010). Nitric oxide, cytochrome C oxidase, and the cellular response to hypoxia. *Arterioscler. Thromb. Vasc. Biol.,* **30** (4): 643-647.

Teixeira, P. F., & Glaser, E. (2013). Processing peptidases in mitochondria and chloroplasts. *Biochim. Biophys. Acta.,* **1833** (2): 360-370.

Thakur, J. K., Arthanari, H., Yang, F., Pan, S. J., Fan, X., Breger, J., Frueh, D. P., Gulshan, K., Li, D. K., Mylonakis, E., Struhl, K., Moye-Rowley, W. S., Cormack, B. P., Wagner, G., & Naar, A. M. (2008). A nuclear receptor-like pathway regulating multidrug resistance in fungi. *Nature,* **452** (7187): 604-609.

Theiss, A. L., & Sitaraman, S. V. (2011). The role and therapeutic potential of prohibitin in disease. *Biochim. Biophys. Acta.,* **1813** (6): 1137-1143.

Thirkettle-Watts, D., McCabe, T. C., Clifton, R., Moore, C., Finnegan, P. M., Day, D. A., & Whelan, J. (2003). Analysis of the alternative oxidase promoters from soybean. *Plant Physiol.,* **133** (3): 1158-1169.

Thomazella, D. P., Teixeira, P. J., Oliveira, H. C., Saviani, E. E., Rincones, J., Toni, I. M., Reis, O., Garcia, O., Meinhardt, L. W., Salgado, I., & Pereira, G. A. (2012). The hemibiotrophic cacao pathogen *Moniliophthora perniciosa* depends on a mitochondrial alternative oxidase for biotrophic development. *New Phytol.,* **194** (4): 1025-1034.

Thrash, J. C., Boyd, A., Huggett, M. J., Grote, J., Carini, P., Yoder, R. J., Robbertse, B., Spatafora, J. W., Rappe, M. S., & Giovannoni, S. J. (2011). Phylogenomic evidence for a common ancestor of mitochondria and the SAR11 clade. *Sci. Rep.,* **1**: 13.

Tieu, Q., & Nunnari, J. (2000). Mdv1p is a WD repeat protein that interacts with the dynamin-related GTPase, Dnm1p, to trigger mitochondrial division. *J. Cell. Biol.,* **151** (2): 353-366.

Tocilescu, M. A., Fendel, U., Zwicker, K., Kerscher, S., & Brandt, U. (2007). Exploring the ubiquinone binding cavity of respiratory complex I. *J. Biol. Chem.,* **282** (40): 29514-29520.

Todd, R. B., Andrianopoulos, A., Davis, M. A., & Hynes, M. J. (1998). FacB, the *Aspergillus nidulans* activator of acetate utilization genes, binds dissimilar DNA sequences. *EMBO J.,* **17** (7): 2042-2054.

Towbin, H., Staehelin, T., & Gordon, J. (1979). Electrophoretic transfer of proteins from polyacrylamide gels to nitrocellulose sheets: procedure and some applications. *Proc. Natl. Acad. Sci. U S A,* **76** (9): 4350-4354.

Trifunovic, A., Wredenberg, A., Falkenberg, M., Spelbrink, J. N., Rovio, A. T., Bruder, C. E., Bohlooly, Y. M., Gidlof, S., Oldfors, A., Wibom, R., Tornell, J., Jacobs, H. T., & Larsson, N. G. (2004). Premature ageing in mice expressing defective mitochondrial DNA polymerase. *Nature,* **429** (6990): 417-423.

Tsukihara, T., Aoyama, H., Yamashita, E., Tomizaki, T., Yamaguchi, H., Shinzawa-Itoh, K., Nakashima, R., Yaono, R., & Yoshikawa, S. (1996). The whole structure of the 13-subunit oxidized cytochrome c oxidase at 2.8 A. *Science,* **272** (5265): 1136-1144.

Turcotte, B., Liang, X. B., Robert, F., & Soontorngun, N. (2010). Transcriptional regulation of nonfermentable carbon utilization in budding yeast. *FEMS Yeast Res.,* **10** (1): 2-13.

Umbach, A. L., Gonzalez-Meler, M. A., Sweet, C. R., & Siedow, J. N. (2002). Activation of the plant mitochondrial alternative oxidase: insights from site-directed mutagenesis. *Biochim. Biophys. Acta.,* **1554** (1-2): 118-128.

Umbach, A. L., & Siedow, J. N. (1993). Covalent and noncovalent dimers of the cyanide-resistant alternative oxidase protein in higher plant mitochondria and their relationship to enzyme activity. *Plant Physiol.,* **103** (3): 845-854.

Umbach, A. L., & Siedow, J. N. (2000). The cyanide-resistant alternative oxidases from the fungi *Pichia stipitis* and *Neurospora crassa* are monomeric and lack regulatory features of the plant enzyme. *Arch. Biochem. Biophys.,* **378** (2): 234-245.

Van Aken, O., Zhang, B., Law, S., Narsai, R., & Whelan, J. (2013). AtWRKY40 and AtWRKY63 modulate the expression of stress-responsive nuclear genes encoding

mitochondrial and chloroplast proteins. *Plant Physiol.,* **162** (1): 254-271.

van der Laan, M., Bohnert, M., Wiedemann, N., & Pfanner, N. (2012). Role of MINOS in mitochondrial membrane architecture and biogenesis. *Trends Cell Biol.,* **22** (4): 185-192.

Vanderauwera, S., Vandenbroucke, K., Inze, A., van de Cotte, B., Muhlenbock, P., De Rycke, R., Naouar, N., Van Gaever, T., Van Montagu, M. C., & Van Breusegem, F. (2012). AtWRKY15 perturbation abolishes the mitochondrial stress response that steers osmotic stress tolerance in Arabidopsis. *Proc. Natl. Acad. Sci. U S A,* **109** (49): 20113-20118.

Vanlerberghe, G. C. (2013). Alternative oxidase: a mitochondrial respiratory pathway to maintain metabolic and signaling homeostasis during abiotic and biotic stress in plants. *Int. J. Mol. Sci.,* **14** (4): 6805-6847.

Vanlerberghe, G. C., Day, D. A., Wiskich, J. T., Vanlerberghe, A. E., & McIntosh, L. (1995). Alternative oxidase activity in tobacco leaf mitochondria (Dependence on tricarboxylic acid cycle-mediated redox regulation and pyruvate activation). *Plant Physiol.,* **109** (2): 353-361.

Vanlerberghe, G. C., & McIntosh, L. (1994). Mitochondrial electron transport regulation of nuclear gene expression. Studies with the alternative oxidase gene of tobacco. *Plant Physiol.,* **105** (3): 867-874.

Vanlerberghe, G. C., & McIntosh, L. (1996). Signals regulating the expression of the nuclear gene encoding alternative oxidase of plant mitochondria. *Plant Physiol.,* **111** (2): 589-595.

Vanlerberghe, G. C., & McIntosh, L. (1997). Alternative oxidase: From gene to function. *Annu. Rev. Plant Physiol. Plant Mol. Biol.,* **48**: 703-734.

Vanlerberghe, G. C., McIntosh, L., & Yip, J. Y. (1998). Molecular localization of a redox-modulated process regulating plant mitochondrial electron transport. *Plant Cell,* **10** (9): 1551-1560.

Vanlerberghe, G. C., Robson, C. A., & Yip, J. Y. (2002). Induction of mitochondrial alternative oxidase in response to a cell signal pathway down-regulating the cytochrome pathway prevents programmed cell death. *Plant Physiol.,* **129** (4): 1829-1842.

Vartak, R., Porras, C. A., & Bai, Y. (2013). Respiratory supercomplexes: structure, function and assembly. *Protein Cell,* **4** (8): 582-590.

Vartiainen, S., Chen, S., George, J., Tuomela, T., Luoto, K. R., O'Dell, K. M., & Jacobs, H. T. (2014). Phenotypic rescue of a Drosophila model of mitochondrial ANT1 disease. *Dis. Model Mech.,* **7** (6): 635-648.

Veiga, A., Arrabaca, J. D., & Loureiro-Dias, M. C. (2003). Cyanide-resistant respiration, a very frequent metabolic pathway in yeasts. *FEMS Yeast Res.,* **3** (3): 239-245.

Vermulst, M., Bielas, J. H., Kujoth, G. C., Ladiges, W. C., Rabinovitch, P. S., Prolla, T. A., & Loeb, L. A. (2007). Mitochondrial point mutations do not limit the natural lifespan of mice. *Nat. Genet.,* **39** (4): 540-543.

Vik, A., & Rine, J. (2001). Upc2p and Ecm22p, dual regulators of sterol biosynthesis in Saccharomyces cerevisiae. *Mol. Cell. Biol.,* **21** (19): 6395-6405.

Vincent, O., & Carlson, M. (1998). Sip4, a Snf1 kinase-dependent transcriptional activator, binds to the carbon source-responsive element of gluconeogenic genes. *EMBO J.,* **17** (23): 7002-7008.

Vogel, F., Bornhovd, C., Neupert, W., & Reichert, A. S. (2006). Dynamic subcompartmentalization of the mitochondrial inner membrane. *J. Cell. Biol.,* **175** (2): 237-247.

von der Malsburg, K., Muller, J. M., Bohnert, M., Oeljeklaus, S., Kwiatkowska, P., Becker, T., Loniewska-Lwowska, A., Wiese, S., Rao, S., Milenkovic, D., Hutu, D. P., Zerbes, R. M., Schulze-Specking, A., Meyer, H. E., Martinou, J. C., Rospert, S., Rehling, P., Meisinger, C., Veenhuis, M., Warscheid, B., van der Klei, I. J., Pfanner, N., Chacinska, A., & van der Laan, M. (2011). Dual role of mitofilin in mitochondrial membrane organization and protein biogenesis. *Dev. Cell,* **21** (4): 694-707.

Vukotic, M., Oeljeklaus, S., Wiese, S., Vogtle, F. N., Meisinger, C., Meyer, H. E., Zieseniss, A., Katschinski, D. M., Jans, D. C., Jakobs, S., Warscheid, B., Rehling, P., & Deckers, M. (2012). Rcf1 mediates cytochrome oxidase assembly and respirasome formation, revealing heterogeneity of the enzyme complex. *Cell Metab.,* **15** (3): 336-347.

Wai, T., & Langer, T. (2016). Mitochondrial dynamics and metabolic regulation. *Trends Endocrino. Metab.*, 27 (2): 105-117.

Walker, J. E. (2013). The ATP synthase: the understood, the uncertain and the unknown. *Biochem. Soc. Trans.,* **41** (1): 1-16.

Wang, H., Liang, X., Huang, J., Zhang, D., Lu, H., Liu, Z., & Bi, Y. (2010). Involvement of ethylene and hydrogen peroxide in induction of alternative respiratory

pathway in salt-treated Arabidopsis calluses. *Plant Cell Physiol.,* **51** (10): 1754-1765.

Wang, W., Wu, Z., Dai, Z., Yang, Y., Wang, J., & Wu, G. (2013). Glycine metabolism in animals and humans: implications for nutrition and health. *Amino Acids,* **45** (3): 463-477.

Wang, Y., & Hekimi, S. (2015). Mitochondrial dysfunction and longevity in animals: Untangling the knot. *Science,* **350** (6265): 1204-1207.

Wang, Z., & Wu, M. (2015). An integrated phylogenomic approach toward pinpointing the origin of mitochondria. *Sci. Rep.,* **5**: 7949.

Wanrooij, S., & Falkenberg, M. (2010). The human mitochondrial replication fork in health and disease. *Biochim. Biophys. Acta.,* **1797** (8): 1378-1388.

Watanabe, C. K., Hachiya, T., Terashima, I., & Noguchi, K. (2008). The lack of alternative oxidase at low temperature leads to a disruption of the balance in carbon and nitrogen metabolism, and to an up-regulation of antioxidant defence systems in *Arabidopsis thaliana* leaves. *Plant Cell Environ.,* **31** (8): 1190-1202.

Watling, J. R., Robinson, S. A., & Seymour, R. S. (2006). Contribution of the alternative pathway to respiration during thermogenesis in flowers of the sacred lotus. *Plant Physiol.,* **140** (4): 1367-1373.

Watters, M. K., Randall, T. A., Margolin, B. S., Selker, E. U., & Stadler, D. R. (1999). Action of repeat-induced point mutation on both strands of a duplex and on tandem duplications of various sizes in Neurospora. *Genetics,* **153** (2): 705-714.

Watt, I. N., Montgomery, M. G., Runswick, M. J., Leslie, A. G., & Walker, J. E. (2010). Bioenergetic cost of making an adenosine triphosphate molecule in animal mitochondria. *Proc. Natl. Acad. Sci. U S A,* **107** (39): 16823-16827.

Weckbecker, D., Longen, S., Riemer, J., & Herrmann, J. M. (2012). Atp23 biogenesis reveals a chaperone-like folding activity of Mia40 in the IMS of mitochondria. *EMBO J.,* **31** (22): 4348-4358.

Weiss, C., Schneider, S., Wagner, E. F., Zhang, X., Seto, E., & Bohmann, D. (2003). JNK phosphorylation relieves HDAC3-dependent suppression of the transcriptional activity of c-Jun. *EMBO J.,* **22** (14): 3686-3695.

Wenz, L. S., Ellenrieder, L., Qiu, J., Bohnert, M., Zufall, N., van der Laan, M., Pfanner, N., Wiedemann, N., & Becker, T. (2015a). Sam37 is crucial for formation of the mitochondrial TOM-SAM supercomplex, thereby promoting beta-barrel biogenesis. *J. Cell. Biol.,* **210** (7): 1047-1054.

Wenz, L. S., Opalinski, L., Wiedemann, N., & Becker, T. (2015b). Cooperation of protein machineries in mitochondrial protein sorting. *Biochim. Biophys. Acta.,* **1853** (5): 1119-1129.

Wenz, L. S., Qiu, J., Becker, T., & Wiedemann, N. (2014). Biogenesis and folding of beta-barrel membrane proteins. *Cell Cycle,* **13** (2): 169-170.

Wideman, J. G., Gawryluk, R. M., Gray, M. W., & Dacks, J. B. (2013). The ancient and widespread nature of the ER-mitochondria encounter structure. *Mol. Biol. Evol.,* **30** (9): 2044-2049.

Williams, K. P., Sobral, B. W., & Dickerman, A. W. (2007). A robust species tree for the alphaproteobacteria. *J. Bacteriol.,* **189** (13): 4578-4586.

Williams, T. A., & Embley, T. M. (2015). Changing ideas about eukaryotic origins. *Philos. Trans. R. Soc. Lond. B. Biol. Sci.,* **370** (1678): 20140318.

Williams, T. A., Foster, P. G., Cox, C. J., & Embley, T. M. (2013). An archaeal origin of eukaryotes supports only two primary domains of life. *Nature,* **504** (7479): 231-236.

Wilson, A. J., & Bhattacharjee, J. K. (1986). Regulation of phosphoenolpyruvate carboxykinase and pyruvate kinase in *Saccharomyces cerevisiae* grown in the presence of glycolytic and gluconeogenic carbon sources and the role of mitochondrial function on gluconeogenesis. *Can. J. Microb.,* **32** (12): 969-972.

Winkler, H., Adam, G., Mattes, E., Schanz, M., Hartig, A., & Ruis, H. (1988). Co-ordinate control of synthesis of mitochondrial and non-mitochondrial hemoproteins: a binding site for the HAP1 (CYP1) protein in the UAS region of the yeast catalase T gene (CTT1). *EMBO J.l,* **7** (6): 1799-1804.

Winterbourn, C. C. (2013). The biological chemistry of hydrogen peroxide. *Methods Enzymol.,* **528**: 3-25.

Worsley Hunt, R., & Wasserman, W. W. (2014). Non-targeted transcription factors motifs are a systemic component of ChIP-seq datasets. *Genome Biol.,* **15** (7): 412.

Wu, D., Wright, D. A., Wetzel, C., Voytas, D. F., & Rodermel, S. (1999). The IMMUTANS variegation locus of Arabidopsis defines a mitochondrial alternative oxidase homolog that functions during early chloroplast biogenesis. *Plant Cell,* **11** (1): 43-55.

Xia, D., Yu, C. A., Kim, H., Xia, J. Z., Kachurin, A. M., Zhang, L., Yu, L., & Deisenhofer, J. (1997). Crystal structure of the cytochrome bc1 complex from bovine

heart mitochondria. *Science,* **277** (5322): 60-66.

Xia, X. J., Zhou, Y. H., Shi, K., Zhou, J., Foyer, C. H., & Yu, J. Q. (2015). Interplay between reactive oxygen species and hormones in the control of plant development and stress tolerance. *J. Exp. Bot.,* **66** (10): 2839-2856.

Yadava, N., Schneider, S. S., Jerry, D. J., & Kim, C. (2013). Impaired mitochondrial metabolism and mammary carcinogenesis. *J. Mammary Gland Biol. Neoplasia,* **18** (1): 75-87.

Yang, H., Tong, J., Lee, C. W., Ha, S., Eom, S. H., & Im, Y. J. (2015). Structural mechanism of ergosterol regulation by fungal sterol transcription factor Upc2. *Nat. Commun.,* **6**: 6129.

Yankovskaya, V., Horsefield, R., Tornroth, S., Luna-Chavez, C., Miyoshi, H., Leger, C., Byrne, B., Cecchini, G., & Iwata, S. (2003). Architecture of succinate dehydrogenase and reactive oxygen species generation. *Science,* **299** (5607): 700-704.

Yasuda, R., Noji, H., Yoshida, M., Kinosita, K., Jr., & Itoh, H. (2001). Resolution of distinct rotational substeps by submillisecond kinetic analysis of F1-ATPase. *Nature,* **410** (6831): 898-904.

Ye, J., Li, J., Xia, R., Zhou, M., & Yu, L. (2015). Prohibitin protects proximal tubule epithelial cells against oxidative injury through mitochondrial pathways. *Free Radic. Res.,* **49** (11): 1393-1403.

Ylikallio, E., & Suomalainen, A. (2012). Mechanisms of mitochondrial diseases. *Ann. Med.,* **44** (1): 41-59.

Yoshikawa, S., Shinzawa-Itoh, K., Nakashima, R., Yaono, R., Yamashita, E., Inoue, N., Yao, M., Fei, M. J., Libeu, C. P., Mizushima, T., Yamaguchi, H., Tomizaki, T., & Tsukihara, T. (1998). Redox-coupled crystal structural changes in bovine heart cytochrome c oxidase. *Science,* **280** (5370): 1723-1729.

Young, E. T., Dombek, K. M., Tachibana, C., & Ideker, T. (2003). Multiple pathways are co-regulated by the protein kinase Snf1 and the transcription factors Adr1 and Cat8. *J. Biol. Chem.,* **278** (28): 26146-26158.

Yuan, X. L., Roubos, J. A., van den Hondel, C. A., & Ram, A. F. (2008). Identification of InuR, a new Zn(II)2Cys6 transcriptional activator involved in the regulation of inulinolytic genes in *Aspergillus niger*. *Mol. Genet. Genomics,* **279** (1): 11-26.

Yukioka, H., Inagaki, S., Tanaka, R., Katoh, K., Miki, N., Mizutani, A., & Masuko, M. (1998). Transcriptional activation of the alternative oxidase gene of the fungus

Magnaporthe grisea by a respiratory-inhibiting fungicide and hydrogen peroxide. *Biochim. Biophys. Acta.,* **1442** (2-3): 161-169.

Zerbes, R. M., van der Klei, I. J., Veenhuis, M., Pfanner, N., van der Laan, M., & Bohnert, M. (2012). Mitofilin complexes: conserved organizers of mitochondrial membrane architecture. *Biol. Chem.,* **393** (11): 1247-1261.

Zeth, K. (2010). Structure and evolution of mitochondrial outer membrane proteins of beta-barrel topology. *Biochim. Biophys. Acta.,* **1797** (6-7): 1292-1299.

Zhang, L., & Hach, A. (1999). Molecular mechanism of heme signaling in yeast: the transcriptional activator Hap1 serves as the key mediator. *Cell. Mol. Life Sci.,* **56** (5-6): 415-426.

Zhang, L., Oh, Y., Li, H., Baldwin, I. T., & Galis, I. (2012). Alternative oxidase in resistance to biotic stresses: *Nicotiana attenuata* AOX contributes to resistance to a pathogen and a piercing-sucking insect but not *Manduca sexta* larvae. *Plant Physiol.,* **160** (3): 1453-1467.

Zhang, Y., Liu, T., Meyer, C. A., Eeckhoute, J., Johnson, D. S., Bernstein, B. E., Nusbaum, C., Myers, R. M., Brown, M., Li, W., & Liu, X. S. (2008). Model-based analysis of ChIP-Seq (MACS). *Genome Biol.,* **9** (9): R137.

Zhang, Z., Huang, L., Shulmeister, V. M., Chi, Y. I., Kim, K. K., Hung, L. W., Crofts, A. R., Berry, E. A., & Kim, S. H. (1998). Electron transfer by domain movement in cytochrome bc1. *Nature,* **392** (6677): 677-684.

Zhao, H., & Eide, D. (1996a). The yeast ZRT1 gene encodes the zinc transporter protein of a high-affinity uptake system induced by zinc limitation. *Proc. Natl. Acad. Sci. U S A,* **93** (6): 2454-2458.

Zhao, H., & Eide, D. (1996b). The ZRT2 gene encodes the low affinity zinc transporter in *Saccharomyces cerevisiae*. *J. Biol. Chem.,* **271** (38): 23203-23210.

Zhao, Q., Wang, J., Levichkin, I. V., Stasinopoulos, S., Ryan, M. T., & Hoogenraad, N. J. (2002). A mitochondrial specific stress response in mammalian cells. *EMBO J.,* **21** (17): 4411-4419.

Zhao, X., Li, G., & Liang, S. (2013). Several affinity tags commonly used in chromatographic purification. *J. Anal. Methods Chem.,* **2013**: 581093.

Zhu, X., Peng, X., Guan, M. X., & Yan, Q. (2009). Pathogenic mutations of nuclear genes associated with mitochondrial disorders. *Acta. Biochim. Biophys. Sin.,* **41** (3): 179-187.

Zhu, Y., Lu, J., Wang, J., Chen, F., Leng, F., & Li, H. (2011). Regulation of thermogenesis in plants: the interaction of alternative oxidase and plant uncoupling mitochondrial protein. *J. Integr. Plant Biol.,* **53** (1): 7-13.

Zickermann, V., Wirth, C., Nasiri, H., Siegmund, K., Schwalbe, H., Hunte, C., & Brandt, U. (2015). Structural biology. Mechanistic insight from the crystal structure of mitochondrial complex I. *Science,* **347** (6217): 44-49.

Zorzano, A., & Claret, M. (2015). Implications of mitochondrial dynamics on neurodegeneration and on hypothalamic dysfunction. *Front. Aging Neurosci.,* **7**: 101.

Appendices

Appendix I. Plasmids and primers used in this study.

Appendix Table 1. Plasmids and cosmids used in this study. All carry ampicillin resistance gene unless noted otherwise.

Plasmids or cosmids	Sources	Comments
pMOcosX X14 D3	FGSC	Cosmid containing *aod-2* gene
pMOcosX X15 B9	FGSC	Cosmid containing *aod-5* gene
p*aod-2*hyg-3	Micheal Chae	*aod-2* and hygromycin resistant gene cloned into pBSKII
p*aod-5*hyg-69	Micheal Chae	*aod-5* and hygromycin resistant gene cloned into pBSKII
p*aod-2*hyg-3 Δ*Not*I	This study	*Not*I site was removed from p*aod-2*hyg-3 by filling in *Not*I-generated overhang with Klenow
p*aod-5*hyg-69 Δ*Not*I	This study	*Not*I site was removed from p*aod-5*hyg-69 by filling in *Not*I-generated overhang with Klenow
p*aod-2*hyg N *Not*I	This study	A *Not*I site was inserted into the 3' end of the ATG of *aod-2* from p*aod-2*hyg-3 Δ*Not*I by mutagenesis
p*aod-2*hyg C *Not*I	This study	A *Not*I site was inserted into the 5' end of the stop codon of *aod-2* from p*aod-2*hyg-3 Δ*Not*I by mutagenesis
p*aod-5*hyg N *Not*I	This study	A *Not*I site was inserted into the 3' end of the ATG of *aod-5* from p*aod-5*hyg-69 Δ*Not*I by mutagenesis
p*aod-5*hyg C *Not*I	This study	A *Not*I site was inserted into the 5' end of the stop codon of *aod-5* from p*aod-5*hyg-69 Δ*Not*I by mutagenesis
pFN-*Not*I-HA3	IDT, Coralville, USA	Plasmid containing the sequence encoding 3×HA tag for cloning, surrounded by *Not*I sites. Kanamycin resistant.
pFN-*Not*I-Myc3	IDT, Coralville, USA	Plasmid containing the sequence encoding 3×Myc tag for cloning, surrounded by *Not*I sites. Kanamycin resistant.

p*aod-2*hyg N-HA	This study	3×HA tag was inserted into the *Not*I site of p*aod-2*hyg N *Not*I
p*aod-2*hyg C-HA	This study	3×HA tag was inserted into the *Not*I site of p*aod-2*hyg C *Not*I
p*aod-2*hyg N-Myc	This study	3×Myc tag was inserted into the *Not*I site of p*aod-2*hyg N *Not*I
p*aod-2*hyg C-Myc	This study	3×Myc tag was inserted into the *Not*I site of p*aod-2*hyg C *Not*I
p*aod-5*hyg N-HA	This study	3×HA tag was inserted into the *Not*I site of p*aod-5*hyg N *Not*I
p*aod-5*hyg C-HA	This study	3×HA tag was inserted into the *Not*I site of p*aod-5*hyg C *Not*I
p*aod-5*hyg N-myc	This study	3×Myc tag was inserted into the *Not*I site of p*aod-5*hyg N *NotI*
p*aod-5*hyg C-myc	This study	3×Myc tag was inserted into the *NotI* site of p*aod-5*hyg C *Not*I

Appendix Table 2. Primers used in this study.

Primer name	Sequence (5' – 3')	Purpose for this study
*aod-5*_seq-1	ACCCCACGATGATGCTAATG	Sequence *aod-5* coding region
*aod-5*_seq-2	AGATACAGCGGCAGCAGGAT	Sequence *aod-5* coding region
*aod-5*_seq-3	GTTTGATAAGCGACTTCCTG	Sequence *aod-5* coding region
*aod-5*_seq-4	TGGCACTAACTCGGATACTC	Sequence *aod-5* coding region
*aod-5*_seq-5	ACTGGAAAGAGATGGTAAGC	Sequence *aod-5* coding region
*aod-5*_seq-6	TTTCTTTTTCGTGACATGCG	Sequence *aod-5* coding region
AOD2N*Not*I	GCCTCTACACTCGATAAGCAATGGCGGCCGCACGGGAACAGAAGCCACGG	Introduce *Not*I site into the N-terminus of AOD2 on the p*aod-2*hyg-3 Δ*Not*I
AOD2C*Not*I	CTTCCTCCCACACGACCCAGCGGCCGCTGACAGTGTTTAGTATACACTCTGCC	Introduce *Not*I site into the C-terminus of AOD2 on the p*aod-2*hyg-3 Δ*Not*I
AOD5N*Not*I	GTCTGTATATATAGAGCTAAGGCACGATGGCGGCCGCCCGGACGACGTTGGACCC	Introduce *Not*I site into the N-terminus of AOD5 on the p*aod-5*hyg-69 Δ*Not*I
AOD5C*Not*I	GCCATAACCAGCTAGCTGTAGCGGCCGCTGATTAGAACCAGTACTGCTGTC TAG	Introduce *Not*I site into the C-terminus of AOD5 on the p*aod-5*hyg-69 Δ*Not*I
aod-2 N Tag sequencing Forward	ACAGAACCTGGTTGCACGAG	Confirm HA or Myc tag at the N terminus of AOD2
aod-2 N Tag sequencing Reverse	AAGGGAACAAAAGCTGGAGC	

aod-2 C Tag sequencing Forward	TCTGACCAGTTGCCTAAATG	Confirm HA or Myc tag at the C terminus of AOD2
aod-2 C Tag sequencing Reverse	GACTTTGGTTTTGCTTAGGG	
aod-5 N Tag gDNA sequencing	CCTATGAGTCGTTTACCCAG	Confirm HA or Myc tag at the N terminus of AOD5
aod-5 C Tag gDNA sequencing	CATTAGGCACCCCAGGCTTT	Confirm HA or Myc tag at the C terminus of AOD5
aod-1 KO Forward	GCTTCCGACACGGGATAATA	Confirm hyg insertion in the *aod-1* knock-out gene
aod-1 KO Reverse	GATGCCTACACTAGACGCGT	
aod-3 KO Forward II	GATCCAGACCTCGACGCTGTCACGACCTTG	Confirm hyg insertion in the *aod-3* knock-out gene
aod-3 KO Reverse II	CCCAATATATGTATCTAGAACCACAGCTGC	
hphF primer for KO genes	GTCGGAGACAGAAGATGATATTGAAGGAG	Amplify hyg cassette for knocking out genes[1]
hphR primer for KO genes	GTTGGAGATTTCAGTAACGTTAAGTGGAT	
aod-1 qPCR primer F	GGGGCGTTAATCATACATTGA	Use qPCR to measure the transcript levels of *aod-1*
aod-1 qPCR primer R	AGTCGCTCACAAACGGATTC	
PEPCK qPCR primer F	CGGCTACACCTCCAAGATG	Use qPCR to measure the transcript levels of PEPCK
PEPCK qPCR primer R	CGAAGCACGAAGAGAAGGTC	
fbp-1 gene qPCR primer F	GCCCATGGCTATGATTTTTG	Use qPCR to measure the transcript levels of FBP
fbp-1 gene qPCR primer R	GCGGTTCATCTTGCTATCG	

β-tubulin qPCR primer F	GCCTCCGGTGTGTACAATG	Use qPCR to measure the transcript levels of β-tubulin
β-tubulin qPCR primer R	CGGAAGCCTCGTTGAAGTAG	
aod-3 gene qPCR primer F	GACCATGAAGGACCTCATCC	Use qPCR to measure the transcript levels of *aod-3*
aod-3 gene qPCR primer R	GTCGAGGTTGCCAAATGTGT	
flavohemoglobin qPCR primer F	CGGCACATGTGTTTCTGAAG	Use qPCR to measure the transcript levels of flavohemoglobin
flavohemoglobin qPCR primer R	CGCAAAATCGTAATGCACAC	
ABC transporter qPCR primer F	TCGGGACGGTTTACTTTTCTC	Use qPCR to measure the transcript levels of ABC transporter
ABC transporter qPCR primer R	TGGCGAGGGCTAGAATAACA	
5-oxoprolinase qPCR primer F	AGATGGGCTCCATGTCCAC	Use qPCR to measure the transcript levels of 5-oxoprolinase
5-oxoprolinase qPCR primer R	CGCAGCTTACCCTTCCAG	
RNA lariat debranching enzyme qPCR primer F	CGAAGAAGAAGACCCAACTGA	Use qPCR to measure the transcript levels of RNA lariat debranching enzyme
RNA lariat debranching enzyme qPCR primer R	GGTTGGGATTCGAAAAGGAC	
NADH ubiquinone oxidoreductase 11.6kD subunit qPCR primer F	CCTGATACTTCCATCCAAACG	Use qPCR to measure the transcript levels of NADH ubiquinone oxidoreductase 11.6 kDa subunit
NADH ubiquinone oxidoreductase 11.6kD subunit qPCR primer R	GAGGATACCCTCGGCCTCTA	
malate synthase qPCR primer F	CAACTACCTCATGGAGGATGC	Use qPCR to measure the transcript levels of malate synthase
malate synthase qPCR primer R	CTTGAGGGCGTACGACTTGT	

NCU03408 hypothetical protein qPCR primer F	TCAAGGGACTGGTGTTGATG	Use qPCR to measure the transcript levels of NCU03408 hypothetical protein
NCU03408 hypothetical protein qPCR primer R	GGTTAGGTAGATGGGGATGGA	
6-phosphofructokinase qPCR primer F	GGAGAGAGGAAATGCGTAGC	Use qPCR to measure the transcript levels of 6-phosphofructokinase
6-phosphofructokinase qPCR primer R	ATGGTCTTGCGCTTTCCA	
fructose bisphophate aldolase qPCR primer F	TCCTCCACACCGACCACT	Use qPCR to measure the transcript levels of fructose bisphophate aldolase
fructose bisphophate aldolase qPCR primer R	CTCCTCGAGCATGCCATC	
NCU04899 malate dehydrogenase qPCR primer F	CGCCAGCTTACCAAGGTCT	Use qPCR to measure the transcript levels of NCU04899 malate dehydrogenase
NCU04899 malate dehydrogenase qPCR primer R	GCTTGAGGAGGAGGGAGAG	
NCU04752 hypothetical protein qPCR primer F	CTTCAAGCGTGATGCTTTCTAA	Use qPCR to measure the transcript levels of NCU04752 hypothetical protein
NCU04752 hypothetical protein qPCR primer R	CGTCTTCTCGTTCAAAGATCTCA	
hydroxyacylglutathione hydrolase qPCR primer F	GGCCTCATGACCCTGAGAT	Use qPCR to measure the transcript levels of hydroxyacylglutathion hydrolase
hydroxyacylglutathione hydrolase qPCR primer R	TCATAATAGCCACCGGATCG	
MSF1 qPCR primer F	CGTTACCATGGTCTCCACAA	Use qPCR to measure the transcript levels of MSF1
MSF1 qPCR primer R	TAGACGACGGTCTCCTGGAC	

NCU01053 hypothetical protein qPCR primer F	CCTTACTCAATCGCGAAGTC	Use qPCR to measure the transcript levels of NCU01053 hypothetical protein
NCU01053 hypothetical protein qPCR primer R	TTTGTCGTCTGCACTTGG	
cytochrome c qPCR primer F	GTGGTCTCAAGAAGGACAAG	Use qPCR to measure the transcript levels of cytochrome c
cytochrome c qPCR primer R	AGCAGTAGCCTCCTTCAT	
NADH ubiquinone oxidoreductase 29.9kD subunit qPCR primer F	GAGCGCTGAACAGATTGCT	Use qPCR to measure the transcript levels of NADH ubiquinone oxidoreductase 29.9kDa subunit
NADH ubiquinone oxidoreductase 29.9kD subunit qPCR primer R	ACCTCCTCAATCAAGCCAGA	
NADP-dependent malic enzyme qPCR primer F	ACAAGGGGACGTCATTCACT	Use qPCR to measure the transcript levels of NADP-dependent malic enzyme
NADP-dependent malic enzyme qPCR primer R	CATGACGTGCGGAATAAGTC	
ATPase-1 qPCR primer F	CGATCTTGATGCTGCTACC	Use qPCR to measure the transcript levels of ATPase-1
ATPase-1 qPCR primer R	GAGTACTGCTTCTGCTTGAG	
26S protease subunit 4 qPCR primer F	CATCGGTACCAAGCGTTAC	Use qPCR to measure the transcript levels of 26S protease subunit 4
26S protease subunit 4 qPCR primer R	CAGCTCCAACATGGTTCTC	
Tom5 qPCR primer F	CCACCTTCACCATTCAACG	Use qPCR to measure the transcript levels of Tom5
Tom5 qPCR primer R	ACGAAGGGAGAGAGGTAAAG	
pyruvate decarboxylase qPCR primer F	ACTTGAGGGTCACCATCTT	Use qPCR to measure the transcript levels of pyruvate decarboxylase
pyruvate decarboxylase qPCR primer R	CCATGGATGTAACGTTCGATAG	

polyketide synthase 3 qPCR primer F	GCAGCTCGAGTCAACATAC	Use qPCR to measure the transcript levels of polyketide synthase 3
polyketide synthase 3 qPCR primer R	AGCCACATCCTGAAGAGTA	
serine/theronine protein kinase-39 qPCR primer F	GGCGTTGAAGGAGATGAACT	Use qPCR to measure the transcript levels of serine/theronine protein kinase-39
serine/theronine protein kinase-39 qPCR primer R	TTCTCGTTATCGTGCTTGCTT	
glycine dehydrogenase qPCR primer F	GAAGAAGTTCTGGCCTAGC	Use qPCR to measure the transcript levels of glycine dehydrogenase
glycine dehydrogenase qPCR primer R	CAGGTACAGAAGAGGTTCAAA	
NCU04392 hypothetical protein qPCR primer F	GCTTTATGCCAGTCATCTTGC	Use qPCR to measure the transcript levels of NCU04392 hypothetical protein
NCU04392 hypothetical protein qPCR primer R	CATGTTTGCCTGCTGACG	
NCU09144 hypothetical protein qPCR primer F	CGAATAACGTTCTTGCTGCAC	Use qPCR to measure the transcript levels of NCU09144 hypothetical protein
NCU09144 hypothetical protein qPCR primer R	CGTGGTAGTTGACCAGTTTCG	
NCU05203 hypothetical protein qPCR primer F	GATGGTGACACATTGCTTCCT	Use qPCR to measure the transcript levels of NCU05203 hypothetical protein
NCU05203 hypothetical protein qPCR primer R	TCTCTCTTCATACGAGTCGATCC	
NCU07678 hypothetical protein qPCR primer F	GACCCATTTCCACGTATCTG	Use qPCR to measure the transcript levels of NCU07678 hypothetical protein
NCU07678 hypothetical protein qPCR primer R	GAAACCCGTGTCTTGATCTAC	

NCU08946 hypothetical protein qPCR primer F	AGCTTGACGCTCAGAGTGC	Use qPCR to measure the transcript levels of NCU08946 hypothetical protein
NCU08946 hypothetical protein qPCR primer R	GTAGTCTGGGCCGAGGTTCT	
ubiquitin qPCR primer F	TTTGACCGGCAAGACCATC	Use qPCR to measure the transcript levels of ubiquitin
ubiquitin qPCR primer R	CCCTCCTTGTCCTGAATCTTT	
zinc ion transporter qPCR primer F	CTTTCCCATGATTCGTCTCC	Use qPCR to measure the transcript levels of zinc ion transporter
zinc ion transporter qPCR primer R	CAATCAAGACTCCGGTACCAA	
NCU05202 hypothetical protein qPCR primer F	GCCGGTTACTATTCCCATTG	Use qPCR to measure the transcript levels of NCU05202 hypothetical protein
NCU05202 hypothetical protein qPCR primer R	CGGTAGACGAGGTAGAAGAA	
NCU00628 hypothetical protein qPCR primer F	ACTTCATCTCGCTCCTTCT	Use qPCR to measure the transcript levels of NCU00628 hypothetical protein
NCU00628 hypothetical protein qPCR primer R	GTAGCCATGGCGAAATAGAG	
mitochondrial hypoxia responsive domain-containing protein qPCR primer F	GTGTCATGTTGGGCATGAAG	Use qPCR to measure the transcript levels of mitochondrial hypoxia responsive domain-containing protein
mitochondrial hypoxia responsive domain-containing protein qPCR primer R	GCCGAGGTAACAAGGAAGG	
ubiquitin conjugating enzyme qPCR primer F	TGTGGGTATTGACCGGAAC	Use qPCR to measure the transcript levels of ubiquitin conjugating enzyme
ubiquitin conjugating enzyme qPCR primer R	GCAGTGATATCGCCCATGTA	

amination-deficient qPCR primer F	AACATTGCTGGTTTCGTCAA	Use qPCR to measure the transcript levels of amination-deficient
amination-deficient qPCR primer R	TTCTTGGACCACCAGTCACC	
pentatricopeptide repeat protein qPCR primer F	TGAGCACCTGCAAAAGTCAC	Use qPCR to measure the transcript levels of pentatricopeptide
pentatricopeptide repeat protein qPCR primer R	ACCCATTCCTGATCGTGTTC	
D-arabinitol dehydrogenase qPCR primer F	ACATCGTCGAGACCTTCAAGA	Use qPCR to measure the transcript levels of D-arabinitol dehydrogenase
D-arabinitol dehydrogenase qPCR primer R	GGCGTAGTGGGCTGTTACTT	
glycine cleavage system H protein qPCR primer F	TGCCAACAATGAGCTAAGG	Use qPCR to measure the transcript levels of glycine cleavage system H protein
glycine cleavage system H protein qPCR primer R	GCCAACGTAACCAGTCTTC	
NCU02732 hypothetical protein qPCR primer F	ACTCGCCTTACTCTGACAA	Use qPCR to measure the transcript levels of NCU02732 hypothetical protein
NCU02732 hypothetical protein qPCR primer R	CAACGACACTACCGCTATTC	
TEM1 qPCR primer F	AGGAGGAAATCTCCAACCA	Use qPCR to measure the transcript levels of TEM1
TEM1 qPCR primer R	ATTGATGCTGTGACTGGTG	
C6 finger domain-containing protein qPCR primer F	GCCATGACCGAAGTTAGAC	Use qPCR to measure the transcript levels of C6 finger domain-containing protein
C6 finger domain-containing protein qPCR primer R	GTTTCTTGACGGGTCCTAAG	

high affinity glucose transporter ght1 qPCR primer F	TCCAGTCACTGCTAGTATCTC	Use qPCR to measure the transcript levels of high affinity glucose transporter ght1
high affinity glucose transporter ght1 qPCR primer R	GTGGCGGTGTATGATGAAG	
NCU06211 malate dehydrogenase qPCR primer F	GCTCGCCCTCTACGATGTC	Use qPCR to measure the transcript levels of NCU06211 malate dehydrogenase
NCU06211 malate dehydrogenase qPCR primer R	AAGGTAGCCGGTGGTTTTG	
ubiquiol-cytochrome c reductase 8 qPCR primer F	CCTACGGTATCAGCCCTAA	Use qPCR to measure the transcript levels of ubiquinol-cytochrome c reductase 8
ubiquiol-cytochrome c reductase 8 qPCR primer R	CACGTCTGAAGGTGTTGAA	

[1] The sequence of the primers originated from the *Neurospora* knock out library project (Colot *et al.* 2006).

Reference

Colot, H. V., Park, G., Turner, G. E., Ringelberg, C., Crew, C. M., Litvinkova, L., Weiss, R. L., Borkovich, K. A., & Dunlap, J. C. (2006). A high-throughput gene knockout procedure for Neurospora reveals functions for multiple transcription factors. *Proc. Natl. Acad. Sci. U S A,* **103** (27): 10352-10357.

Appendix II. Optimal KCl concentration for extraction of nuclear proteins

To determine the KCl concentration to be used for extraction of nuclear proteins from gradient purified nuclei, I grew strain AOD2-C-HA-8 in the absence of CM, isolated gradient purified nuclei from the cultures, and mixed the nuclei with different concentrations of KCl dissolved in the nuclear suspension buffer for 1.5 hr at 4 ºC (see section 2.11 and Appendix Fig. 1 legend for buffer composition and volumes). After centrifugation for 30 min at 13,000 rpm (16,000 × g) at 4 ºC in a Sorvall Biofuge® fresco centrifuge, the supernatant was desalted using Zeba™ desalting columns. The desalted supernatant, as well as the pellet obtained after centrifugation, were subjected to SDS-PAGE, blotted to nitrocellulose, and analyzed by Western blot.

As shown on the left panel of Appendix Fig. 1, the amount of AOD2 protein was slightly increased as the concentration of KCl was increased, whereas an increase in Histone H3 with KCl concentration was not apparent. In the absence of KCl, neither AOD2 nor Histone H3 protein was detected, indicating that KCl causes the release of nuclear proteins from gradient purified nuclei. For both proteins, there was a decrease in the amount of protein remaining in the nuclear pellet that corresponded with increasing KCl concentration (Appendix Fig. 1, right panel). Although the highest concentration of KCl used gave the most efficient extraction of AOD2, I reasoned that it would also be the most likely to interfere with protein-protein interactions. Since the extracted proteins were to be used for co-immunoprecipitation experiments, I chose a final KCl concentration of 0.2 M to achieve reasonable extraction efficiency and minimal effects on protein-protein interactions.

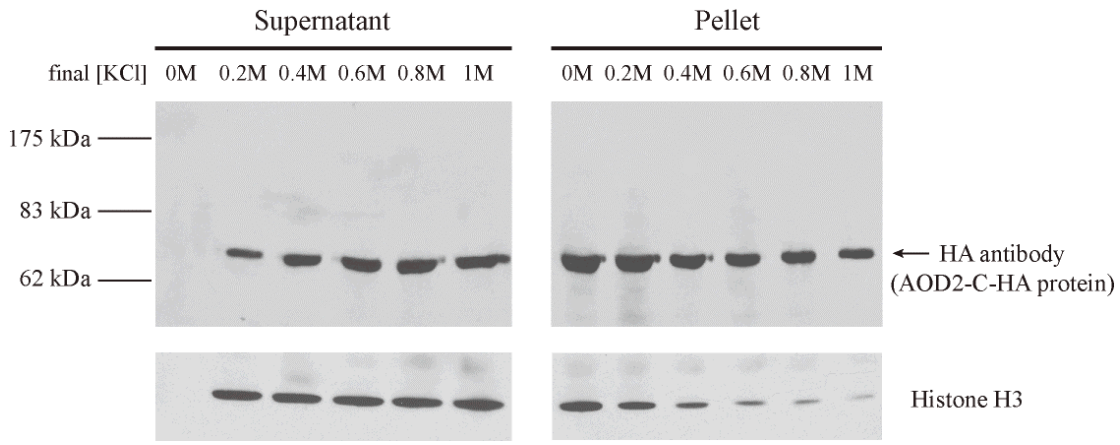

Appendix Figure 1. Test for different KCl concentrations for extraction of nuclear proteins. 40 µL of gradient purified nuclei containing 100 µg of protein from strain AOD2-C-HA-8 grown in the absence of CM were gently mixed with 40 µL 0 M, 0.4 M, 0.8 M, 1.2 M, 1.6 M, or 2 M KCl dissolved in nuclear suspension buffer (25 mM sucrose, 50 mM Tris-HCl [pH7.5], 5 mM $MgCl_2$, 10 mM $CaCl_2$) containing 1 mM PMSF and protease inhibitors (final concentrations of 2 µg/mL aprotinin, 1 µg/mL leupeptin, and 1 µg/mL pepstatin A). Thus, the final KCl concentrations used were 0 M, 0.2 M, 0.4 M, 0.6 M, 0.8 M, and 1 M, respectively. The mixing was performed for 1.5 hr at 4 ºC using an Orbitron Rotator I (Boekel Scientific, Feasterville, USA). The resulting nuclear mixture was centrifuged at 13,000 rpm (16,000 × g) for 30 min at 4 ºC in a Sorvall Biofuge® fresco centrifuge. The pellet was dissolved in 100 µL cracking buffer (section 2.12) and heated to 95 ˚C for 5 min. It was then subjected to SDS-PAGE, blotted to nitrocellulose, and analyzed by Western blot. The supernatant was desalted using Zeba™ Spin Desalting columns (Thermo Scientific, Rockford, USA, see section 2.11). 20 µL of 5X cracking buffer (section 2.12) was added and the sample was heated to 95 ˚C for 5 min. The sample was then subjected to SDS-PAGE, blotted to nitrocellulose, and analyzed by Western blot.

Appendix III. Characterization of a potential *aod-1* precursor protein band.

When performing cell fractionation experiments, I noticed that the AOX antibody-stained strips from Western blots of cytosolic fractions usually contained an additional band with a slightly higher molecular weight than the mature AOX found in the mitochondrial fractions. This band was often more evident in the –CM cytosolic fraction (Fig. 3.3, indicated by the arrows). Occasionally, lower levels of the band were also seen in the +CM cytosolic fraction. These observations lead us to suspect that the band might represent a precursor protein of AOX still carrying its N-terminal mitochondrial targeting signal. This was of interest because it would mean that some AOX protein was being translated in the cytosol in non-inducing conditions, but was not being imported into mitochondria, since the –CM mitochondria lanes contained no AOX. This suggested the hypothesis that at least some AOX was expressed and translated in *N. crassa*, even in the absence of CM. However, an unknown post-translational control mechanism for AOX might prevent mitochondrial import, thus sequestering AOX in the cytosol under non-inducing conditions.

A second possibility was that the band represented AOD3. A gene encoding the AOD3 protein was discovered when the *N. crassa* genome sequence was examined by a BLAST search with the AOD1 protein sequence as the probe. AOD3 was reported to be 55% identical to the AOD1 protein (Tanton *et al.* 2003). The antibody against AOD1, which was used in my studies, was produced against the last 122 amino acids of AOD1 (Tanton *et al.* 2003). This region of AOD1 is reasonably conserved in AOD3 (Appendix Fig. 2). Thus, it is possible that the anti-AOX antibody might detect AOD3 if it existed in the cytosolic fraction. However, it should be noted that previous work gave no evidence of AOD3 mRNA expression following growth in the presence or absence of CM (Tanton *et al.* 2003).

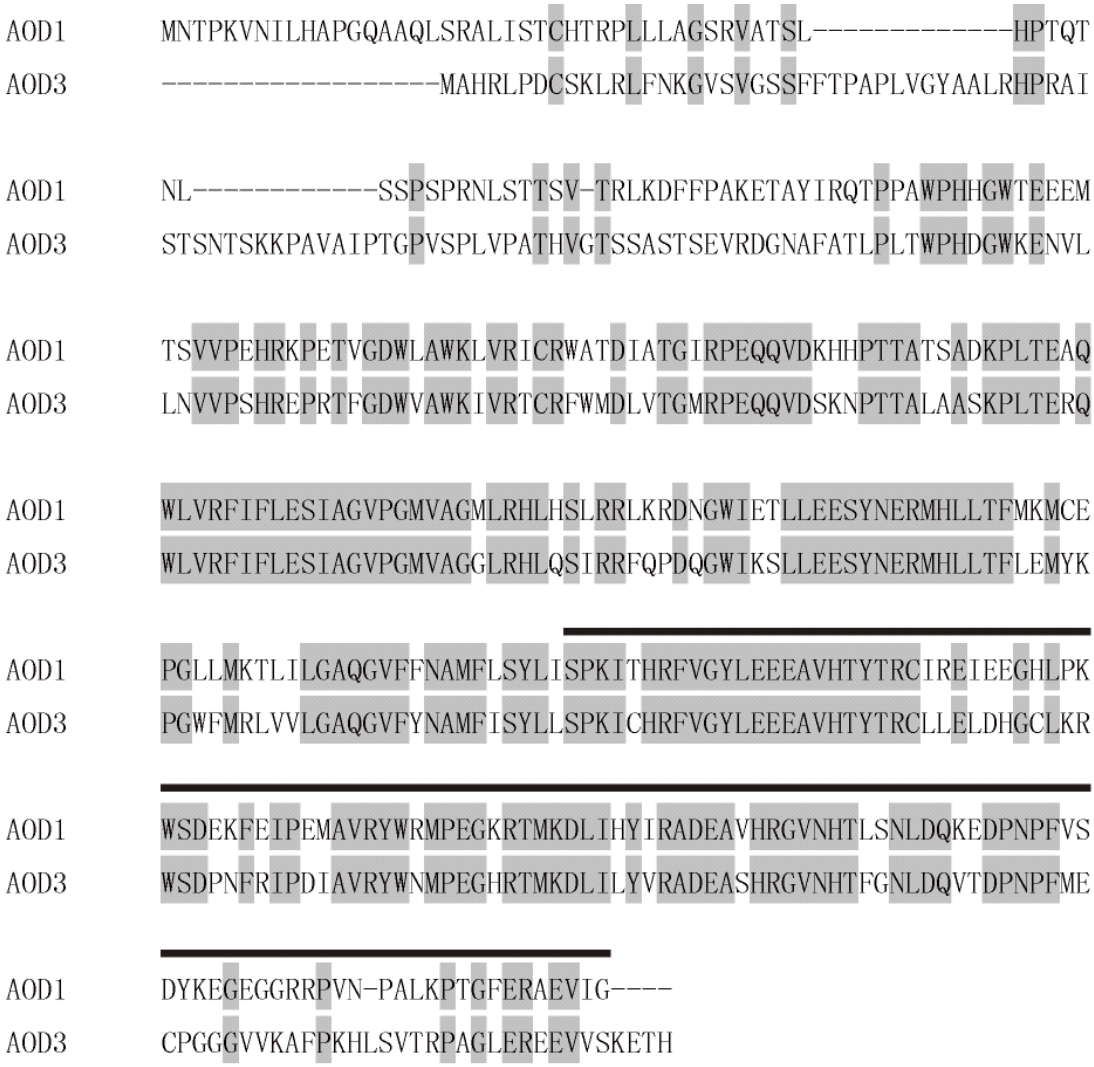

Appendix Figure 2. Alignment of AOD1 and AOD3. Protein sequences of AOD1 and AOD3 were retrieved from FungiDB (Stajich *et al.* 2012). Alignment was performed using the Clustal Omega program (Sievers *et al.* 2011). Amino acids that are highlighted in grey represent identical amino acids. Black bars on the top of the AOD1 sequence indicate the position of the last 122 amino acids in the protein, which was used as the antigen to produce the AOD1 antibody. Note that this alignment data is slightly different from that published in Tanton *et al.* (2003).

A third alternative was that the cytosolic band was a non-specific protein band recognized by our antibody.

As an initial step for testing these three possibilities, I wished to determine if the band was present in an *aod-1 aod-3* double knock-out strain. If the band represented an AOD1 preprotein or AOD3, it would not be present in the cytosolic fraction of the double knock-out. Δ*aod-1* (96H9) and Δ*aod-3* (44H6) strains were available in the FGSC knock-out library, where individual genes are replaced with a hygromcyin resistant cassette. The mutants were crossed reciprocally using either the Δ*aod-1* (mating type *A*) or Δ*aod-3* (mating type *a*) as a female, and the other as a male. The progeny were examined for knock-out alleles at both loci by PCR analysis. The progeny were also tested on medium containing antimycin A, as sensitivity to the drug should indicate inability to produce the AOD1 protein and be diagnostic for the Δ*aod-1*:hygR allele. 20 progeny from the cross using Δ*aod-1* as the female, and 17 progeny from the cross using Δ*aod-3* as the female, were not able to grow in the presence of antimycin A.

Genomic DNA was isolated from 10 of the antimycin A sensitive progeny (eight from the Δ*aod-1* female cross and two from the Δ*aod-3* female cross). PCR was performed to amplify the *aod-1* and *aod-3* loci using primers upstream and downstream of the gene replacement sites (Appendix Fig. 3A, B). Because the knock out cassette containing the hygromycin gene gave a PCR product similar in size to the product from the *aod-1* gene, I performed a restriction digest of the PCR product to distinguish between them (Appendix Fig. 3B). The hygromycin PCR product contained an *EcoR*I restriction site whereas the *aod-1* gene did not. Two progeny, 44H6-3 and 44H6-4 (from the cross using Δ*aod-3* as the female), were confirmed as Δ*aod-1* Δ*aod-3* mutants (Appendix Fig. 3C).

Appendix Figure 3. The unknown band observed in cytosolic fractions is not AOX. A. Diagram of genomic regions containing the *aod-1* (left side) and *aod-3* (right side) loci. Half arrows indicate the position of forward (top) and reverse (bottom) primers for PCR amplification of each gene. The predicted size of the PCR products is shown below with full arrows on both sides indicating the size of fragments. B. As in A except the loci containing the replacement hygromycin resistance cassettes (Hyg) are shown. For the *aod-1* replacement, the position of the *EcoR*I site in the hygromycin cassette is indicated, as are the size of predicted *EcoR*I fragments. The *aod-1* gene contains no *EcoR*I sites. C. Genomic DNA was isolated from the indicated progeny strains of the Δ*aod-1* × Δ*aod-3* cross, and a wild-type (NCN251) control. The DNA was subjected to PCR amplification using the primers shown in A. For the *aod-1* PCR, the products were subjected to digestion with *EcoR*I. DNA was then electrophoresed on 1% agarose gels containing ethidium bromide and photographed. Sizes of fragments obtained from the PCR with *EcoR*I digestion for the *aod-1* PCR (left side) and without *EcoR*I digestion for the *aod-3* PCR (right side) are indicated on the right. *Hind*III digested lamda DNA was used as a size marker as indicated on the left. D. Cytosolic and mitochondrial fractions were isolated from the control strain (NCN251) and double mutant 44H6-3, each grown in the absence (-CM) and presence (+CM) of CM. Following electrophoresis, and electro-blotting, the membrane was decorated with antibody to Tom70 (loading control for mitochondria) and AOX, as indicated on the right. Arrows indicate the presence of the extra band in the cytosol of both the control and double mutant strain.

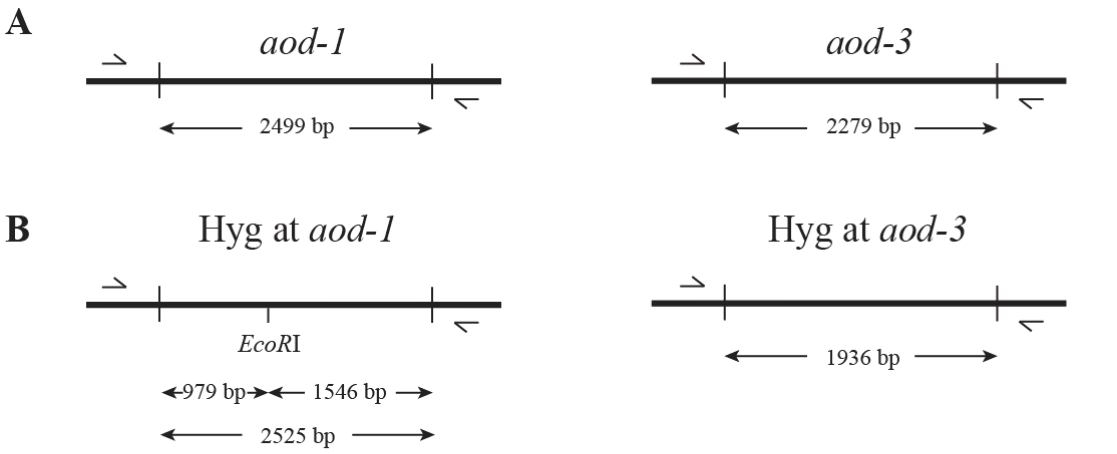
A
aod-1
2499 bp
aod-3
2279 bp
B
Hyg at aod-1
EcoRI
979 bp
1546 bp
2525 bp
Hyg at aod-3
1936 bp

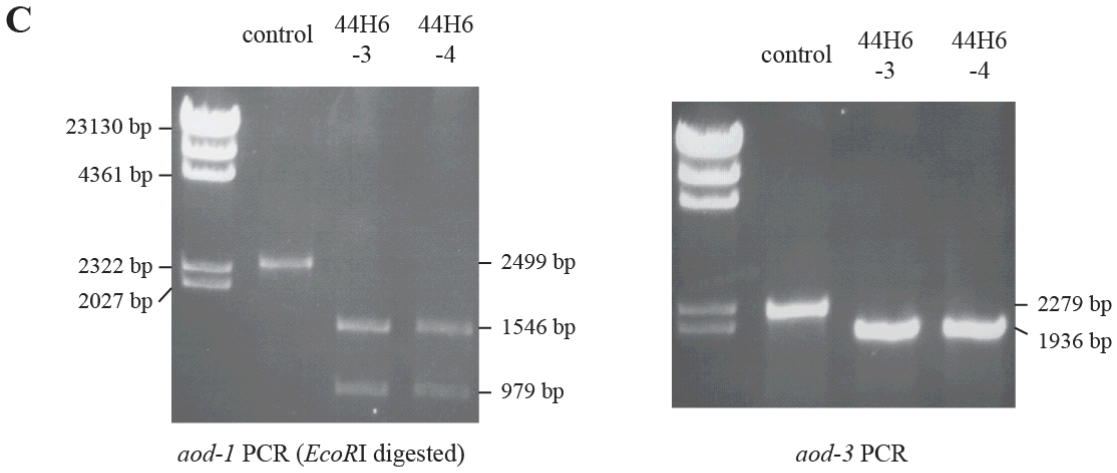
C
control
44H6 -3
44H6 -4
23130 bp
4361 bp
2322 bp
2027 bp
2499 bp
1546 bp
979 bp
aod-1 PCR (EcoRI digested)
control
44H6 -3
44H6 -4
2279 bp
1936 bp
aod-3 PCR

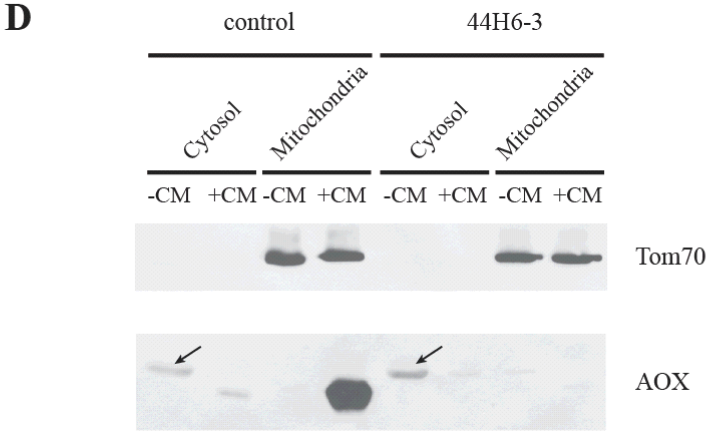
D
control
44H6-3
Cytosol
Mitochondria
Cytosol
Mitochondria
-CM +CM -CM +CM -CM +CM -CM +CM
Tom70
AOX

Cytosolic and mitochondrial fractions were then isolated from strain 44H6-3 grown in both the presence and absence of CM. Western blot analysis showed that the unknown band was still present in 44H6-3 -CM cytosolic fraction even though neither of the AOX proteins can be expressed from the strain (Appendix Fig. 3D). This result demonstrated that the extra band was due to non-specific binding of the anti-AOX antibody to an unknown protein in the cytosolic fraction.

Reference

Tanton, L. L., Nargang, C. E., Kessler, K. E., Li, Q., & Nargang, F. E. (2003). Alternative oxidase expression in *Neurospora crassa*. *Fungal Genet. Biol.,* **39** (2): 176-190.

Appendix IV. Investigation of phosphorylation and redox status of AOD2 and AOD5

Appendix IV. 1. Phosphorylation status

It was conceivable that a post-translational modification of AOD2 or AOD5 was responsible for changing the protein from an inactive to an active form. One common post-translational modification is phosphorylation. Phosphorylation was an attractive hypothesis because the *S. cerevisiae* homologue of AOD2 (Rds2p) is phosphorylated when cells are grown on medium that is shifted from glucose to ethanol (Soontorngun *et al.* 2007).

A Phos-tag is a chemical that binds two manganese ions that have high affinity to phosphate. When the tag is co-polymerized with acrylamide, it can greatly retard the mobility of phosphorylated proteins during electrophoresis, resulting in separation of the phosphorylated and non-phosphorylated forms of a protein. I examined AOD2 and AOD5 by phos-tag gel electrophoresis after growing cells in both the presence and absence of CM.

As a control to test whether Phos-tag SDS-PAGE was able to separate and detect phosphorylated proteins, I analyzed β-casein, a phosphorylated protein from bovine milk. Lanes containing the protein exhibited a readily detectable band near the top in the Phos-tag SDS-PAGE (Appendix Fig. 4A). However, the mobility of the band was obviously increased following treatment with calf intestine phosphatase (CIP) (Appendix Fig. 4A).

Analysis of nuclear proteins from strain AOD2-N-HA-3 was then carried out following treatment or no treatment with CIP. Samples were analyzed by Western blot using antibodies against the HA tag. Two phos-tag SDS-PAGE gels gave inconsistent results (Appendix Fig. 4B). One of them showed that when cells were grown in the

Appendix Figure 4. Phos-tag gel analysis of AOD2 and AOD5. A. 2 μg, 5 μg, and 10 μg of β-casein (Sigma-Aldrich, USA) were not treated, and/or treated with calf intestine phosphatase (CIP) for 3 hr at 37 ° C as indicated on the figure. Samples were electrophoresed on a phos-tag (100 μM) gel. The gel was stained with Coomassie blue. B. The wild-type control strain (NCN251) and strain AOD2-N-HA-3 were grown in the presence or absence of CM. Gradient purified nuclei were isolated from the cultures. The nuclear proteins were extracted, treated with or without CIP, and then subjected to phos-tag (100 μM) SDS-PAGE. The gel was blotted to nitrocellulose membrane and probed with antibodies against the HA tag. Left and right panels are two replicates with inconsistent results. Asterisks indicate bands with faster mobility when proteins were treated with CIP compared to those without CIP treatment. Arrowheads on the right panel indicate retarded protein bands in CIP untreated samples when compared to the CIP treated samples. C. As in B except strain AOD5-C-Myc-4 was used and detection of the tagged AOD5 protein was done using anti-Myc antibody. Black arrows indicate bands unique to AOD5-C-Myc-4 when compared to the wild-type control.

A

β-casein (μg)	2	2	2	5	5	5	10	10	10
CIP buffer (μL)	0	0.4	0.4	0	1	1	0	2	2
CIP (units)	0	0	0.2	0	0	0.5	0	0	1

B

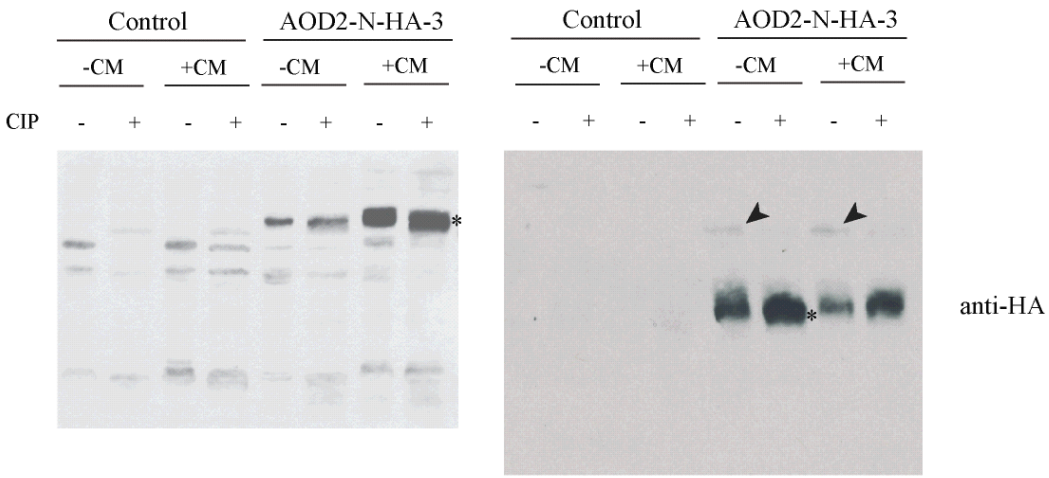

C

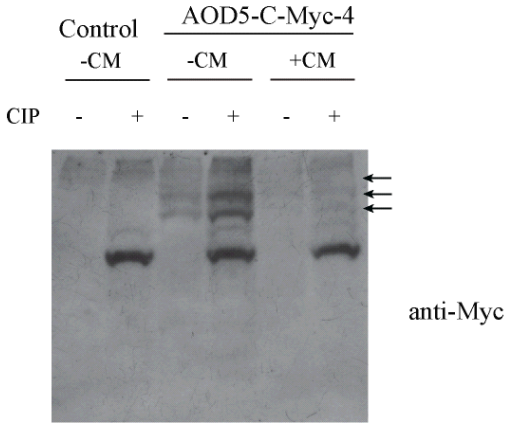

presence of CM, AOD2 exhibited faster electrophoretic mobility when dephosphorylated by CIP compared to no CIP treatment (Appendix Fig. 4B, left panel). In contrast, the electrophoretic mobility of AOD2 from –CM cultures was not affected by CIP treatment. However, the opposite result was obtained in a second phos-tag SDS-PAGE gel, where AOD2 from –CM cultures showed faster electrophoretic mobility when treated with CIP. On this gel AOD2 from the +CM culture displayed no difference in electrophoretic mobility, regardless of whether the nuclear proteins had been treated with CIP or not (Appendix Fig. 4B, right panel). Furthermore, a faint band was observed when AOD2 was untreated, while only the major band was seen when AOD2 was dephosphorylated (Appendix Fig. 4B, right panel arrowheads). Unfortunately, the latter result was seen in proteins from both induced and non-induced cultures. These data suggest that a minor fraction of AOD2 proteins are phosphorylated under both conditions.

I then examined the phosphorylation of AOD5 using the strain AOD5-C-Myc-4. The blots of the phos-tag SDS-PAGE using the anti-Myc tag antibody showed several non-specific bands that were also present in the untagged control sample. However, there were three bands that were unique to the tagged AOD5 samples (Appendix Fig. 4C, indicated by the arrows). However, no obvious band shifts were observed in CIP treated AOD5 when compared to the CIP untreated, regardless of whether the AOD5 was from +CM or -CM cultures. These observations make it unlikely that phosphorylation status influences AOD5 activity.

Appendix IV.2. Redox status

I was also interested in determining if AOD2 or AOD5 undergo changes in their redox state when cells are grown in the presence of CM, since it is conceivable

that inhibition of mitochondrial protein synthesis by CM might lead to oxidative stress. Furthermore, in addition to the multiple cysteine residues in the DNA binding domain of AOD2 and AOD5 ($CysX_2CysX_6CysX_{5\text{-}12}CysX_2CysX_{6\text{-}8}Cys$) that is conserved in fungal $Zn(II)Cys_6$ cluster transcription factors (MacPherson *et al.* 2006), there are five cysteine residues that are found C terminal to the DNA binding domain in both AOD2 and AOD5. Potentially, these could form intra- or inter-molecular disulfide bonds in response to oxidative stress and alter the function of the proteins. To investigate the redox status of AOD2 and AOD5, I isolated gradient purified nuclei from wild-type, AOD2-C-HA-8, and AOD5-N-HA-1 grown in the presence and the absence of CM. Extracted nuclear proteins were treated with or without a reducing agent (β-mercaptoethanol). The proteins were run on an SDS-PAGE gel. As shown in Appendix Fig. 5, neither AOD2 nor AOD5 show different electrophoretic mobilities under any conditions. This result suggested that no binding partners were associated with AOD2 or AOD5 through disulfide bonds. Furthermore, lack of any detectable changes in electrophoretic mobility also makes it unlikely that intra-molecular disulfide bonds exist in the unreduced samples.

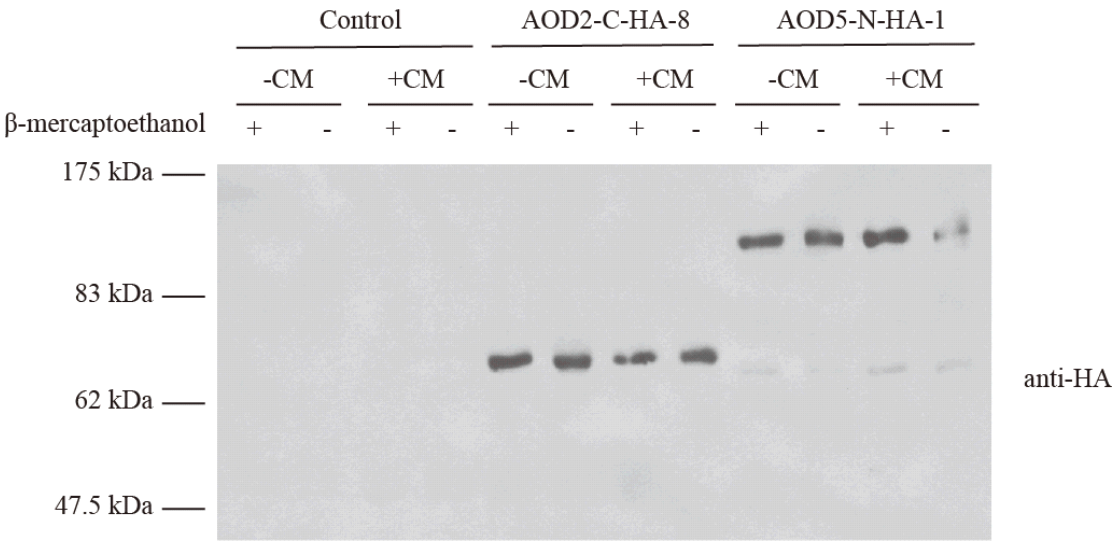

Appendix Figure 5. Redox status of AOD2 and AOD5. Gradient purified nuclei were isolated from the control strain (NCN251), strain AOD2-C-HA-8, and strain AOD5-N-HA-1 each grown in the presence and absence of CM. Extracted proteins were mixed with gel loading buffer (cracking buffer, see section 2.12) with or without β-mercaptoethanol which reduces disulfide bonds within or between proteins. Samples were subjected to SDS-PAGE and transferred to nitrocellulose. The blots were examined with antibody against the HA tag. Molecular weight markers are indicated on the left.

Reference

MacPherson, S., Larochelle, M., & Turcotte, B. (2006). A fungal family of transcriptional regulators: the zinc cluster proteins. *Microbiol. Mol. Biol. Rev.,* **70** (3): 583-604.

Soontorngun, N., Larochelle, M., Drouin, S., Robert, F., & Turcotte, B. (2007). Regulation of gluconeogenesis in *Saccharomyces cerevisiae* is mediated by activator and repressor functions of Rds2. *Mol. Cell. Biol.,* **27** (22): 7895-7905.